



# OROBANCHACEAE PLANTS OF ISRAEL AND PALESTINE. CHEMICAL AND MEDICINAL TREASURES

Abdullatif Azab<sup>[a]\*</sup>

**Keywords:** *Orobanchaceae*; trixagol; iridoids; phenylethanoids; strigolactones; parasitic plants, medicinal activities, immunomodulation.

*Orobanchaceae* plant family is one of the most interesting plant families in our region. It is represented by small number of plants and some of them attracted major interest while others have been almost completely neglected. Even the ethnobotanical uses of these plants in the reviewed region are very limited. The present day knowledge about these plants indicates contradicting research tendencies, interesting natural products that were isolated from some of these plants, along with massive lack of information about the chemical and medicinal properties of others. Many review articles were published about this family, but each one of them lacks some essential information or includes ambiguities. This article will present the known information in helpful tables and figures, but will mainly emphasize the areas where intensive research efforts are needed. In the discussion section, the parasitic nature of these plants will be elaborated, and some synthetic and biosynthetic paths will be introduced.

\*Corresponding Authors

Fax: +972-4-6205906

E-Mail: [eastern\\_plants@gmail.com](mailto:eastern_plants@gmail.com)

[a] Eastern Plants Research Institute, Box 868, Arara, Israel 30026

## INTRODUCTION

*Orobanchaceae* plant family includes around 2060 species, classified in 90 genera.<sup>1</sup> In the reviewed region, it is represented by 17 species, and this number is debated among scholars.<sup>2</sup> For example, G. Domina and A. Danin have defined a new species in 2014, and they named it *Orobanche cohenii*.<sup>2</sup> But searching the website “Flora of Israel Online”, that was established by Prof. A. Danin himself and still has his name on homepage, shows that this species is not included in the 18 species presented there.<sup>3</sup> Interestingly, ancient human societies did not utilize these plants for their needs.

The major botanical property of *Orobanchaceae* plants is their parasitic nature, which was very extensively studied. Many aspects of this parasitism were investigated, such as the genetics of this property,<sup>4</sup> and the chemical basis of it.<sup>5</sup> For example, the cyclohexene oxide-type sphaeropsidone (Figure 1), induces parasitism of *Orobanche* plants, which is a genus in the *Orobanchaceae* family.

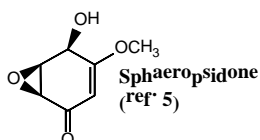


**Figure 1.** Sphaeropsidone, natural parasitism inducer of *Orobanche* plants

Among the four genera that are represented in the reviewed region, *Orobanche* plants are the most parasitic, and many attempts were made to control them. An extensive presentation of this topic will be introduced in the discussion

section, but we will indicate here some of these publications. *Orobanche crenata* and *Orobanche aegyptiaca* are among the most harmful species of this genus, and a method of controlling them (Imazapic, C<sub>14</sub>H<sub>17</sub>N<sub>3</sub>O<sub>3</sub>) in parsley crops was reported.<sup>6</sup> Another study that investigated the mechanism of parasitic activity of *O. aegyptiaca*, revealed the involvement of horizontal genes transfer.<sup>7</sup> *O. crenata* is harmful to many crops, especially *Fabaceae* plants, and so, it causes many agricultural damages to *Vicia faba* production, which is a major food source in the Middle East, particularly in Egypt. So, a method of biocontrol of this parasitic plant was developed based on the allelopathic property of *Euroca sativa* seed powder.<sup>8</sup> But as we mentioned above, all genera of this plant family are parasitic, and a notable study of this property of one of the most studied plants of this family, *Cistanche tubulosa*, was performed and it revealed the mechanism that this parasite attaches itself to the roots of host plants.<sup>9</sup>



**Figure 2.** *Bellardia trixago* (Orobanchaceae)

Finally, in the reviewed region, the *Orobanchaceae* plant family is represented by four genera that include 17 species namely *Bellardia trixago*, *Cistanche fissa*, *Cistanche salsa*,

*Cistanche tubulosa*, *Odontites aucheri*, *Orobanche aegyptiaca*, *Orobanche cernua*, *Orobanche crenata*, *Orobanche cumana*, *Orobanche hermonis*, *Orobanche lavandulacea*, *Orobanche mutelii*, *Orobanche palaestina*, *Orobanche pubescens*, *Orobanche schultzei*, *Parentucellia flaviflora* and *Parentucellia viscosa*.

## ETHNOBOTANICAL USES

Generally, cultures of the Middle East and particularly these of reviewed region, have almost ignored the *Orobanchaceae* plant family. There is very partial documentation of ethnobotanical uses of these plants, contrary to some nations in the Far East or Europe. But these peoples mostly used species that do not grow in Israel and Palestine, so we will not cite these reports here. And yet, some of the literature that we will cite about the species that grow here, were published about other regions in the world. In Table 1, we summarized these published uses.

**Table 1.** Ethnomedicinal and ethnobotanical uses of *Orobanchaceae* plants

Species	Region, uses, methods, references
<i>Bellardia trixago</i>	Spain. Flowers are sucked as food. <sup>10</sup>
<i>Cistanche salsa</i>	Korea. As part of a traditional formulation named PJBH, to activate brain function, promote memory and lengthen life span. <sup>11</sup>
<i>Cistanche tubulosa</i>	Pakistan. Whole plant powder used against diarrhea, <sup>12</sup> blood purifier, epistaxis, cough, fever, bleeding nose, laxative, digestive, remove the pain of stomach, flavoring agent in pot herbs, <sup>13,14</sup> aprodisiac. <sup>15</sup> India. Fertility of males and females, jaundice, whooping cough, stomach aches, diabetes. <sup>16</sup> Ethiopia. Whole plant powder with butter to treat burns. <sup>17</sup>
<i>Orobanche aegyptiaca</i>	Nepal. Seeds are used as toys. <sup>18</sup>
<i>Orobanche crenata</i>	Italy. Food. Young shoots are prepared and consumed in various ways. <sup>19</sup>
<i>Orobanche mutelii</i>	Turkey. Harmful to melon crops. <sup>20</sup>

## SELECTED PUBLISHED REVIEW ARTICLES: PRESENTATION AND DISCUSSION

Aside from very few review articles about the parasitic properties of the entire *Orobanchaceae* plant family, there are no reviews about its medicinal, ethnobotanical and chemical composition of the plants. Different genera, species or even natural products contained in the plants, were reviewed, and in our humble opinion, some of them have high quality. So, the need for a comprehensive article like this one is felt.

The most recent review article was published by R. Shi and her colleagues.<sup>21</sup> This article is outstanding in terms of

the very good photos, tables, listing of traditional uses of the plants, citation of modern research published results and numerous structures of natural products that were isolated from the plants of the genus of *Orobanche*. Another strength that this article is its global presentation of the plants of this genus. But it showed some shortcomings also, especially in the cited literature, particularly if an interested reader is interested to follow, and learn more about some presented work. For example, the work of “Han, 2017” has been cited no less than 27 times. When reading the references part of the article, it is cited as “Studies on the Chemical Composition, Content Determination and Antioxidant Activity of *Orobanche Aegyptiaca* Pers, Inner. Mongolia. Med. Univ.”. Searching the internet for this work or any other citations of it, did not lead to a single result. But as we mentioned earlier, this review is one of the best published about this genus, due to its comprehensiveness. Another outstanding review about the genus of *Orobanche* natural products was published by F. Scharenberg and C. Zidorn.<sup>22</sup> It is a vast article that focuses on these compounds and some of their medicinal activities.

The genus of *Cistanche* was even more covered than *Orobanche*. L-I. Wang and her colleagues published a short review about the composition and the pharmacological activities of the Chinese traditional medicine formulation named *Cistanches Herba*, which contains five species of this genus.<sup>23</sup> Despite the fact that only two of them grow in the reviewed region (*C. salsa* and *C. tubulosa*), this review is highly informative. Z. Li and his colleagues published a short review article about the same formulation.<sup>24</sup> They name it *Herba Cistanches* (*Rou Cong-Rong*, in Chinese), and they presented its ancient use in traditional Chinese medicine, that go back to 250 BC, its composition and medicinal activities. The most recent review article about this formulation was published by H. Lei *et al.*<sup>25</sup> It is comprehensive, with two clear advantages over previous review articles. First, it indicates the plant species from which each natural product was isolated. Secondly, the natural products are arranged in general structure that presents each one of them as a derivative of this structure. Along with the three cited review articles (ref. 23-25), the publication of Y. Jiang and P-F. Tu, give a comprehensive view of the chemical composition and the medicinal activities of this unique formulation.<sup>26</sup>

But this formulation was reviewed not just in general scope as in references 23-26, but some reviews elaborated on some specific activities. An excellent review article of this type was published by C. Gu *et al.* that presented various medicinal activities of this formulation but focused on neuropharmacological aspects.<sup>27</sup> N. Wang and her colleagues focused on antiaging activity in their excellent, comprehensive review article about this formulation.<sup>28</sup> Their review has more advantages which are, linking to traditional medicine, presenting various activities and showing the structures of major active ingredients.

Review articles about single species of the *Orobanchaceae* plant family, in our region, are very limited. Among these species, only *Cistanche tubulosa* and *Orobanche crenata* have been reviewed. *C. tubulosa* was reviewed by A. E. Al-Snafi, and the article presents many medicinal activities that this plant showed.<sup>29</sup> This good article lacks two topics: traditional medicine and structures of at least major active natural products, even though some

of them are indicated. C. Genovese and his colleagues reviewed the chemical composition and the biological activities of *O. crenata*.<sup>30</sup> This very good review is very informative, with excellent tables and figures but lacks introduction to use in traditional medicine.

Finally, R. Halouzka and his colleagues summarized in a very useful review article the analytical methods of isolation and quantification of strigolactones (see general structure in Figure 3).<sup>31</sup> These natural products are found in *Orobanche* and *Striga* genera, but the second one is not represented in the reviewed region and not included in this article.

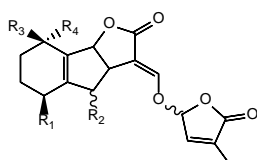


Figure 3. General structure of Strigolactone (ref. 31)

## MEDICINAL ACTIVITIES AND CHEMICAL COMPOSITION

Scanning the published literature about the plants of *Orobanchaceae* family that grow in the reviewed region, revealed an interesting but not completely understood result. Few species are extensively studied, others are very limitedly studied and many have been completely ignored. Moreover, some “classical” medicinal properties that are usually tested and published for other plant families, are not mentioned at all. For example, there are no publications that report antidiabetic or related activities, for any of these plants. On the contrary, there is relatively considerable amount of publications that reported isolation and characterization of structurally interesting natural products and of brain related activities.

Summary of these findings are shown in the following tables, that appear according to alphabetical order of the names of the species. An absence of published reports has been clearly indicated.

### *Bellardia trixago*

Table 2. Biological, medicinal and other properties of *Bellardia trixago*

Activity/Property	Major Findings/Reference
Antifungal	Resin of the plant was analyzed, and 8 known flavonoids were identified. Some of these compounds were methylated and found active against the fungus <i>Cladosporium herbarum</i> . <sup>32</sup>
Insecticidal	Essential oil of whole plant was prepared and analyzed by GC-MS. A detailed list of compounds is presented. New natural products are not reported, but this EO showed antifeedant activity against <i>Spodoptera littoralis</i> . <sup>33</sup> Aerial parts were

	extracted with dichloromethane and extract showed weak antifeedant activity against <i>Spodoptera litura</i> . Extract was analyzed and detailed list of (known) compounds and structures are provided. <sup>34</sup>
Chemical composition	Isolation and characterization of new compounds have been reported. The structures of most of them are shown in Figure 4. <sup>35,36</sup> Malonate ester of compound A in Figure 4. <sup>37</sup> Isolation of known, active, interesting natural products found in this plant has been reported. <sup>38,39</sup>

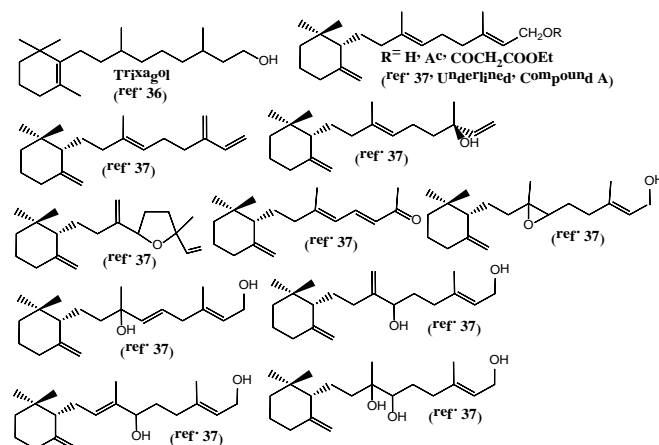


Figure 4. New compounds isolated from *Bellardia trixago*

### *Cistanche fissa*.

There are no publications relevant to this review article.

### *Cistanche salsa*

Table 3. Biological, medicinal and other properties of *Cistanche salsa*

Activity/Property	Major Findings/Reference
Analgesic	Stems were extracted with 80% aqueous ethanol, assisted with microwave radiation. Extract showed antinociceptive activity in mice, that was tested with three methods. <sup>40</sup>
Anticancer and related activities	Whole plant was extracted with 50 % aqueous ethanol, and this extract showed anti-proliferative activity against prostate cancer cells in rats. <sup>41</sup>
Bones related activities	Whole plant was extracted with methanol and extract was fractionized by several organic solvents, yielding and new compound [ <i>R</i> -HDOA, see Chemical composition below]. This compound showed anti-osteoporotic activity in mice. <sup>42</sup>
Brain related activities	Phenylethanoid glycoside-rich extracts were prepared by extracting different parts of the plant with organic solvents.

	These extracts showed activity against neurotoxicity of MPTP in mice. <sup>43-46</sup> <i>Echinacoside</i> (phenylethanoid glycoside) was isolated from stem methanolic extract, and it alleviated hypobaric hypoxia-induced memory impairment in mice. <sup>47</sup>
Hepatoprotection	Phenylethanoid-rich (mainly <i>Echinacoside</i> ) stem methanolic extract showed protective activity against ethanol-induced hepatotoxicity in mice. <sup>48</sup>
Enzyme inhibition	Whole plant was extracted with methanol and extract was chromatographed obtaining five new compounds (see Chemical composition below). These compounds inhibited the production of NO that was induced by LPS. <sup>49</sup>
Immune system related activities	Three studies that were published in the same year by the same research group, reporting immunomodulatory and immunostimulant effect of extracts of the plant. <sup>50-52</sup>
Chemical composition	<i>R</i> -HDOA (Figure 5) was isolated and its structure was confirmed by spectroscopic analyses and by laboratory synthesis of it. <sup>42</sup> Five new phenylpropanoid-substituted diglycosides were isolated (Figure 5). <sup>49</sup> Six new <i>Salsasides</i> were isolated from the stems of the plant. Their structures are presented in the review article that we cited earlier (ref. 25). <sup>53</sup> This publication did not report new compounds, but it is interesting since it presents the HPLC method of isolation of active glycosides of this plant. <sup>54</sup>

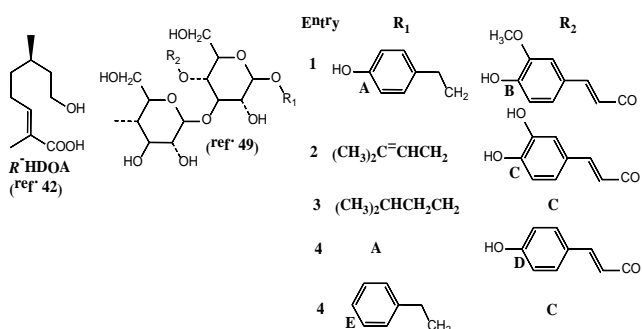


Figure 5. New compounds isolated from *Cistanche salsa*

**Cistanche tubulosa**

Table 4. Biological, medicinal and other properties of *Cistanche tubulosa*

Activity/Property	Major Findings/Reference
Anticancer and related activities	Commercial mixture of phenylethanoids that was isolated from the plant, showed activity against B16-F10 cancer cells. <sup>55</sup> Whole plant aqueous extract showed activity against human colon cancer cells. <sup>56</sup> Commercial mixture of phenylethanoids that was isolated from

	the plant, showed activity against H22 hepatocellular carcinoma cells. <sup>57</sup>
Antidiabetic, anti-hyperlipidemic	Stem ethanolic extract showed antidiabetic and hypolipidemic activities in db/db mice model. <sup>58</sup> Roots were extracted with 70 % aqueous ethanol and extract was hypocholesterolemic in mice. <sup>61</sup>
Antioxidant, anti-inflammatory	Commercial Echinacoside (Figure 6), a major compound in the extracts of the plant, and various extracts, showed antioxidant (DPPH, trolox) and anti-inflammatory activity in STZ-nicotineamide-induced diabetic rats. <sup>59</sup> Ultrasonic-assisted extraction of aerial parts yielded new polysaccharide (rhamnose, mannose, glucose, and galactose), which showed <i>in vitro</i> antioxidant activity. <sup>60</sup>
Bone, muscle, eye, growth and hair related activities	Commercial echinacoside and acteoside (Figure 6) showed anti-osteoporotic activity in rat model. <sup>62</sup> Commercial extract (no other details) showed novel eye protection against blue light emission, that was confirmed by 6 methods, <i>in vitro</i> and <i>in vivo</i> . <sup>63</sup> Stems were extracted with 30 % aqueous ethanol and this extract enhanced muscles activity, in forced immobilized rats. <sup>64</sup> Commercial mixed extract of the plant with <i>Laminaria japonica</i> , was orally (pills) administered to healthy female human who suffered hair loss and unhealthy scalp. This supplementation improved both conditions. <sup>65</sup> Stems aqueous extract was chromatographed to obtain nearly pure echinacoside, with small amount of acteoside and tubuloside A (Figure 6). This powder was fed to rats and it stimulated growth hormone, suggesting antiaging activity. <sup>66</sup>
Brain related activities	Commercial echinacoside and acteoside showed anti-Alzheimer activity in rat model. <sup>62</sup> Patented phenylethanoid glycosides pills produced from plant extract found efficient for treating moderate Alzheimer disease (AD). <sup>67</sup> Phenylethanoid glycosides-rich stem aqueous extract was showed anti-Alzheimer disease-like activity in rat model, and slowed memory loss and improved other brain functions. <sup>68</sup> Stem aqueous extract that contained mainly echinacoside, acteoside and isoacteoside (Figure 6), inhibited aggregation of amyloid-β in AD-like model in rats. <sup>69</sup> A decoction was prepared from Herb <i>Cistanche</i> , a traditional Chinese medicine, which is a mixture of <i>C. tubulosa</i> and <i>C. deserticola</i> (not included in this review). This decoction was rich with phenylethanoid glycosides, and it was supplied to rats that were exposed to



	several stress methods. The decoction showed antidepressant and cognitive improvement activities. <sup>70</sup> Aqueous extract of Herb <i>Cistanche</i> that contained mainly <i>C. tubulosa</i> , was supplied to rats that were subjected to various depression inducers. The extract showed clear antidepressant activity, confirmed by behavioral and brain chemical tests. <sup>71,72</sup> Plant nano-powder was orally supplied to rats that were exposed to various stress methods. Results showed antidepressant and neuroprotective (dopaminergic neurons) activities. <sup>73</sup>
Cardiovascular system related activities	Echinacoside and acteoside that were extracted with water from the stems of the plant, showed blood glucose lowering and hypotensive effect <i>in vitro</i> . <sup>74</sup>
Hepatoprotection	Methanolic extract from fresh stems have hepatoprotective effects against D-galactosamine/lipopolysaccharide (LPS)-induced liver injury in mice. The extract was rich with phenylethanoid glycosides and their acetyls. <sup>75</sup> Roots were extracted with 70 % aqueous ethanol, to obtain phenylethanoid glycosides-rich extract. It showed activity against hepatic fibrosis in rats. <sup>76</sup>
Nutrition, toxicity	The group that published Ref. 68 tested the safety of their capsules (Memoregain®) and found it safe. <sup>77</sup>
Reproductive system, sex	Commercial Echinacoside, and various extracts, showed steroidogenesis in STZ-nicotineamide-induced diabetic rats <sup>59</sup> Stems were extracted with 70 % aqueous ethanol and this extract enhanced sex hormone levels in rats. <sup>78</sup>
Chemical composition	Four new tubulosides were isolated and characterized. One of them, tubuloside A is shown in Figure 6. <sup>79</sup> New iridoid glycosides, kankanosides A-D, kankanol and kankanoside E (Figure 6) were isolated from the methanolic extract of dried stems. <sup>80</sup> Interesting studies of chemical composition and methods for their determination have been reported though no new compounds were detected. <sup>81-84</sup>

**Odontites aucheri**

There are no publications relevant to this review article.

**Orobanche aegyptiaca**

Whole plant aqueous extract showed hypotensive activity.<sup>85</sup>

**Orobanche cernua**

A new phenylethanoid, 3'-O-methyl isocrenatoside, was isolated from fresh whole plant and characterized (Figure 7).

This compound, along with other two known compounds were active against human lung cancer cell lines.<sup>86</sup> Stems of the plant were extracted with 70 % aqueous ethanol and this extract showed strong antioxidant activity (DPPH),<sup>87</sup> and their ethanolic extract showed protective effect against UVB-induced human skin photoaging.<sup>88</sup>

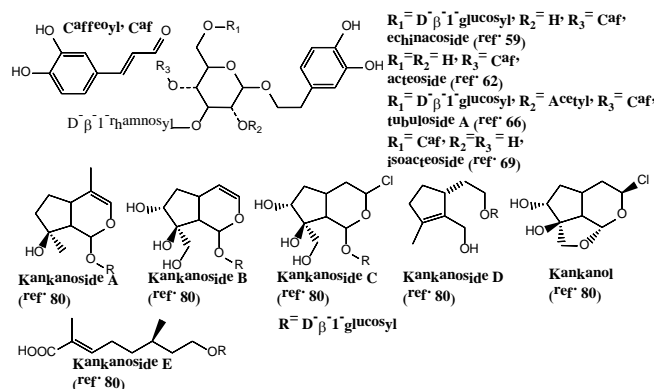


**Figure 6.** New compounds isolated from *Cistanche tubulosa*

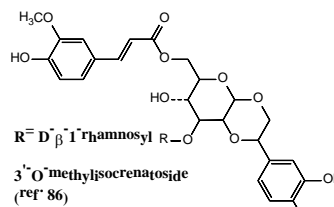


**Figure 7.** 3'-O-methyl isocrenatoside isolated from *Orobanche cernua*

**Orobanche crenata**

**Table 5.** Biological, medicinal and other properties of *Orobanche crenata*

Activity/Property	Major Findings/Reference
Analgesic	Whole plant was successively extracted with chloroform and 70 % aqueous methanol, and the organic solvent was removed. The water solution was fractionized with ethyl acetate and chloroform. The ethyl acetate fraction showed analgesic activity in hot plate method in mice. <sup>89</sup>
Antibacterial, antifungal	Acetone extract of leaves showed activity against several bacteria and fungi species. <sup>90</sup> Aerial parts were separately extracted with methanol and water. Both extracts showed antioxidant activity (DPPH, ABTS). <sup>91</sup> Leaves were extracted with 80 % aqueous methanol and extract was fractionized to obtain phenolics-rich fraction. This fraction showed activity against 8 fungi species. <sup>93</sup>
Anticancer	Methanolic extract of the plant (parts not indicated) was prepared and showed activity against several cancer cell lines. <sup>92</sup> Whole plant was successively

	extracted with <i>n</i> -hexane, ethyl acetate, acetone, methanol and water. Essential oil was also prepared. All products were tested for general chemical composition and activity against B16F10 melanoma cancer cells. <sup>94</sup>
Antioxidant	Acetone extract of leaves showed antioxidant activity (DPPH). <sup>90</sup> Aerial parts were separately extracted with methanol and water. Both extracts were tested against 18 bacteria species. Methanolic extract was active in 17 cases, but aqueous extract was not. <sup>91</sup> Methanolic extract of the plant (parts not indicated) was prepared and antioxidant activity (FRAP, DPPH) was tested. <sup>92</sup> Whole plant was successively extracted with <i>n</i> -hexane, ethyl acetate, acetone, methanol and water. Essential oil was also prepared. All products were tested for antioxidant activity (DPPH, FRAP, TEAC). <sup>94</sup>
Antispasmodic, muscles related activities	Whole plant ethyl acetate fraction (see analgesic) showed smooth muscles relaxation effect and antispasmodic activity in mice. <sup>89</sup>
Diuretic	Whole plant ethyl acetate fraction (see analgesic) showed diuretic activity in mice. <sup>89</sup>
Hypotensive	Whole plant ethyl acetate fraction (see analgesic) showed hypotensive activity in mice. <sup>89</sup>
Chemical composition	Crenatoside was isolated and characterized from aerial parts of the plant (Figure 8). <sup>95</sup>

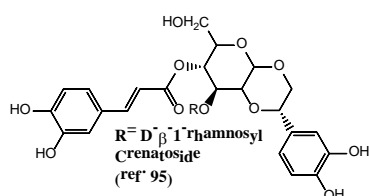


**Figure 8.** Crenatoside isolated from *Orobanche crenata*

#### *Orobanche cumana* and *Orobanche hermonis*

There are no publications relevant to this review article.

#### *Orobanche lavandulacea*

Whole plant was successively extracted with *n*-hexane, ethyl acetate, acetone, methanol and water. Essential oil was also prepared. All products were tested for general chemical composition and activity against B16F10 melanoma cancer cells.<sup>94</sup> Whole plant was successively extracted with *n*-hexane, ethyl acetate, acetone, methanol and water. Essential oil was also prepared. All products were tested for antioxidant activity (DPPH, FRAP, TEAC).<sup>94</sup>

#### *Orobanche mutellii*, *Orobanche palaestina*, *Orobanche pubescens*, *Orobanche schultzei*, and *Parentucellia flaviflora*

There are no publications relevant to this review article.

#### *Parentucellia viscosa*

Aerial parts were extracted with dichloromethane and extract showed notable antifeedant activity against *Spodoptera litura*. Extract was analyzed and detailed list of (known) compounds and structures are provided.<sup>34</sup>

General chemical composition and analysis of polar compounds in the plant, in order to compare with other plants of the *Orobanchaceae* family. New compounds are not reported, but the study confirmed the presence of known active compounds found in other plants of this family.<sup>96</sup> Other authors found a new compound, gardoside methyl ester (Figure 9).<sup>97</sup>

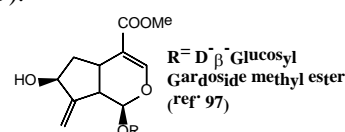


**Figure 9.** Gardoside methyl ester isolated from *Parentucellia viscosa*

## DISCUSSION

The previous section of “Medicinal activities and chemical composition” reveals a dismal picture about the medicinal and chemical research of the *Orobanchaceae* family in the reviewed region of Israel and Palestine. A minority of them was sufficiently studied and published, while the majority was not. Nine species out of 17 have no medicinal activities-type articles and their chemical composition is unknown. Some other species were very limitedly studied.

Although the *Cistanche* genus is represented by 3 species and the *Orobanche* genus by 10, the number of publications about *Cistanche* is way higher, and they are much more frequent. This is due to the massive use of *Cistanche* plants in East Asian traditional medicines, and especially, the successful medicinal formulation “*Cistanches Herba*” in Chinese traditional medicine. So, the interest of East Asian researchers in the species *Cistanche tubulosa* yielded many important publications (see previous section and discussion below).

One of the major research finding was that of the active natural products in the *Cistanche* plants and study the various conditions of growth or cultivation that affect the qualities and the quantities of these compounds in the plants. In this regard, Y. Wang *et al.* published one of the most comprehensive works.<sup>98</sup> Geographically, they sampled plants from all over the world but mainly focused on China and Mongolia. They tested the presence and concentrations of seven phenylethanoid glycosides and found several conditions that affect these compounds.

Even though *Cistanche salsa* was moderately studied for medicinal activities, its chemical composition drew major interest of researchers. On this basis, many works about its cultivation conditions were published, such as the study of X. Sun *et al.*<sup>99</sup> In addition, J-Y. Liu *et al.* developed a method to increase the production of phenylethanoid glycosides (echinacoside, acteoside, 2'-acetylacteoside) by feeding the plants with precursors such as tyrosine, phenylalanine, caffeic acid and cucumber juice.<sup>100</sup> J. Chen *et al.* reported that cultivation of the plant under administration of hydrogen peroxide, upregulated the genes responsible for the production of these important natural products, and their biosynthesis was enhanced.<sup>101</sup>

As we mentioned above, *Cistanche tubulosa* was and still extensively investigated, since it is an important ingredient of "Cistanches Herba". An early, interesting botanical study of this plant was published by T. S. Rangan and N. S. Rangaswamy, focusing on the parasitic nature of this species, and biochemical parasite-host relationship.<sup>102</sup> T. Deyama *et al.* published an outstanding work of isolation of phenylethanoid glycosides from this plant, and a comprehensive spectroscopic identification of them. Moreover, their major biological activities are presented.<sup>103</sup> S-Y. Zhao *et al.* reported that microwave processing of the plant increased the production of acteoside.<sup>104</sup> They report that this treatment activates  $\beta$ -glucosidase that hydrolyses echinacoside to acteoside, and for this purpose, several  $\beta$ -glucosidases were tested. C. Xei *et al.* developed a very efficient method (high-speed counter-current chromatography) for isolation of echinacoside and acteoside from this plant.<sup>105</sup> Y. Li *et al.* developed a unique method using ultraperformance liquid chromatography-quadrupole time-of-flight mass spectrometry to identify echinacoside metabolites, produced by human intestinal bacteria.<sup>106</sup> Q. Cui *et al.* reported the development of very similar method to identify metabolites of echinacoside and acteoside in rat plasma, bile, urine and feces.<sup>107</sup>

Attempts to achieve an increase in the amount of the important phenylethanoids found in *Cistanche tubulosa*, were not limited to growing the plant under various conditions, which promoted their production. G. Guchhait and A. K. Misra reported a short synthesis of the trisaccharide major unit in these compounds (see Figure 6).<sup>108</sup> The compound that they reported is shown in Figure 10.

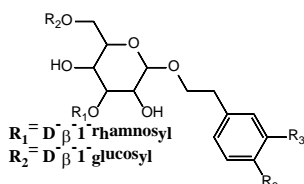


**Figure 10.** Trisaccharide prepared by Guchhait & Misra (ref. 108)

In the reported synthesis,  $R_1=R_2=H$ , meaning that the aromatic ring is not substituted in positions 3, 4. Authors claim that they prepared the core trisaccharide of Kankanoside F. But in this compound, which was first isolated by M. Yoshikawa and his colleagues, the aromatic ring is doubly hydroxylated ( $R_3=OH$ ).<sup>109</sup> Additional synthetic steps are needed to hydroxylate the aromatic ring. M. Yoshikawa and his colleagues report that these compounds (the isolated kankanosides F and G) have vasorelaxant activity. Finally, in this regard, this research

group published an excellent review article about the active natural products of *Cistanche tubulosa*.<sup>110</sup>

A detailed and relatively easy to perform synthesis of trixagol (Figure 4) found in *Bellardia trixago* was published by R. J. Armstrong and Larry Weiler.<sup>111</sup> A. F. Barrero and his colleagues published a unique report on the use of this plant for the synthesis of enantiospecific odorant products.<sup>112</sup> For example, the important natural product dihydro- $\gamma$ -ionone is present only in small amounts in *Bellardia trixago* and other plants. So, this group reported its synthesis from another natural product present in the plant in larger concentration. The synthesis is shown in Figure 11.

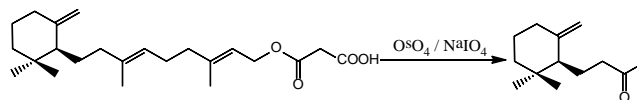


**Figure 11.** Synthesis of dihydro- $\gamma$ -ionone.

Relying on the success previous synthesis (60 % isolated yield) of dihydro- $\gamma$ -ionone, this group used that compound to prepare other natural products present in small quantities in the same plant, such as Siccanochromene F.<sup>113</sup> Finally, a comprehensive work of the synthesis and use of this compound and its closely related structures, was published by A. Barakat and his colleagues.<sup>114</sup>

Among the plants of the *Orobanchaceae* family, species of the *Orobanche* genus are more parasitic than other genera, and among these, *O. crenata* is the most aggressive.<sup>115</sup> The research of this species is ranging between two contradictions: on one hand, attempts to use it as food and utilize its medicinal properties (Table 5), and on the other hand, efforts to understand its parasitic mechanism, and develop methods to control it.

Strigolactones (Figure 3) are produced by different host plants and they play major role of growth stimulation of *O. crenata*. On this basis, I. Trabelsi and her colleagues published their research about various factors that affect the production of strigolactones, and consequently, possible methods to control *O. crenata*.<sup>116</sup> R. Matusova and her colleagues investigated the biosynthetic paths of strigolactones, and discovered the involvement of carotenoids as starting materials.<sup>117</sup>

As we mentioned earlier, there are no published studies about the medicinal/biological properties of *Orobanche cumana*. But as a harmful weed, many researches were published. One of them studied the effect of Helio lactone (Figure 12), a growth stimulant produced by sunflower (*Helianthus annuus*) on the parasitic activity of *O. crenata* and *O. cumana* (and other plants that are not included in this article).<sup>118</sup>

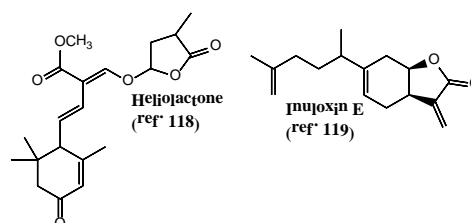


**Figure 12.** Growth stimulants of *Orobanche* plants

But not only sunflower is infected by *O. cumana*, wild plants of the same family (*Asteraceae*) are parasitized by this plant, such as *Dittrichia viscosa* (False yellowhead), that grows in the Mediterranean basin. The host-parasite relationship in this case was studied revealed that the host species produces a growth stimulant, Inuloxin E (Figure 12).<sup>119</sup>

So, *Orobanche* plant species are real challenge. Many efforts have been made to control them and the review article of S. Habimana is a good summary of these efforts of different types.<sup>120</sup> But they are also a very rich source of active natural products, that have unique structures with useful sub-units for organic synthesis. For this reason, many analytical methods were developed for their isolation and quantification. The review article of S. V. Luca and his colleagues presents the structures of the major compounds and the various methods that were developed for their isolation.<sup>121</sup>

## CONCLUSIONS

Generally, plants of the *Orobanchaceae* family in Israel and Palestine, were very limitedly studied. The medicinal and biological activities of most of these plants have never been published. These plants have parasitic activity and understanding these parasite-host relationships might result in controlling these parasites. The species that were studied are sources of unique natural products.

There is a great lack of using the isolated natural products of these plants for synthesis of new analogues and modifications, thus it is a real need to investigate the medical uses of pure compounds isolated from these unique plants.

## REFERENCES

- <sup>1</sup>McNeal, J. R., Bennett, J. R., Wolfe, A. D., Mathews, S., Phylogeny and origins of holoparasitism in *Orobanchaceae*, *Am. J. Bot.*, **2013**, *100*, 971-983. DOI: 10.3732/ajb.1200448
- <sup>2</sup>Domina, G., Danin, A., *Orobanche cohenii* (*Orobanchaceae*) a new species from Israel, *Fl. Medit.*, **2014**, *24*, 63-69. DOI: 10.7320/FIMedit24.063
- <sup>3</sup>Flora of Israel Online, *Orobanchaceae* <https://flora.org.il/en/plants/systematics/orobanchaceae/>
- <sup>4</sup>Bennett, J. R., Mathews, S., Phylogeny of the Parasitic Family *Orobanchaceae* Inferred from Phytochrome A, *Am. J. Bot.*, **2006**, *93*, 1039-1051. DOI: 10.3732/ajb.93.7.1039
- <sup>5</sup>Goyet, V., Wada, S., Cui, S., Wakatake, T., Shirasu, K., Montiel, G., Simier, P., Yoshida, S., Haustorium Inducing Factors for Parasitic *Orobanchaceae*. *Front. Plant Sci.*, **2019**, *10*, Article 1056, 8 pages. DOI: 10.3389/fpls.2019.01056
- <sup>6</sup>Goldwasser, Y., Eizenberg, H., Golan, S., Kleifeld, Y., Control of *Orobanche crenata* and *Orobanche aegyptiaca* in parsley, *Crop Prot.*, **2003**, *22*, 295-305. [https://doi.org/10.1016/S0261-2194\(02\)00152-7](https://doi.org/10.1016/S0261-2194(02)00152-7)
- <sup>7</sup>Zhang, D., Qi, J., Yue, J., Huang, J., Sun, T., Li, S., Wen, J-F., Hettenhausen, C., Wu, J., Wang, L., Zhuang, H., Wu, J., Sun, G., Root parasitic plant *Orobanchaeegyptiaca* and shoot parasitic plant *Cuscuta australis* obtained Brassicaceae-specific *strictosidine synthase*-like genes by horizontal gene transfer, *BMC Plant Biol.*, **2014**, *14*, Article 19, 14 pages. DOI: 10.1186/1471-2229-14-19
- <sup>8</sup>El-Dabaa, M. A., Ahmed, S. A., Messiha, N. K., El-Masry, R. R., The allelopathic efficiency of *Eruca sativa* seed powder in controlling *Orobanche crenata* infected *Vicia faba* cultivars, *Bull. Natl. Res. Cent.*, **2019**, *43*, Article 37, 8 pages. <https://doi.org/10.1186/s42269-019-0079-9>
- <sup>9</sup>Ilahi, I., Rehman, S., Iqbal, Z., Some studies on the mode of parasitization of *Cistanche tubulosa* on various host plants, *Pak. J. Plant Sci.*, **2009**, *15*, 1545-1552. <https://www.researchgate.net/publication/237844823>
- <sup>10</sup>Tardio, J., Santyana, M. P., Morales, R., Ethnobotanical review of wild edible plants in Spain, *Bot. J. Linn. Soc.*, **2006**, *152*, 27-71. <https://doi.org/10.1111/j.1095-8339.2006.00549.x>
- <sup>11</sup>Kumar, H., Song, S-Y., More, S. V., Kang, S-M., Kim, B-W., Kim, I-S., Choi, D-K., Traditional Korean East Asian Medicines and Herbal Formulations for Cognitive Impairment, *Molecules*, **2013**, *18*, 14670-14693. DOI: 10.3390/molecules181214670
- <sup>12</sup>Qureshi, R., Bhatti, G. R., Memon, R. A., Ethnomedicinal Uses of Herbs from Northern Part of Nara Desert, Pakistan, *Pak. J. Bot.*, **2010**, *42*, 839-851. <https://www.researchgate.net/publication/228374017>
- <sup>13</sup>Mahmood, A., Mahmood, A., Tabassum, A., Ethnomedicinal Survey of Plants from District Sialkot, Pakistan, *J. Appl. Pharm.*, **2011**, *2*, 2012-2220. <https://www.consortiumpublisher.ca/index.php/jap/article/viewFile/164/154>
- <sup>14</sup>Alamgeer, A., Younis, W., Asif, H., Sharif, A., Riaz, H., Bukhari, I. A., Assiri, A. M., Traditional medicinal plants used for respiratory disorders in Pakistan: a review of the ethno-medicinal and pharmacological evidence, *Chin. Med.*, **2018**, *13*, Article 48, 29 pages. <https://doi.org/10.1186/s13020-018-0204-y>
- <sup>15</sup>Shah, A., Poudel, R. C., Ishtiaq, M., Sarvat, R., Shahzad, H., Abbas, A., Shoaib, S., Nuzhat, R., Noor, U. D., Mahmooda, H., Summaya, A., Ifra, A., Ihsan, U., Ethnobotanical study of medicinal plants of Namal valley, Salt Range, Pakistan, *Appl. Ecol. Environ. Res.*, **2019**, *17*, 4725-4805. DOI: 10.15666/aeer/1702\_47254805
- <sup>16</sup>Salahuddin, K., Suresh, G., Manish, V., Virendra, S., Nalin, T., Ethnobotanical Survey of Some Parasitic Plants Growing in Girnar forest of Junagadh District of Gujarat, India, *Int. Res. J. Biol. Sci.*, **2013**, *2*, 59-62. <http://www.isca.in/IJBS/Archive/v2/i4/11.ISCA-IRJBS-2013-042.pdf>
- <sup>17</sup>Meragiaw, M., Asfaw, Z., Argaw, M., The Status of Ethnobotanical Knowledge of Medicinal Plants and the Impacts of Resettlement in Delanta, Northwestern Wello, Northern Ethiopia, *Evid. Based Complement. Alternat. Med.*, **2016**, Article 5060247, 24 pages. <http://dx.doi.org/10.1155/2016/5060247>
- <sup>18</sup>O'Neill, A. R., Rana, S. K., An ethnobotanical analysis of parasitic plants (Parijibi) in the Nepal Himalaya, *J. Ethnobiol. Ethnomed.*, **2016**, *12*, Article 14, 15 pages. DOI: 10.1186/s13002-016-0086-y
- <sup>19</sup>Biscotti, N., Bonsanto, D., Del Viscio, G., The traditional food use of wild vegetables in Apulia (Italy) in the light of Italian ethnobotanical literature, *Ital. Bot.*, **2018**, *5*, 1-24. DOI: 10.3897/italianbotanist.5.22297
- <sup>20</sup>Akan, H., Aydogdu, M., Korkut, M. M., Balos, M. M., An ethnobotanical research of the Kalecik mountain area (Şanlıurfa, South-East Anatolia), *Biol. Divers. Conser.*, **2013**, *6*, 84-90. <https://dergipark.org.tr/en/pub/biodicon/issue/55883/765704>
- <sup>21</sup>Shi, R., Zhang, C., Gong, X., Yang, M., Ji, M., Jiang, L., Leonti, M., Yao, R., Minhui Li, M., The genus *Orobanche* as food and medicine: An ethnopharmacological review, *J. Ethnopharmacol.*, **2020**, *263*, 113154-113174. <https://doi.org/10.1016/j.jep.2020.113154>



- <sup>22</sup>Scharenberg, F., Zidorn, C., Genuine and Sequestered Natural Products from the Genus *Orobanche* (Orobanchaceae, Lamiales), *Molecules*, **2018**, *23*, 2821-2851. DOI: 10.3390/molecules23112821
- <sup>23</sup>Wang, L-l., Ding, H., Shi, Y., Lai, Q-h., Yu, H-s., Zhang, L-j., Song, X-b., Research Progress on Chemical Constituents of *Cistanches Herba* and their Pharmacological Effects, *Chin. Herb. Med.*, **2015**, *7*, 6 pages. <http://www.tiprpress.com/chmen/article/abstract/chm20150101>
- <sup>24</sup>Li, Z., Lin, H., Gu, L., Gao, J., Tzeng, C-M., Herba *Cistanche* (Rou Cong-Rong): One of the Best Pharmaceutical Gifts of Traditional Chinese Medicine, *Front. Pharmacol.*, **2016**, *7*, Article 41, 7 pages. DOI: 10.3389/fphar.2016.00041
- <sup>25</sup>Lei, H., Wang, X., Zhang, Y., Cheng, T., Mi, R., Xu, X., Zu, X., Zhang, W., Herba *Cistanche* (Rou Cong Rong): A Review of Its Phytochemistry and Pharmacology, *Chem. Pharm. Bull.*, **2020**, *68*, 694-712. <https://doi.org/10.1248/cpb.c20-00057>
- <sup>26</sup>Jiang, Y., Tu, P-F., Analysis of chemical constituents in *Cistanche* species, *J. Chromatogr. A*, **2009**, *1216*, 1970-1799. DOI: 10.1016/j.chroma.2008.07.031
- <sup>27</sup>Gu, C., Yang, X., Huang, L., *Cistanches Herba*: A Neuropharmacology Review, *Front. Pharmacol.*, **2016**, *7*, Article 289, 10 pages. DOI: 10.3389/fphar.2016.00289
- <sup>28</sup>Wang, N., Ji, S., Zhang, H., Mei, S., Qiao, L., Jin, X., Herba *Cistanches*: Anti-aging, *Aging Dis.*, **2017**, *8*, 740-759. <http://dx.doi.org/10.14336/AD.2017.0720>
- <sup>29</sup>Al-Snafi, A. E., Bioactive Metabolites and Pharmacology of *Cistanche Tubulosa*- A Review, *IOSR J. Pharm.*, **2020**, *10*, 37-46. <https://www.researchgate.net/publication/338901804>
- <sup>30</sup>Genovese, C., D'Angeli, F., Attanasio, F., Caserta, G., Scarpaci, K. S., Nicolosi, D., Phytochemical composition and biological activities of *Orobanche crenata* Forssk.: a review, *Nat. Prod. Res.*, **2020**, *34*, 1-17. DOI: 10.1080/14786419.2020.1739042
- <sup>31</sup>Halouzka, R., Zeljkovic, S. C., Klejdus, B., Tarkowski, P., Analytical methods in strigolactone research, *Plant Methods*, **2020**, *16*, Article 76, 13 pages. <https://doi.org/10.1186/s13007-020-00616-2>
- <sup>32</sup>Tomas-Barberan, F. A., Cole, M. D., Garcia-Viguera, C., Tomas-Lorente, F., Guirado, A., Epicuticular flavonoids from *Bellardia trixago* and their antifungal fully methylated derivatives, *Int. J. Crude Drug Res.*, **1990**, *28*, 57-60. <https://doi.org/10.3109/13880209009082777>
- <sup>33</sup>Formisano, C., Rigano, D., Senatore, F., Simmonds, M. S., Bisio, A., Bruno, M., Sergio Rosselli, S., Essential oil composition and antifeedant properties of *Bellardia trixago* (L.) All. (sin. *Bartsia trixago* L.) (Scrophulariaceae), *Biochem. Syst. Ecol.*, **2008**, *36*, 454-457. DOI: 10.1016/j.bse.2007.11.003
- <sup>34</sup>Morimoto, M., Chemical defense against insects in *Heterotheca subaxillaris* and three Orobanchaceae species using exudates from trichomes, *Pest Manag. Sci.*, **2019**, *75*, 2474-2481. DOI: 10.1002/ps.5395
- <sup>35</sup>de Pascual, T. J., Caballero, C., Caballero, M., Medarde, M., Barrero, A. F., Grande, M., *Trixago*, natural  $\gamma$ -cyclogeranylgeraniol from *Bellardia trixago* (L.) all., *Tetrahedron Lett.*, **1978**, *19*, 3491-3494. DOI: 10.1016/S0040-4039(00)70554-5
- <sup>36</sup>de Pascual, T. J., Caballero, C., Caballero, M., Medarde, M., Barrero, A. F., Grande, M., Minor Components with the  $\gamma$ -cyclogeranyl Geraniol Skeleton from *Bellardia trixago* (L.) ALL., *Tetrahedron*, **1982**, *38*, 1837-1842. [https://doi.org/10.1016/0040-4020\(82\)80260-3](https://doi.org/10.1016/0040-4020(82)80260-3)
- <sup>37</sup>Barrero, A. F., Sanchez, J. F., Cuenca, F. G., Dramatic variation in diterpenoids of different populations of *Bellardia trixago*, *Phytochemistry*, **1988**, *27*, 3676-3678. [https://doi.org/10.1016/0031-9422\(88\)80795-7](https://doi.org/10.1016/0031-9422(88)80795-7)
- <sup>38</sup>Ersoz, T., Yalcin, F. N., Tasdemir, D., Sticher, O., Calis, I., Iridoid and Lignan Glucosides from *Bellardia trixago* (L.) All., *Turk. J. Med. Sci.*, **1998**, *28*, 397-400. <https://dergipark.org.tr/en/download/article-file/129923>
- <sup>39</sup>Venditti, A., Serrilli, A. M., Bianco, A., Iridoids from *Bellardia trixago* (L.) All., *Nat. Prod. Res.*, **2013**, *27*, 1413-1416. DOI: 10.1080/14786419.2012.746342
- <sup>40</sup>Kartbaeva, E. B., Donald, G. R., Sakipova, Z. B., Ibragimova, L. N., Bekbolatova, E. N., Ternynko, I. I., Fernandes, P. D., Boylan, F., Antinociceptive activity of *Cistanche salsa* stolons, growing in the Republic of Kazakhstan, *Braz. J. Pharmacog.*, **2017**, *27*, 587-591. <http://dx.doi.org/10.1016/j.bjp.2017.05.013>
- <sup>41</sup>Jeon, E., Chung, K-S., An, H-J., Anti-proliferation effects of *Cistanches salsa* on the progression of benign prostatic hyperplasia, *Can. J. Physiol. Pharmacol.*, **2016**, *94*, 104-111. <https://doi.org/10.1139/cjpp-2015-0112>
- <sup>42</sup>Yamaguchi, K., Shinohara, C., Kojima, S., Sodeoka, M., Tsuji, T., (2E,6R)-8-Hydroxy-2,6-dimethyl-2-octenoic Acid, a Novel Anti-osteoporotic Monoterpene, Isolated from *Cistanche salsa*, *Bioscience, Biotechnol. Biochem.*, **1999**, *63*, 731-735. DOI: 10.1271/bbb.63.731
- <sup>43</sup>Geng, X., Song, L., Pu, X., Tu, P., Neuroprotective Effects of Phenylethanoid Glycosides from *Cistanche salsa* against 1-Methyl-4-phenyl-1,2,3,6-tetrahydropyridine (MPTP)-Induced Dopaminergic Toxicity in C57 Mice, *Biol. Pharm. Bull.*, **2004**, *27*, 797-801. DOI: 10.1248/bpb.27.797
- <sup>44</sup>Tian, X-F., Pu, X-P., Phenylethanoid glycosides from *Cistanche salsa* inhibit apoptosis induced by 1-methyl-4-phenylpyridinium ion in neurons, *J. Ethnopharmacol.*, **2005**, *97*, 59-63. DOI: 10.1016/j.jep.2004.10.014
- <sup>45</sup>Pu, X., Song, Z., Li, Y., Tu, P., Li, H., Acteoside from *Cistanche salsa* inhibits apoptosis by 1-methyl-4-phenylpyridinium ion in cerebellar granule neurons, *Planta Med.*, **2003**, *69*, 65-66. DOI: 10.1055/s-2003-37029
- <sup>46</sup>Sheng, G., Pu, X., Lei, L., Tu, P., Li, C., Tubuloside B from *Cistanche salsa* rescues the PC12 neuronal cells from 1-methyl-4-phenylpyridinium ion-induced apoptosis and oxidative stress, *Planta Med.*, **2002**, *68*, 966-970. DOI: 10.1055/s-2002-35667
- <sup>47</sup>Zheng, H., Su, Y., Sun, Y., Tang, T., Zhang, D., He, X., Wang, J., Echinacoside alleviates hypobaric hypoxia-induced memory impairment in C57 mice, *Phytother. Res.*, **2019**, *33*, 1150-1160. <https://doi.org/10.1002/ptr.6310>
- <sup>48</sup>Wang, Y-f., Zhao, J-j., Hai, P-l., Xue, P-f., Li, H., Li, M-h., Protective Effect of Total Glycosides from *Cistanche salsa* on Experimental Liver Injury, *Nat. Prod. Res. Develop.*, **2015**, *27*, 1076-1080. DOI: 10.16333/j.1001-6880.2015.06.025 [Chinese]
- <sup>49</sup>Ahn, J., Chae, H-S., Chin, Y-W., Kim, J., Dereplication-Guided Isolation of New Phenylpropanoid-Substituted Diglycosides from *Cistanche salsa* and Their Inhibitory Activity on NO Production in Macrophage, *Molecules*, **2017**, *22*, 1138-1153. DOI: 10.3390/molecules22071138
- <sup>50</sup>Maruyama, S., Yamada, K., Tachibana, H., Immunomodulatory factors of *Cistanche salsa*, *J. Trad. Med.*, **2008**, *25*, 87-89. DOI: 10.11339/jtm.25.87
- <sup>51</sup>Maruyama, S., Shuichi Hashizume, S., Tanji, T., Yamada, K., Tachibana, H., *Cistanche salsa* Extract Enhanced Antibody Production in Human Lymph Node Lymphocytes, *Pharmacologyonline*, **2008**, *2*, 341-348. [https://pharmacologyonline.silae.it/files/archives/2008/vol2/30\\_Maruyama.pdf](https://pharmacologyonline.silae.it/files/archives/2008/vol2/30_Maruyama.pdf)
- <sup>52</sup>Maruyama, S., Akasaka, T., Yamada, K., Tachibana, H., *Cistanche salsa* extract acts similarly to protein-bound polysaccharide-K (PSK) on various types of cell lines, *J. Trad. Med.*, **2008**, *25*, 166-169. DOI: 10.11339/jtm.25.166

- <sup>53</sup>Lei, L., Jiang, Y., Liu, X-M., Tu, P-F., Wu, L-J., Chen, F-K., New Glycosides from *Cistanche salsa*. *Helvet. Chim. Acta*, **2007**, *90*, 79-85. DOI: 10.1002/hlca.200790024
- <sup>54</sup>Kartbaeva, E. B., Sakipova, Z. B., Ibragimova, L. N., Kapsalyamova, E. N., Ternynko, I. I., Compositional study of phenolic compounds of *Cistanche salsa* (*C. A. Mey*) *G.Beck*, growing in the Republic of Kazakhstan, *J. Chem. Pharmaceut. Res.*, **2015**, *7*, 120-122. <https://www.researchgate.net/publication/294733262>
- <sup>55</sup>Li, J., Li, J., Aipire, A., Gao, L., Huo, S., Luo, J., Zhang, F., Phenylethanoid Glycosides from *Cistanche tubulosa* Inhibits the Growth of B16-F10 Cells both *in Vitro* and *inVivo* by Induction of Apoptosis via Mitochondria-dependent Pathway, *J. Cancer*,**2016**, *7*, 1877-1887. DOI: 10.7150/jca.15512
- <sup>56</sup>Al-Menhali, A. S., Jameela, S. A., Latiff, A. A., Elrayess, M. A., Alsayrafi, M., Jaganjac, M., *Cistanche tubulosa* induces reactive oxygen species-mediated apoptosis of primary and metastatic human colon cancer cells, *J. Appl. Pharmaceut. Sci.*, **2017**, *7*, 39-45. DOI: 10.7324/JAPS.2017.70507
- <sup>57</sup>Yuan, P., Li, J., Aipire, A., Yang, Y., Xia, L., Wang, X., Li, Y., Jinyao Li, J., *Cistanche tubulosa* phenylethanoid glycosides induce apoptosis in H22 hepatocellular carcinoma cells through both extrinsic and intrinsic signaling pathways, *BMC Complement. Alternat. Med.*, **2018**, *18*, Article 275, 10 pages. <https://doi.org/10.1186/s12906-018-2201-1>
- <sup>58</sup>Xiong, W-T., Gu, L., Wang, C., Sun, H-X., Liu, X., Anti-hyperglycemic and hypolipidemic effects of *Cistanche tubulosa* in type 2 diabetic db/db mice, *J. Ethnopharmacol.*, **2013**, *150*, 935-945. DOI: 10.1016/j.jep.2013.09.027
- <sup>59</sup>Kong, Z-L., Johnson, A., Ko, F-C., He, J-L., Cheng, S-C., Effect of *Cistanche Tubulosa* Extracts on Male Reproductive Function in Streptozotocin–Nicotinamide-Induced Diabetic Rats, *Nutrients*, **2018**, *10*, 1562-1583. DOI: 10.3390/nu10101562
- <sup>60</sup>Zhang, W., Huang, J., Wang, W., Li, Q., Chen, Y., Feng, W., Zheng, D., Zhao, T., Mao, G., Yang, L., Wu, X., Extraction, purification, characterization and antioxidant activities of polysaccharides from *Cistanche tubulosa*, *Int. J. Biol. Macromolec.*, **2016**, *93*, 448-458. <https://doi.org/10.1016/j.ijbiomac.2016.08.079>
- <sup>61</sup>Shimoda, H., Tanaka, J., Takahara, Y., Takemoto, K., Shan, S-J., Su, M-H., The hypocholesterolemic effects of *Cistanche tubulosa* extract, a Chinese traditional crude medicine, in mice, *Am. J. Chin. Med.*, **2009**, *37*, 1125-1138. DOI: 10.1142/S0192415X09007545
- <sup>62</sup>Chen, Y., Li, Y-Q., Fang, J-Y., Li, P., Li, F., Establishment of the concurrent experimental model of osteoporosis combined with Alzheimer's disease in rat and the dual-effects of echinacoside and acteoside from *Cistanche tubulosa*, *J. Ethnopharmacol.*, **2020**, *257*, 112834-112853. DOI: 10.1016/j.jep.2020.112834
- <sup>63</sup>Wu, M-R., Lin, C-H., Ho, J-D., Hsiao, G., Cheng, Y-W., Novel Protective Effects of *Cistanche Tubulosa* Extract Against Low-Luminance Blue Light-Induced Degenerative Retinopathy, *Cell Physiol. Biochem.*, **2018**, *51*, 63-79. DOI: 10.1159/000495162
- <sup>64</sup>Kimbara, Y., Shimada, Y., Kuboyama, T., Tohda, C., *Cistanche tubulosa* (Schenk) Wight Extract Enhances Hindlimb Performance and Attenuates Myosin Heavy Chain IId/IIX Expression in Cast-Immobilized Mice, *Evid. Based Complement. Alternat. Med.*, **2019**, Article 9283171, 10 pages. <https://doi.org/10.1155/2019/9283171>
- <sup>65</sup>Seok, J., Kim, T. S., Kwon, H. J., Lee, S. P., Kang, M. H., Kim, B. J., Kim, M. N., Efficacy of *Cistanche Tubulosa* and *Laminaria Japonica* Extracts (MK-R7) Supplement in Preventing Patterned Hair Loss and Promoting Scalp Health, *Clin. Nutr. Res.*, **2015**, *4*, 124-131. <http://dx.doi.org/10.7762/cnr.2015.4.2.124>
- <sup>66</sup>Wu, C-J., Chien, M-Y., Lin, N-H., Lin, Y-C., Chen, W-Y., Chen, C-H., Tzen, J. T., Echinacoside Isolated from *Cistanche tubulosa* Putatively Stimulates Growth Hormone Secretion via Activation of the Ghrelin Receptor, *Molecules*, **2019**, *24*, 720-730, DOI: 10.3390/molecules24040720
- <sup>67</sup>Guo, O., Zhou, Y., Wang, C-J., Huang, Y-M., Lee, Y-T., Su, M-H., Lu, J., An Open-Label, Nonplacebo-Controlled Study on *Cistanche tubulosa* Glycoside Capsules (Memoregain®) for Treating Moderate Alzheimer's Disease, *Am. J. Alzheimer's Dis. Other Dement.*, **2013**, *28*, 363-370. DOI: 10.1177/1533317513488907
- <sup>68</sup>Wu, C-R., Lin, H-C., Su, M-H., Reversal by aqueous extracts of *Cistanche tubulosa* from behavioral deficits in Alzheimer's disease-like rat model: relevance for amyloid deposition and central neurotransmitter function, *BMC Complement. Alternat. Med.*, **2014**, *14*, Article 202, 11 pages. DOI: 10.1186/1472-6882-14-202
- <sup>69</sup>Chao, C-L., Huang, H-W., Huang, H-C., Chao, H-F., Yu, S-W., Su, M-H., Wang, C-J., Lin, H-C., Inhibition of Amyloid Beta Aggregation and Deposition of *Cistanche tubulosa* Aqueous Extract, *Molecules*, **2019**, *24*, 687-698, DOI: 10.3390/molecules24040687
- <sup>70</sup>Wang, D., Wang, H., Gu, L., The Antidepressant and Cognitive Improvement Activities of the Traditional Chinese Herb *Cistanche*, *Evid. Based Complement. Alternat. Med.*, **2017**, Article 3925903, 9 pages. DOI: 10.1155/2017/3925903
- <sup>71</sup>Li, Y., Peng, Y., Ma, P., Yang, H., Xiong, H., Wang, M., Peng, C., Tu, P., Li, X., Antidepressant-Like Effects of *Cistanche tubulosa* Extract on Chronic Unpredictable Stress Rats Through Restoration of Gut Microbiota Homeostasis, *Front. Pharmacol.*, **2018**, *9*, Article 967, 14 pages. DOI: 10.3389/fphar.2018.00967
- <sup>72</sup>Li, Y., Peng, Y., Ma, P., Wang, M., Peng, C., Tu, P., Li, X., *In vitro* and *in vivo* metabolism of *Cistanche tubulosa* extract in normal and chronic unpredictable stress-induced depressive rats, *J. Chromatogr. B*, **2019**, *1125*, Article 121728, 14 pages. DOI: 10.1016/j.jchromb.2019.121728
- <sup>73</sup>Xu, Q., Fan, W., Ye, S-F., Cong, Y-B., Qin, W., Chen, S-Y., Cai, J., *Cistanche tubulosa* Protects Dopaminergic Neurons through Regulation of Apoptosis and Glial Cell-Derived Neurotrophic Factor: *in vivo* and *in vitro*. *Front. Aging Neurosci.*, **2016**, *8*, Article 295, 14 pages. DOI: 10.3389/fnagi.2016.00295
- <sup>74</sup>Shimada, H., Urabe, Y., Okamoto, Y., Li, Z., Kawase, A., Morikawa, T., Tu, P., Muraoka, O., Iwaki, M., Major constituents of *Cistanche tubulosa*, echinacoside and acteoside, inhibit sodium dependent glucose cotransporter 1-mediated glucose uptake by intestinal epithelial cells, *J. Funct. Foods*, **2017**, *39*, 91-95. <https://doi.org/10.1016/j.jff.2017.10.013>
- <sup>75</sup>Morikawa, T., Pan, Y., Ninomiya, K., Imura, K., Matsuda, H., Yoshikawa, M., Yuan, D., Muraoka, O., Acylated phenylethanoid oligoglycosides with hepatoprotective activity from the desert plant *Cistanche tubulosa*, *Bioorg. Med. Chem.*, **2010**, *18*, 1882-1890. DOI: 10.1016/j.bmc.2010.01.047
- <sup>76</sup>You, S-P., Zhao, J., Ma, L., Tudimat, M., Zhang, S-L., Liu, T., Preventive effects of phenylethanol glycosides from *Cistanche tubulosa* on bovine serum albumin-induced hepatic fibrosis in rats, *DARU J. Pharmaceut. Sci.*, **2015**, *23*, Article 52, 13 pages. DOI: 10.1186/s40199-015-0135-4
- <sup>77</sup>Liao, P-L., Li, C-H., Tse, L-S., Kang, J-J., Cheng, Y-W., Safety assessment of the *Cistanche tubulosa* health food product Memoregain®: Genotoxicity and 28-day repeated dose toxicity test, *Food Chem. Toxicol.*, **2018**, *118*, 581-588. <https://doi.org/10.1016/j.fct.2018.06.012>
- <sup>78</sup>Wang, T., Chen, C., Yang, M., Deng, B., Kirby, G. M., Zhang, X., *Cistanche tubulosa* ethanol extract mediates rat sex hormone levels by induction of testicular steroidogenic enzymes, *Pharmaceut. Biol.*, **2016**, *54*, 481-487. DOI: 10.3109/13880209.2015.1050114
- <sup>79</sup>Kobayashi, H., Ogushi, H., Takizawa, N., Miyase, T., Ueno, A., Usmanghani, K., Ahmad, M., New Phenylethanoid Glycosides from *Cistanche tubulosa* (SCHRENK) HOOK. f.

- I., *Chem. Pharm. Bull.*, **1987**, *35*, 3309-3314. DOI: 10.1248/cpb.35.3309
- <sup>80</sup>Xie, H., Morikawa, T., Matsuda, H., Nakamura, S., Muraoka, O., Yoshikawa, M., Monoterpane Constituents from *Cistanche tubulosa* - Chemical Structures of Kankanosides A-E and Kankanol, *Chem. Pharm. Bull.*, **2006**, *54*, 669-675. <https://doi.org/10.1248/cpb.54.669>
- <sup>81</sup>Cai, H., Bao, Z., Jiang, Y., Wang, X.-y., Fan, X.-t., Aierken, M., Tu, P.-f., Study on processing method of *Cistanche tubulosa*, *Chin. J. Chin. Mater. Med.*, **2007**, *32*, 1289-1291. [Chinese] <https://pubmed.ncbi.nlm.nih.gov/17879727>
- <sup>82</sup>Zheng, S., Jiang, X., Wu, L., Wang, Z., Huang, L., Chemical and Genetic Discrimination of *Cistanche* Herba Based on UPLC-QTOF/MS and DNABarcoding, *PLOS ONE*, **2014**, *9*, Article e98061, 11 pages. DOI: 10.1371/journal.pone.0098061
- <sup>83</sup>Wang, X., Wang, X., Guo, Y., Rapidly Simultaneous Determination of Six Effective Components in *Cistanche tubulosa* by Near Infrared Spectroscopy, *Molecules*, **2017**, *22*, 843-851. DOI: 10.3390/molecules22050843
- <sup>84</sup>Pei, W., Guo, R., Zhang, J., Li, X., Extraction of Phenylethanoid Glycosides from *Cistanche tubulosa* by High-Speed Shearing Homogenization Extraction, *J. AOAC Int.*, **2019**, *102*, 63-68. <https://doi.org/10.5740/jaoacint.18-0039>
- <sup>85</sup>Sharaf, A., Youssef, M., Pharmacologic investigation on *Orobanchaegyptiac* with a special study on its hypotensive action, *Plant Food Hum. Nutr.*, **1971**, *20*, 255-269. <https://doi.org/10.1007/BF01104902>
- <sup>86</sup>Qu, Z.-y., Zhang, Y.-w., Zheng, S.-W., Yao, C.-l., Jin, Y.-p., Zheng, P.-h., Sun, C.-h., Wang, Y.-p., A new phenylethanoid glycoside from *Orobancha cernua* Loefling, *Nat. Prod. Res.*, **2016**, *30*, 948-953. DOI: 10.1080/14786419.2015.1084305
- <sup>87</sup>Bai, Z. F., Lu, J. K., Wang, X. Q., Liu, Y., Anti-oxidant Properties of Extracts from *Orobancha cernua* var. *Cumana*. *Chin. J. Exp. Trad. Med. Formulae*, **2012**, *18*, 232-235. [http://en.cnki.com.cn/Article\\_en/CJFDTOTAL-ZSFX201218070.htm](http://en.cnki.com.cn/Article_en/CJFDTOTAL-ZSFX201218070.htm)
- <sup>88</sup>Gao, W., Wang, Y.-S., Qu, Z.-Y., Hwang, E., Ngo, H. T., Wang, Y.-P., Bae, J., Yi, T.-H., *Orobancha cernua* Loefling Attenuates Ultraviolet B-mediated Photoaging in Human Dermal Fibroblasts, *Photochem. Photobiol.*, **2018**, *94*, 733-743. DOI: 10.1111/php.12908
- <sup>89</sup>EI-Shabrawy, O. A., Melek, F. R., Ibrahim, M., Radwan, A. S., Pharmacological Evaluation of the Glycosidated Phenylpropanoids Containing Fraction from *Orobancha crenata*, *Arch. Pharm. Res.*, **1989**, *12*, 22-25. <http://www.koreascience.or.kr/article/JAKO198903038898508.pub>
- <sup>90</sup>Genovese, C., Acquaviva, R., Ronsisvalle, S., Tempera, G., Malfa, G. A., D'Angeli, F., Ragusa, S., Nicolosi, D., *In vitro* evaluation of biological activities of *Orobancha crenata* Forssk. leaves extract, *Nat. Prod. Res.*, **2019**, *33*, 1-5. DOI: 10.1080/14786419.2018.1552697
- <sup>91</sup>Abbes, Z., El Abed, N., Amri, M., Kharrat, M., Ben Hadj, S. A., Antioxidant and Antibacterial Activities of the Parasitic Plants *Orobancha foetida* and *Orobancha crenata* Collected on Faba Bean in Tunisia, *J. Anim. Plant Sci.*, **2014**, *24*, 310-314. <https://www.researchgate.net/publication/264310780>
- <sup>92</sup>Hegazy, M. G., Imam, A. A., Abdelghany, B. E., Evaluation of cytotoxic and anticancer effect of *Orobancha crenata* methanolic extract on cancer cell lines, *Tumor Biol.*, **2020**, *42*, 1-11. DOI: 10.1177/1010428320918685
- <sup>93</sup>Gatto, M. A., Sanzani, S. M., Tardia, P., Linsalata, V., Perialice, M., Sergio, L., Di Venere, D., Antifungal activity of total and fractionated phenolic extracts from two wild edible herbs, *Nat. Sci.*, **2013**, *5*, 895-902. DOI: 10.4236/ns.2013.58108
- <sup>94</sup>Ben Attia, I., Zucca, P., Marincola, F. C., Nieddu, M., Piras, A., Rosa, A., Rescigno, A., Chaieb, M., Evaluation of the Antioxidant and Cytotoxic Activities on Cancer Cell Line of Extracts of Parasitic Plants Harvested in Tunisia, *Pol. J. Food Nutr. Sci.*, **2020**, *70*, 253-263. DOI: 10.31883/pjfn/122040
- <sup>95</sup>Afifi, M. S., Lahloub, M. F., el-Khayaat, S. A., Anklin, C. G., Ruegger, H., Sticher, O., Crenatoside: a novel phenylpropanoid glycoside from *Orobancha crenata*, *Planta Med.*, **1993**, *59*, 59-62. DOI: 10.1055/s-2006-959701
- <sup>96</sup>Venditti, A., Ballero, M., Serafini, M., Bianco, A., Polar compounds from *Parentucellia viscosa* (L.) Caruel from Sardinia, *Nat. Prod. Res.*, **2015**, *29*, 602-606. DOI: 10.1080/14786419.2014.973409
- <sup>97</sup>Bianco, A., Passacantilli, P., Righi, G., Nicoletti, M., Iridoid glucosides from *Parentucellia viscosa*, *Phytochemistry*, **1985**, *24*, 1843-1845. DOI: 10.1016/s0031-9422(00)82566-2
- <sup>98</sup>Wang, Y., Zhang, L., Du, Z., Pei, J., Huang, L., Chemical Diversity and Prediction of Potential Cultivation Areas of *Cistanche* Herbs, *Sci. Rep.*, **2019**, *9*, Article 19737, 13 pages. <https://doi.org/10.1038/s41598-019-56379-x>
- <sup>99</sup>Sun, X., Pei, J., Lin, Y., Li, B., Zhang, L., Ahmad, B., Huang, L., Revealing the impact of the environment on *Cistanche salsa*: from global ecological regionalization to soil microbial community characteristics, *J. Agric. Food Chem.*, **2020**, *68*, 8720-8731. <https://doi.org/10.1021/acs.jafc.0c01568>
- <sup>100</sup>Liu, J.-Y., Guo, Z.-G., Zeng, Z.-L., Improved accumulation of phenylethanoid glycosides by precursor feeding to suspension culture of *Cistanche salsa*, *Biochem. Eng. J.*, **2007**, *33*, 88-93. <https://doi.org/10.1016/j.bej.2006.09.002>
- <sup>101</sup>Chen, J., Yan, Y.-X., Guo, Z.-G., Identification of hydrogen peroxide responsive ESTs involved in phenylethanoid glycoside biosynthesis in *Cistanche salsa* cell culture, *Biol. Plantarum*, **2015**, *59*, 695-700. DOI: 10.1007/s10535-015-0541-y
- <sup>102</sup>Rangan, T. S., Rangaswamy, N. S., Morphogenic investigations on parasitic angiosperms. I. *Cistanche tubulosa* (Orobanchaceae) *Can. J. Bot.*, **1968**, *46*, 263-266. <https://doi.org/10.1139/b68-043>
- <sup>103</sup>Deyama, T., Kobayashi, H., Nishibe, S., Tu, P., Isolation, structure elucidation and bioactivities of phenylethanoid glycosides from *Cistanche*, *Forsythia* and *Plantago* plants, *Stud. Nat. Prod. Chem.*, **2006**, *33*, 645-674. <https://kundoc.com/pdf-isolation-structure-elucidation-and-bioactivities-of-phenylethanoid-glycosides-f.html>
- <sup>104</sup>Zhao, S.-Y., He, X.-Y., Jia, B.-G., Peng, Q.-Y., Liu, X., Production of acteoside from *Cistanche tubulosa* by  $\beta$ -glucosidase, *Pak. J. Pharm. Sci.*, **2011**, *24*, 135-141. <https://pubmed.ncbi.nlm.nih.gov/21454161>
- <sup>105</sup>Xie, C., Xu, X., Liu, Q., Xie, Z., Yang, M., Huang, J., Yang, D., Isolation and purification of echinacoside and acteoside from *cistanche tubulosa* (Schrenk) wight by high-speed counter-current chromatography, *J. Liq. Chromatogr. Relat. Technol.*, **2012**, *35*, 2602-2609. DOI: 10.1080/10826076.2011.63727
- <sup>106</sup>Li, Y., Zhou, G., Xing, S., Tu, P., Li, X., Identification of Echinacoside Metabolites Produced by Human Intestinal Bacteria Using Ultraperformance Liquid Chromatography-Quadrupole Time-of-Flight Mass Spectrometry, *J. Agric. Food Chem.*, **2015**, *63*, 6764-6771. DOI: 10.1021/acs.jafc.5b02881
- <sup>107</sup>Cui, Q., Pan, Y., Bai, X., Zhang, W., Chen, L., Liu, X., Systematic characterization of the metabolites of echinacoside and acteoside from *Cistanche tubulosa* in rat plasma, bile, urine and feces based on UPLC-ESI-Q-TOF-MS, *Biomed. Chromatogr.*, **2016**, *30*, 1406-1415. DOI: 10.1002/bmc.3698
- <sup>108</sup>Guchhait, G., Misra, A. K., Short synthesis of the common trisaccharide core of kankanose and kankanoside isolated from *Cistanche tubulosa*, *Beilstein J. Org. Chem.*, **2013**, *9*, 705-709. DOI: 10.3762/bjoc.9.80
- <sup>109</sup>Yoshikawa, M., Matsuda, H., Morikawa, T., Xie, H., Nakamura, S., Muraoka, O., Phenylethanoid oligoglycosides and acylated oligosugars with vasorelaxant activity from



- Cistanche tubulosa*, *Bioorg. Med. Chem.*, **2006**, *14*, 7468-7475. DOI: 10.1016/j.bmc.2006.07.018
- <sup>110</sup>Morikawa, T., Xie, H., Pan, Y., Ninomiya, K., Yuan, D., Jia, X., Yoshikawa, M., Nakamura, S., Matsuda, H., Muraoka, O., A Review of Biologically Active Natural Products from a Desert Plant *Cistanche tubulosa*, *Chem. Pharm. Bull.*, **2019**, *67*, 675-689. DOI: 10.1248/cpb.c19-00008
- <sup>111</sup>Armstrong, R. J., Weiler, L., Synthesis of (±)-trixagol by an electrophilic cyclization of an allylsilane, *Can. J. Chem.*, **2011**, *61*, 2530-2539. DOI: 10.1139/v83-436
- <sup>112</sup>Barrero, A. F., Herrador, M. M., Arteaga, P., Castillo, A., Arteaga, A. F., Use of the Plant *Bellardia trixago* for the Enantiospecific Synthesis of Odorant Products, *Nat. Prod. Commun.*, **2011**, *6*, 439-442. <https://doi.org/10.1177/1934578X1100600403>
- <sup>113</sup>Castillo, A., Silva, L., Briones, D., Quílez del Moral, J. F., Barrero, A. F., Collective Synthesis of Natural Products Sharing the Dihydro- $\gamma$ -Ionone Core, *Eur. J. Org. Chem.*, **2015**, *15*, 3266-3273. DOI: 10.1002/ejoc.201500208
- <sup>114</sup>Barakat, A., Al-Majid, A. M., Mabkhot, Y. N., Al-Othman, Z. A., A Practical Chemo-enzymatic Approach to Highly Enantio-Enriched 10-Ethyl-7,8-dihydro- $\gamma$ -ionone Isomers: A Method for the Synthesis of 4,5-Didehydro- $\alpha$ -Ionone, *Int. J. Mol. Sci.*, **2012**, *13*, 5542-5553. DOI: 10.3390/ijms13055542
- <sup>115</sup>Fernandez-Aparicio, M., Flores, F., Rubiales, D., The Effect of *Orobancha crenata* Infection Severity in Faba Bean, Field Pea, and Grass Pea Productivity, *Front. Plant Sci.*, **2016**, *7*, Article 1409, 8 pages. DOI: 10.3389/fpls.2016.01409
- <sup>116</sup>Trabelsi, I., Yoneyama, K., Abbes, Z., Amri, M., Xie, X., Kisugi, T., Kim, H. I., Kharrat, M., Yoneyama, K., Characterization of strigolactones produced by *Orobancha foetida* and *Orobancha crenata* resistant faba bean (*Vicia faba* L.) genotypes and effects of phosphorous, nitrogen, and potassium deficiencies on strigolactone production. *S. Afr. J. Bot.*, **2017**, *108*, 15-22. <http://dx.doi.org/10.1016/j.sajb.2016.09.009>
- <sup>117</sup>Matusova, R., Rani, K., Verstappen, F. W., Franssen, M. C., Beale, M. H., Bouwmeester, H. J., The Strigolactone Germination Stimulants of the Plant-Parasitic *Striga* and *Orobancha* spp. Are Derived from the Carotenoid Pathway, *Plant Physiol.*, **2005**, *139*, 920-934. DOI: 10.1104/pp.105.061382
- <sup>118</sup>Ueno, K., Furumoto, T., Umeda, S., Mizutani, M., Takikawa, H., Batchvarova, R., Sugimoto, Y., Heliolactone, a non-sesquiterpene lactone germination stimulant for root parasitic weeds from sunflower, *Phytochemistry*, **2014**, *108*, 122-128. DOI: 10.1016/j.phytochem.2014.09.018
- <sup>119</sup>Masi, M., Fernandez-Aparicio, M., Zatout, R., Boari, A., Cimmino, A., Evidente, A., Inuloxin E, a New Seco-Eudesmanolide Isolated from *Dittrichia viscosa*, Stimulating *Orobancha cumana* Seed Germination, *Molecules*, **2019**, *24*, 3479-3489, DOI: 10.3390/molecules24193479
- <sup>120</sup>Habimana, S., Nduwumuremyi, A., Chinama R. J., Management of *orobanche* in field crops- A review, *J. Soil Sci. Plant Nutr.*, **2014**, *14*, 43-62. DOI: 10.4067/S0718-95162014005000004
- <sup>121</sup>Luca, S. V., Miron, A., Ignatova, S., Skalicka-Wozniak, K., An overview of the two-phase solvent systems used in the countercurrent separation of phenylethanoidglycosides and iridoids and their biological relevance, *Phytochem. Rev.*, **2019**, *18*, 377-403. DOI: 10.1007/s11101-019-09599-y

Received: 10.11.2020.

Accepted: 08.12.2020.





# SYNTHESIS OF 5-SUBSTITUTED-1,3,4-OXADIAZOLE CLUBBED PYRAZOLE AND DIHYDROPYRIMIDINE DERIVATIVES AS POTENT BIOACTIVE AGENTS

Bonny Y. Patel,<sup>[a]\*</sup> Tushar J. Karkar<sup>[b]</sup> and Malay J. Bhatt<sup>[c]</sup>

**Keywords:** Pyrazole; 3,4-dihydropyrimidin-2(1H)-one; 1,3,4-Oxadiazole; Antimicrobial; Antitubercular; MIC.

A series of 4-fluorophenylpyrazole clubbed 1,3,4-oxadiazole and 3,4-dihydropyrimidin-2(1H)-ones were prepared by cyclization of Biginelli-type adducts. Their structures were assigned on the basis of known spectral techniques. All the scaffolds were evaluated for *in vitro* antimicrobial activity by broth microdilution bioassay method and *in vitro* antitubercular property by microplate alamar blue assay method. Compounds **3j** and **3l** containing -OH and -CH<sub>3</sub> groups were found to act as potent antimicrobials and antitubercular candidates with relatively low cytotoxicity on VERO cells.

\* Corresponding Authors

E-Mail: bonny.y.patel@gmail.com

[a] Department of Chemistry, School of Science, RK University, Rajkot, 360020, Gujarat, India

[b] C.B. Patel Computer & J. N. M Patel Science College (DRB), Bharthana (Vesu), New City Light Road, Surat, Gujarat, India

[c] HVHP Institute of Post Graduate Studies and Research, Sarva Vidyalaya Campus, Near Railway Station, Kadi, Gujarat, India

Recognizing these particulars and our continuing endeavours toward the development of bioactive agents,<sup>20-22</sup> emphasis is given to the development of new prototypes as potent antimicrobial as well as antitubercular molecules. These include the lead of the three medicinally important pharmacophores - DHPMs, pyrazole and 1,3,4-oxadiazole in one hybrid molecular framework.

## INTRODUCTION

Resistance of microbes is a major hurdle for the treatment of several infectious diseases. The WHO has considered antimicrobial drug resistance (AMR) to be one of the utmost threats to human life. The structural modifications in existing drugs have shown astonishing results in the field of drug discovery programs. In view of this, novel scaffold architecture by molecular hybridization approach is considered as the best tool for the development of newer potent agents.<sup>1,2</sup> Nowadays, Biginelli type reaction has captured the attention of numbers of medicinal chemists for dihydropyrimidines (DHPMs) synthesis having varied bioactivity.<sup>3-5</sup> Pyrazoles engage a diverse alcove in synthetic heterocycles as a chief motif in medicinal chemistry because of their wide array of biological effects, including antimicrobial, antidepressant, anticonvulsant, antipyretic, anti-influenza and anticancer activities.<sup>6-8</sup> Various catalysts such as Sc(OTf)<sub>3</sub>, Mg(ClO<sub>4</sub>)<sub>2</sub> and H<sub>2</sub>SO<sub>4</sub> were used to synthesize pyrazole derivatives in multicomponent reaction.<sup>9-11</sup>

In recent years, oxadiazole is a frequently utilized pharmacophore due to its metabolic profile and capability to engage in hydrogen bonding with the receptor site. The presence of azole group in oxadiazole uplifts lipophilicity and influences the easy ability of the drug to target leads to generate numerous biological activities like hypoglycaemic, anti-HIV, analgesic, anti-inflammatory, antitubercular.<sup>12,13</sup> Oxadiazole have displayed remarkable inhibitory potential against important biological targets like tyrosinase, monoamine oxidase (MAO) and cathepsin K.<sup>14-19</sup>

## EXPERIMENTAL

The required chemicals were purchased from Aldrich and E. Merck and used without further purification. Buchi Rotavapor was used for distillation. Melting points were determined in the Gallenkamp apparatus and are uncorrected. The completion of the reaction and the purity of all compounds was checked on aluminum-coated TLC plates G60, F<sub>245</sub> (E. Merck) using hexane and ethyl acetate (7:3) as eluent and visualized under UV light (λ 254 and 365 nm), or iodine vapor. Elemental analysis was carried out by a Perkin-Elmer 2400 CHN analyzer. <sup>1</sup>H NMR spectra were recorded on a Bruker Avance II 400 MHz and <sup>13</sup>C NMR spectra on Varian Mercury-400, 100 MHz in DMSO-*d*<sub>6</sub> as a solvent and TMS as a reference standard for chemical shifts. IR spectra were recorded on a Perkin-Elmer FT-IR spectrophotometer, while mass spectra were scanned on a Shimadzu LCMS 2010 spectrometer.

### Ethyl-4-(3-(4-fluorophenyl)-1-phenyl-1H-pyrazol-4-yl)-6-methyl-2-oxo-1,2,3,4-tetrahydropyrimidine-5-carboxylate (1)

Compound **1** was prepared according to the literature method.<sup>23</sup>

### 4-(3-(4-Fluorophenyl)-1-phenyl-1H-pyrazol-4-yl)-6-methyl-2-oxo-1,2,3,4-tetrahydro-pyrimidine-5-carbohydrazide (2)

Compound **1** (0.01 mol) was dissolved in 1,4-dioxane (20 mL) and to this, hydrazine hydrate (99 %, 0.01 mol) was added, followed by the addition of a catalytic amount of

conc. H<sub>2</sub>SO<sub>4</sub> and allowed to stir for 5 h at 100 °C. After cooling, the reaction mixture was poured into ice-cold water. Product, obtained as off-white precipitate, was filtered, washed with water, dried and recrystallized from ethanol (95 %) to obtain compound **2**.

Yield: 73 %, m.p. 224-225 °C. IR (KBr): 3454, 3340 (N-H), 3060 (C-H<sub>arom</sub>), 1689 (C=O), 1582 (C=N), 1512 (C=C), 1124 (C-F) cm<sup>-1</sup>. <sup>1</sup>H NMR (400 MHz, DMSO-*d*<sub>6</sub>, δ ppm): 1.95 (s, 2H, NH<sub>2</sub>), 2.34 (s, 3H, -CH<sub>3</sub>), 5.16 (s, 1H, CH<sub>pyrimidine</sub>), 5.87 (s, 1H, -NHNH<sub>2</sub>), 6.91 (s, 1H, NH-C-Ph), 7.30-7.89 (m, 10H, Ar-H), 9.03 (s, 1H, NH-C-CH<sub>3</sub>). <sup>13</sup>C NMR (100 MHz, DMSO-*d*<sub>6</sub>, δ ppm): 17.9 (-CH<sub>3</sub>), 50.6 (-CH<sub>pyrimidine</sub>), 123.3 (-CH<sub>pyrazole</sub>), 118.5-149.1 (Ar-C), 150.3 (C=O, NHCONH), 166.2 (C=O). LCMS (ESI) *m/z*: 406.16 [M]<sup>+</sup>. Anal. calcd. for C<sub>21</sub>H<sub>19</sub>FN<sub>6</sub>O<sub>2</sub>: C, 62.06; H, 4.71; N, 20.68. Found: C, 62.00; H, 4.62; N, 20.73 %.

**General procedure of synthesis of 4-(3-(4-fluorophenyl)-1-phenyl-1H-pyrazol-4-yl)-6-methyl-5-(5-aryl-1,3,4-oxadiazol-2-yl)-3,4-dihydro-2(1H)-ones (3a-o)**

Compound **2** (0.01 mol) with various derivatives of aromatic acids (0.01 mol) were dissolved and stirred in one pot having phosphoryl chloride (POCl<sub>3</sub>) (20 mL). The mixture was refluxed at 80 °C for 6 h. After completion of the reaction (TLC), the mixture was slowly quenched on crushed ice. The precipitates were filtered, washed with NaHCO<sub>3</sub> to remove excess POCl<sub>3</sub> trace followed by water, dried and recrystallized from ethanol (95 %) to furnish final compounds.

**4-(3-(4-Fluorophenyl)-1-phenyl-1H-pyrazol-4-yl)-6-methyl-5-(5-phenyl-1,3,4-oxadiazol-2-yl)-3,4-dihydro-2(1H)-one (3a)**

Yield: 71 %, m.p. 241-242 °C. IR (KBr): 3223 (NH), 3061 (C-H<sub>arom</sub>), 2983 (H-C=C<), 2848 (C-H, CH<sub>3</sub>), 1685 (C=O), 1598 (C=N), 1527 (C=C), 1281 (C-O-C), 1122 (C-F) cm<sup>-1</sup>. <sup>1</sup>H NMR (400 MHz, DMSO-*d*<sub>6</sub>, δ ppm): 2.36 (s, 3H, -CH<sub>3</sub>), 5.18 (s, 1H, CH<sub>pyrimidine</sub>), 6.88 (s, 1H, NH-C-Ph), 7.28-8.06 (m, 14H, Ar-H), 8.14 (s, 1H, CH<sub>pyrazole</sub>), 9.10 (s, 1H, NH-C-CH<sub>3</sub>). <sup>13</sup>C NMR (100 MHz, DMSO-*d*<sub>6</sub>, δ ppm): 15.1 (-CH<sub>3</sub>), 53.6 (C<sub>pyrimidine</sub>), 123.2 (C<sub>pyrazole</sub>), 113.5-149.5 (Ar-C), 150.4 (C=O), 160.3, 164.1 (C<sub>oxadiazole</sub>), 161.6 (C-F). LCMS (ESI) *m/z*: 492.17 [M]<sup>+</sup>. Anal. calcd. for C<sub>29</sub>H<sub>21</sub>FN<sub>6</sub>O<sub>2</sub>: C, 68.28; H, 4.30; N, 17.06. Found: C, 68.19; H, 4.41; N, 17.11 %.

**5-(5-(2-Chlorophenyl)-1,3,4-oxadiazol-2-yl)-4-(3-(4-fluorophenyl)-1-phenyl-1H-pyrazol-4-yl)-6-methyl-3,4-dihydro-2(1H)-one (3b)**

Yield: 65 %, m.p. 218-220 °C. IR (KBr): 3221 (NH), 3062 (C-H<sub>arom</sub>), 2981 (H-C=C<), 2850 (C-H, CH<sub>3</sub>), 1691 (C=O), 1597 (C=N), 1514 (C=C), 1288 (C-O-C), 1107 (C-F), 754 (C-Cl) cm<sup>-1</sup>. <sup>1</sup>H NMR (400 MHz, DMSO-*d*<sub>6</sub>, δ ppm): 2.28 (s, 3H, -CH<sub>3</sub>), 5.18 (s, 1H, CH<sub>pyrimidine</sub>), 6.89 (s, 1H, NH-C-Ph), 7.28-8.20 (m, 13H, Ar-H), 8.28 (s, 1H, CH<sub>pyrazole</sub>), 9.16 (s, 1H, NH-C-CH<sub>3</sub>). <sup>13</sup>C NMR (100 MHz, DMSO-*d*<sub>6</sub>, δ ppm): 15.2 (CH<sub>3</sub>), 53.5 (C<sub>pyrimidine</sub>), 123.6 (C<sub>pyrazole</sub>), 135.3 (C-Cl), 113.2-149.7 (Ar-C), 150.6 (C=O), 160.1, 164.4 (C<sub>oxadiazole</sub>), 161.4 (C-F). LCMS (ESI) *m/z*: 526.13 [M]<sup>+</sup>. Anal. calcd. for

C<sub>28</sub>H<sub>20</sub>ClFN<sub>6</sub>O<sub>2</sub>: C, 68.82; H, 3.83; N, 15.95. Found: C, 63.79; H, 3.85; N, 15.93 %.

**5-(5-(3-Chlorophenyl)-1,3,4-oxadiazol-2-yl)-4-(3-(4-fluorophenyl)-1-phenyl-1H-pyrazol-4-yl)-6-methyl-3,4-dihydro-2(1H)-one (3c)**

Yield: 59 %, m.p. 186-188 °C. IR (KBr): 3222 (NH), 3063 (C-H<sub>arom</sub>), 2980 (H-C=C<), 2852 (C-H, CH<sub>3</sub>), 1691 (C=O), 1599 (C=N), 1517 (C=C), 1280 (C-O-C), 1110 (C-F), 754 (C-Cl) cm<sup>-1</sup>. <sup>1</sup>H NMR (400 MHz, DMSO-*d*<sub>6</sub>, δ ppm): 2.30 (s, 3H, -CH<sub>3</sub>), 5.16 (s, 1H, CH<sub>pyrimidine</sub>), 6.85 (s, 1H, NH-C-Ph), 7.29-8.16 (m, 13H, Ar-H), 8.24 (s, 1H, CH<sub>pyrazole</sub>), 9.15 (s, 1H, NH-C-CH<sub>3</sub>). <sup>13</sup>C NMR (100 MHz, DMSO-*d*<sub>6</sub>, δ ppm): 15.0 (CH<sub>3</sub>), 53.3 (C<sub>pyrimidine</sub>), 123.4 (C<sub>pyrazole</sub>), 135.2 (C-Cl), 113.3-149.5 (Ar-C), 150.7 (C=O), 160.3, 164.6 (C<sub>oxadiazole</sub>), 161.2 (C-F). LCMS (ESI) *m/z*: 526.13 [M]<sup>+</sup>. Anal. calcd. for C<sub>28</sub>H<sub>20</sub>ClFN<sub>6</sub>O<sub>2</sub>: C, 68.82; H, 3.83; N, 15.95. Found: C, 63.90; H, 3.80; N, 15.85 %.

**5-(5-(4-Chlorophenyl)-1,3,4-oxadiazol-2-yl)-4-(3-(4-fluorophenyl)-1-phenyl-1H-pyrazol-4-yl)-6-methyl-3,4-dihydro-2(1H)-one (3d)**

Yield: 63 %, m.p. 225-227 °C. IR (KBr): 3293 (NH), 3066 (C-H<sub>arom</sub>), 2978 (H-C=C<), 2929 (C-H, CH<sub>3</sub>), 1680 (C=O), 1591 (C=N), 1504 (C=C), 1219 (C-O-C), 1155 (C-F), 752 (C-Cl) cm<sup>-1</sup>. <sup>1</sup>H NMR (400 MHz, DMSO-*d*<sub>6</sub>, δ ppm): 2.31 (s, 3H, CH<sub>3</sub>), 5.26 (s, 1H, CH<sub>pyrimidine</sub>), 6.82 (s, 1H, NH-C-Ph), 7.20-8.05 (m, 13H, Ar-H), 8.16 (s, 1H, CH<sub>pyrazole</sub>), 9.04 (s, 1H, NH-C-CH<sub>3</sub>). <sup>13</sup>C NMR (100 MHz, DMSO-*d*<sub>6</sub>, δ ppm): 15.3 (CH<sub>3</sub>), 53.9 (C<sub>pyrimidine</sub>), 123.8 (C<sub>pyrazole</sub>), 135.6 (C-Cl), 113.0-149.7 (Ar-C), 150.5 (C=O), 160.6, 164.4 (C<sub>oxadiazole</sub>), 161.7 (C-F). LCMS (ESI) *m/z*: 526.13 [M]<sup>+</sup>. Anal. calcd. for C<sub>28</sub>H<sub>20</sub>ClFN<sub>6</sub>O<sub>2</sub>: C, 68.82; H, 3.83; N, 15.95. Found: C, 63.75; H, 3.86; N, 15.89 %.

**4-(3-(4-Fluorophenyl)-1-phenyl-1H-pyrazol-4-yl)-6-methyl-5-(5-(2-nitrophenyl)-1,3,4-oxadiazol-2-yl)-3,4-dihydro-2(1H)-one (3e)**

Yield: 58 %, m.p. 233-235 °C. IR (KBr): 3224 (NH), 3063 (C-H<sub>arom</sub>), 2981 (H-C=C<), 2862 (C-H, CH<sub>3</sub>), 1687 (C=O), 1606 (C=N), 1531 (C=C), 1508 (-N=O), 1234 (C-O-C), 1150 (C-F) cm<sup>-1</sup>. <sup>1</sup>H NMR (400 MHz, DMSO-*d*<sub>6</sub>, δ ppm): 2.37 (s, 3H, CH<sub>3</sub>), 5.20 (s, 1H, CH<sub>pyrimidine</sub>), 6.85 (s, 1H, NH-C-Ph), 7.22-8.15 (m, 13H, Ar-H), 8.20 (s, 1H, CH<sub>pyrazole</sub>), 9.04 (s, 1H, NH-C-CH<sub>3</sub>). <sup>13</sup>C NMR (100 MHz, DMSO-*d*<sub>6</sub>, δ ppm): 15.2 (CH<sub>3</sub>), 54.0 (C<sub>pyrimidine</sub>), 122.9 (C<sub>pyrazole</sub>), 113.0-149.7 (Ar-C), 147.3 (C-NO<sub>2</sub>), 150.4 (C=O), 160.2, 164.1 (C<sub>oxadiazole</sub>), 161.5 (C-F). LCMS (ESI) *m/z*: 537.16 [M]<sup>+</sup>. Anal. calcd. for C<sub>28</sub>H<sub>20</sub>FN<sub>7</sub>O<sub>4</sub>: C, 62.57; H, 3.75; N, 18.24. Found: C, 62.53; H, 3.69; N, 18.21 %.

**4-(3-(4-Fluorophenyl)-1-phenyl-1H-pyrazol-4-yl)-6-methyl-5-(5-(3-nitrophenyl)-1,3,4-oxadiazol-2-yl)-3,4-dihydro-2(1H)-one (3f)**

Yield: 60 %, m.p. 250-252 °C. IR (KBr): 3221 (NH), 3060 (C-H<sub>arom</sub>), 2985 (H-C=C<), 2854 (C-H, CH<sub>3</sub>), 1680 (C=O), 1603 (C=N), 1533 (C=C), 1507 (-N=O), 1231 (C-O-C),

1155 (C-F)  $\text{cm}^{-1}$ .  $^1\text{H}$  NMR (400 MHz, DMSO- $d_6$ ,  $\delta$  ppm): 2.35 (s, 3H, CH<sub>3</sub>), 5.23 (s, 1H, CH<sub>pyrimidine</sub>), 6.86 (s, 1H, NH-C-Ph), 7.20-8.21 (m, 13H, Ar-H), 8.29 (s, 1H, CH<sub>pyrazole</sub>), 9.08 (s, 1H, NH-C-CH<sub>3</sub>).  $^{13}\text{C}$  NMR (100 MHz, DMSO- $d_6$ ,  $\delta$  ppm): 15.1 (CH<sub>3</sub>), 54.4 (C<sub>pyrimidine</sub>), 123.1 (C<sub>pyrazole</sub>), 113.4-149.9 (Ar-C), 147.6 (C-NO<sub>2</sub>), 150.5 (C=O), 160.1, 164.6 (C<sub>oxadiazole</sub>), 161.3 (C-F). LCMS (ESI)  $m/z$ : 537.10 [M]<sup>+</sup>. Anal. calcd. for C<sub>28</sub>H<sub>20</sub>FN<sub>7</sub>O<sub>4</sub>: C, 62.57; H, 3.75; N, 18.24. Found: C, 62.52; H, 3.61; N, 18.20 %.

**4-(3-(4-Fluorophenyl)-1-phenyl-1H-pyrazol-4-yl)-6-methyl-5-(5-(4-nitrophenyl)-1,3,4-oxadiazol-2-yl)-3,4-dihydropyrimidin-2(1H)-one (3g)**

Yield: 66 %, m.p. 269-271 °C. IR (KBr): 3211 (NH), 3059 (C-H<sub>arom</sub>), 2980 (H-C=C<), 2848 (C-H, CH<sub>3</sub>), 1693 (C=O), 1598 (C=N), 1527 (C=C), 1504 (N=O), 1284 (C-O-C), 1157 (C-F)  $\text{cm}^{-1}$ .  $^1\text{H}$  NMR (400 MHz, DMSO- $d_6$ ,  $\delta$  ppm): 2.40 (s, 3H, CH<sub>3</sub>), 5.21 (s, 1H, CH<sub>pyrimidine</sub>), 6.80 (s, 1H, NH-C-Ph), 7.29-8.23 (m, 13H, Ar-H), 8.31 (s, 1H, CH<sub>pyrazole</sub>), 9.24 (s, 1H, NH-C-CH<sub>3</sub>).  $^{13}\text{C}$  NMR (100 MHz, DMSO- $d_6$ ,  $\delta$  ppm): 15.7 (CH<sub>3</sub>), 54.7 (C<sub>pyrimidine</sub>), 123.4 (C<sub>pyrazole</sub>), 113.2-149.2 (Ar-C), 147.1 (C-NO<sub>2</sub>), 150.6 (C=O), 160.4, 164.9 (C<sub>oxadiazole</sub>), 161.6 (C-F). LCMS (ESI)  $m/z$ : 537.13 [M]<sup>+</sup>. Anal. calcd. for C<sub>28</sub>H<sub>20</sub>FN<sub>7</sub>O<sub>4</sub>: C, 62.57; H, 3.75; N, 18.24. Found: C, 62.62; H, 3.78; N, 18.29 %.

**4-(3-(4-Fluorophenyl)-1-phenyl-1H-pyrazol-4-yl)-5-(5-(2-hydroxyphenyl)-1,3,4-oxadiazol-2-yl)-6-methyl-3,4-dihydropyrimidin-2(1H)-one (3h)**

Yield: 68 %, m.p. 179-181 °C. IR (KBr): 3409 (OH), 3216 (NH), 3062 (C-H<sub>arom</sub>), 2984 (H-C=C<), 2845 (C-H, CH<sub>3</sub>), 1697 (C=O), 1602 (C=N), 1525 (C=C), 1280 (C-O-C), 1151 (C-F)  $\text{cm}^{-1}$ .  $^1\text{H}$  NMR (400 MHz, DMSO- $d_6$ ,  $\delta$  ppm): 2.35 (s, 3H, CH<sub>3</sub>), 5.22 (s, 1H, CH<sub>pyrimidine</sub>), 6.82 (s, 1H, NH-C-Ph), 7.02-8.07 (m, 13H, Ar-H), 8.18 (s, 1H, CH<sub>pyrazole</sub>), 9.16 (s, 1H, NH-C-CH<sub>3</sub>), 9.20 (s, 1H, OH).  $^{13}\text{C}$  NMR (100 MHz, DMSO- $d_6$ ,  $\delta$  ppm): 15.0 (CH<sub>3</sub>), 53.4 (C<sub>pyrimidine</sub>), 123.2 (C<sub>pyrazole</sub>), 113.2-149.7 (Ar-C), 150.1 (C=O), 157.3 (C-OH), 160.1, 164.4 (C<sub>oxadiazole</sub>), 161.8 (C-F). LCMS (ESI)  $m/z$ : 508.16 [M]<sup>+</sup>. Anal. calcd. for C<sub>28</sub>H<sub>21</sub>FN<sub>6</sub>O<sub>3</sub>: C, 66.14; H, 4.16; N, 16.53. Found: C, 66.23; H, 4.12; N, 16.58 %.

**4-(3-(4-Fluorophenyl)-1-phenyl-1H-pyrazol-4-yl)-5-(5-(3-hydroxyphenyl)-1,3,4-oxadiazol-2-yl)-6-methyl-3,4-dihydropyrimidin-2(1H)-one (3i)**

Yield: 57 %, m.p. 271-273 °C. IR (KBr): 3412 (OH), 3217 (NH), 3064 (C-H<sub>arom</sub>), 2987 (H-C=C<), 2848 (C-H, CH<sub>3</sub>), 1698 (C=O), 1609 (C=N), 1528 (C=C), 1252 (C-O-C), 1151 (C-F)  $\text{cm}^{-1}$ .  $^1\text{H}$  NMR (400 MHz, DMSO- $d_6$ ,  $\delta$  ppm): 2.34 (s, 3H, CH<sub>3</sub>), 5.19 (s, 1H, CH<sub>pyrimidine</sub>), 6.80 (s, 1H, NH-C-Ph), 6.99-8.14 (m, 13H, Ar-H), 8.20 (s, 1H, CH<sub>pyrazole</sub>), 9.14 (s, 1H, NH-C-CH<sub>3</sub>), 9.19 (s, 1H, OH).  $^{13}\text{C}$  NMR (100 MHz, DMSO- $d_6$ ,  $\delta$  ppm): 15.3 (CH<sub>3</sub>), 53.1 (C<sub>pyrimidine</sub>), 123.4 (C<sub>pyrazole</sub>), 113.0-149.8 (Ar-C), 150.4 (C=O), 157.6 (C-OH), 160.2, 164.3 (C<sub>oxadiazole</sub>), 161.2 (C-F). LCMS (ESI)  $m/z$ : 508.16 [M]<sup>+</sup>. Anal. calcd. for C<sub>28</sub>H<sub>21</sub>FN<sub>6</sub>O<sub>3</sub>: C, 66.14; H, 4.16; N, 16.53. Found: C, 66.26; H, 4.20; N, 16.61 %.

**4-(3-(4-Fluorophenyl)-1-phenyl-1H-pyrazol-4-yl)-5-(5-(4-hydroxyphenyl)-1,3,4-oxadiazol-2-yl)-6-methyl-3,4-dihydropyrimidin-2(1H)-one (3j)**

Yield: 73 %, m.p. 237-239 °C. IR (KBr): 3418 (OH), 3219 (NH), 3062 (C-H<sub>arom</sub>), 2981 (H-C=C<), 2853 (C-H, CH<sub>3</sub>), 1692 (C=O), 1605 (C=N), 1526 (C=C), 1278 (C-O-C), 1160 (C-F)  $\text{cm}^{-1}$ .  $^1\text{H}$  NMR (400 MHz, DMSO- $d_6$ ,  $\delta$  ppm): 2.37 (s, 3H, CH<sub>3</sub>), 5.22 (s, 1H, CH<sub>pyrimidine</sub>), 6.83 (s, 1H, NH-C-Ph), 6.96-8.17 (m, 13H, Ar-H), 8.21 (s, 1H, CH<sub>pyrazole</sub>), 9.16 (s, 1H, NH-C-CH<sub>3</sub>), 9.20 (s, 1H, OH).  $^{13}\text{C}$  NMR (100 MHz, DMSO- $d_6$ ,  $\delta$  ppm): 15.0 (CH<sub>3</sub>), 53.3 (C<sub>pyrimidine</sub>), 123.0 (C<sub>pyrazole</sub>), 113.6-149.9 (Ar-C), 150.6 (C=O), 158.4 (C-OH), 160.6, 164.7 (C<sub>oxadiazole</sub>), 161.8 (C-F). LCMS (ESI)  $m/z$ : 508.16 [M]<sup>+</sup>. Anal. calcd. for C<sub>28</sub>H<sub>21</sub>FN<sub>6</sub>O<sub>3</sub>: C, 66.14; H, 4.16; N, 16.53. Found: C, 66.19; H, 4.22; N, 16.60 %.

**4-(3-(4-Fluorophenyl)-1-phenyl-1H-pyrazol-4-yl)-5-(5-(4-methoxyphenyl)-1,3,4-oxadiazol-2-yl)-6-methyl-3,4-dihydropyrimidin-2(1H)-one (3k)**

Yield: 64 %, m.p. 184-186 °C. IR (KBr): 3216 (NH), 3063 (C-H<sub>arom</sub>), 2985 (H-C=C<), 2944 (OCH<sub>3</sub>), 2850 (C-H, CH<sub>3</sub>), 1698 (C=O), 1606 (C=N), 1527 (C=C), 1281 (C-O-C), 1163 (C-F)  $\text{cm}^{-1}$ .  $^1\text{H}$  NMR (400 MHz, DMSO- $d_6$ ,  $\delta$  ppm): 2.39 (s, 3H, CH<sub>3</sub>), 3.60 (s, 3H, OCH<sub>3</sub>), 5.19 (s, 1H, CH<sub>pyrimidine</sub>), 6.84 (s, 1H, NH-C-Ph), 7.01-8.14 (m, 13H, Ar-H), 8.20 (s, 1H, CH<sub>pyrazole</sub>), 9.17 (s, 1H, NH-C-CH<sub>3</sub>).  $^{13}\text{C}$  NMR (100 MHz, DMSO- $d_6$ ,  $\delta$  ppm): 15.2 (CH<sub>3</sub>), 53.6 (C<sub>pyrimidine</sub>), 55.6 (OCH<sub>3</sub>), 123.7 (C<sub>pyrazole</sub>), 113.4-149.8 (Ar-C), 150.1 (C=O), 160.1, 164.5 (C<sub>oxadiazole</sub>), 161.9 (C-F). LCMS (ESI)  $m/z$ : 522.17 [M]<sup>+</sup>. Anal. calcd. for C<sub>29</sub>H<sub>23</sub>FN<sub>6</sub>O<sub>3</sub>: C, 66.66; H, 4.44; N, 16.08. Found: C, 66.71; H, 4.53; N, 16.17 %.

**4-(3-(4-Fluorophenyl)-1-phenyl-1H-pyrazol-4-yl)-6-methyl-5-(5-*p*-tolyl-1,3,4-oxadiazol-2-yl)-3,4-dihydropyrimidin-2(1H)-one (3l)**

Yield: 74 %, m.p. 213-215 °C. IR (KBr): 3219 (NH), 3068 (C-H<sub>arom</sub>), 2986 (H-C=C<), 2856, 2860 (C-H, CH<sub>3</sub>), 1701 (C=O), 1602 (C=N), 1531 (C=C), 1284 (C-O-C), 1165 (C-F)  $\text{cm}^{-1}$ .  $^1\text{H}$  NMR (400 MHz, DMSO- $d_6$ ,  $\delta$  ppm): 2.37 (s, 3H, CH<sub>3</sub>Pyrimidine), 2.44 (s, 3H, CH<sub>3</sub>arom), 5.21 (s, 1H, CH<sub>pyrimidine</sub>), 6.86 (s, 1H, NH-C-Ph), 7.07-8.18 (m, 13H, Ar-H), 8.22 (s, 1H, CH<sub>pyrazole</sub>), 9.18 (s, 1H, NH-C-CH<sub>3</sub>).  $^{13}\text{C}$  NMR (100 MHz, DMSO- $d_6$ ,  $\delta$  ppm): 15.0 (CH<sub>3</sub>Pyrimidine), 21.2 (CH<sub>3</sub>arom), 53.2 (C<sub>pyrimidine</sub>), 123.2 (C<sub>pyrazole</sub>), 113.1-149.7 (Ar-C), 150.2 (C=O), 160.2, 164.2 (C<sub>oxadiazole</sub>), 161.4 (C-F). LCMS (ESI)  $m/z$ : 506.19 [M]<sup>+</sup>. Anal. calcd. for C<sub>29</sub>H<sub>23</sub>FN<sub>6</sub>O<sub>2</sub>: C, 66.76; H, 4.58; N, 16.59. Found: C, 66.77; H, 4.52; N, 16.68 %.

***N*-((5-(4-(3-(4-fluorophenyl)-1-phenyl-1H-pyrazol-4-yl)-6-methyl-2-oxo-1,2,3,4-tetrahydropyrimidin-5-yl)-1,3,4-oxadiazol-2-yl)methyl)benzamide (3m)**

Yield: 61 %, m.p. 227-229 °C. IR (KBr): 3221 (NH), 3061 (C-H<sub>arom</sub>), 2984 (H-C=C<), 2921 (C-H, CH<sub>2</sub>), 2852 (C-H, CH<sub>3</sub>), 1703 (C=O), 1605 (C=N), 1528 (C=C), 1281 (C-O-C), 1160 (C-F)  $\text{cm}^{-1}$ .  $^1\text{H}$  NMR (400 MHz, DMSO- $d_6$ ,  $\delta$  ppm): 2.36 (s, 3H, CH<sub>3</sub>), 4.06 (s, 2H, CH<sub>2</sub>), 5.25 (s, 1H, CH<sub>pyrimidine</sub>), 6.87 (s, 1H, NH-C-Ph), 7.10-8.20 (m, 14H, Ar-H), 8.24 (s, 1H, CH<sub>pyrazole</sub>), 8.68 (s, 1H, NHCO), 9.17 (s, 1H, NH-C-CH<sub>3</sub>).  $^{13}\text{C}$  NMR (100 MHz, DMSO- $d_6$ ,  $\delta$  ppm): 15.4



(CH<sub>3</sub>), 43.4 (CH<sub>2</sub>), 53.5 (C<sub>pyrimidine</sub>), 123.6 (C<sub>pyrazole</sub>), 113.0-149.1 (Ar-C), 150.7 (C=O), 160.4, 164.3 (C<sub>oxadiazole</sub>), 161.5 (C-F), 167.5 (NHCO). LCMS (ESI) *m/z*: 549.19 [M]<sup>+</sup>. Anal. calcd. for C<sub>30</sub>H<sub>24</sub>FN<sub>7</sub>O<sub>3</sub>: C, 66.57; H, 4.40; N, 17.84. Found: C, 66.55; H, 4.46; N, 17.88 %.

**5-(5-Benzyl-1,3,4-oxadiazol-2-yl)-4-(3-(4-fluorophenyl)-1-phenyl-1H-pyrazol-4-yl)-6-methyl-3,4-dihydropyrimidin-2(1H)-one (3n)**

Yield: 62 %, m.p. 195-197 °C. IR (KBr): 3219 (NH), 3066 (C-H<sub>arom</sub>), 2987 (H-C=C<), 2923 (C-H, CH<sub>2</sub>), 2854 (C-H, CH<sub>3</sub>), 1705 (C=O), 1604 (C=N), 1531 (C=C), 1284 (C-O-C), 1166 (C-F) cm<sup>-1</sup>. <sup>1</sup>H NMR (400 MHz, DMSO-*d*<sub>6</sub>, δ ppm): 2.34 (s, 3H, CH<sub>3</sub>), 4.01 (s, 2H, CH<sub>2</sub>), 5.22 (s, 1H, CH<sub>pyrimidine</sub>), 6.86 (s, 1H, NH-C-Ph), 7.12-8.19 (m, 14H, Ar-H), 8.22 (s, 1H, CH<sub>pyrazole</sub>), 9.15 (s, 1H, NH-C-CH<sub>3</sub>). <sup>13</sup>C NMR (100 MHz, DMSO-*d*<sub>6</sub>, δ ppm): 15.1 (CH<sub>3</sub>), 31.2 (CH<sub>2</sub>), 53.7 (C<sub>pyrimidine</sub>), 123.3 (C<sub>pyrazole</sub>), 113.4-149.6 (Ar-C), 150.4 (C=O), 160.1, 164.7 (C<sub>oxadiazole</sub>), 161.7 (C-F). LCMS (ESI) *m/z*: 506.19 [M]<sup>+</sup>. Anal. calcd. for C<sub>29</sub>H<sub>23</sub>FN<sub>6</sub>O<sub>2</sub>: C, 68.76; H, 4.58; N, 16.59. Found: C, 68.85; H, 4.65; N, 16.62 %.

**4-(3-(4-fluorophenyl)-1-phenyl-1H-pyrazol-4-yl)-6-methyl-5-(5-styryl-1,3,4-oxadiazol-2-yl)-3,4-dihydropyrimidin-2(1H)-one (3o)**

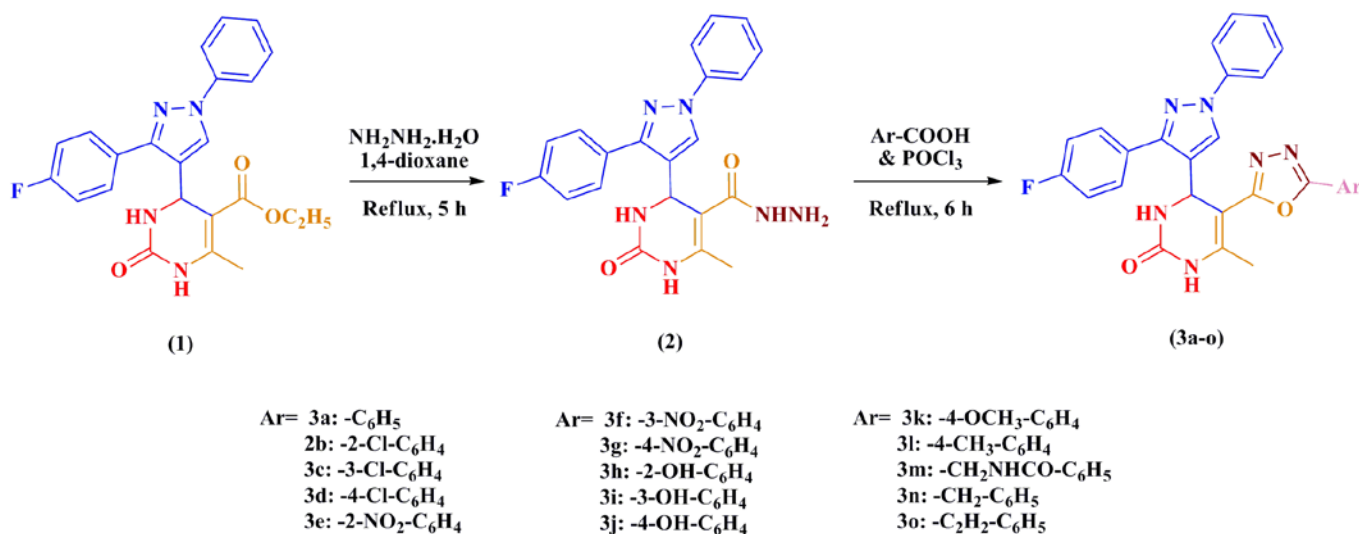
Yield: 72 %, m.p. 275-277 °C. IR (KBr): 3224 (NH), 3151 (C-H<sub>arom</sub>), 3024 (H-C=C-H), 2980 (H-C=C<), 2920 (C-H, CH<sub>3</sub>), 1708 (C=O), 1597 (C=N), 1500 (C=C), 1217 (C-O-C), 1178 (C-F) cm<sup>-1</sup>. <sup>1</sup>H NMR (400 MHz, DMSO-*d*<sub>6</sub>, δ ppm): 2.26 (s, 3H, CH<sub>3</sub>), 5.44 (s, 1H, CH<sub>pyrimidine</sub>), 6.42 (d, 1H, CH=CH<sub>arom</sub>), 6.46 (d, 1H, CH=CH<sub>oxadiazole</sub>), 7.06 (s, 1H, NH-C-Ph), 7.13-7.97 (m, 14H, Ar-H), 8.00 (s, 1H, CH<sub>pyrazole</sub>), 9.21 (s, 1H, NH-C-CH<sub>3</sub>). <sup>13</sup>C NMR (100 MHz, DMSO-*d*<sub>6</sub>, δ ppm): 15.1 (CH<sub>3</sub>), 53.4 (C<sub>pyrimidine</sub>), 123.1 (C<sub>pyrazole</sub>), 123.1 (CH=CH<sub>oxadiazole</sub>), 133.1 (CH=CH<sub>arom</sub>), 113.4-149.8 (Ar-C), 150.1 (C=O), 159.9, 164.0 (C<sub>oxadiazole</sub>), 161.2 (C-F). LCMS (ESI) *m/z*: 518.19 [M]<sup>+</sup>. Anal. calcd. for C<sub>30</sub>H<sub>23</sub>FN<sub>6</sub>O<sub>2</sub>: C, 69.49; H, 4.47; N, 16.21. Found: C, 69.45; H, 4.44; N, 16.32 %.

## RESULTS AND DISCUSSION

Scheme 1 shows the synthesis of targeted compounds. Compound 2 was synthesized by adopting the well-known approach of Biginelli reaction by means of diaryl-pyrazole-4-carbaldehyde followed by the addition of NH<sub>2</sub>-NH<sub>2</sub> (hydrazine hydrate). This adduct was treated with different aryl acid derivatives in one-pot to produce the final compounds 4-(3-(4-fluorophenyl)-1-phenyl-1H-pyrazol-4-yl)-6-methyl-5-(5-aryl-1,3,4-oxadiazol-2-yl)-3,4-dihydropyrimidin-2(1H)-ones **3a-o**.

Synthesized molecules were characterized by well known spectroscopic techniques before evaluating their *in vitro* antimicrobial activity. IR spectrum of compound **3a-o** showed characteristic absorption band of the carbonyl group at 1710-1680 cm<sup>-1</sup>, while absorption band appeared at 3293-3212 cm<sup>-1</sup> corresponding to a secondary amine. The vibrations appeared at 3151-3058, 2998-2978 and 2929-2845 cm<sup>-1</sup> corresponding to C-H stretching of the aromatic ring, H-C=C< and -CH<sub>3</sub>, respectively. Absorption bands at 1609-1592, 1533-1500 cm<sup>-1</sup> corresponding to >C=N-, >C=C< stretching of the aromatic ring, while absorption displayed at 1289-1217 cm<sup>-1</sup> was due to C-O-C stretching in oxadiazole ring.

In <sup>1</sup>H NMR, the appearance of three singlet peaks at δ = 2.26-2.40, 5.17-5.45 and 9.04-9.24 ppm were due to three protons of the methyl group, -CH of the pyrimidine ring and proton of -NH of pyrimidine ring (-NH-C-CH<sub>3</sub>), respectively. The appearance of singlet peak at δ = 6.80-7.06 ppm was due to one proton of -NH of pyrimidine ring (-NH-C-Ph). <sup>13</sup>C NMR of compound **3a-o** showed a characteristic signal at δ = 150.2-151.3 ppm due to carbonyl carbon of pyrimidine scaffold as well as the appearance of a signal around δ = 15.0-15.2 ppm assignable to the carbon of the methyl group. Moreover, the mass spectrum had shown a molecular ion peak corresponding to molecular formula **3a-o** along with other fragment peaks, which were in agreement with the proposed molecular weight and elemental analysis of the anticipated structure of compounds.



**Scheme 1.** Synthetic pathway of novel compounds **3a-o**



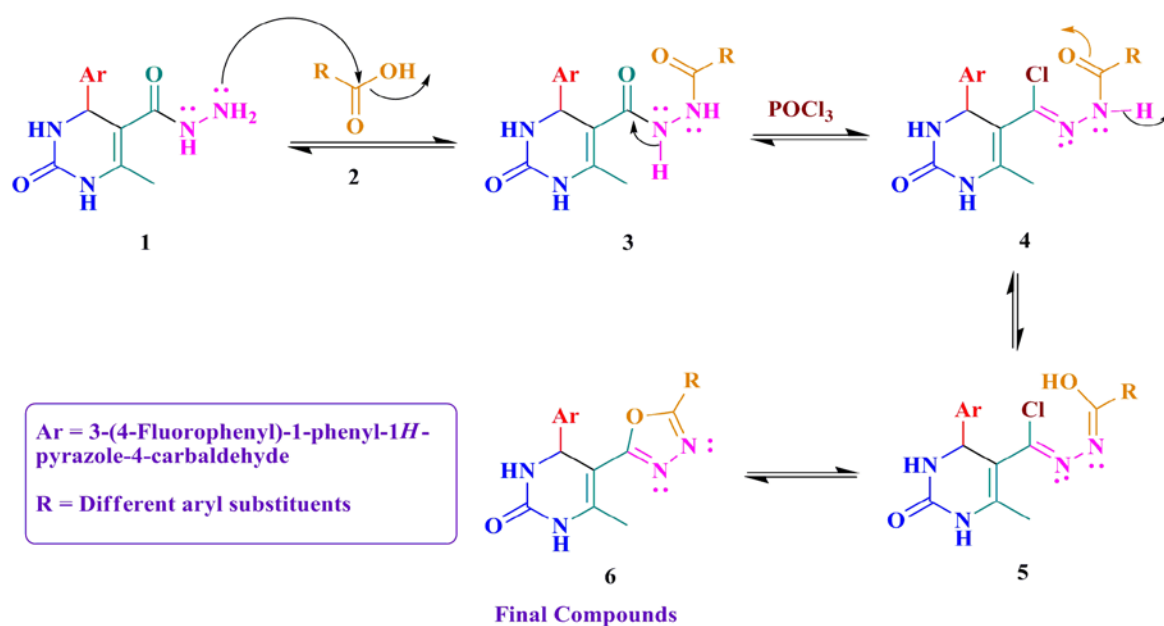


**Figure 1.** Plausible mechanistic pathway of synthesized analogs

A plausible mechanistic path for compounds **3a-o** is suggested in Figure 1. Biginelli hydrazide (**1**) was transformed to targeted compounds (**6**) by intermolecular nucleophilic attack on the carbonyl carbon of different aromatic acids (**2**) followed by the cyclocondensation (removal of HCl) (**5**) in the presence of phosphorus oxychloride (POCl<sub>3</sub>).

#### Antimicrobial activity

Amongst the synthesized compounds **3a-o**, several compounds revealed the antimicrobial influence that ranged from good to excellent. On the basis of antibacterial screening results given in Table 1, compounds **3j** (-4-OH-C<sub>6</sub>H<sub>4</sub>), **3k** (-4-OCH<sub>3</sub>-C<sub>6</sub>H<sub>4</sub>) and **3l** (-4-CH<sub>3</sub>-C<sub>6</sub>H<sub>4</sub>) displayed noteworthy antibacterial activities against *E. coli*, *P. aeruginosa*, *S. aureus*, *S. pyogenes* compared to chloramphenicol and Ciprofloxacin used as standard drugs. MIC values of antifungal activity were determined by means of conventional broth microdilution bioassay method using Nystatin and Griseofulvin as a reference standard.<sup>24</sup> Compounds **3h** (-2-OH-C<sub>6</sub>H<sub>4</sub>) and **3l** (-4-CH<sub>3</sub>-C<sub>6</sub>H<sub>4</sub>) unveiled remarkable inhibitory effect at MIC = 12.5 µg mL<sup>-1</sup> against selected fungal strains.

#### Antitubercular and cytotoxic activity

Synthesized oxadiazole hybrid molecules **3a-o** were screened for their *in vitro* antitubercular activity at 6.25 µg mL<sup>-1</sup> against *Mycobacterium tuberculosis* H<sub>37</sub>Rv strain in BACTEC 12B medium using the microplate alamar blue assay (MABA).<sup>25</sup> In an initial screen, the compounds which shown more than or equal to 90 % inhibition were retested at and below 6.25 µg mL<sup>-1</sup> by using 2-fold dilution to determine the definite MIC. In preliminary *in vitro* screening, compounds **3d**, **3h**, **3j**, **3k** and **3l** inhibited Mtb in the range of 92-98 %. In secondary level screening, two

compounds **3j** (-4-OH-C<sub>6</sub>H<sub>4</sub>) and **3l** (-4-CH<sub>3</sub>-C<sub>6</sub>H<sub>4</sub>) inhibited Mtb with MIC of 0.03 µg mL<sup>-1</sup> correspond to the same MIC as the reference standard isoniazid.

Compounds revealing comparatively low MICs were tested for cytotoxicity (IC<sub>50</sub>) in VERO cell lines. Their selectivity index (SI) was calculated as per the following formula IC<sub>50</sub>/MIC. The compounds **3h**, **3j** and **3l** were somehow less toxic than **3d** and **3k**. Basically, the compounds with MIC ≤ 6.25 µg mL<sup>-1</sup> and SI ≥ 10 are remarkable compounds and MIC ≤ 1 µg mL<sup>-1</sup> in the newly synthesized compound may be considered as excellent leadership, which makes compounds **3j** and **3l** promising bioactive molecules for future research. The results of the antitubercular studies, actual IC<sub>50</sub> and SI of tested compounds were reported in Table 2.

#### Determination of 50 % IC<sub>50</sub> in VERO cells (Cytotoxicity assay)

Compounds were tested for cytotoxicity (IC<sub>50</sub>) in VERO cells at concentrations less than or equal to 62.5 µg mL<sup>-1</sup> or 10 times the MIC for *M. tuberculosis* H<sub>37</sub>Rv. After 72 h of exposure, viability was assessed on the basis of cellular conversion of MTT into a formazan product using the Promega CellTiter 96 Non-radioactive Cell Proliferation Assay. The Selectivity Index (SI = IC<sub>50</sub>/MIC) was also determined; it was considered significant when SI > 10.

#### Structure-activity relationship study

In this manuscript, 1,3,4-oxadiazole motifs were used to impart electronic location on the hankering of molecules. It is observed that the electron releasing group on the phenyl nucleus of 1,3,4-oxadiazole enhanced, whereas electron-withdrawing substituent caused a substantial decrease in the biological potency.

**Table 1.** Antimicrobial screening of the compounds **3a-o**.

No.	-Ar	MINIMUM INHIBITORY CONCENTRATIONS, MIC, in $\mu\text{g mL}^{-1}$						
		Gram-negative		Gram-positive		Fungi		
		<i>E.C.</i> <sup>a</sup>	<i>P.A.</i> <sup>b</sup>	<i>S.A.</i> <sup>c</sup>	<i>S.P.</i> <sup>d</sup>	<i>C.A.</i> <sup>e</sup>	<i>A.N.</i> <sup>f</sup>	<i>A.C.</i> <sup>g</sup>
<b>3a</b>	-C <sub>6</sub> H <sub>5</sub>	500	250	500	250	500	N.A. <sup>h</sup>	N.A.
<b>3b</b>	-2-Cl-C <sub>6</sub> H <sub>4</sub>	125	250	500	100	500	NA.	NA.
<b>3c</b>	-3-Cl-C <sub>6</sub> H <sub>4</sub>	100	100	100	500	NA.	NA.	500
<b>3d</b>	-4-Cl-C <sub>6</sub> H <sub>4</sub>	25	62.5	25	100	500	NA.	NA.
<b>3e</b>	-2-NO <sub>2</sub> -C <sub>6</sub> H <sub>4</sub>	1000	500	500	500	NA.	250	NA.
<b>3f</b>	-3-NO <sub>2</sub> -C <sub>6</sub> H <sub>4</sub>	1000	1000	500	500	250	100	250
<b>3g</b>	-4-NO <sub>2</sub> -C <sub>6</sub> H <sub>4</sub>	500	100	1000	1000	500	NA.	NA.
<b>3h</b>	-2-OH-C <sub>6</sub> H <sub>4</sub>	100	1000	1000	500	NA.	100	12.5
<b>3i</b>	-3-OH-C <sub>6</sub> H <sub>4</sub>	1000	100	500	50	NA.	1000	NA.
<b>3j</b>	-4-OH-C <sub>6</sub> H <sub>4</sub>	12.5	25	1000	100	1000	1000	100
<b>3k</b>	-4-OCH <sub>3</sub> -C <sub>6</sub> H <sub>4</sub>	100	250	500	12.5	50	1000	1000
<b>3l</b>	-4-CH <sub>3</sub> -C <sub>6</sub> H <sub>4</sub>	500	500	25	1000	100	12.5	NA.
<b>3m</b>	-CH <sub>2</sub> NHCOC <sub>6</sub> H <sub>5</sub>	1000	1000	250	500	1000	NA.	50
<b>3n</b>	-CH <sub>2</sub> -C <sub>6</sub> H <sub>5</sub>	500	1000	100	500	NA.	50	1000
<b>3o</b>	-C <sub>2</sub> H <sub>2</sub> -C <sub>6</sub> H <sub>5</sub>	1000	500	250	1000	1000	500	1000
<b>S.d.<sup>i</sup> 1</b>	Chloramphenicol	50	50	50	50	-	-	-
<b>S.d. 2</b>	Ciprofloxacin	25	25	50	50	-	-	-
<b>S.d. 3</b>	Nystatin	-	-	-	-	100	100	100
<b>S.d. 4</b>	Griseofulvin	-	-	-	-	500	100	100

<sup>a</sup>*E.C.*: *Escherichia coli* MTCC 443; <sup>b</sup>*P.A.*: *Pseudomonas aeruginosa* MTCC 1688; <sup>c</sup>*S.A.*: *Staphylococcus aureus* MTCC 96; <sup>d</sup>*S.P.*: *Staphylococcus pyogenes* MTCC 442; <sup>e</sup>*C.A.*: *Candida albicans* MTCC 227; <sup>f</sup>*A.N.*: *Aspergillus niger* MTCC 282; <sup>g</sup>*A.C.*: *Aspergillus clavatus* MTCC 1323; <sup>h</sup>N.A.: No activity; <sup>i</sup>S.d.: Standard drug.

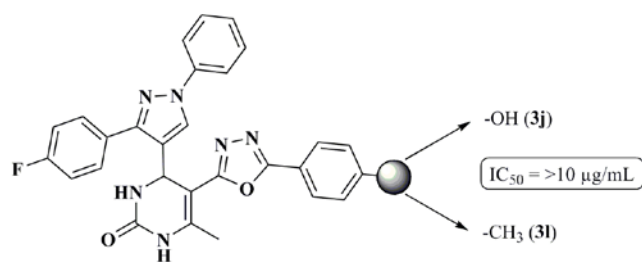
**Table 2.** *In vitro* antitubercular screening data of oxadiazole analogs **3a-o**.

No.	-Ar	% Inhibition, at $6.25 \mu\text{g mL}^{-1}$	MIC <sup>a</sup> , $\mu\text{g mL}^{-1}$	IC <sub>50</sub> <sup>b</sup> , VERO cells	SI <sup>c</sup> =IC <sub>50</sub> /MIC
<b>3a</b>	-C <sub>6</sub> H <sub>5</sub>	65	n.d. <sup>f</sup>	n.d.	n.d.
<b>3b</b>	-2-ClC <sub>6</sub> H <sub>4</sub>	55	n.d.	n.d.	n.d.
<b>3c</b>	-3-ClC <sub>6</sub> H <sub>4</sub>	52	n.d.	n.d.	n.d.
<b>3d</b>	-4-ClC <sub>6</sub> H <sub>4</sub>	92	6.25	7.2	1.15
<b>3e</b>	-2-NO <sub>2</sub> C <sub>6</sub> H <sub>4</sub>	48	n.d.	n.d.	n.d.
<b>3f</b>	-3-NO <sub>2</sub> C <sub>6</sub> H <sub>4</sub>	71	n.d.	n.d.	n.d.
<b>3g</b>	-4-NO <sub>2</sub> C <sub>6</sub> H <sub>4</sub>	62	n.d.	n.d.	n.d.
<b>3h</b>	-2-HOC <sub>6</sub> H <sub>4</sub>	93	3.13	>10	>3.19
<b>3i</b>	-3-HOC <sub>6</sub> H <sub>4</sub>	82	n.d.	n.d.	n.d.
<b>3j</b>	-4-HOC <sub>6</sub> H <sub>4</sub>	98	0.03	>10	333
<b>3k</b>	-4-MeOC <sub>6</sub> H <sub>4</sub>	96	1.56	8.9	5.70
<b>3l</b>	-4-CH <sub>3</sub> -C <sub>6</sub> H <sub>4</sub>	97	0.03	>10	333
<b>3m</b>	-CH <sub>2</sub> NHCOC <sub>6</sub> H <sub>5</sub>	81	n.d.	n.d.	n.d.
<b>3n</b>	-CH <sub>2</sub> C <sub>6</sub> H <sub>5</sub>	73	n.d.	n.d.	n.d.
<b>3o</b>	-C <sub>2</sub> H <sub>2</sub> C <sub>6</sub> H <sub>5</sub>	84	n.d.	n.d.	n.d.
<b>R.S.<sup>d</sup></b>	INH <sup>e</sup>	99	0.03	-	-

<sup>a</sup>Minimum inhibitory concentration against H<sub>37</sub>Rv strain of *M. tuberculosis* ( $\mu\text{g mL}^{-1}$ ). <sup>b</sup>Measurement of cytotoxicity in VERO cells: 50% inhibitory concentrations ( $\mu\text{g mL}^{-1}$ ). <sup>c</sup>Selectivity index (*in vitro*): IC<sub>50</sub> in VERO cells/MIC against *M. tuberculosis*. <sup>d</sup>R.S.: Reference Standard; <sup>e</sup>INH: Isoniazid; <sup>f</sup>n.d.: Not determined.

Compounds **3h**, **3j**, **3k** and **3l**, substituted with inductively electron-donating groups like methyl, methoxy (on *para*) and hydroxyl (on *ortho* and *para*), showed the maximum inhibitory antimicrobial as well as antitubercular influence

with an IC<sub>50</sub> of >10  $\mu\text{g mL}^{-1}$ . Looking at the MIC values, it may be concluded that electron-donating groups at the *para* position of the phenyl ring induced a positive effect on bio-activity.



## CONCLUSION

The pivotal point of the present work was to focus on the development of novel structural hybrids based on DHPMs and pyrazole clubbed 1,3,4-oxadiazole, which could be useful as effective antimicrobial as well as antitubercular agents. It is concluded from biological activity that the structural and electronic diversity of these compounds influences their activity. Synthesized scaffolds **3h**, **3j**, **3k** and **3l** having an electron-donating group such as -OH, -OCH<sub>3</sub>, -CH<sub>3</sub> are found as the most potent antimicrobials and antitubercular candidates. Moreover, most active compounds (i.e., **3j** and **3l**) were conveyed with moderately low cytotoxicity. Consequently, this hybrid nucleus may unlock a moderately simplistic route to new potent antimicrobials and antitubercular scaffolds.

## ACKNOWLEDGEMENTS

Authors are thankful to MK Bhavnagar University, Bhavnagar and RK University, Rajkot, for supporting the research.

## REFERENCES

- Moellering Jr, R. C., Discovering new antimicrobial agents, *Int. J. Antimicrob. Agents*, **2011**, *37*, 2-9. DOI: 10.1016/j.ijantimicag.2010.08.018
- Dartois, V., Barry, C. E., A medicinal chemists' guide to the unique difficulties of lead optimization for tuberculosis, *Bioorg. Med. Chem. Lett.*, **2013**, *23(17)*, 4741-4750. DOI: 10.1016/j.bmcl.2013.07.006
- Safari, S., Ghavimi, R., Razzaghi-Asl, N., Sepehri, S., Synthesis, biological evaluation and molecular docking study of dihydropyrimidine derivatives as potential anticancer agents, *J. Heterocyclic Chem.*, **2020**, 1023-1033. DOI: 10.1002/jhet.3822
- Kappe, C. O., Shishkin, O. V., Uray, G., Verdino, P., Synthesis and reactions of Biginelli compounds, part 19-X-ray structure, conformational analysis, enantioseparation, and determination of absolute configuration of the mitotic kinesin Eg5 inhibitor monastrol, *Tetrahedron*, **2000**, *56*, 1859-1862. DOI: 10.1016/S0040-4020(00)00116-2
- Deshmukh, M. B., Salunkhe, S. M., Patil, D. R., Anbhule, P. V., A novel and efficient one step synthesis of 2-amino-5-cyano-6-hydroxy-4-aryl pyrimidines and their antibacterial activity, *Eur. J. Med. Chem.*, **2009**, *44*, 2651-2654. DOI: 10.1016/j.ejmech.2008.10.018
- Shih, S. R., Chu, T. Y., Reddy, G. R., Tseng, S. N., Chen, H. L., Tang, W. F., Wu, M., Yeh, J. Y., Chao, Y. S., Hsu, J. T. A., Hsieh H. P., Horng J. T., Pyrazole compound BPR1P0034 with potent and selective anti-influenza virus activity, *J. Biomed. Sci.*, **2010**, *17*, 1-9. DOI: 10.1186/1423-0127-17-13
- Kumar, H., Saini, D., Jain, S., Jain, N., Pyrazole scaffold: a remarkable tool in the development of anticancer agents, *Eur. J. Med. Chem.*, **2013**, *70*, 248-258. DOI: 10.1016/j.ejmech.2013.10.004
- Abdel-Aziz, M., Abu-Rahma, G. E. D. A., Hassan, A. A., Synthesis of novel pyrazole derivatives and evaluation of their antidepressant and anticonvulsant activities, *Eur. J. Med. Chem.*, **2009**, *44*, 3480-3487. DOI: 10.1016/j.ejmech.2009.01.032
- Malvar, Dd. C., Ferreira, R. T., de Castro, R. A., de Castro, L. L., Freitas, A. C. C., Costa, E. A., Florentino, I. F., Mafra, J. C. M., de Souza, G. E. P., Vanderlinde, F. A., Antinociceptive, anti-inflammatory and antipyretic effects of 1,5-diphenyl-1H-pyrazole-3-carbohydrazide, a new heterocyclic pyrazole derivative, *Life Sci.*, **2014**, *95*, 81-88. DOI: 10.1016/j.lfs.2013.12.005
- Fatemeh Mirjalili, B. B., Bamoniri, A., Amrollahi, M. A., Emtiazi, H., Mg(ClO<sub>4</sub>)<sub>2</sub>: An efficient catalyst for the synthesis of 1,3,5-trisubstituted pyrazoles, *Dig. J. Nanomater.*, **2010**, *5*, 897-902. DOI: http://www.chalcogen.ro/897\_Mirjalili.pdf
- Polshettiwar, V., Varma, R. S., Greener and rapid access to bio-active heterocycles: room-temperature synthesis of pyrazoles and diazepines in an aqueous medium, *Tetrahedron Lett.*, **2008**, *49*, 397-400. DOI: 10.1016/j.tetlet.2007.11.017
- Iyer, V. B., Gurupadayya, B., Koganti, V. S., Inturi, B., Chandan, R. S., Design, synthesis and biological evaluation of 1,3,4-oxadiazoles as promising anti-inflammatory agents, *Med. Chem. Res.*, **2017**, *26*, 190-204. DOI: 10.1007/s00044-016-1740-6
- Shingare, R. M., Patil, Y. S., Sangshetti, J. N., Patil, R. B., Rajani, D. P., Madje, B. R., Synthesis, Biological Evaluation and Docking Study of Some Novel Isoxazole Clubbed 1,3,4-Oxadiazoles Derivatives, *Med. Chem. Res.*, **2018**, *27*, 1283-1291. DOI: 10.1007/s00044-018-2148-2
- Shingalapur, R. V., Hosamani, K. M., Keri, R. S., Hugar, M. H., Derivatives of benzimidazole pharmacophore: synthesis, anticonvulsant, antidiabetic and DNA cleavage studies, *Eur. J. Med. Chem.*, **2010**, *45*, 1753-1759. DOI: 10.1016/j.ejmech.2010.01.007
- Ahsan, M. J., Samy, J. G., Khalilullah, H., Nomani, M. S., Saraswat, P., Gaur, R., Singh, A., Molecular properties prediction and synthesis of novel 1,3,4-oxadiazole analogues as potent antimicrobial and antitubercular agents, *Bioorg. Med. Chem. Lett.*, **2011**, *21*, 7246-7250. DOI: 10.1016/j.bmcl.2011.10.057
- Ingale, N., Maddi, V., Palkar, M., Ronad, P., Mamledesai, S., Vishwanathswamy, A. H. M., Satyanarayana, D., Synthesis and evaluation of anti-inflammatory and analgesic activity of 3-[(5-substituted-1,3,4-oxadiazol-2-yl-thio)acetyl]-2H-chromen-2-ones, *Med. Chem. Res.*, **2012**, *21*, 16-26. DOI: 10.1007/s00044-010-9494-z
- Macaev, F., Rusu, G., Pogrebnoi, S., Gudima, A., Stingaci, E., Vlad, L., Shvets, N., Kandemirli, F., Dimoglo, A., Reynolds, R., Synthesis of novel 5-aryl-2-thio-1,3,4-oxadiazoles and the study of their structure-anti-mycobacterial activities, *Bioorg. Med. Chem.*, **2005**, *13*, 4842-4850. DOI: 10.1016/j.bmc.2005.05.011
- Khan, M. T., Choudhary, M. I., Khan, K. M., Rani, M., Atta-ur-Rahman, Structure-activity relationships of tyrosinase inhibitory combinatorial library of 2,5-disubstituted-1,3,4-oxadiazole analogues, *Bioorg. Med. Chem.*, **2005**, *13*, 3385-3395. DOI: 10.1016/j.bmc.2005.03.012
- Ke, S., Li, Z., Qian, X., 1,3,4-Oxadiazole-3(2H)-carboxamide derivatives as potential novel class of monoamine oxidase (MAO) inhibitors: synthesis, evaluation, and role of urea moiety, *Bioorg. Med. Chem.*, **2008**, *16*, 7565-7572. DOI: 10.1016/j.bmc.2008.07.026
- Desai, N. C., Vaghani, H. V., Patel, B. Y., Karkar, T. J., Synthesis and Antimicrobial Activity of Fluorine Containing Pyrazole-clubbed Dihydropyrimidinones, *Indian J. Pharm.*

- Sci.*, **2018**, 80, 242–252. DOI: 10.4172/pharmaceutical-sciences.1000351
- <sup>21</sup>Desai, N. C., Bhatt, N., Dodiya, A., Karkar, T., Patel, B., Bhatt, M., Synthesis, characterization and antimicrobial screening of thiazole based 1,3,4-oxadiazoles heterocycles, *Res. Chem. Intermed.*, **2016**, 42, 3039-3053. DOI: 10.1007/s11164-015-2196-x
- <sup>22</sup>Desai, N. C., Shihory, N., Bhatt, M., Patel, B., Karkar, T., Studies on antimicrobial evaluation of some 1-((1-(1 *H*-benzo[*d*]imidazol-2-yl) ethylidene) amino)-6-((arylidene) amino)-2-oxo-4-phenyl-1,2-dihydropyridine-3,5-dicarbonitriles, *Synth. Commun.* **2015**, 45, 2701-2711. DOI: 10.1080/00397911.2015.1102286
- <sup>23</sup>Trivedi, A. R., Bhuvra, V. R., Dholariya, B. H., Dodiya, D. K., Kataria, V. B., Shah, V. H., Novel dihydropyrimidines as a potential new class of antitubercular agents, *Bioorg. Med. Chem. Lett.*, **2010**, 20, 610-6102. DOI: 10.1016/j.bmcl.2010.08.046
- <sup>24</sup>Desai, N. C., Patel, B. Y., Dave, B. P., Synthesis and antimicrobial activity of novel quinoline derivatives bearing pyrazoline and pyridine analogues, *Med. Chem. Res.*, **2017**, 26, 109-119. DOI: 10.1007/s00044-016-1732-6
- <sup>25</sup>Desai, N. C., Trivedi, A. R., Somani, H. C., Bhatt, K. A., Design, Synthesis, and Biological Evaluation of 1,4-dihydropyridine Derivatives as Potent Antitubercular Agents, *Chem. Biol. Drug Des.*, **2015**, 86, 370-377. DOI: 10.1111/cbdd.12502

**This paper was presented at the International Conference "**

**CONFERENCE ON MOLECULAR STRUCTURE & INSTRUMENTAL APPROACHES"**

**at RK University, Rajkot (Gujarat-India) on 26-27th November 2020**

Received: 04.12.2020.

Accepted: 11.12.2020.





# NOVEL 1,2,3-TRIAZOLE-1,4-DIHYDROPYRIDINE-3,5-DICARBONITRILE DERIVATIVES: SYNTHESIS AND ANTIBACTERIAL EVALUATION

Bhagwati Gauni,<sup>[a]</sup> Krunal Mehariya,<sup>[b]</sup> Anamik Shah,<sup>[c]</sup>\* Srinivas Murty Duggirala<sup>[d]</sup>\*

**Keywords:** Antibacterial; 1,4-Dihydropyridines, 1,2,3-Triazoles.

The purpose of this study was the synthesis of a novel series of 1,2,3-triazole-1,4-dihydropyridine-3,5-dicarbonitrile derivatives (**3a-3o**) via Cu(I) catalyzed reaction between a terminal alkyne and substituted alkyl or aryl azides. The synthesized triazoles were characterized by <sup>1</sup>H NMR, <sup>13</sup>C NMR, and single crystal X-Ray. They were screened *in vitro* for antibacterial activity against a set of 10 bacterial cultures by the broth microdilution method. The significant antibacterial activity with MIC: 50 µg mL<sup>-1</sup> was displayed by compounds **3j** and **3h** against *Pseudomonas aeruginosa* and compounds **3c** and **3g** against *Salmonella paratyphi* as well as compound **3f** against *Enterobacter aerogenes*, *Klebsiella pneumoniae*, *Proteus vulgaris*, and *Shigella flexneri*. Compound **3e** was the only compound that was found to inhibit *Escherichia coli* with MIC: 200 µg mL<sup>-1</sup>.

\* Corresponding Authors

E-Mail: [b.gauni@gmail.com](mailto:b.gauni@gmail.com)

[a] Department of Microbiology, Gujarat Vidyapith, Sadra-382320, D; Gandhinagar, Gujarat, India

[b] National Facility for Drug Discovery Complex, Department of Chemistry, Saurashtra University, Rajkot-360005, India

[c] Gujarat Vidyapith, Nr. Income Tax Office, Ashram Rd, Ahmedabad, Gujarat 380014

[d] Department of Microbiology, Gujarat Vidyapith, Sadra-382320, D; Gandhinagar, Gujarat, India

Azoles are a class of heterocyclic compounds having a five-membered ring that consists of at least one nitrogen atom and one more heteroatom like nitrogen, oxygen, or sulfur in the ring. They are present in many biologically active compounds as well as they are excellent ligands for the synthesis of coordinated polymers and metal-organic frameworks.<sup>5</sup> 1,2,3-Triazole is a component of this family and can be efficiently synthesized by the copper-catalyzed click reaction of azides with alkynes.<sup>6</sup>

## INTRODUCTION

Antibiotic resistance is presently contemplated as a chief public health issue.<sup>1</sup> As per the WHO report of April 2019, currently, every year, almost 700,000 people die as a result of drug-resistant diseases and this situation will push about 24 million people into extreme poverty by 2030. Due to the re-emergence of devastating bacterial infections, antimicrobial resistance has left behind the relevance of modern medicines.<sup>2</sup> Therefore, the development of new compounds with antimicrobial activity is the crucial mission of this century.

The involvement of medicinal chemistry in the biological and pharmaceutical field is broad that accounts for drug development, detection, design, and recognition of bioactive compounds. Heterocyclic compounds are of crucial importance in medicinal chemistry. They are getting strong interest in the context to synthesize and process different types of compounds having pharmacological and biological properties.<sup>3</sup> Currently, a general trend of research is synthesizing new drugs by modification of existing biologically active matrices and molecular design of the structural entities.<sup>4</sup> In search of new antimicrobials, medicinal chemists generally confide in N-heterocyclic compounds. In this line, 1,2,3-triazoles have been scrutinized as a substantial class of synthetically versatile heterocyclic compounds.

Triazole is a significant heterocyclic skeleton with extensive biological activities and 1,2,3-Triazoles are the influential class in the triazole series.<sup>5</sup> These compounds are engaging for synthesis since they acquire diversified pharmacological properties functioning as antimicrobial,<sup>7,8,9,10,11,12</sup> antimalarial,<sup>13</sup> antiviral,<sup>14</sup> antitumoral,<sup>15</sup> anti-inflammatory,<sup>11</sup> antitubercular,<sup>16</sup> anti-HIV,<sup>17</sup> activities.

These diverse pharmacological activities are accredited to a 1,2,3-triazole moiety and it can apply various noncovalent interactions that can enhance the solubility and binding ability to biomolecular targets.<sup>18</sup> 1,2,3-Triazole can function as the isostere of amide, ester, carboxylic acid, and other heterocycles that makes it a common pharmacophore in several drugs.<sup>14</sup> Thus, 1,2,3-triazole derivatives play a compelling role in the development of new drugs.

There are several 1,2,3-triazole containing molecules on the market or are in the final stage of clinical trials. Promising pharmaceuticals based on 1,2,3-triazoles include the anticancer compound carboxyamidotriazole (CAI), the nucleoside derivative non-nucleoside reverse transcriptase inhibitor tert-butyl dimethyl spiroamino oxathiole dioxide (also known as TSAO), β-lactam antibiotic Tazobactam, the cephalosporin Cefatrizine (Figure-1).<sup>19</sup>

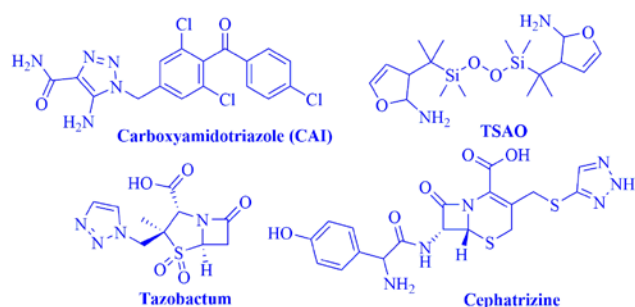


**Figure 1.** Promising pharmaceuticals based on 1,2,3-triazoles

The approach for developing an expanding set of powerful, selective, and modular blocks that work reliably in both small- and large-scale applications is called click chemistry.<sup>20</sup> Copper-catalyzed azide-alkyne cycloaddition (CuAAC) for the reactions that are capable of building blocks of complex compounds has been widely applied in pharmacological and medicinal applications. On that account, CuAAC has thoroughly emerged in research within the past few years in the fields of organic synthesis, polymer chemistry as well as biochemistry.<sup>21,22</sup> The concept of “click” chemistry was established by Sharpless and co-workers in 2001.<sup>23</sup> Click chemistry comprising good yield, temperature, mild reaction condition, and few by-products, has found applications in many research fields. The 1,2,3-triazole having aromatic five-membered heterocyclic ring containing  $\pi$ -excessive three nitrogen atoms and two carbon atoms with two double bonds have attracted significant attention over recent decades due to their extensive biological activities used in the pharmacological and medicinal applications.<sup>20</sup> Described more than one century ago behavior of 1,4-dihydropyridine derivatives (1,4-DHPs) is exhibiting a wide range of biological activity.

New derivatives of 1,2,3-triazole-linked 1,2,4-triazino[5,6-*b*] indole by the Cu(I)-catalyzed click reaction were determined for their binding modes to three enzyme active sites by molecular docking study. Some of these derivatives were found to bind to active sites of dihydrodipicolinate reductase of *Escherichia coli*, undecaprenyl diphosphate synthase (UPPS) of *Micrococcus luteus* and fibrinogen-binding MSCRAMM, clumping factor A *Staphylococcus aureus* via hydrogen bonds and hydrophobic interactions, respectively.<sup>24</sup>

Methyl derivative of acridone-1,2,3-triazole displayed significant antibacterial activity against *Staphylococcus aureus* (MRSA) with MIC: 19.6  $\mu\text{g mL}^{-1}$  and it also played a key role in bond interaction with Ala 7 and hydrophobic interaction into DHFR active site of dihydropteroate synthase (DHPS) in methicillin-resistant *Staphylococcus aureus* (MRSA). Most of the tested compounds displayed moderate activity against *Escherichia coli* and *Klebsiella pneumoniae* with the MIC values between 56.6 - 74.0  $\mu\text{g mL}^{-1}$ .<sup>25</sup>

Some vanillin-derived 1,2,3-triazoles and bis 1,2,3-triazoles substituted with various aromatic rings synthesized using click chemistry concept were found to have potent antibacterial activity. Among them, mono 1,2,3-triazoles, compounds having electron-withdrawing -Br and -NO<sub>2</sub> groups at 3- and 4- position of aryl group were more active

against Gram-positive bacteria (MIC: 5  $\mu\text{g mL}^{-1}$ ). Methyl derivative of bis 1,2,3-triazoles was the most active in the series for most of the Gram-positive and Gram-negative strains (MIC: 5  $\mu\text{g mL}^{-1}$ ). It was found as a lead inhibitor of bacterial DNA synthesis due to conformational fitting in the active site of targeted protein Thymidylate kinase (TMPK), which is an essential enzyme in bacterial DNA biosynthesis.<sup>26</sup>

Among few fluorinated chalcone-triazole hybrids obtained from propargylated chalcones and organic azides, derivative with a 4-nitro group (MIC: 0.0032  $\mu\text{mol mL}^{-1}$ ) was found to be more potent than the standard Ciprofloxacin (MIC: 0.0047  $\mu\text{mol mL}^{-1}$ ) against *E. coli* and *S. epidermidis*. While compound with -OMe functional group was also active against *E. coli* with MIC value of 0.0032  $\mu\text{mol mL}^{-1}$ . The activity results displayed the synergistic effect of biological activity when two pharmacophoric units, i.e., chalcone and 1,2,3-triazole are conjugated. Furthermore, the docking study revealed that the most potent derivative with a 4-NO<sub>2</sub> group was found to form the most stable binding confirmation into the active site of topoisomerase II DNA gyrase B. Thus, these chalcone triazole conjugates could be thought to possibly inhibit DNA topoisomerase.<sup>27</sup>

2-Chloro-6-fluorobenzyl substituted 1,2,3-triazole and 2,4-dichlorobenzylTriazole among ten 1,4-disubstituted 1,2,3-triazoles having benzhydryl piperazine chemical scaffold were found to have excellent antibacterial activity against Gram-positive *S. aureus* (zone of inhibition 16.33 mm and 16.45 mm respectively) and Gram-negative *E. coli* (zone of inhibition 15.63 mm and 16.15 mm respectively). By docking study, it was also found that these two compounds make several hydrogen bonds with DNA Gyrase B of bacteria.<sup>28</sup>

Functionalized 1,2,3-triazole nucleosides, 4-chlorophenyl derivative **3a**, and 3-methylthiophen derivative **3b** displayed significant antibacterial activity against many Gram-positive and Gram-negative organisms. The 4-chlorophenyl derivative of functionalized 1,2,3-triazole nucleosides inhibited *E. coli* ATCC 10536 with a zone of inhibition of 30 mm that was nearer to zone obtained by standard Cefotaxime (34 mm). While 3-methylthiophen derivative inhibited *M. luteus* ATCC 10240 (35 mm) that was higher than standard (28 mm) at the concentration of 40  $\mu\text{g mL}^{-1}$ .<sup>29</sup>

In the library of 1,2,3-triazolyl-1,4-dihydropyridine hybrids, derivatives with methyl ester, ethyl ester, cyano, phenacyl, and benzyl functional group showed equipotent activity (10  $\mu\text{g mL}^{-1}$ ) to the standard Tetracycline against *Proteus mirabilis* with MIC: 10  $\mu\text{g mL}^{-1}$ . In more, cyano, phenacyl, and benzyl derivatives of 1,2,3-triazolyl-1,4-dihydropyridine hybrids were equal potent against *Escherichia coli* with MIC: 30  $\mu\text{g mL}^{-1}$  and more potent against *Klebsiella pneumoniae* (MIC: 8  $\mu\text{g mL}^{-1}$ ) compared to reference drug (MIC: 10  $\mu\text{g mL}^{-1}$ ).<sup>30</sup>

Some 1,2,3-triazole-linked  $\beta$ -lactam-bile acid conjugates showed moderate to good antifungal and antibacterial activity against *Candida albicans*, *Candida neoformans*, *Fusarium oxysporum*, *Escherichia coli*, and *Staphylococcus aureus*.<sup>31</sup> Between the series of 5-(4-methyl-1,2,3-triazole)methyl oxazolidinones, the compound with substitution of the isopropylcarbonyl group at the piperazine C4 position was found to be potent against all tested

susceptible and resistant Gram-positive pathogenic bacteria.<sup>32</sup> In one study, octyl triazole derivatives of the glycol derived novel tetrahydrofuran 1,2,3-triazoles displayed both antibacterial and antifungal activity at MIC: 12.5  $\mu\text{g mL}^{-1}$ .<sup>33</sup> 1,2,3-triazole-linked pentasubstituted 1,4-dihydropyridine derivative having the presence of fluorine at the para and chlorine at the meta position of the aromatic ring inhibited *B. subtilis* and *S. aureus* at 64  $\mu\text{g mL}^{-1}$ .<sup>34</sup> 1-benzyl/aryl-4-[(1-aryl-1H-1,2,3-triazol-4-yl)methoxy]-methyl-1H-1,2,3-triazole derivative having 3-nitrophenyl substituent was found to be best inhibitory against *E. coli* (32 mm), *P. aeruginosa* (12 mm), *S. aureus* (31 mm) and *B. subtilis* (13 mm) compared to standard drug Amoxicillin (30 mm, 10 mm, 30 mm and 12 mm respectively).<sup>35</sup>

In view of the noteworthy bio-potential of the 1,2,3-triazole nucleus to develop novel bioactive therapeutic agents, we targeted our work on the synthesis and evaluation of the novel 1,2,3-triazole-1,4-dihydropyridine-3,5-dicarbonitrile derivatives as antibacterial agents against ten bacteria. The synthesized compounds had contributed to some key structures with interesting antibacterial activity.

In the present study, to improve the inhibitory function of 1,4-dihydropyridine-3,5-dicarbonitrile, the functionalized derivatives 3a-3o were synthesized via CuAAC click chemistry from 1,4-dihydropyridine-3,5-dicarbonitrile and relevant aryl/alkyl azides. The biological importance scaffolds DHPs with 1,2,3-triazole combine together in a single scaffold for increasing importance in pharmaceutical and biological fields. We search for the design and synthesis of pharmacologically important new heterocycles linked in antibacterial activity. The synthesized compounds had contributed to some key structures with interesting antibacterial activity.

## EXPERIMENTAL

Compound solvents and reagents were reagent grade and used without purification unless otherwise noted. The melting points were recorded on a Fargo melting point apparatus and are uncorrected. Reaction progress was monitored using analytical thin-layer chromatography (TLC) on 0.25mmMerck F-254 silica gel glass plates. Visualization was achieved by UV light (254 nm). Mass spectra were recorded on the Shimadzu GC-MS-QP-2010 model using the Direct Injection Probe technique. <sup>1</sup>H and <sup>13</sup>C NMR spectra were recorded with a Bruker AVANCE 400 MHz spectrometer; Chemical shifts are reported in parts per million ( $\delta$ ) using Tetramethylsilane (TMS) as the internal standard with coupling constants (*J*) reported in hertz (Hz). The peak shapes are denoted as follows: s, singlet; d, doublet; t, triplet; q, quartet; m, multiplet; dd, a double doublet. Here, Ar and Ph are representing aromatic ring while -OCH<sub>3</sub>(-OMe) is representing methoxy group.

In this study, 1,2,3-triazole-1,4-dihydropyridine-3,5-dicarbonitrile derivatives (3a-3o) were synthesized. All of them are reported for the first time here. The initial synthesis of the 1,2,3-triazole-1,4-dihydropyridine-3,5-dicarbonitrile derivatives is illustrated in Scheme-1. Different 1,4-dihydropyridine-3,5-dicarbonitrile derivatives 1a-b were synthesized by substituted propargylated benzaldehyde derivatives with 3-aminocrotonitrile in glacial acetic acid

in a stoppered flask and stirred for 1 hour at room temperature under nitrogen atmosphere. The 1,3-dipolar cycloaddition between propargylated 1,4-dihydropyridine-3,5-dicarbonitrile derivatives and alkyl and aryl-substituted azides derivatives under click chemistry conditions produced novel 1,2,3-triazole-1,4-dihydropyridine-3,5-dicarbonitrile derivatives 3a-3o were synthesized in quantitative yields. Different aromatic azides with various substitutions, including electron-withdrawing and electron-donating groups, have been used. The propargylation of -CH<sub>2</sub> group of the different 1,2,3-triazole 1,4-dihydropyridine-3,5-dicarbonitrile derivatives was confirmed by the presence of a signal at  $\delta$  5.20–5.26 s (2H, -CH<sub>2</sub>). The formation of 1,2,3-triazoles was confirmed by the resonance of the proton in the 1,2,3 triazole ring at a  $\delta$  8.70–8.80 s (1H, -CH) as a single. The structure was further supported by the <sup>13</sup>C NMR spectra, which showed the C-atom signals corresponding to triazole derivatives.

### Preparation of propargylated-1,4-dihydropyridine-3,5-dicarbonitrile derivatives (1a-1b)

A mixture of propargylated benzaldehyde derivatives (0.01 mol) and 3-aminocrotonitrile (0.02 mol) was taken in glacial acetic acid in a flask and stirred for 1 hour at room temperature. During the reaction, progress and the completion of the reaction were checked by silica gel-G F254 thin layer chromatography using ethyl acetate: hexane (3:2) as a mobile phase. After the completion of the reaction, the crystalline product was separated which was filtered and washed with diethyl ether.

### General procedure for preparation of compounds 3a-3o

To a solution of propargylated-1,4-dihydropyridine-3,5-dicarbonitrile derivatives (1a-1b) (0.01 mol) in dry DMF (5 mL), anhydrous sodium hydride (15 mmol) was added and stirred for 5 min. After adding propargyl bromide (12 mmol), the resulting mixture was stirred at room temperature overnight. Upon completion of the reaction, water (20 mL) was added and the whole was extracted with dichloromethane (3  $\times$  30 mL). The combined organic layers were washed with brine and dried over Na<sub>2</sub>SO<sub>4</sub>. The organic layer was concentrated in vacuum and the residue was purified by silica gel (60–120 mesh) column chromatography using hexane–ethyl acetate.

### Antimicrobial activity of synthesized 1,2,3-triazole derivatives

Minimum Inhibition Concentration (MIC) of all 1,2,3-triazole-1,4-dihydropyridine-3,5-dicarbonitrile derivatives was determined by using the two-fold microdilution method, the standard methodology that is given by NCCLS.<sup>44</sup> Both Gram-positive and Gram-negative bacterial strains used for the *in-vitro* antibacterial study were procured from culture collection centers. Bacterial cultures of *Salmonella typhi* (MTCC 733), *Salmonella paratyphi* (MTCC 735), *Escherichia coli* (MTCC 1610 T) and *Proteus vulgaris* (MTCC 1771 T) were procured from MTCC, IMTECH, Chandigarh, whereas cultures of *Klebsiella pneumoniae* (MCC 3094), *Pseudomonas aeruginosa* (MCC 3097), *Enterobacter aerogenes* (MCC 3092) and *Shigella flexneri* (MCC 3095) were procured from NCMR, NCCS, Pune.



Clinical isolates of *Serratia marcescens* and *Bacillus subtilis* were collected from a local pathology laboratory in Ahmedabad and identified using biochemical tests prescribed in Bergey's Manual of Determinative Bacteriology, Sixth Edition.<sup>47</sup> The bacterial cultures were maintained on nutrient agar slants at  $2\pm 4$  °C. For the microdilution method, a standardized inoculum for each bacterial strain was prepared to get the inoculum size of approximately  $5\times 10^5$  CFU mL<sup>-1</sup> in each well. A stock solution (10  $\mu$ g mL<sup>-1</sup>) of each compound was prepared in DMSO. Further dilutions of stock solution were prepared in DMSO to get working concentration ranging from 25  $\mu$ g mL<sup>-1</sup> to 2000  $\mu$ g mL<sup>-1</sup>. 100  $\mu$ L of each dilution was distributed in 96 well microtiter plates with double strength (2X) Mueller Hinton broth (MH broth) to obtain an actual concentration ranging from 12.5  $\mu$ g mL<sup>-1</sup> to 1000  $\mu$ g mL<sup>-1</sup> in each test well of a microtiter plate.

For standard, Penicillin and Tetracycline antibiotic solutions were prepared in working concentration ranging from 25  $\mu$ g mL<sup>-1</sup> to 2000  $\mu$ g mL<sup>-1</sup> was used which was added in the same way as test solutions to get actual concentrations ranging from 12.5  $\mu$ g mL<sup>-1</sup> to 1000  $\mu$ g mL<sup>-1</sup> in standard wells. These microtiter plates were then kept at 37 °C for 24-36 h incubation. Each test and growth control well were inoculated with 50  $\mu$ L of a bacterial suspension having standard inoculum size. Following the incubation period, bacterial growth was detected by optical density using Biolog Microplate Reader. MIC values were defined as the lowest concentration of each compound that completely inhibited microbial growth.<sup>45,46</sup>

#### 4-(3-Methoxy-4-((1-(3-nitrophenyl)-1H-1,2,3-triazol-4-yl)-methoxy)phenyl)-2,6-dimethyl-1,4-dihydropyridine-3,5-dicarbonitrile (3a)

To a solution of 1-azido-3-nitrobenzene (1.2 mmol) and 2,6-dimethyl-4-(3-(prop-2-yn-1-yloxy)phenyl)-1,4-dihydropyridine-3,5-dicarbonitrile (**1a**, 1.0 mmol) were added to a mixture of copper(II) sulfate pentahydrate solution (0.01 mmol) and sodium ascorbate (0.25 mmol) dissolved in *t*-BuOH:H<sub>2</sub>O (1:1 mixture, 3 mL) at room temperature. The reaction mixture was stirred at room temperature for 3-6 h, and monitored by TLC. The resulting mixture was poured into CHCl<sub>3</sub> (5 mL) and H<sub>2</sub>O (3 mL), and the organic layer was separated. The aqueous layer was extracted with CHCl<sub>3</sub> (5 mL) three times. The combined organic layer was concentrated in vacuo. The residue was purified by short column chromatography on silica gel (60-120 mesh) eluted with ethyl acetate: hexane (6:4) to give **3a**; <sup>1</sup>H NMR (DMSO-*d*<sub>6</sub>)  $\delta$  2.04 s (6H, 2 $\times$ CH<sub>3</sub>), 3.76 s (3H, -OCH<sub>3</sub>), 4.36 s (3H, -CH), 5.22 s (2H, -CH<sub>2</sub>), 6.80-6.82 d (1H, *J* = 8.2 Hz, Ar-H), 6.88-6.89 d (1H, *J* = 1.48 Hz, Ar-H), 7.89-7.93 d (1H, *J* = 8.20 Hz, Ar-H), 8.33-8.35 t (1H, *J* = 6.88 Hz, Ar-H), 8.43-8.45 t (1H, *J* = 7.84 Hz, Ar-H), 8.77 s (1H, Ar-H), 9.21 s (1H, Ar-H), 9.49 s (1H, -NH); <sup>13</sup>C NMR (DMSO-*d*<sub>6</sub>)  $\delta$  17.73, 55.50, 61.55, 82.77, 111.55, 113.90, 114.88, 119.35, 119.81, 123.17, 123.50, 126.18, 131.51, 137.11, 137.49, 144.30, 146.40, 146.83, 148.49, 149.02.

By following the same procedure, the following compounds were synthesized. Analytical data and yields of 1,2,3-triazole 1,4-dihydropyridine-3,5-dicarbonitrile derivatives (**3a-3o**) is given in Table 1.

#### 4-(4-((1-(3-Chlorophenyl)-1H-1,2,3-triazol-4-yl)methoxy)-3-methoxyphenyl)-2,6-dimethyl-1,4-dihydropyridine-3,5-dicarbonitrile (3b)

Compound **3b** was prepared from 1-azido-3-chlorobenzene (1.2 mmol), 2,6-dimethyl-4-(3-(prop-2-yn-1-yloxy)phenyl)-1,4-dihydropyridine-3,5-dicarbonitrile (**1a**, 1.0 mmol), copper(II) sulfate pentahydrate solution (0.01 mmol) and sodium ascorbate (0.25 mmol); <sup>1</sup>H NMR (DMSO-*d*<sub>6</sub>)  $\delta$  2.04 s (6H, 2 $\times$ CH<sub>3</sub>), 3.76 s (3H, -OCH<sub>3</sub>), 4.39 s (3H, -CH), 5.22 s (2H, -CH<sub>2</sub>), 6.81-6.87 d (2H, *J* = 24.2 Hz, 2 $\times$ Ar-H), 7.20-7.22 d (1H, *J* = 6.04 Hz, Ar-H), 7.58-7.63 t (2H, *J* = 6.92 Hz, Ar-H), 7.95 s (2H, 2 $\times$ ArH), 8.08 s (2H, 2 $\times$ ArH), 9.03 s (1H, Ar-H), 9.49 s (1H, NH); <sup>13</sup>C NMR (DMSO-*d*<sub>6</sub>)  $\delta$  17.74, 55.50, 61.58, 82.78, 111.55, 113.88, 118.74, 119.35, 119.81, 119.96, 123.20, 128.54, 131.59, 134.18, 137.46, 137.57, 144.02, 146.40, 146.85, 149.01.

#### 4-(3-((1-(4-Cyanophenyl)-1H-1,2,3-triazol-5-yl)methoxy)phenyl)-2,6-dimethyl-1,4-dihydropyridine-3,5-dicarbonitrile (3c)

Compound **3c** was prepared from 4-azidobenzonitrile (1.2 mmol), 2,6-dimethyl-4-(3-(prop-2-yn-1-yloxy)phenyl)-1,4-dihydropyridine-3,5-dicarbonitrile (**1a**, 1.0 mmol), copper(II) sulfate pentahydrate solution (0.01 mmol) and sodium ascorbate (0.25 mmol); <sup>1</sup>H NMR (DMSO-*d*<sub>6</sub>)  $\delta$  2.04 s (6H, 2 $\times$ CH<sub>3</sub>), 4.39 s (1H, -CH), 5.28 s (2H, -CH<sub>2</sub>), 6.89-6.92 t (2H, *J* = 6.12 Hz, 2 $\times$ Ar-H), 7.08-7.09 d (1H, *J* = 6.04 Hz, Ar-H), 7.34-7.38 t (2H, *J* = 7.80 Hz, Ar-H), 8.10-8.12 d (2H, *J* = 8.48 Hz, 2 $\times$ Ar-H), 8.16-8.18 d (2H, *J* = 8.56 Hz, 2 $\times$ Ar-H), 9.12 s (1H, Ar-H), 9.53 s (1H, -NH); <sup>13</sup>C NMR (DMSO-*d*<sub>6</sub>)  $\delta$  17.13, 60.92, 82.47, 111.11, 113.25, 114.52, 118.07, 119.24, 120.37, 120.53, 123.13, 130.01, 134.25, 139.44, 144.32, 145.67, 146.76, 158.25.

#### 4-(3-Methoxy-4-((1-(*p*-tolyl)-1H-1,2,3-triazol-4-yl)methoxy)phenyl)-2,6-dimethyl-1,4-dihydropyridine-3,5-dicarbonitrile (3d)

Compound **3d** was prepared from 1-azido-4-methylbenzene (1.2 mmol), 2,6-dimethyl-4-(3-(prop-2-yn-1-yloxy)phenyl)-1,4-dihydropyridine-3,5-dicarbonitrile (**1b**, 1.0 mmol), copper(II) sulfate pentahydrate solution (0.01 mmol) and sodium ascorbate (0.25 mmol); <sup>1</sup>H NMR (DMSO-*d*<sub>6</sub>)  $\delta$  2.04 s (6H, 2 $\times$ CH<sub>3</sub>), 2.38 s (3H, CH<sub>3</sub>), 3.76 s (3H, -OCH<sub>3</sub>), 4.36 s (1H, -CH), 5.21 s (2H, -CH<sub>2</sub>), 6.80-6.98 dd (2H, *J* = 8.16 and 1.24 Hz, 2 $\times$ Ar-H), 7.21-7.23 d (1H, *J* = 8.24 Hz, Ar-H), 7.39-7.41 d (2H, *J* = 8.12 Hz, 2 $\times$ Ar-H), 7.79-7.81 d (2H, *J* = 8.24 Hz, 2 $\times$ Ar-H), 8.90 s (1H, Ar-H), 9.49 s (1H, -NH); <sup>13</sup>C NMR (DMSO-*d*<sub>6</sub>)  $\delta$  17.74, 20.54, 55.48, 61.61, 82.79, 111.53, 113.82, 119.35, 119.81, 120.01, 122.88, 130.21, 134.30, 137.39, 138.36, 143.70, 146.39, 146.90, 149.01, 162.26.

#### 4-(3-Methoxy-4-((1-(4-methoxyphenyl)-1H-1,2,3-triazol-4-yl)methoxy)phenyl)-2,6-dimethyl-1,4-dihydropyridine-3,5-dicarbonitrile (3e)

Compound **3e** was prepared from 1-azido-4-methoxybenzene (1.2 mmol), 4-(3-methoxy-4-(prop-2-yn-1-yloxy)phenyl)-2,6-dimethyl-1,4-dihydropyridine-3,5-dicarbonitrile (**1b**, 1.0 mmol), copper(II) sulfate



pentahydrate solution (0.01 mmol) and sodium ascorbate (0.25 mmol);  $^1\text{H}$  NMR (DMSO- $d_6$ )  $\delta$  2.04 s (6H,  $2\times\text{CH}_3$ ), 3.76 s (3H,  $\text{CH}_3$ ), 3.84 s (3H,  $-\text{OCH}_3$ ), 4.36 s (1H,  $-\text{CH}$ ), 5.20 s (2H,  $-\text{CH}_2$ ), 6.79–6.82 dd (2H,  $J = 1.60$  and  $1.60$  Hz, Ar-H), 6.87–6.87 d (1H,  $J = 1.56$  Hz, Ar-H), 7.13–7.16 d (2H,  $J = 8.96$  Hz,  $2\times\text{Ar-H}$ ), 7.21–7.23 d (1H,  $J = 8.24$  Hz, Ar-H), 7.82–7.84 d (1H,  $J = 8.92$  Hz, Ar-H), 8.85 s (1H, Ar-H), 9.49 s (1H,  $-\text{NH}$ );  $^{13}\text{C}$  NMR (DMSO- $d_6$ )  $\delta$  17.74, 30.73, 55.48, 55.53, 61.62, 82.79, 111.52, 113.80, 114.85, 119.36, 119.80, 121.82, 122.98, 129.96, 137.36, 143.57, 146.39, 146.91, 148.99, 159.28, 162.27.

**4-(4-((1-(4-Fluorophenyl)-1H-1,2,3-triazol-4-yl)methoxy)-3-methoxyphenyl)-2,6-dimethyl-1,4-dihydropyridine-3,5-dicarbonitrile (3f)**

Compound **3f** was prepared from 1-azido-4-fluorobenzene (1.2 mmol), 4-(3-methoxy-4-(prop-2-yn-1-yloxy)phenyl)-2,6-dimethyl-1,4-dihydropyridine-3,5-dicarbonitrile (**1b**, 1.0 mmol), copper(II) sulfate pentahydrate solution (0.01 mmol) and sodium ascorbate (0.25 mmol);  $^1\text{H}$  NMR (DMSO- $d_6$ )  $\delta$  2.04 s (6H,  $2\times\text{CH}_3$ ), 3.76 s (3H,  $-\text{OCH}_3$ ), 4.36 s (1H,  $-\text{CH}$ ), 5.22 s (2H,  $-\text{CH}_2$ ), 6.80–6.82 d (1H,  $J = 7.80$  Hz, Ar-H), 6.88 s (1H, Ar-H), 7.21–7.23 d (1H,  $J = 8.08$  Hz, Ar-H), 7.47–7.49 d (2H,  $J = 8.24$  Hz,  $2\times\text{Ar-H}$ ), 7.97 s, (2H,  $2\times\text{ArH}$ ), 8.94 s (1H, Ar-H), 9.50 s (1H,  $-\text{NH}$ );  $^{13}\text{C}$  NMR (DMSO- $d_6$ )  $\delta$  17.74, 55.48, 61.58, 82.79, 111.53, 113.84, 116.59, 116.82, 119.36, 119.81, 122.49, 122.58, 123.26, 133.11, 137.42, 143.86, 146.40, 146.87, 149.01, 160.44, 162.88.

**4-(4-((1-(4-Cyanophenyl)-1H-1,2,3-triazol-4-yl)methoxy)-3-methoxyphenyl)-2,6-dimethyl-1,4-dihydropyridine-3,5-dicarbonitrile (3g)**

Compound **3g** was prepared from 4-azidobenzonitrile (1.2 mmol), 4-(3-methoxy-4-(prop-2-yn-1-yloxy)phenyl)-2,6-dimethyl-1,4-dihydropyridine-3,5-dicarbonitrile (**1b**, 1.0 mmol), copper(II) sulfate pentahydrate solution (0.01 mmol) and sodium ascorbate (0.25 mmol);  $^1\text{H}$  NMR (DMSO- $d_6$ )  $\delta$  2.04 s (6H,  $2\times\text{CH}_3$ ), 3.76 s (3H,  $\text{OCH}_3$ ), 4.36 s (1H,  $-\text{CH}$ ), 5.25 s (2H,  $-\text{CH}_2$ ), 6.80–6.82 d (2H,  $J = 7.80$  Hz,  $2\times\text{Ar-H}$ ), 6.88 s (1H, Ar-H), 7.20–7.22 d (1H,  $J = 7.96$  Hz, Ar-H), 8.10–8.19 dd (4H,  $J = 7.76$  and  $7.76$  Hz,  $4\times\text{Ar-H}$ ), 9.12 s (1H, Ar-H), 9.50 s (1H,  $-\text{NH}$ );  $^{13}\text{C}$  NMR (DMSO- $d_6$ )  $\delta$  17.74, 55.50, 61.53, 82.77, 111.10, 111.55, 113.91, 118.08, 119.36, 119.81, 120.54, 123.25, 134.26, 137.50, 139.44, 144.36, 146.41, 146.81, 149.02.

**2,6-Dimethyl-4-(3-((1-(3-nitrophenyl)-1H-1,2,3-triazol-5-yl)methoxy)phenyl)-1,4-dihydropyridine-3,5-dicarbonitrile (3h)**

Compound **3h** was prepared from 1-azido-3-nitrobenzene (1.2 mmol), 2,6-dimethyl-4-(3-(prop-2-yn-1-yloxy)phenyl)-1,4-dihydropyridine-3,5-dicarbonitrile (**1a**, 1.0 mmol), copper(II) sulfate pentahydrate solution (0.01 mmol) and sodium ascorbate (0.25 mmol);  $^1\text{H}$  NMR (DMSO- $d_6$ )  $\delta$  2.04 s (6H,  $2\times\text{CH}_3$ ), 4.39 s (1H,  $-\text{CH}$ ), 5.29 s (2H,  $-\text{CH}_2$ ), 6.89–6.93 d (2H,  $J = 7.56$  Hz,  $2\times\text{Ar-H}$ ), 7.08–7.10 d (1H,  $J = 6.80$  Hz, Ar-H), 7.35–7.38 t (1H,  $J = 6.72$  Hz, Ar-H), 7.90–7.94 t (1H,  $J = 7.68$  Hz, Ar-H), 8.34–8.44 dd (2H,  $J = 7.68$ ,  $2\times\text{Ar-H}$ ), 8.76 s (1H, Ar-H), 9.22 s (1H, Ar-H), 9.54 s (1H,  $-\text{NH}$ );  $^{13}\text{C}$  NMR (DMSO- $d_6$ )  $\delta$  17.73, 60.94, 82.47, 113.25, 114.54,

114.88, 119.23, 120.36, 123.19, 123.38, 126.18, 130.01, 131.54, 137.12, 144.25, 145.67, 146.76, 148.49, 158.26.

**4-(3-((1-Benzyl-1H-1,2,3-triazol-5-yl)methoxy)phenyl)-2,6-dimethyl-1,4-dihydropyridine-3,5-dicarbonitrile (3i)**

Compound **3i** was prepared from (azidomethyl)benzene (1.2 mmol), 2,6-dimethyl-4-(3-(prop-2-yn-1-yloxy)phenyl)-1,4-dihydropyridine-3,5-dicarbonitrile (**1a**, 1.0 mmol), copper(II) sulfate pentahydrate solution (0.01 mmol) and sodium ascorbate (0.25 mmol);  $^1\text{H}$  NMR (DMSO- $d_6$ )  $\delta$  2.04 s (6H,  $2\times\text{CH}_3$ ), 4.38 s (1H,  $-\text{CH}$ ), 5.15 s (2H,  $-\text{CH}_2$ ), 5.62 s (2H,  $-\text{CH}_2$ ), 6.87–6.89 d (2H,  $J = 7.44$  Hz,  $2\times\text{Ar-H}$ ), 7.01–7.03 d (1H,  $J = 8.60$  Hz, Ar-H), 7.34–7.40 m (6H,  $6\times\text{Ar-H}$ ), 8.32 s (1H, Ar-H), 9.54 s (1H, Ar-H), 9.54 s (1H,  $-\text{NH}$ );  $^{13}\text{C}$  NMR (DMSO- $d_6$ )  $\delta$  17.74, 52.84, 60.98, 82.49, 113.15, 114.49, 119.27, 120.17, 124.77, 127.94, 128.14, 128.75, 129.91, 135.95, 145.65, 146.76, 158.38.

**2,6-Dimethyl-4-(3-((1-(p-tolyl)-1H-1,2,3-triazol-5-yl)methoxy)phenyl)-1,4-dihydropyridine-3,5-dicarbonitrile (3j)**

Compound **3j** was prepared from 1-azido-4-methylbenzene (1.2 mmol), 2,6-dimethyl-4-(3-(prop-2-yn-1-yloxy)phenyl)-1,4-dihydropyridine-3,5-dicarbonitrile (**1a**, 1.0 mmol), copper(II) sulfate pentahydrate solution (0.01 mmol) and sodium ascorbate (0.25 mmol);  $^1\text{H}$  NMR (DMSO- $d_6$ )  $\delta$  2.04 s (6H,  $2\times\text{CH}_3$ ), 2.38 s (3H,  $-\text{CH}_3$ ), 4.39 s (1H,  $-\text{CH}$ ), 5.25 s (2H,  $-\text{CH}_2$ ), 6.89–6.93 d (2H,  $J = 7.48$  Hz,  $2\times\text{Ar-H}$ ), 7.07–7.09 d (1H,  $J = 6.92$  Hz, Ar-H), 7.36–7.41 t (3H,  $J = 12.44$  Hz,  $3\times\text{Ar-H}$ ), 7.79–7.80 d (2H,  $J = 7.20$  Hz,  $2\times\text{Ar-H}$ ), 8.91 s (1H, Ar-H), 9.55 s (1H,  $-\text{NH}$ );  $^{13}\text{C}$  NMR (DMSO- $d_6$ )  $\delta$  17.73, 20.55, 24.22, 61.00, 82.49, 113.21, 114.51, 119.25, 120.02, 120.28, 122.76, 129.98, 130.20, 134.31, 138.36, 143.63, 145.68, 146.75, 158.35.

**4-(3-Methoxy-4-((1-(2-nitrophenyl)-1H-1,2,3-triazol-4-yl)methoxy)phenyl)-2,6-dimethyl-1,4-dihydropyridine-3,5-dicarbonitrile (3k)**

Compound **3k** was prepared from 1-azido-2-nitrobenzene (1.2 mmol), 4-(3-methoxy-4-(prop-2-yn-1-yloxy)phenyl)-2,6-dimethyl-1,4-dihydropyridine-3,5-dicarbonitrile (**1b**, 1.0 mmol), copper(II) sulfate pentahydrate solution (0.01 mmol) and sodium ascorbate (0.25 mmol);  $^1\text{H}$  NMR (DMSO- $d_6$ )  $\delta$  2.04 s (6H,  $2\times\text{CH}_3$ ), 3.76 s (3H,  $-\text{OCH}_3$ ), 4.36 s (3H,  $-\text{CH}$ ), 5.22 s (2H,  $-\text{CH}_2$ ), 6.80–6.82 d (1H,  $J = 8.2$  Hz, ArH), 6.88–6.89 d (1H,  $J = 1.48$  Hz, ArH), 7.89–7.93 d (1H,  $J = 8.20$  Hz, ArH), 8.33–8.35 t (1H,  $J = 6.88$  Hz, ArH), 8.43–8.45 t (1H,  $J = 7.84$  Hz, ArH), 8.77 s (1H, ArH), 9.21 s (1H, ArH), 9.49 s (1H,  $-\text{NH}$ );  $^{13}\text{C}$  NMR (DMSO- $d_6$ )  $\delta$  17.73, 55.50, 61.55, 82.77, 111.55, 113.90, 114.88, 119.35, 119.81, 123.17, 123.50, 126.18, 131.51, 137.11, 137.49, 144.30, 146.40, 146.83, 148.49, 149.02.

**4-(4-((1-Benzyl-1H-1,2,3-triazol-4-yl)methoxy)-3-methoxyphenyl)-2,6-dimethyl-1,4-dihydropyridine-3,5-dicarbonitrile (3l)**

Compound **3l** was prepared from (azidomethyl)benzene (1.2 mmol), 4-(3-methoxy-4-(prop-2-yn-1-yloxy)phenyl)-2,6-dimethyl-1,4-dihydropyridine-3,5-dicarbonitrile (**1b**, 1.0 mmol), copper(II) sulfate pentahydrate solution (0.01

mmol) and sodium ascorbate (0.25 mmol);  $^1\text{H}$  NMR (DMSO- $d_6$ )  $\delta$  2.05 s (6H,  $2\times\text{CH}_3$ ), 3.77 s (3H,  $-\text{CH}_3$ ), 4.35 s (1H,  $-\text{CH}$ ), 5.12 s (2H,  $-\text{CH}_2$ ), 5.62 s (2H,  $-\text{CH}_2$ ), 6.77–6.85 t (2H,  $J = 6.88$  Hz,  $2\times\text{Ar-H}$ ), 7.14–7.16 d (1H,  $J = 8.24$  Hz, Ar-H), 7.33–7.40 m (5H,  $5\times\text{Ar-H}$ ), 8.29 s (1H, Ar-H), 9.49 (s, 1H,  $-\text{NH}$ );  $^{13}\text{C}$  NMR (DMSO- $d_6$ )  $\delta$  17.74, 52.81, 55.43, 61.66, 82.80, 111.46, 113.68, 119.35, 119.75, 124.81, 127.96, 128.13, 128.75, 135.97, 137.25, 146.37, 146.90, 148.95.

#### 4-(3-((1-(4-Bromophenyl)-1H-1,2,3-triazol-5-yl)methoxy)phenyl)-2,6-dimethyl-1,4-dihydropyridine-3,5-dicarbonitrile (3m)

Compound **3m** was prepared from 1-azido-4-bromobenzene (1.2 mmol), 2,6-dimethyl-4-(3-(prop-2-yn-1-yloxy)phenyl)-1,4-dihydropyridine-3,5-dicarbonitrile (**1a**, 1.0 mmol), copper(II) sulfate pentahydrate solution (0.01 mmol) and sodium ascorbate (0.25 mmol);  $^1\text{H}$  NMR (DMSO- $d_6$ )  $\delta$  2.05 s (6H,  $2\times\text{CH}_3$ ), 4.39 s (1H,  $-\text{CH}$ ), 5.25 s (2H,  $-\text{CH}_2$ ), 6.89–6.92 t (2H,  $J = 6.20$  Hz,  $2\times\text{Ar-H}$ ), 7.08–7.09 t (1H,  $J = 6.96$  Hz, Ar-H), 7.34–7.38 t (1H,  $J = 7.56$  Hz, Ar-H), 7.80–7.82 d (2H,  $J = 8.16$  Hz,  $2\times\text{Ar-H}$ ), 7.89–7.91 d (2H,  $J = 8.24$  Hz,  $2\times\text{Ar-H}$ ), 9.00 s (1H, Ar-H), 9.54 s (1H,  $-\text{NH}$ );  $^{13}\text{C}$  NMR (DMSO- $d_6$ )  $\delta$  17.74, 60.95, 82.48, 113.23, 114.51, 119.24, 120.32, 121.40, 122.06, 122.93, 129.99, 132.76, 135.74, 143.97, 145.67, 146.75, 158.30.

#### 4-(3-((1-(Cyanomethyl)-1H-1,2,3-triazol-5-yl)methoxy)phenyl)-2,6-dimethyl-1,4-dihydropyridine-3,5-dicarbonitrile (3n)

Compound **3n** was prepared from 2-azidoacetonitrile (1.2 mmol), 2,6-dimethyl-4-(3-(prop-2-yn-1-yloxy)phenyl)-1,4-dihydropyridine-3,5-dicarbonitrile (**1a**, 1.0 mmol), copper(II) sulfate pentahydrate solution (0.01 mmol) and sodium ascorbate (0.25 mmol);  $^1\text{H}$  NMR (DMSO- $d_6$ )  $\delta$  2.05 s (6H,  $2\times\text{CH}_3$ ), 4.38 s (1H,  $-\text{CH}$ ), 5.20 s (2H,  $-\text{CH}_2$ ), 6.89 s (2H,  $2\times\text{Ar-H}$ ), 7.03–7.05 d (1H,  $J = 7.32$  Hz, Ar-H), 7.33–7.36 t (1H,  $J = 7.36$  Hz, Ar-H), 8.41 s (1H, Ar-H), 9.54 s (1H,  $-\text{NH}$ );  $^{13}\text{C}$  NMR (DMSO- $d_6$ )  $\delta$  17.74, 60.69, 82.47, 113.13, 114.48, 115.04, 119.26, 120.25, 125.62, 129.95, 143.32, 145.67, 146.77, 158.27.

#### 4-(4-((1-(4-Cyanobenzyl)-1H-1,2,3-triazol-4-yl)methoxy)-3-methoxyphenyl)-2,6-dimethyl-1,4-dihydropyridine-3,5-dicarbonitrile (3o)

Compound **3o** was prepared from 4-(azidomethyl)benzonitrile (1.2 mmol), 4-(3-methoxy-4-(prop-2-yn-1-yloxy)phenyl)-2,6-dimethyl-1,4-dihydropyridine-3,5-dicarbonitrile (**1b**, 1.0 mmol), copper(II) sulfate pentahydrate solution (0.01 mmol) and sodium ascorbate (0.25 mmol);  $^1\text{H}$  NMR (DMSO- $d_6$ )  $\delta$  2.05 s (6H,  $2\times\text{CH}_3$ ), 3.73 s (3H,  $-\text{OCH}_3$ ), 4.35 s (1H,  $-\text{CH}$ ), 5.14 s (2H,  $-\text{CH}_2$ ), 5.75 s (2H,  $-\text{CH}_2$ ), 6.77–6.79 m (1H, Ar-H), 6.85–6.86 d (1H,  $J = 1.68$  Hz, Ar-H), 7.17–7.16 d (1H,  $J = 8.32$  Hz, Ar-H), 7.46–7.48 d (2H,  $J = 8.12$  Hz,  $2\times\text{Ar-H}$ ), 7.85–7.87 d (2H,  $J = 8.16$  Hz,  $2\times\text{Ar-H}$ ), 8.34 s (1H, Ar-H), 9.49 s (1H, Ar-H);  $^{13}\text{C}$  NMR (DMSO- $d_6$ )  $\delta$  17.73, 52.16, 55.45, 61.64, 82.79, 110.92, 111.48, 113.76, 118.51, 119.35, 119.76, 125.14, 128.70, 132.72, 137.30, 141.43, 143.16, 146.38, 146.84, 148.98.

## Crystal Structure Determination

Crystal data of **3d** and **3e** were made on a Rigaku SCX mini diffractometer using graphite monochromated Mo-K $\alpha$  radiation. The crystal to detector distance is fixed at 52 mm with a detector. The data were collected at a temperature of  $20\pm 1^\circ\text{C}$  to a maximum  $2\theta$  value of  $55.0^\circ$ . A total of 540 oscillation images were collected. The first and second sweep of data was done using  $\omega$  oscillations from  $-120.0$  to  $60.0^\circ$  in  $1.0^\circ$  steps. The exposure rate was  $8.0$  [sec/°]. The detector swing angle was  $-30.80^\circ$ . The crystal-to-detector distance was 52.00 mm. The readout was performed in the 0.146 mm pixel mode. Both crystals of **3d** and **3e** crystallize in triclinic space group P-1(#2). Figure 2 and 3 represents the ORTEP of the molecules **3d** and **3e**, respectively, with thermal ellipsoids drawn at 50% probability.

## Crystal Structure Determination and Refinements (3d)

A colorless prism crystal of **3d** having M.F.  $\text{C}_{26}\text{H}_{24}\text{N}_6\text{O}_2\cdot\text{C}_2\text{H}_6\text{OS}$  and approximate dimensions of  $0.455 \times 0.321 \times 0.300$  mm was mounted on a glass fiber. Data Reduction of the 13915 reflections that were collected, 6245 were unique ( $R_{\text{int}} = 0.0551$ ), equivalent reflections were merged. Data were collected and processed using Crystal Clear.<sup>36</sup> The linear absorption coefficient  $\mu$ , for Mo-K $\alpha$  radiation, is  $1.582\text{ cm}^{-1}$ . Empirical absorption correction was applied, which resulted in transmission factors ranging from 0.445 to 0.954. The data were corrected for Lorentz and polarization effects. The structure was solved by direct methods<sup>37</sup> and expanded using Fourier techniques. The non-hydrogen atoms were refined anisotropically. Hydrogen atoms were refined using the riding model. Hydrogen atoms associated with heteroatoms were refined independently in the isotropic approximation. The final cycle of full-matrix least-squares refinement [ $\text{SHELXL97}$ ,  $\sum w(F_o^2 - F_c^2)^2$  where  $w = \text{Least Squares weights}$ ] on  $F^2$  was based on 6245 observed reflections and 343 variable parameters and converged. The standard deviation of observation of unit weight was 1.03 and calculated by  $\sum w(F_o^2 - F_c^2)^2 / (N_o^2 - N_v)^{1/2}$ , where:  $N_o =$  number of observations  $N_v =$  number of variables. Unit weights were used. The maximum and minimum peaks on the final difference Fourier map corresponded to 0.67 and  $-0.55\text{ e } \text{\AA}^{-3}$  respectively. Neutral atom scattering factors were taken from Cromer and Waber.<sup>38</sup> Anomalous dispersion effects were included in F Calculation<sup>39</sup> the values for  $\Delta f'$  and  $\Delta f''$  were those of Creagh and McAuley.<sup>40</sup> The values for the mass attenuation coefficients are those of Creagh and Hubbell.<sup>41</sup> All calculations were performed using the crystal structure.<sup>42</sup> Crystallographic software package except for refinement, which was performed using [Direct Methods (SHELXD)] SHELXL-97.<sup>43</sup> Crystal Lattice Parameters  $a = 7.9223(9)\text{ \AA}$ ,  $b = 11.361(2)\text{ \AA}$ ,  $c = 16.227(2)\text{ \AA}$ ,  $\alpha = 73.440(4)^\circ$ ,  $\beta = 89.413(4)^\circ$ ,  $\gamma = 79.452(4)^\circ$ ,  $V = 1374.9(3)\text{ \AA}^3$ ,  $Z$  value is 2,  $D_{\text{cal}} = 1.258\text{ g cm}^{-3}$ ,  $F_{000} = 616.00$ ,  $\mu(\text{Mo-K}\alpha) = 2.054\text{ cm}^{-1}$ , Radiation is Mo-K $\alpha$  ( $\lambda = 0.71075\text{ \AA}$ ). Final refinement parameters:  $R_1$  [ $I > 2\sigma(I)$ ] = 0.0960,  $wR_2 = 0.3082$ ,  $R$  (All reflections) = 0.1310, Goodness of Fit Indicator = 1.095, Max Shift/Error in Final Cycle = 0.001, Maximum peak in Final Diff. Map =  $0.67\text{ e } \text{\AA}^{-3}$ , Minimum peak in Final Diff. Map =  $-0.55\text{ e } \text{\AA}^{-3}$  X-ray diffraction results were deposited at the Cambridge Crystallographic Data Center (CCDC 1969216). The X-ray crystal structure determination shows that the interatomic distances 1.355(5)  $\text{\AA}$  for  $\text{N}_2\text{-C}_{20}$  is near to that of a typical Aromatic C–N bond

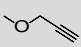
(1.47). The bond length for 1.153(6) Å for C<sub>9</sub>-N<sub>5</sub> and 1.145(7) Å for C<sub>8</sub>-N<sub>6</sub> are near to that of a typical C≡N Cyano bond length (1.16). The bond angles for C<sub>4</sub>-C<sub>5</sub>-C<sub>6</sub>, C<sub>2</sub>-C<sub>3</sub>-C<sub>4</sub> which illustrate that 123.7(4)°, 124.2(3)° of C<sub>2</sub>, C<sub>3</sub>, C<sub>4</sub>, C<sub>5</sub>, C<sub>6</sub> all adopt sp<sup>2</sup> hybrid orbit to form C=C double bonds. The bond angles for C<sub>12</sub>-O<sub>1</sub>-C<sub>16</sub> and C<sub>13</sub>-O<sub>2</sub>-C<sub>17</sub> is 117.1(4)° and 118.9(4)°, which illustrate that C<sub>12</sub>, O<sub>1</sub>, C<sub>16</sub>, C<sub>13</sub>, O<sub>2</sub>, C<sub>17</sub> all adopt sp<sup>2</sup> hybrid orbit to form C-O-C Single bond. In this molecule, N<sub>2</sub>-N<sub>3</sub>-N<sub>4</sub> bond angle is 107.6(4)° of the 1,2,3-triazole core is planar. A study of torsion angles of N<sub>2</sub>, N<sub>3</sub>, N<sub>4</sub>, C18 is 0.6(5) and C<sub>19</sub>, N<sub>2</sub>, N<sub>3</sub>, N<sub>4</sub> is -0.3(5)°.

### Crystal Structure Determination and Refinements (3e)

A colorless prism crystal of **3e** having M.F. C<sub>26</sub>H<sub>24</sub>N<sub>6</sub>O<sub>3</sub>·C<sub>2</sub>H<sub>6</sub>OS and approximate dimensions of 0.670 × 0.560 × 0.560 mm was mounted on a glass fiber. Data Reduction of the 14263 reflections that were collected, 6382 were unique ( $R_{int} = 0.0248$ ), equivalent reflections were merged. Data were collected and processed using Crystal Clear.<sup>36</sup> The linear absorption coefficient  $\mu$ , for Mo-K $\alpha$  radiation, is 1.603 cm<sup>-1</sup>. Empirical absorption correction was applied, which resulted in transmission factors ranging from 0.684 to 0.914. The data were corrected for Lorentz and polarization effects. The structure was solved by direct methods<sup>37</sup> and expanded using Fourier techniques. The non-hydrogen atoms were refined anisotropically. Hydrogen atoms associated with heteroatom were refined independently in the isotropic approximation. The final cycle of full-matrix least-squares refinement [SHELXL97,  $\Sigma w(F_o^2 - F_c^2)^2$  where  $w = \text{Least Squares weights}$ ] on  $F^2$  was based on 6382 observed reflections and 352 variable parameters and converged. The standard deviation of observation of unit weight was 1.51 and calculated by  $\Sigma w(F_o^2 - F_c^2)^2 / (N_o^2 - N_v)^{1/2}$ , where:  $N_o$  = number of observations,  $N_v$  = number of variables. Unit weights were used. The maximum and minimum peaks on the final difference Fourier map corresponded to 1.87 and

-0.71 e Å<sup>-3</sup>, respectively. Neutral atom scattering factors were taken from Cromer and Waber.<sup>38</sup> Anomalous dispersion effects were included in F Calculation<sup>39</sup>; the values for  $\Delta f'$  and  $\Delta f''$  were those of Creagh and McAuley.<sup>40</sup> The values for the mass attenuation coefficients are those of Creagh and Hubbell.<sup>41</sup> All calculations were performed using the crystal structure.<sup>42</sup> Crystallographic software package except for refinement, which was performed using Direct Methods (SHELXD and SHELXL-97).<sup>43</sup> Crystal Lattice Parameters  $a = 9.570(1)$  Å,  $b = 10.577(2)$  Å,  $c = 14.595(2)$  Å,  $\alpha = 73.440(4)^\circ$ ,  $\beta = 89.413(4)^\circ$ ,  $\gamma = 79.452(4)^\circ$ ,  $V = 1374.9(3)$  Å<sup>3</sup>,  $Z$  value is 2,  $D_{cal} = 1.258$  g cm<sup>-3</sup>,  $F_{000} = 616.00$ ,  $\mu(\text{Mo-K}\alpha) = 2.054$  cm<sup>-1</sup>, Radiation is Mo-K $\alpha$  ( $\lambda = 0.71075$  Å). Final refinement parameters:  $R_1 [I > 2\sigma(I)] = 0.1057$ ,  $wR_2 = 0.3850$ ,  $R$  (All reflections) = 0.1315, Goodness of Fit Indicator = 1.512, Max Shift/Error in Final Cycle = 0.004, Maximum peak in Final Diff. Map = 1.87 e Å<sup>-3</sup>, Minimum peak in Final Diff. Map = -0.71 e Å<sup>-3</sup>. X-ray diffraction results were deposited at the Cambridge Crystallographic Data Center (CCDC 1996628). The X-ray crystal structure determination shows that the interatomic distances 1.434(5) Å for N<sub>4</sub>-C<sub>20</sub> is near to that of a typical Aromatic C-N bond (1.47). The bond length for 1.154(6) Å for C<sub>9</sub>-N<sub>2</sub> and 1.150(7) Å for C<sub>8</sub>-N<sub>3</sub> are near to that of a typical C≡N Cyano bond length (1.16). The bond angles for C<sub>2</sub>-C<sub>3</sub>-C<sub>4</sub> and C<sub>4</sub>-C<sub>5</sub>-C<sub>6</sub>, which illustrate that 124.6(4)°, 124.1(4)° of C<sub>2</sub>, C<sub>3</sub>, C<sub>4</sub>, C<sub>5</sub>, C<sub>6</sub> all adopt sp<sup>2</sup> hybrid orbit to form C=C double bonds. The bond angles for C<sub>12</sub>-O<sub>2</sub>-C<sub>17</sub> and C<sub>23</sub>-O<sub>3</sub>-C<sub>26</sub> is 116.9(3)° and 118.4(4)°, which illustrate that C<sub>12</sub>, O<sub>2</sub>, C<sub>17</sub>, C<sub>23</sub>, O<sub>3</sub>, C<sub>26</sub> all adopt sp<sup>2</sup> hybrid orbit to form C-O-C Single bond. In this molecule, the N<sub>4</sub>-N<sub>5</sub>-N<sub>6</sub> bond angle is 106.4(3)° of the 1,2,3-triazole core is the planar aromatic ring. A study of the torsion angles, asymmetric parameters and least-squares plane calculations reveals that the three-membered ring of 1,2,3 triazole C<sub>19</sub>-N<sub>4</sub>-N<sub>5</sub>-N<sub>6</sub> is -0.4(4)° and N<sub>4</sub>-N<sub>5</sub>-N<sub>6</sub>-C<sub>18</sub> is -0.398(5)° are showing that the 1,2,3 triazole ring in the same plane. A study of torsion angles of N<sub>2</sub>, N<sub>3</sub>, N<sub>4</sub>, C18 is 0.6(5) and C<sub>19</sub>, N<sub>2</sub>, N<sub>3</sub>, N<sub>4</sub> is -0.3(5)°.

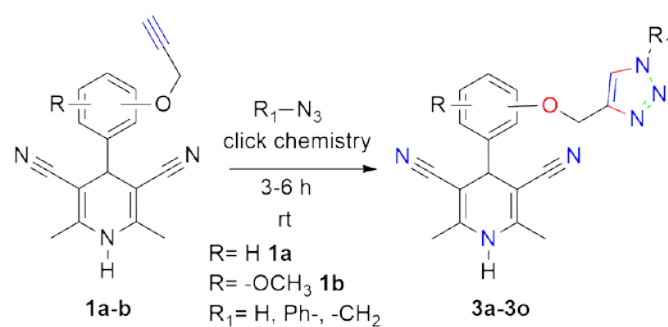
**Table 1.** Analytical data and yields of 1,2,3-triazole 1,4-dihydropyridine-3,5-dicarbonitrile derivatives (3a-3o).

Compound		R	R <sub>1</sub>	MF	MW	M.P. (°C)	Yield (%)
<b>3a</b>	<b>3</b>	H	-3-O <sub>2</sub> NPh	C <sub>24</sub> H <sub>19</sub> N <sub>7</sub> O <sub>3</sub>	453.45	256-257	70
<b>3b</b>	<b>3</b>	H	-3-ClPh	C <sub>24</sub> H <sub>19</sub> ClN <sub>6</sub> O	442.90	228-229	72
<b>3c</b>	<b>3</b>	H	-4-NCPH	C <sub>25</sub> H <sub>19</sub> N <sub>7</sub> O	433.46	220-221	75
<b>3d</b>	<b>4</b>	3-OMe	-4-MePh	C <sub>26</sub> H <sub>24</sub> N <sub>6</sub> O <sub>2</sub>	452.50	264-265	68
<b>3e</b>	<b>4</b>	3-OMe	-4-MeOPH	C <sub>26</sub> H <sub>24</sub> N <sub>6</sub> O <sub>3</sub>	468.50	268-269	71
<b>3f</b>	<b>4</b>	3-OMe	-4-FPh	C <sub>25</sub> H <sub>21</sub> FN <sub>6</sub> O <sub>2</sub>	456.47	258-259	70
<b>3g</b>	<b>4</b>	3-OMe	-4-NCPH	C <sub>26</sub> H <sub>21</sub> N <sub>7</sub> O <sub>2</sub>	463.49	270-271	73
<b>3h</b>	<b>3</b>	H	-2-O <sub>2</sub> NPh	C <sub>24</sub> H <sub>19</sub> N <sub>7</sub> O <sub>3</sub>	453.45	250-251	68
<b>3i</b>	<b>3</b>	H	-CH <sub>2</sub> Ph	C <sub>25</sub> H <sub>22</sub> N <sub>6</sub> O	422.48	260-261	67
<b>3j</b>	<b>3</b>	H	-4-MePh	C <sub>25</sub> H <sub>22</sub> N <sub>6</sub> O	422.48	240-241	70
<b>3k</b>	<b>4</b>	3-OMe	-2-O <sub>2</sub> NPh	C <sub>25</sub> H <sub>21</sub> N <sub>7</sub> O <sub>4</sub>	483.47	266-267	61
<b>3l</b>	<b>4</b>	3-OMe	-CH <sub>2</sub> Ph	C <sub>26</sub> H <sub>24</sub> N <sub>6</sub> O <sub>2</sub>	452.50	268-269	69
<b>3m</b>	<b>3</b>	H	-4-BrPh	C <sub>24</sub> H <sub>19</sub> BrN <sub>6</sub> O	487.35	202-203	69
<b>3n</b>	<b>3</b>	H	-CH <sub>2</sub> CN	C <sub>20</sub> H <sub>17</sub> N <sub>7</sub> O	371.39	240-241	65
<b>3o</b>	<b>4</b>	3-OMe	-CH <sub>2</sub> (4-NC)Ph	C <sub>27</sub> H <sub>23</sub> N <sub>7</sub> O <sub>2</sub>	477.51	272-273	75



## RESULTS AND DISCUSSIONS

The general route for the synthesis of 1,2,3-triazole-1,4-dihydropyridine-3,5-dicarbonitrile derivatives (**3a-3o**) was developed with the reaction of **1a-1o** alkynes with alkyl and aryl azides at room temperature for 3-6 h.



Scheme-1

**Scheme 1.** The general route for the synthesis of 1,2,3-triazole-1,4-dihydropyridine-3,5-dicarbonitrile derivatives.

The yield and melting points of prepared derivatives are given in Table 1. The structure of compounds **3d** and **3e** are given in Figures 2 and 3, respectively. The other structural data are given in Supplementary material.

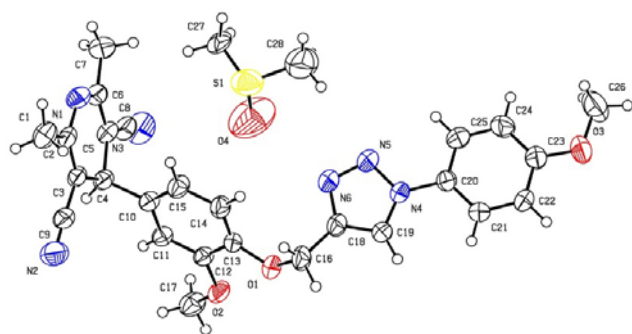


**Figure 2.** PLATON version of **3d** with data block ellipsoid plot drawn at 50% probability (CCDC 1969216).

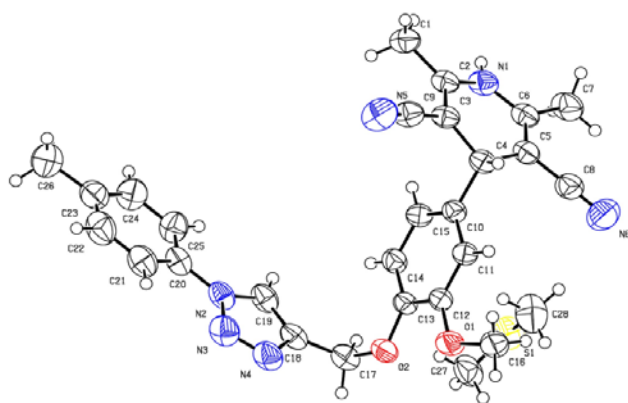


**Figure 3.** PLATON version of **3e** with data block ellipsoid plot drawn at 50% probability (CCDC 1996628).

## Antimicrobial activity of synthesized 1,2,3-triazole derivatives

Results of antibacterial activity of 1,2,3-triazole derivatives are represented in Table 1 and Figure 4. For *S. flexneri*, nine of the compounds show good potency. Compounds **3b** and **3d** displayed more potency with MIC value of  $100 \mu\text{g mL}^{-1}$  due to the presence of 3-Cl and 4-Me groups respectively, while compounds **3a** and **3e** displayed twofold lower MIC ( $200 \mu\text{g mL}^{-1}$ ) compared to standard due to the presence of 3-O<sub>2</sub>N and 4-OMe group attached to triazole ring. In more, compounds **3i**, **3k**, **3l**, and **3n** ( $400 \mu\text{g mL}^{-1}$ ) were found to be equipotent compared to the standard antibiotic Tetracycline. Compounds **3h**, **3j**, and **3f** displayed prominent activity having MIC values of  $50 \mu\text{g mL}^{-1}$  similar to Tetracycline against *P. aeruginosa* and *P. vulgaris* respectively and this potency was observed due to the presence of 2-NO<sub>2</sub>, 4-Me and 4-F groups attached to the triazole rings of **3h**, **3j**, and **3f** respectively. Comparatively, the derivative of 1,2,3-triazolyl-1,4-dihydropyridine having the propargyloxy group at the ortho position of the phenyl ring inhibited *P. mirabilis* and *K. pneumoniae* with the MIC:  $70 \mu\text{g mL}^{-1}$ .<sup>30</sup>

The MIC value of compound **3i** was  $12.5 \mu\text{g mL}^{-1}$  which is twofold lower than Tetracycline ( $25 \mu\text{g mL}^{-1}$ ) against *S. marcescens* that is due to the methylene group attached to the triazole ring. The MIC value of compound **3f** was found to be similar to Tetracycline against *E. aerogenes*. The compound **3e** was the only one that is active against *E. coli* (MIC:  $50 \mu\text{g mL}^{-1}$ ) due to the presence of 4-OMe group attached to the triazole ring.

## The meta-analysis of antibacterial activity

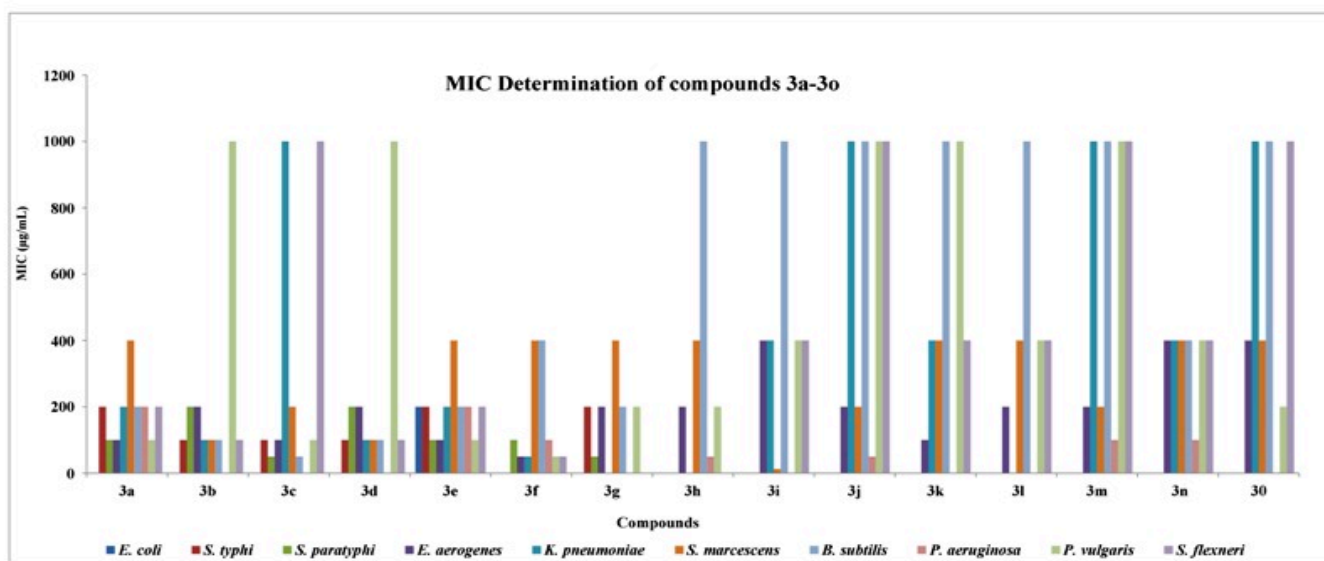
A meta-analysis of our experimental findings of antibacterial activity was done by Orange3-3.27.1-Miniconda software. As shown in Figures 5 and 6, if we compare the observations among compounds with different groups, it can be seen that various functional groups at the various position of core structure inhibited different test organisms with varying MICs. Compound **3k** (3-MeO at R) inhibited *K. pneumoniae* and *S. flexneri* with MIC:  $400 \mu\text{g mL}^{-1}$  that is lower than MIC shown by compound **3h**. On the other hand, compound **3h** (-H at R) inhibited *P. aeruginosa* with MIC:  $50 \mu\text{g mL}^{-1}$  that is much lower than the MIC given by compound **3k**. Compound **3h** also inhibited *P. vulgaris* with MIC:  $50 \mu\text{g mL}^{-1}$  that is much lower than the MIC given by **3k** (MIC:  $1000 \mu\text{g mL}^{-1}$ ). In comparison to standard antibiotic Tetracycline, compound **3h** inhibited *P. aeruginosa* with similar MIC:  $50 \mu\text{g mL}^{-1}$ . Compounds **3i** and **3l** have common functional group -CH<sub>2</sub>Ph at R<sub>1</sub> but a different functional group at R, i.e., -H and -OMe. Inhibitory activity of both compounds was nearly similar for all organisms, but compound **3i** (-H) inhibited *S. marcescens* with MIC  $12.5 \mu\text{g mL}^{-1}$  that compared to **3l** (-OMe group) with MIC:  $400 \mu\text{g mL}^{-1}$ . Besides, for *K. pneumoniae* MIC value of  $400 \mu\text{g mL}^{-1}$  was observed with compound **3i** while  $>1000 \mu\text{g mL}^{-1}$  was observed with compound **3l**. Furthermore, compounds **3a** and **3h** are different from the functional group at the R<sub>1</sub> position, i.e., -3-O<sub>2</sub>N and -2-O<sub>2</sub>NPh, respectively. Compound **3a** with -3-O<sub>2</sub>NPh inhibited *S. typhi* and *S. paratyphi* with MIC of  $200 \mu\text{g mL}^{-1}$  and  $100 \mu\text{g mL}^{-1}$  compared to **3h** that inhibited both organisms with  $>1000 \mu\text{g mL}^{-1}$ .



**Table 2.** Antibacterial activity of 1,2,3-triazole-1,4-dihydropyridine-3,5-dicarbonitrile derivatives (**3a-3o**).

Compound	EC	ST	SP	EA	KP	SM	BS	PA	PV	SF
	MIC ( $\mu\text{g mL}^{-1}$ )									
<b>3a</b>	-	200	100	100	200	400	200	200	100	200
<b>3b</b>	-	100	200	200	100	100	100	-	1000	100
<b>3c</b>	-	100	50	100	1000	200	50	-	100	1000
<b>3d</b>	-	100	200	200	100	100	100	-	1000	100
<b>3e</b>	200	200	100	100	200	400	200	200	100	200
<b>3f</b>	-	-	100	50	50	400	400	100	50	50
<b>3g</b>	-	200	50	200	-	400	200	-	200	-
<b>3h</b>	-	-	-	200	-	400	1000	50	200	-
<b>3i</b>	-	-	-	400	400	12.5	1000	-	400	400
<b>3j</b>	-	-	-	200	1000	200	1000	50	1000	1000
<b>3k</b>	-	-	-	100	400	400	1000	-	1000	400
<b>3l</b>	-	-	-	200	-	400	1000	-	400	400
<b>3m</b>	-	-	-	200	1000	200	1000	100	1000	1000
<b>3n</b>	-	-	-	400	400	400	400	100	400	400
<b>3o</b>	-	-	-	400	1000	400	1000	-	200	1000
Tetracycline	12.5	12.5	12.5	50	100	25	-	50	50	400
Penicillin	-	-	-	-	-	-	100	-	-	-

Legend: EC – *E. coli*, SP – *S. typhi*, SP – *S. paratyphi*, EA – *E. aerogenes*, KP – *K. pneumoniae*, SM – *S. marcescens*, BS – *B. subtilis*, PA – *P. aeruginosa*, PV – *P. vulgaris*, SF – *S. flexneri*.

**Figure 4.** MIC Determination of compounds **3a-3o**

Compound **3a** also inhibited *K. pneumoniae* and *S. flexneri* with MIC: 200  $\mu\text{g mL}^{-1}$  compared to MIC: 1000  $\mu\text{g mL}^{-1}$  given by compound **3h**. Compound **3a** (MIC: 200  $\mu\text{g mL}^{-1}$ ) was shown to be more potent against *S. flexneri* compared to standard antibiotic Tetracycline (MIC: 400  $\mu\text{g mL}^{-1}$ ).

If we compare the compounds **3d** and **3j**, it can be observed that **3d** inhibited *S. typhi* and *S. paratyphi* with MIC: 100 and 200  $\mu\text{g mL}^{-1}$  respectively that is lower than the MIC >1000  $\mu\text{g mL}^{-1}$  given by compound **3j**. Compound **3d** also inhibited *K. pneumoniae*, *B. subtilis*, and *S. flexneri* with lower MIC (100  $\mu\text{g mL}^{-1}$ ) compared to MIC (1000  $\mu\text{g mL}^{-1}$ ) given by **3j**. Compound **3j** having -H at R position

inhibited *P. aeruginosa* with MIC: 50  $\mu\text{g mL}^{-1}$  that is much lower than MIC >1000  $\mu\text{g mL}^{-1}$  given by compound **3d**. Compound **3j** showed equal potency with the standard for *P. aeruginosa* by inhibiting it with MIC: 50  $\mu\text{g mL}^{-1}$  that is similar to the MIC: 50  $\mu\text{g mL}^{-1}$  given by standard Tetracycline. Compound **3d** (MIC 100  $\mu\text{g mL}^{-1}$ ) was found to be more potent than standard (MIC: 400  $\mu\text{g mL}^{-1}$ ) against *S. flexneri* while equipotent to the standard against *K. pneumoniae* with MIC 100  $\mu\text{g mL}^{-1}$ . Among compounds **3c** and **3g**, both are having common functional group -4-NCPH at R<sub>1</sub> but different functional groups (-H and 3-MeO respectively) at R position. Compound **3c** inhibited *B. subtilis* with MIC: 50  $\mu\text{g mL}^{-1}$  compared to MIC 200  $\mu\text{g mL}^{-1}$  given by compound **3g**.



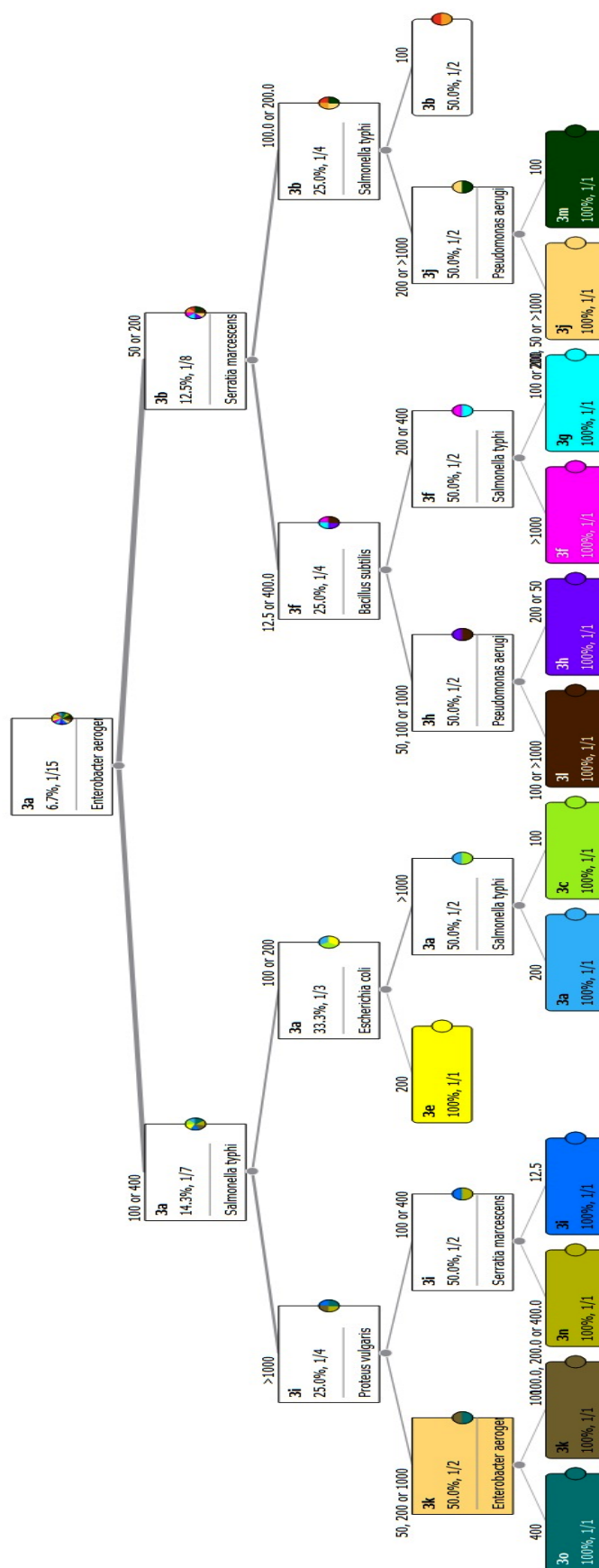


**Figure 6.** A meta-analysis of antibacterial activity of various synthesized triazole compounds (3a-3o).

Compound **3e** was the only compound (-4-MeOPh) that inhibited *E. coli* with MIC: 200  $\mu\text{g mL}^{-1}$  between compounds **3d**, **3e**, **3f**, **3g**, **3k**, **3l** and **3o** having common 3-MeO at R but different functional groups at R<sub>1</sub>. From the literature, it was found that cyano, phenacyl, and benzyl derivatives of 1,2,3-triazolyl-1,4-dihydropyridine hybrids were potent against *Escherichia coli* with MIC: 30  $\mu\text{g mL}^{-1}$ .<sup>30</sup> Some fluorinated chalcone-triazole hybrids having -OMe functional group was also reported to be active against *E. coli* with MIC value of 0.0032  $\mu\text{mol mL}^{-1}$ .<sup>27</sup>

Compound **3e** (MIC 200  $\mu\text{g mL}^{-1}$ ) was also found to be more potent against *S. flexneri* compared to standard (MIC 400  $\mu\text{g mL}^{-1}$ ). Among the compounds **3g** and **3o** (common 3-OMe at R but -4-NCPH at R<sub>1</sub>), compound **3g** inhibited *S. typhi* and *S. paratyphi* with MIC 200 and 50, respectively. Between the compounds, **3f** and **3m**, compound **3f** (3-OMe at R and -4 FPh at R<sub>1</sub>) inhibited *S. typhi*, *E. aerogenes*, *K. pneumoniae*, *P. vulgaris*, *S. flexneri* with MIC 100, 50, 50, 50 and 50  $\mu\text{g mL}^{-1}$  respectively that is lower than the MIC obtained by compound **3m** (-H at R and -4BrPh at R<sub>1</sub>).

Compound **3f** was found to equipotent to standard against *P. vulgaris* and *E. aerogenes* with MIC: 50  $\mu\text{g mL}^{-1}$  while more potent compared to standard (MIC 400  $\mu\text{g mL}^{-1}$  and 100  $\mu\text{g mL}^{-1}$ ) against *S. flexneri* and *K. pneumoniae* (MIC: 50  $\mu\text{g mL}^{-1}$ ). Between the compounds, **3g** and **3o** that possesses common -3-OMe but -4-CNPh and -4-CNCH<sub>2</sub>Ph groups at R<sub>1</sub> position exhibited almost similar activity against test organisms except for **3g** that inhibited *S. typhi* and *S. paratyphi* with MIC: 200 and 50  $\mu\text{g mL}^{-1}$  respectively, which is lower than the MIC (>1000  $\mu\text{g mL}^{-1}$ ) given by compound **3o**.

## CONCLUSION

This study reports the successful synthesis of 1,2,3-triazole-1,4-dihydropyridine-3,5-dicarbonitrile derivatives (**3a-3o**) in good yields and antibacterial activity of these derivatives containing triazole moiety against a wide range of bacterial strains. Besides, both crystal structures of **3d** and **3e** were herein reported for the first time. The *in vitro* antibacterial activity study revealed that all the compounds tested showed potent antibacterial activity which support the importance of these compounds as candidates for therapeutically efficient agents against bacteria. Among all compounds, **3e** inhibited all test bacterial strains.

This probably occurs due to the presence of -4-MeOPh group in the structure of compound **3e**. The lowest MIC was displayed by compounds **3j** and **3h** due to the presence of -4-MePh and -2-O<sub>2</sub>NPh groups at the fourth and second positions, respectively. These results confirmed that the integration of various functional groups to the 1,2,3-triazole moiety was greatly beneficial for the antibacterial activities, which could not only intensify the inhibition remarkably but also broaden their antimicrobial spectrum. These compounds are found to be promising for future antibacterial drugs.

## ACKNOWLEDGMENTS

The authors would like to express their thanks to the National Facility for Drug Discovery Complex, Department of Chemistry, Saurashtra University, Rajkot as well as Department of Microbiology, Gujarat Vidyapith, Sadra for the Laboratory Facility.

## REFERENCES

- López-Pueyo, M. J., Barcenilla-Gaite, F., Amaya-Villar, R., Garnacho-Monteroc, J., Antibiotic multiresistance in critical care units, *Intensive Medicine*, **2011**, *35*(1), 41-53. <https://doi.org/10.1016/j.medin.2010.07.011>
- New report calls for urgent action to avert antimicrobial resistance crisis, <https://www.who.int/news-room/detail/29-04-2019-new-report-calls-for-urgent-action-to-avert-antimicrobial-resistance-crisis> (Accessed on 29/07/2019).
- Gomtsyan, A., Heterocycles in drugs and drug discovery, *Chem. Heterocycl. Comp.*, **2012**, *48*, 7-10. <https://doi.org/10.1007/s10593-012-0960-z>
- Mishra, B. B., Kumar, D., Mishra, A., Mohapatra, P. P., Tiwari, V. K., Cyclo-Release Strategy in Solid-Phase Combinatorial Synthesis of Heterocyclic Skeletons, *In Advances in Heterocyclic Chemistry*, Katritzky, A. R., Academic Press publications, San Diego, USA, **2012**, *107*, 42-95. <https://doi.org/10.1016/B978-0-12-396532-5.00002-0>
- Belay, Y., Coetzee, L.C., Williams, D.B.G., Muller, A., Synthesis of novel 1,2,3-triazole based polycarboxylic acid functionalised ligands for MOF systems, *Tetrahedron Lett.*, **2019**, *60*, 501-503. <https://doi.org/10.1016/j.tetlet.2019.01.014>
- Yoo, E. J., Ahlquist, M., Kim, S. H., Bae, I., Fokin, V. V., Sharpless, K. B., Chang, S., Copper-Catalyzed synthesis of N-Sulfonyl-1,2,3-triazoles: Controlling Selectivity, *Angew. Chem. Int. Ed. Engl.*, **2007**, *46*, 1730-1733. <https://doi.org/10.1002/anie.200604241>
- Bourne, Y., Kolb H. C., Radic, Z., Sharpless, K. B., Taylor, P., Marchot, P., Freeze-frame inhibitor captures acetylcholinesterase in a unique conformation, *Proc. Natl. Acad. Sci. USA*, **2004**, *101*, 1449-1454. <https://doi.org/10.1073/pnas.0308206100>
- Chen, M., Lu, S. L., Yuan, G. P., Yang, S., Du, X., Synthesis and Antibacterial Activity of some Heterocyclic  $\beta$ -Enamino Ester Derivatives with 1,2,3-triazole, *Heterocycl. Commun.*, **2000**, *5*, 421-426. <https://doi.org/10.1515/HC.2000.6.5.421>
- Reddy, B. J., Reddy, V. P., Goud, G. L., Rao, Y. J., Synthesis of novel 1-benzyl/aryl-4-[(1-aryl-1H-1,2,3-triazol-4-yl)methoxy]methyl-1H-1,2,3-triazole derivatives and evaluation of their antimicrobial activity, *Russ. J. Gen. Chem.*, **2016**, *6*, 1424-1429. <https://doi.org/10.1134/S107036321606030X>
- Fu, X., Albermann, C., Zhang, C., Thorson, J. S., Diversity of Vancomycin Structure via Chemoselective Ligation, *Org. Lett.*, **2005**, *7*, 1513-155. <https://doi.org/10.1021/ol0501626>
- Zhang, B., Comprehensive review on the antibacterial activity of 1,2,3-triazole Hybrids, *Eur. J. Med. Chem.*, **2019**, *168*, 357-372. <https://doi.org/10.1016/j.ejmech.2019.02.055>
- Yan, W., Wang, X., Li, K., Li, T. X., Wang, J. J., Yao, K. C., Cao, L. L., Zhao, S. S., Ye, Y. H., Design, synthesis, and antifungal activity of carboxamide derivatives possessing 1,2,3-triazole as potential succinate dehydrogenase inhibitors, *Pestic. Biochem. Physiol.*, **2019**, *156*, 160-169. <https://doi.org/10.1016/j.pestbp.2019.02.017>



- <sup>13</sup>Devender, N., Gunjan, S., Chhabra, S., Singh, K., Pasam, V. R., Shukla, S. K., Sharma, A., Jaiswal, J., Singh, S. K., Kumar, Y., Lal, J., Trivedi, A. K., Tripathi, R., Tripathi, R. P., Identification of  $\beta$ -Amino Alcohol Grafted 1,4,5 Trisubstituted 1,2,3-Triazoles as Potent Antimalarial agents, *Eur. J. Med. Chem.*, **2016**, *109*, 187-198. <https://doi.org/10.1016/j.ejmech.2015.12.038>
- <sup>14</sup>Bonandi, E., Christodoulou, M. S., Fumagalli, G., Perdicchia, D., Rastelli, G., Passarella, D., The 1,2,3-triazole ring as a bioisostere in medicinal Chemistry, *Drug Discovery Today*, **2017**, *22(10)*, 1572-1581. <http://dx.doi.org/doi:10.1016/j.drudis.2017.05.014>
- <sup>15</sup>Pokhodylo, N., Shyyka, O., Matychuk, V., Synthesis and anticancer activity evaluation of new 1,2,3-triazole-4-carboxamide derivatives, *Med. Chem. Res.*, **2014**, *23*, 2426-2438. <http://dx.doi.org/doi:10.1007/s00044-013-0841-8>
- <sup>16</sup>Boechat, N., Ferreira, V. F., Ferreira, S. B., Ferreira, M. L. G., Da Silva, F. C., Bastos, M. M., Costa, M. S., Lourenco, M. C. S., Pinto, A. C., Krettli, A. U., Aguiar, A. C., Teixeira, B. M., Da Silva, N. V., Martins, P. R. C., Bezerra, F. A. F. M., Camilo, A. L. S., Da Silva, G. P., Costa, C. P. C., Novel 1,2,3-Triazole Derivatives for Use against Mycobacterium tuberculosis H37Rv (ATCC 27294) Strain, *J. Med. Chem.*, **2011**, *54*, 5988-5999. <https://doi.org/10.1021/jm2003624>
- <sup>17</sup>Da Silva, F. C., De Souza, M. C., Frugulhetti, Castro, H. C., Souza S. L., De Souza, T. M., Rodrigues, D. Q., Souza, A. M., Abreu, P. A., Passamani, F., Rodrigues, C. R., and Ferreira, V. F., Synthesis, HIV-RT inhibitory activity and SAR of 1-benzyl-1H-1,2,3-triazole derivatives of carbohydrates, *Eur. J. Med. Chem.*, **2009**, *44*, 373-383. <https://doi.org/10.1016/j.ejmech.2008.02.047>
- <sup>18</sup>Gao, C., Chang, L., Xu, Z., Yan, X. F., Ding, C., Zhao, F., Wu, X., Feng, L. S., Recent advances of tetrazole derivatives as potential antitubercular and antimalarial agents, *Eur. J. Med. Chem.*, **2019**, *163*, 404-412. <https://doi.org/10.1016/j.ejmech.2018.12.001>
- <sup>19</sup>Agalave, S. G., Maujan, S. R., Pore, V. S., Click Chemistry: 1,2,3-Triazoles as Pharmacophores, *Chem. -Asian J.*, **2011**, *10*, 2696-2718. <https://doi.org/10.1002/asia.201100432>
- <sup>20</sup>Kolb, H. C., Finn, M. G., Sharpless, K. B., Click Chemistry: Diverse Chemical Function from a Few Good Reactions, *Angew. Chem.-Int. Ed. Engl.*, **2001**, *11*, 2004-2021. [https://doi.org/10.1002/1521-3773\(20010601\)40:11<2004::AID-ANIE2004>3.0.CO;2-5](https://doi.org/10.1002/1521-3773(20010601)40:11<2004::AID-ANIE2004>3.0.CO;2-5)
- <sup>21</sup>Steve, N., Michel, B., Sravendra, R., Wolfgang, H. B., The CuAAC: Principles, Homogeneous and Heterogeneous Catalysts, and Novel Developments and Applications, *Macromol. Rapid Comm.*, **2020**, *41*, 1900359-1900391, <https://doi.org/10.1002/marc.201900359>
- <sup>22</sup>Rolf, H., Kinetics and reaction mechanisms: selected examples from the experience of forty years, *Pure Appl. Chem.*, **2009**, *61*, 613-628, <https://doi.org/10.1351/pac198961040613>
- <sup>23</sup>Palacios, F., Herran, E., Rubiales, G., Alonso, C., Regioselective synthesis of pyridines and dihydropyridines derived from  $\beta$ -amino acids and aminophosphonates by reaction of N-vinylc phosphazenes with  $\alpha$ ,  $\beta$ -unsaturated ketones, *Tetrahedron*, **2007**, *63*, 5669-5676. <https://doi.org/10.1016/j.tet.2007.03.146>
- <sup>24</sup>Keivanloo, A., Sepehri, S., Bakherad, M., Eskandari, M., Click Synthesis of 1,2,3-Triazoles-Linked 1,2,4-Triazino[5,6-b]indole, Antibacterial Activities and Molecular Docking Studies, *Chemistry Select*, **2020**, *5(13)*, 4091-4098. <https://doi.org/10.1002/slct.202000266>
- <sup>25</sup>Aarjane, M., Slassi, S., Tazi, B., Maouloua, M., Amine, A., Synthesis, antibacterial evaluation and molecular docking studies of novel series of acridone-1,2,3-triazole derivatives, *Struct. Chem.*, **2020**, *1-9*, <https://doi.org/10.1007/s11224-020-01512-0>
- <sup>26</sup>Hussain, M., Qadri, T., Hussain, Z., Saeed, A., Channar, P. A., Shehzadi, S. A., Hassan, M., Larik, F. A., Mahmood, T., Malik, A., Synthesis, antibacterial activity and molecular docking study of vanillin derived 1,4-disubstituted 1,2,3-triazoles as inhibitors of bacterial DNA synthesis, *Heliyon*, **2019**, *5(11)*, e02812. <https://doi.org/10.1016/j.heliyon.2019.e02812>
- <sup>27</sup>Yadav, P., Lal, K., Kumar, L., Kumar, A., Kumar, A., Paul, A. K., Kumar, R., Designed chalcone-1,2,3-triazole conjugates as potential antimicrobial agents synthesis, crystal structure and antimicrobial potential of some fluorinated chalcone-1,2,3-triazole conjugates, *Eur. J. Med. Chem.*, **2018**, *155*, 263-274. <http://doi.org/10.1016/j.ejmech.2018.05.055>
- <sup>28</sup>Govindaiah, S., Sreenivasa, S., Ramakrishna, R. A., Rao, T. M. C., Nagabhushana, H., Regioselective Synthesis, Antibacterial, Molecular Docking and Fingerprint Applications of 1-Benzhydrylpiperazine Derivatized 1,4-Disubstituted 1,2,3-Triazoles, *Chemistry Select*, **2018**, *3*, 8111-8117, <https://doi.org/10.1002/slct.201801364>
- <sup>29</sup>Morsy, H. A., Mohammed, S. M., Hamid, A. M. A., Moustafa, A. H., El-Sayed, H. A., Click Synthesis of 1,2,3-Triazole Nucleosides Based on Functionalized Nicotinonitriles, *Russ. J. Org. Chem.*, **2020**, *56(1)*, 143-147. <https://doi.org/10.1134/S1070428020010224>
- <sup>30</sup>Archana, S., Dinesh, M., Ranganathan, R., Ponnuswamy, A., Kalaiselvi, P., Chellammal, S., Subramanian, G., Murugavel, S., Water mediated one-pot synthesis and biological evaluation of 1,2,3-triazolyl-1,4-dihydropyridine hybrids, *Res. Chem. Intermed.*, **2017**, *43(1)*, 187-202. <https://doi.org/10.1007/s11164-016-2614-8>
- <sup>31</sup>Vatmurge, N. S., Hazra, B. G., Pore, V. S., Shirazi, F., Deshpande, M. V., Kadreppa, S., Chattopadhyay, S., Gonnade, R. G., Synthesis and biological evaluation of bile acid dimers linked with 1,2,3-triazole and bis- $\beta$ -lactam, *Org. Bioorg. Chem.*, **2008**, *6*, 3823-3830. <https://doi.org/10.1039/b809221d>
- <sup>32</sup>Phillips, O. A., Udo, E. E., Abdel-Hamid, M. E., Varghese, R., Synthesis and antibacterial activity of novel 5-(4-methyl-1H-1,2,3-triazole) methyl oxazolidinones, *Eur. J. Med. Chem.*, **2009**, *44(8)*, 3217-3227. <https://doi.org/10.1016/j.ejmech.2009.03.024>
- <sup>33</sup>Reddy, L. V. R., Reddy, P. V., Mishra, N. N., Shukla, P. K., Yadav, G., Srivastava, R., Shaw, A. K., Synthesis and biological evaluation of glycal-derived novel tetrahydrofuran1,2,3-triazoles by 'click' chemistry, *Carbohydr. Res.*, **2010**, *345(11)*, 1515-1521. <https://doi.org/10.1016/j.carres.2010.03.031>
- <sup>34</sup>Singh, H., Sindhu, J., Khurana, J. M., Sharma, C., Aneja, K. R., A Facile Eco-Friendly One-Pot Five-Component Synthesis of Novel 1,2,3-Triazole-Linked Pentasubstituted 1,4-Dihydropyridines and their Biological and Photophysical Studies, *Aust. J. Chem.*, **2013**, *66*, 1088-1096. <http://dx.doi.org/10.1071/CH13217>
- <sup>35</sup>Reddy, B. J., Reddy, V. P., Goud, G. L., Rao, Y. J., Premkumar, Supriya, K., Synthesis of novel 1-benzyl/aryl-4-[(1-aryl-1H-1,2,3-triazol-4-yl)methoxy]methyl]-1H-1,2,3-triazole derivatives and evaluation of their antimicrobial activity, *Russ. J. Gen. Chem.*, **2016**, *6*, 1424-1429. <https://doi.org/10.1134/S107036321606030X>
- <sup>36</sup>Pflugrath, J. W., The finer things in X-ray diffraction data Collection, *Acta Cryst. Sect. D.*, **1999**, *55*, 1718-1725. <https://doi.org/10.1107/S090744499900935X>
- <sup>37</sup>Altomare, A., Cascarano, G., Giacovazzo, C., Guagliardi, A., Burla, M., Polidori, G., Camalli, M., SIR92 - a program for automatic solution of crystal structures by direct methods, *J. Appl. Cryst.*, **1994**, *27*, 435. <https://doi.org/10.1107/S002188989400021X>
- <sup>38</sup>Cromer, D. T., Waber, J. T., *Atomic Scattering Factors for X-Rays, International Tables for X-ray Crystallography*, volume-4, The Kynoch Press, Birmingham, England, Table 2.2 A, 71-147, **1974**.
- <sup>39</sup>Ibers, J. A., Hamilton, W. C., Dispersion corrections and crystal structure refinements, *Acta Cryst.*, **1964**, *17*, 781-782. <https://doi.org/10.1107/S0365110X64002067>

- <sup>40</sup>Creagh, D. C., McAuley, W. J., *The International Tables for X-Ray Crystallography*, (A.J.C. Wilson, ed.), Volume-C Table 4.2.6.8, Kluwer Academic Publishers, Boston, 219-222, **1992**. <https://doi.org/10.1107/97809553602060000592>
- <sup>41</sup>Creagh, D. C., Hubbell, J. H., *The International Tables for X-Ray Crystallography*, (A.J.C. Wilson, ed.), Volume-C Table 4.2.4.3, Kluwer Academic Publishers, Boston, 200-206, **1992**. <https://doi.org/10.1107/97809553602060000592>
- <sup>42</sup>Crystal Structure Analysis Package, (CrystalStructure 4.0) Rigaku Corporation (2000-2010) Tokyo 196-8666, Japan.
- <sup>43</sup>Sheldrick, G. M., A short history of SHELX, *Acta Cryst., Sect. A.* **2008**, 64, 112-122. <https://doi.org/10.1107/S0108767307043930>
- <sup>44</sup>Wayne, P. A., CLSI. *Methods for Dilution Antimicrobial Susceptibility Tests for Bacteria That Grow Aerobically*, 11<sup>th</sup> Edition. CLSI Standard M07, **2018**. <https://clsi.org/standards/products/microbiology/documents/m07/>
- <sup>45</sup>Valgas, C., De-Souza, S. M., Smania, E. F., Smania, Jr. A., Screening methods to determine antibacterial activity of natural products, *Braz. J. Microbiol.*, **2007**, 38, 369-380. <https://doi.org/10.1590/S1517-83822007000200034>
- <sup>46</sup>Wiegand, I., Hilpert, K., Hancock, R. E., Agar and broth dilution methods to determine the minimal inhibitory concentration (MIC) of antimicrobial substances, *Nat. Protoc.*, **2008**, 3, 163-175. <https://doi.org/10.1038/nprot.2007.521>
- <sup>47</sup>Breed, R. S., Murray, E. G. D., Hitchens, A. P., *Bergey's Manual of Determinative Bacteriology*, 6<sup>th</sup> Edition, The Williams & Wilkins Company: Baltimore, USA, pp. 443-544, **1948**.

**This paper was presented at the International Conference "**

**CONFERENCE ON MOLECULAR STRUCTURE & INSTRUMENTAL APPROACHES"**

**at RK University, Rajkot (Gujarat-India) on 26-27th November 2020**

Received: 04.12.2020.

Accepted: 11.12.2020



# SYNTHESIS AND CHARACTERIZATION OF SOME DISTYRYL-DERIVATIVES FOR AGRICULTURAL USES

Shaban A. A. Abdel-Raheem,<sup>[a]\*</sup> Adel M. Kamal El-Dean,<sup>[b]</sup> Reda Hassanien,<sup>[c]</sup> Mohamed E. A. El-Sayed<sup>[a]</sup> and Aly A. Abd-Ella<sup>[d]</sup>

**Keywords:** Synthesis, distyryl-containing compounds, agricultural bioactivity, acetamiprid, cowpea aphid.

Three distyryl-containing compounds, namely, 2-((cyanomethyl)thio)-4,6-distyrylnicotinonitrile (**2**), 3-amino-4,6-distyrylthieno[2,3-*b*]pyridine-2-carbonitrile (**3**) and 2-((2-cyanoethyl)thio)-4,6-distyrylnicotinonitrile (**4**) have been prepared and characterized by elemental and spectroscopic analyses. The three compounds contain the pyridine moiety and are considered neonicotinoids analogues. Because neonicotinoids were considered the most effective pesticides, the biological activity of the distyryl-containing compounds as potential insecticides against cowpea aphid, *Aphis craccivora* Koch was evaluated. The agricultural bioactivity results of these compounds showed that the insecticidal activity varied from good to moderate against cowpea aphid insects.

\* Corresponding Authors

E-Mail: drshaban202025@gmail.com

- [a] Soil, Water, and Environment Research Institute, Agriculture Research Center, Giza, Egypt  
 [b] Chemistry Department, Faculty of Science, Assiut University, 71516 Assiut, Egypt  
 [c] Chemistry Department, Faculty of Science, New Valley University, El-Kharja, 72511, Egypt  
 [d] Plant Protection Department, Faculty of Agriculture, Assiut University, 71526 Assiut, Egypt

## Introduction

It is known that heterocyclic compounds, especially pyridine derivatives, are widely used and different important applications for these compounds have been previously reported.<sup>1-6</sup> So, the chemists around the world focused on the synthesis and the applications of these compounds. Some neonicotinoids contain pyridine moiety in their structure. Different advantages of neonicotinoids insecticides such as their high efficacy with lack cross-resistance, low mammalian toxicity, a novel mode of action specific for (nAChRs) and protection of great range of crops, resulted in a large use of these compounds in the field of crop protection at the present time.<sup>7-13</sup>

Genotoxic effect, oxidative stress, DNA damage, and clastogenic effect are different results that were found when the exposure to imidacloprid as neonicotinoid insecticide was monitored in some modern researches after long-term exposure of rabbits to that insecticide.<sup>14-17</sup> So, in view of the above results, the work in this paper was planned to prepare some neonicotinoids analogues compounds and screening their toxicological activity as insecticides against cowpea aphid, *Aphis craccivora* Koch (Homoptera: Aphididae) hoping to be with a higher insecticidal activity and lower toxicity.

## Experimental

Melting points of the prepared compounds were determined by the means of a Fisher-Johns apparatus. IR spectra and elemental analyses were determined by a Pye-

Unicam SP3-100 spectrophotometer using the KBr disk technique and a Vario EL C, H, N, S analyzer, respectively. <sup>1</sup>H NMR, <sup>13</sup>C NMR, and DEPT 135 spectra measurement was accomplished via a Bruker 400 MHz spectrometer in the presence of TMS as an internal reference. Chemical shifts are given in  $\delta$  (ppm). The purity of the synthesized compounds was checked by TLC. 3-Cyano-4,6-distyrylpyridin-2(1*H*)-thione (**1**) was prepared according to the reported method.<sup>5</sup> The neonicotinoid insecticide (acetamiprid, purity > 98 %) was purchased from Sigma-Aldrich (France). Batches of cowpea aphid were gathered from faba bean, *Vicia faba* L., growing on the fields of the experimental farm of Assiut University. Compounds **2-4** and acetamiprid were screened for their insecticidal activity against the gathered cowpea aphids.

### 2-((Cyanomethyl)thio)-4,6-distyrylnicotinonitrile (2).

A mixture of compound (**1**) (2 g, 0.006 mol), chloroacetonitrile (0.006 mol), and fused sodium acetate (0.6 g, 0.007 mol) in ethanol (25 mL) was heated under reflux for 30 min. The formed precipitate was collected and recrystallized from ethanol-dioxane mixture (1:2) as pale yellow crystals of compound **2**. Yield 89 %. m. p. 121-122 °C. IR ( $\nu$ ) (KBr): 3026 (C-H aromatic), 2978, 2931, 2848 (C-H aliphatic), 2246 (C $\equiv$ N aliphatic), 2211 (C $\equiv$ N conjugated), 1634 (C=N) cm<sup>-1</sup>. <sup>1</sup>H NMR (DMSO-*d*<sub>6</sub>, 400 MHz):  $\delta$  = 7.20-8.08 (m, 15H, 2CH=CH and Ar-H), 4.36 (s, 2H, CH<sub>2</sub>). <sup>13</sup>C NMR (DMSO-*d*<sub>6</sub>, 100 MHz):  $\delta$  = 162.45, 159.37, 149.51, 137.68, 136.12, 135.56, 130.44, 129.90, 129.44, 128.07, 126.48, 118.10, 116.10, 115.19, 102.07, 16.39. DEPT 135 (DMSO-*d*<sub>6</sub>, 100 MHz):  $\delta$  = 136.12 (CH), 135.56 (CH), 130.44 (CH), 129.90 (CH), 129.43 (CH), 128.06 (CH), 126.48 (CH), 115.19 (CH), 16.39 (CH<sub>2</sub>). Anal. Calcd. for C<sub>24</sub>H<sub>17</sub>N<sub>3</sub>S: C, 75.96; H, 4.52; N, 11.07; S, 8.45. Found: C, 75.97; H, 4.49; N, 11.06; S, 8.47.

### 3-Amino-4,6-distyrylthieno[2,3-*b*]pyridine-2-carbonitrile (3)

In addition to the procedure reported before,<sup>18</sup> compound (**3**) was synthesized here by suspending of compound (**2**) (0.005 mol) in sodium ethoxide solution (0.5 g of sodium in

31 mL of absolute ethanol) and heating for 5 min under reflux. The formed product after cooling was collected and recrystallized from ethanol-dioxane mixture (1:2) as orange crystals of compound **3**. Yield 90 % m. p. 156-157 °C. IR ( $\nu$ ) (KBr): 3383, 3314, 3199 (NH<sub>2</sub>), 3019 (C-H aromatic), 2917 (C-H aliphatic), 2198 (C≡N) cm<sup>-1</sup>. <sup>1</sup>H NMR (DMSO-*d*<sub>6</sub>, 400 MHz):  $\delta$  = 7.31-7.86 (m, 16H, 2CH=CH, NH of NH<sub>2</sub> and Ar-H), 6.18 (s, 1H, NH of NH<sub>2</sub>). <sup>13</sup>C NMR (DMSO-*d*<sub>6</sub>, 100 MHz):  $\delta$  = 160.43, 156.61, 151.90, 144.76, 144.31, 135.19, 129.35, 129.21, 128.11, 128.05, 127.79, 127.34, 123.00, 117.25, 115.87, 76.23. DEPT 135 (DMSO-*d*<sub>6</sub>, 100 MHz):  $\delta$  = 129.35 (CH), 129.20 (CH), 128.11 (CH), 128.05 (CH), 127.79 (CH), 127.34 (CH), 123.00 (CH), 117.24 (CH). The mass spectrum of compound **3** showed a molecular ion peak at  $m/z$  = 379.2 (M<sup>+</sup>, 29.47 %) which is in agreement with its molecular formula (C<sub>24</sub>H<sub>17</sub>N<sub>3</sub>S). Anal. Calcd. for C<sub>24</sub>H<sub>17</sub>N<sub>3</sub>S: C, 75.96; H, 4.52; N, 11.07; S, 8.45. Found: C, 75.98; H, 4.47; N, 11.09; S, 8.46.

#### 2-((2-Cyanoethyl)thio)-4,6-distyrylnicotinonitrile (**4**)

A mixture of compound (**2**) (2 g, 0.006 mol), acrylonitrile (0.006 mol) and fused sodium acetate (0.6 g, 0.007 mol) in ethanol (25 mL) was heated under reflux for 3 h. The formed precipitate was collected and recrystallized from ethanol-dioxane mixture (1:2) as yellow crystals of compound **4**. Yield 88 %. m. p. 158-159 °C. IR ( $\nu$ ) (KBr): 3024 (C-H aromatic), 2917, 2849 (C-H aliphatic), 2250 (C≡N aliphatic), 2211 (C≡N conjugated) cm<sup>-1</sup>. <sup>1</sup>H NMR (DMSO-*d*<sub>6</sub>, 400 MHz):  $\delta$  = 7.19-7.92 (m, 15H, 2CH=CH and Ar-H), 3.51-3.54 (t, 2H, CH<sub>2</sub>CN), 2.99-3.02 (t, 2H, SCH<sub>2</sub>). <sup>13</sup>C NMR (DMSO-*d*<sub>6</sub>, 100 MHz):  $\delta$  = 162.17, 157.40, 149.83, 138.63, 136.81, 135.67, 130.36, 129.82, 129.43, 128.05, 126.97, 119.63, 115.45, 114.72, 102.54, 25.98, 18.12. DEPT 135 (DMSO-*d*<sub>6</sub>, 100 MHz):  $\delta$  = 136.80 (CH), 135.67 (CH), 130.36 (CH), 129.82 (CH), 129.43 (CH), 128.05 (CH), 126.97 (CH), 114.71 (CH), 25.98 (CH<sub>2</sub>), 18.12 (CH<sub>2</sub>). Anal. Calcd. for C<sub>25</sub>H<sub>19</sub>N<sub>3</sub>S: C, 76.31; H, 4.87; N, 10.68; S, 8.15. Found: C, 76.49; H, 4.86; N, 10.69; S, 8.17.

#### Laboratory bioassay

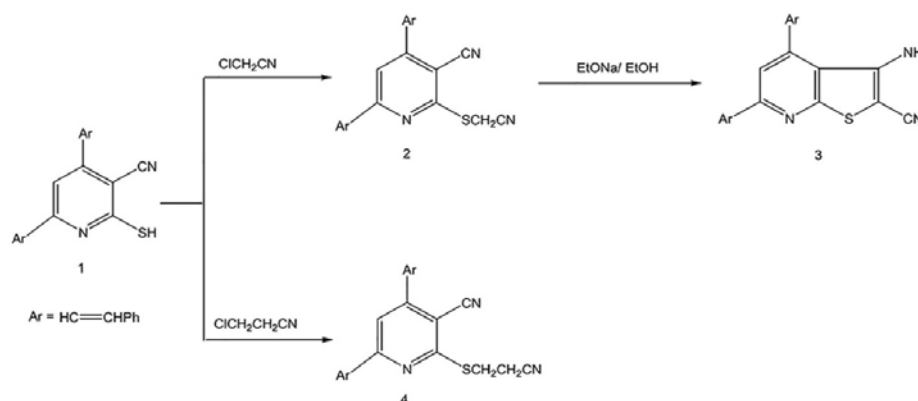
The insecticidal activity of the prepared compounds was evaluated via leaf dip bioassay method.<sup>19</sup> Laboratory screening data are reported here for the title compounds to

find out the concentrations that are required to kill 50 % (LC<sub>50</sub>) of the gathered insects. Number of six concentrations of each synthesized compound plus 0.1 % Triton X-100 (surfactant) was used. 20 adults and 20 nymphs of cowpea aphids, almost of the same size, were dipped 3 times in every concentration for ten seconds. The cowpea aphids were dried at RT for 0.5 h. Cowpea aphids control batches were also used. The aphids after drying were transferred to Petri dishes (9 centimeters diameter) and grasped for 24 and 48 h at photoperiod of 12:12 (light/ dark), 22 ± 2 °C and 60 ± 5 % relative humidity. Aphids mortality was counted after 24 and 48 h of test by means of a binocular microscope. The aphids that not capable of coordinating forward movement were considered dead. Toxicological activity check of the title compounds was repeated twice, and the results were corrected using Abbott's formula.<sup>20</sup> Slope values and median lethal concentrations (LC<sub>50</sub>) of the prepared compounds were calculated through a probit regression analysis program and recorded in ppm.<sup>21</sup>

## RESULTS AND DISCUSSION

The synthesis of the title compounds was started from (**1**) which was prepared according to the reported method.<sup>5</sup> Refluxing of compound **1** with chloroacetonitrile in ethanol containing slightly excess amounts of fused sodium acetate for 30 min resulted in the formation of 2-((cyanomethyl)thio)-4,6-distyrylnicotinonitrile (**2**). The latter compound underwent intramolecular Thorpe-Ziegler cyclization upon refluxing in ethanol containing catalytic amounts of sodium ethoxide for 5 min to give the corresponding thienopyridine compound 3-amino-4,6-distyrylthieno[2,3-*b*]pyridine-2-carbonitrile (**3**) (Scheme 1).

Spectroscopic data and elemental analyses of compounds **2** and **3** were in agreement with their proposed structure. IR spectrum of compound **2** showed absorption bands at 2246 and 2211 cm<sup>-1</sup> characteristic for (C≡N aliphatic) and (C≡N conjugated) groups. The absorption band of (C≡N conjugated) of compound **2** was disappeared when cyclised to give the thienopyridine **3** and was replaced by 3383 and 3199 cm<sup>-1</sup> for NH<sub>2</sub>. <sup>1</sup>H NMR spectrum (DMSO-*d*<sub>6</sub>, 400 MHz) of compound **2** showed singlet signal at 4.36 for (CH<sub>2</sub>) group. The signal of (CH<sub>2</sub>) group of compound **2** in the <sup>1</sup>H NMR spectrum was disappeared when cyclised to give compound **3**.



**Scheme 1.** Synthesis of distyryl compounds.



**Table 1.** Insecticidal activity of acetamiprid and compounds **2-4** against the cowpea aphid nymphs after 24 and 48 h of treatment.

24 h after treatment				48 h after treatment		
Compd.	Slope ± SE	LC <sub>50</sub> (ppm)	Toxic ratio	Slope ± SE	LC <sub>50</sub> (ppm)	Toxic ratio
Acetamipri	0.34±0.02	0.045	1	0.42±0.03	0.006	1
<b>2</b>	0.44±0.03	0.064	0.703	0.48±0.03	0.013	0.462
<b>3</b>	0.38±0.03	0.097	0.464	0.49±0.04	0.018	0.333
<b>4</b>	0.41±0.03	0.052	0.865	0.48±0.03	0.010	0.600

**Table 2.** Insecticidal activity of acetamiprid and compounds **2-4** against the cowpea aphid adults after 24 and 48 h of treatment.

24 h after treatment				48 h after treatment		
Compd.	Slope ± SE	LC <sub>50</sub> (ppm)	Toxic ratio	Slope ± SE	LC <sub>50</sub> (ppm)	Toxic ratio
Acetamipri	0.24±0.02	0.225	1	0.32±0.03	0.023	1
<b>2</b>	0.36±0.02	0.322	0.699	0.39±0.03	0.035	0.657
<b>3</b>	0.39±0.03	0.754	0.298	0.45±0.03	0.049	0.469
<b>4</b>	0.36±0.02	0.282	0.798	0.41±0.03	0.034	0.676

DEPT 135 (DMSO-*d*<sub>6</sub>, 100 MHz) spectrum of compound **2** showed characteristic signal at 16.39 for (CH<sub>2</sub>) group. The signal of (CH<sub>2</sub>) group of compound **2** in the DEPT 135 spectrum was disappeared when cyclised to give compound **3**. The mass spectrum of compound **3** showed a molecular ion peak at *m/z* = 379.2 (M<sup>+</sup>, 29.47 %) which is in agreement with its molecular formula (C<sub>24</sub>H<sub>17</sub>N<sub>3</sub>S).

Reflux of compound **1** with acrylonitrile in ethanol containing slightly excess amounts of fused sodium acetate for 3 h resulted in the formation of 2-((2-cyanoethyl)thio)-4,6-distyrylnicotinonitrile (**4**) (Scheme 1). The chemical structure of compound **4** was confirmed by elemental and spectral analyses. IR spectrum of compound **4** showed absorption bands at 2250 and 2211 cm<sup>-1</sup> characteristic for (2C≡N) groups. <sup>1</sup>H NMR spectrum (DMSO-*d*<sub>6</sub>, 400 MHz) of compound **4** showed two triplet signals at 3.51-3.54 and 2.99-3.02 for (2CH<sub>2</sub>) groups. DEPT 135 (DMSO-*d*<sub>6</sub>, 100 MHz) spectrum of compound **4** showed characteristic signals at 25.98 and 18.12 for (2CH<sub>2</sub>) groups.

#### Insecticidal activity test for the cowpea aphid nymphs.

Compounds **2**, **3**, and **4** were investigated for their insecticidal activities against the nymphs of the collected aphids, and the results are presented in table 1. The insecticidal activity results indicated that, after 24 h of

treatment compounds **2**, **3**, and **4** exhibited high to low insecticidal activity against the cowpea aphid nymphs and the LC<sub>50</sub> values ranged from 0.052 to 0.097 ppm, whereas the LC<sub>50</sub> value of acetamiprid was 0.045 ppm. Whilst after 48 h of treatment, the insecticidal activity of compounds **2**, **3**, and **4** against cowpea aphid nymphs varied from strong to weak with LC<sub>50</sub> values assorted from 0.01 to 0.018 ppm, but the LC<sub>50</sub> value of acetamiprid was 0.006 ppm. These results indicate that compounds **2** and **4** have a high insecticidal activity close to that of acetamiprid insecticide against cowpea aphid nymphs after 24 and 48 h of test.

#### Insecticidal activity test for the adults of cowpea aphid

Compounds **2**, **3**, and **4** were investigated also for their insecticidal activity against the adults of the collected aphids, and the results are presented in table 2. From the results obtained after 24 h of insecticidal activity test, it was found that the compounds **2**, **3**, and **4** have strong to weak activity and LC<sub>50</sub> values ranged from 0.282 to 0.754 ppm, while 0.225 ppm was the LC<sub>50</sub> value of acetamiprid. Compound **4** possess a high insecticidal activity, and its LC<sub>50</sub> value is 0.282 ppm. After 48 h of the agricultural bioactivity test as insecticides, the insecticidal activity of compounds **2**, **3**, and **4** against cowpea aphid adults varied from high to low with LC<sub>50</sub> values ranged from 0.034 to 0.049 ppm, whilst the LC<sub>50</sub> value of acetamiprid was 0.023 ppm. Thus, compounds **2** and **4** showed a high insecticidal activity close to that of acetamiprid insecticide against cowpea aphid adults after 24 and 48 h of treatment.

#### Structure-action relationship

It is interesting to note that the insecticidal activity of the compound 2-((2-cyanoethyl)thio)-4,6-distyrylnicotinonitrile (**4**) with two cyano groups in its structure is more than that of the compound 2-((cyanomethyl)thio)-4,6-distyrylnicotinonitrile (**2**) that contains also two cyano groups in its structure, which may be due to the presence of the chain (CH<sub>2</sub>CH<sub>2</sub>CN) in compound **4** instead (CH<sub>2</sub>CN) in compound **2**. The insecticidal activity of the opened form of compounds **2** is more than that of its closed form, the compound 3-amino-4,6-distyrylthieno[2,3-*b*]pyridine-2-carbonitrile (**3**), which may be due to the presence of two cyano group in the former and one cyano group in the latter.

#### CONCLUSION

Three distyryl-containing compounds, which are considered neonicotinoid analogs, were prepared. The agricultural bioactivity as potential insecticides against

cowpea aphid, *Aphis craccivora* Koch for these compounds was investigated. The data obtained from this investigation proved that these compounds have insecticidal activities varied from good to moderate against cowpea aphids in comparison of acetamiprid insecticide as a reference.

## REFERENCES

- Bakhite, E. A., Abd-Ella, A. A., El-Sayed, M. E. A., Abdel-Raheem, Sh. A. A., Pyridine derivatives as insecticides. Part 1: Synthesis and toxicity of some pyridine derivatives against Cowpea Aphid, *Aphis craccivora* Koch (Homoptera: Aphididae), *J. Agric. Food Chem.*, **2014**, 62(41), 9982–9986. DOI: [10.1021/jf503992y](https://doi.org/10.1021/jf503992y)
- Bakhite, E. A., Abd-Ella, A. A., El-Sayed, M. E. A., Abdel-Raheem, Sh. A. A., Pyridine derivatives as insecticides. Part 2: Synthesis of some piperidinium and morpholinium cyanopyridinethiolates and their insecticidal activity, *J. Saud. Chem. Soc.*, **2017**, 21(1), 95–104. <https://doi.org/10.1016/j.jscs.2016.02.005>
- Kamal El-Dean, A. M., Abd-Ella, A. A., Hassanien, R., El-Sayed, M. E. A., Zaki, R. M., Abdel-Raheem, Sh. A. A., Chemical design and toxicity evaluation of new pyrimidothienotetrahydroisoquinolines as potential insecticidal agents, *Toxicol. Rep.*, **2019**, 6, 100–104. <https://doi.org/10.1016/j.toxrep.2018.12.004>
- Altaf, A. A., Shahzad, A., Gul, Z., Rasool, N., Badshah, A., Lal, B., Khan, E., A Review on the Medicinal Importance of Pyridine Derivatives, *J. Drug Des. Med. Chem.*, **2015**, 1, 1–11. DOI: [10.11648/j.jddmc.20150101.11](https://doi.org/10.11648/j.jddmc.20150101.11)
- Kamal El-Dean, A. M., Abd-Ella, A. A., Hassanien, R., El-Sayed, M. E. A., Abdel-Raheem, Sh. A. A., Design, Synthesis, Characterization, and Insecticidal Bioefficacy Screening of Some New Pyridine Derivatives, *ACS Omega*, **2019**, 4, 8406–8412. DOI: [10.1021/acsomega.9b00932](https://doi.org/10.1021/acsomega.9b00932)
- Al-Taifi, E. A., Abdel-Raheem, Sh. A. A., Bakhite, E. A., Some reactions of 3-cyano-4-(*p*-methoxyphenyl)-5-oxo-5,6,7,8-tetrahydroquinoline-2(1*H*)-thione; Synthesis of new tetrahydroquinolines and tetrahydrothieno[2,3-*b*]quinolines, *Assiut University Journal of Chemistry (AUJC)*, **2016**, 45, 24–32.
- Zhang, N., Tomizawa, M., Casida, J. E.,  $\alpha$ -Nitro Ketone as an Electrophile and Nucleophile: Synthesis of 3-Substituted 2-Nitromethylenetetrahydrothiophene and tetrahydrofuran as *Drosophila* Nicotinic Receptor Probes, *J. Org. Chem.*, **2004**, 69, 876–881. DOI: [10.1021/jo035457g](https://doi.org/10.1021/jo035457g)
- Shimomura, M., Yokota, M., Ihara, M., Akamatsu, M., Sattelle, D. B., Matsuda, K., Role in the Selectivity of Neonicotinoids of Insect-Specific Basic Residues in Loop D of the Nicotinic Acetylcholine Receptor Agonist Binding Site, *Mol. Pharmacol.*, **2006**, 70, 1255–1263. DOI: [10.1124/mol.106.026815](https://doi.org/10.1124/mol.106.026815)
- Tomizawa, M., Casida, J. E., Selective toxicity of neonicotinoids attributable to specificity of insect and mammalian nicotinic receptors, *Annu. Rev. Entomol.*, **2003**, 48, 339–364. DOI: [10.1146/annurev.ento.48.091801.112731](https://doi.org/10.1146/annurev.ento.48.091801.112731)
- Tomizawa, M., Talley, T., Maltby, D., Durkin, K. A., Medzihradsky, K. F., Burlingame, A. L., Taylor, P., Casida, J. E., Mapping the elusive neonicotinoid binding site, *Proc. Natl. Acad. Sci. U.S.A.*, **2007**, 104, 9075–9080. DOI: [10.1073/pnas.0703309104](https://doi.org/10.1073/pnas.0703309104)
- Kagabu, S., Ishihara, R., Nishimura, K., Naruse, Y., Insecticidal and neuroblocking potencies of variants of the imidazolidine moiety of imidacloprid-related neonicotinoids and the relationship to partition coefficient and charge density on the pharmacophore, *J. Agric. Food Chem.*, **2007**, 55, 812–818. DOI: [10.1021/jf0623440](https://doi.org/10.1021/jf0623440)
- Yang, Z. B., Hu, D. Y., Zeng, S., Song, B. A., Novel hydrazone derivatives containing pyridine amide moiety: Design, synthesis, and insecticidal activity, *Bioorg. Med. Chem. Lett.*, **2016**, 26, 1161–1164. DOI: [10.1016/j.bmcl.2016.01.047](https://doi.org/10.1016/j.bmcl.2016.01.047)
- Tian, Z., Shao, X., Li, Z., Qian, X., Huang, Q., Synthesis, insecticidal activity and QSAR of novel nitromethylene neonicotinoids with tetrahydropyridine fixed cis configuration and exo-ring ether modification, *J. Agric. Food Chem.*, **2007**, 55, 2288–2292. DOI: [10.1021/jf063418a](https://doi.org/10.1021/jf063418a)
- Stivaktakis, P. D., Kavvalakis, M. P., Tzatzarakis, M. N., Alegakis, A. K., Panagiotakis, M. N., Fragkiadaki, P., Vakonaki, E., Ozcagli, E., Hayes, W. A., Rakitskii, V. N., Tsatsakis, A. M., Long-term exposure of rabbits to imidacloprid as quantified in blood induces genotoxic effect, *Chemosphere*, **2016**, 149, 108–113. <http://dx.doi.org/10.1016/j.chemosphere.2016.01.040>
- Vardavas, A. I., Ozcagli, E., Fragkiadaki, P., Stivaktakis, P. D., Tzatzarakis, M. N., Kaloudis, K., Tsardi, M., Datseri, G., Tsiaoussis, J., Tsitsimpikou, C., Carvalho, F., Tsatsakis, A. M., DNA damage after long-term exposure of rabbits to imidacloprid and sodium tungstate, *Toxicol. Lett.*, **2016**, 258S, S247–S248. <http://dx.doi.org/10.1016/j.toxlet.2016.06.1878>
- Vardavas, A. I., Ozcagli, E., Fragkiadaki, P., Stivaktakis, P. D., Tzatzarakis, M. N., Alegakis, A. K., Vasilakia, F., Kaloudisa, K., Tsiaoussis, J., Kouretas, D., Tsitsimpikou, Ch., Carvalho, F., Tsatsakis, A. M., The metabolism of imidacloprid by aldehyde oxidase contributes to its clastogenic effect in New Zealand rabbits, *Mutat. Res. Genet. Toxic. Environ. Mutag.*, **2018**, 829–830, 26–32. <https://doi.org/10.1016/j.mrgentox.2018.03.002>
- Stivaktakis, P., Kavvalakis, M., Goutzourelas, N., Stagos, D., Tzatzarakis, M., Kyriakakis, M., Rezaee, R., Kouretas, D., Hayes, W., Tsatsakis, A., Evaluation of oxidative stress in long-term exposed rabbits to subtoxic levels of imidacloprid, *Toxicol. Lett.*, **2014**, 229S, No. S228. <http://dx.doi.org/10.1016/j.toxlet.2014.06.764>
- Ho, Y. W., Wang, I. J., Studies on the synthesis of some styryl-3-cyano-2(1*H*)-pyridinethiones and polyfunctionally substituted 3-aminothieno[2,3-*b*]pyridine derivatives, *J. Heterocycl. Chem.*, **1995**, 32(3), 819–825. <https://doi.org/10.1002/jhet.5570320323>
- O'Brien, P. J., Abdel-Aal, Y. A., Ottea, J. A., Graves, J. B., Relationship of insecticide resistance to carboxylesterases in *Aphis gossypii* (Homoptera: Aphididae) from Midsouth cotton, *J. Econ. Entomol.*, **1992**, 85, 651–657. DOI: [10.1093/jee/85.3.651](https://doi.org/10.1093/jee/85.3.651)
- Abbott, W. S., A method of computing the effectiveness of an insecticide, *J. Econ. Entomol.*, **1925**, 18, 265–267. <https://doi.org/10.1093/jee/18.2.265a>
- Probit Analysis: A Statistical Treatment of the Sigmoid Response Curve; Finney, D. J., Ed.; Cambridge University Press: Cambridge, U.K., **1952**. <https://doi.org/10.1093/aesa/45.4.686>

Received: 11.11.2020.

Accepted: 13.12.2020.



## QUALITY CONTROL PARAMETERS OF PRICKLES OF *BOMBAX CEIBA* LINN.

V. B. Savalia,<sup>[a]\*</sup> D. J. Pandya<sup>[a]</sup> and N. R. Sheth<sup>[b]</sup>

**Keywords:** *Bombax ceiba* Linn.; pharmacognostic; phytochemical; prickles; quality control.

*Bombax ceiba* Linn. is a deciduous tree known as Red silk cotton tree. *Bombax ceiba* stem, stem bark and prickles are used for the treatment of rheumatism, swellings, asthma and inflammation of the legs. The stem bark of *Bombax ceiba* is official in the ayurvedic Pharmacopoeia of India recommends its use in acne. Prickles are also used and recommended in anti-acne marketed formulation. However, limited work was carried out on the prickles toward establishing quality control parameters. Studies were therefore carried out to determine the phytochemical and pharmacognostic profile of prickles of *Bombax ceiba* Linn. The study, including determination of macroscopic, microscopic characters, ash values, extractive values, loss on drying, phytochemical screening, total phenolic content, TLC and HPTLC fingerprinting were carried out. Successive extracts were prepared using Soxhlet extraction. The phytochemical analysis of extracts revealed the presence of tannin, saponin, phenol, carbohydrate, steroids, triterpenoids and flavonoids. Total phenolic and tannin content of methanol extract was found 327.78±1.09mg GAE/gm equivalent and 4.98±0.22% w/w, respectively. The mobile phase showing distinct spots in TLC was found in Toluene: Ethyl acetate (9.5:0.5) and (9:1) for petroleum ether and methanol extracts, respectively. HPTLC fingerprinting shows 8 & 3 peaks at 366nm for petroleum ether and methanol extract, respectively.

\*Corresponding Authors

Fax: 9712489122

E-Mail: vaibhavi.savalia@rku.ac.in

- [a] School of Pharmacy, R K University, Kasturbadham, Bhavnagar Highway, Rajkot. 360020. Gujarat, India.  
[b] Vice-Chancellor, Gujarat Technological University, Near Visat Three Roads, Visat Gandhinagar Highway, Chandkheda, Ahmedabad. 382424 Gujarat, India.

parameters like total tannin, total phenolic, total ash, loss on drying, TLC and HPTLC fingerprinting.<sup>8,9</sup> Therefore, the present research of *Bombax ceiba* prickles was taken up to establish quality control parameters of prickles, which will help in the identification of crude drug as well as in the standardization of the formulation. In our present investigation, we have carried out macroscopic, microscopic, ash values, extractive values, fluorescence analysis, phytochemical screening, total tannin, phenolic content, qualitative TLC as well as HPTLC analysis of prickles of *Bombax ceiba* plant.

### INTRODUCTION

*Bombax ceiba* L. is a tall deciduous tree, buttressed at base, belongs to the Bombacaceae family.<sup>1</sup> *Bombax ceiba* scientific synonyms are *Bombax malabaricum* and *Salmalia malabarica*. The plant is also known as a silk-cotton tree, shalmali and shemlo. The plant is used for the treatment of gastrointestinal, skin diseases, gynecological, urinogenital disorders, general debility, diabetes and impotence. The plant parts like root, stem, stem bark and prickles are used for the treatment of rheumatism, swellings, bone fracture, asthma, snake bite, edema, hotness and inflammation of legs in several parts of Indian continent.<sup>2</sup> The bark of *Bombax ceiba* (*B. ceiba*) is official in The Ayurvedic Pharmacopoeia of India and it recommends its use in the treatment of acne.<sup>3</sup> Prickles of *B. ceiba* have been employed to treat acne face in many tribal communities.<sup>3</sup> According to *Charak Samhita*, the plant is among the top ten drugs to treat sepsis, bowel regulator and tissue regenerator.<sup>4</sup> According to *Sushrut Samhita* stem bark is useful in removing acne, hemorrhagic disorders, wound healing and in burns.<sup>5</sup> Patnakar has studied the *in-vitro* and *in-vivo* anti-acne potential of bark and thorns and results shown that an alcoholic extract of bark and thorns possess anti-acne potential.<sup>6</sup> It is interesting to note that prickles of *B. ceiba* are now an important ingredient of Himalaya's acne-n-pimple cream.<sup>7</sup> However, limited work has been carried out on the prickles toward establishing its physio-chemical & pharmacognostic quality control

### MATERIALS AND METHODS

#### Chemical and reagents

Gallic acid, Folin Ciocalteu reagent, and methanol were purchased from S.D. Fine Chemicals Ltd. Mumbai, India. Whatman (Florham Park, NJ) No. 1 filter paper was used for the filtration of the samples. All other chemicals and solvents used were purchased from Merck Chemicals, Mumbai, India. 10 X 10 cms HPTLC aluminum plate precoated with silica gel 60 F<sub>254</sub> (0.2mm thickness) of Merck Pvt. Ltd. (India) were used for HPTLC analysis.

#### Collection of plant material, extraction and sample preparation

Prickles of *Bombax ceiba* (*B. ceiba*) were collected in the month of August-September 2007, from Gir Forest, Junagadh, Gujarat. The identity of the plant was also confirmed by the Department of Botany, Christ College, Saurashtra University, Rajkot. And Herbarium voucher specimen no. SU/DPS/Herb/07-08/2 was deposited at the Department of Pharmaceutical Sciences, Saurashtra University, Rajkot.

Sun-dried Prickle of *Bombax ceiba* was powdered by pulverizer and passed through 40 # sieve and stored in an airtight bottle. The powdered materials were used for further investigation. The powder of the drug, weighing about 150 g, was successively extracted in soxhlet apparatus with solvents of increasing polarity as follows, petroleum ether, benzene, chloroform, acetone, methanol and water. All extracts were concentrated by distilling the solvent and the extracts were dried on a water bath at 50 °C. Dried extracts were used further for fluorescence analysis, phytochemical screening, total tannin, total phenolic, TLC and HPTLC analysis.



**Figure 1.** Prickles of *Bombax ceiba*

#### Macroscopy and microscopy

In organoleptic evaluation, various sensory parameters of the prickle, such as color, odor, taste, shape and texture of the prickle were recorded. Fresh prickles were taken for microscopic studies. Sun-dried Prickles of *Bombax ceiba* were powdered by a pulverizer. Powder passed through 40 # sieve was used to study microscopical characters. For the microscopical studies, transverse sections of prickle were prepared and stained as per the standard procedure.<sup>10,11</sup> The powder microscopy was performed according to the method described by Khandelwal.<sup>12</sup>

#### Physico-chemical investigations

The dried prickle powder was used for the determination of loss on drying, ash values, extractive values, foaming index and swelling index.<sup>13</sup>

#### Fluorescence analysis

Then consistency, percentage yield, fluorescence examination of all successive extracts by color in daylight and ultraviolet light 366 nm were also studied which may help to confirm the purity of the drug.<sup>14</sup>

#### Preliminary phytochemical investigation

For the preliminary phytochemical investigation of prickle, extracts were done according to methods described in Harborne (1973) and Kokate (1997).<sup>15,16</sup> The different extracts obtained by successive solvent extraction were tested

separately for the presence of various phytoconstituents, viz. alkaloids, glycosides, carbohydrates, Phenolics and tannins, phytosterols, fixed oils and fats, proteins and amino acids, flavonoids, saponins, gums and mucilage.

#### Determination of total tannin content

Total tannin content was estimated for methanol extract of prickle of *Bombax ceiba* by the method described in Indian Pharmacopoeia, 1996.<sup>17,18</sup> Accurately weighed 0.08 g of methanol extract of *Bombax ceiba* prickle powder were heated gently with 100 ml of water. From this 100 ml solution, 10 ml was taken into another conical flask. 10 ml of indigo carmine solution and 300 ml water were added to the flask. This solution was heated at 60-70 °C and then titrated with 0.1 N KMnO<sub>4</sub> until royal blue color changes to bottle green and then titrated dropwise until the solution becomes bottle green to golden yellow in color. Similarly, Blank reading was taken by using 10 ml of the indigo carmine solution alone with 300 ml of water. Total tannin content was calculated using the following formula.

$$\varphi = \frac{(A - B) \times N \times 4.157}{0.1 \times m_{\text{sample}}} \quad (1)$$

where,

$\varphi$  = % of total tannin content,

A = blank reading,

B = test reading,

$m_{\text{sample}}$  = sample weight in g,

N = normality of KMnO<sub>4</sub> solution

#### Determination of total phenolic content

The total phenolic content of methanol extract of prickle was determined by the Folin-Ciocalteu method.<sup>19</sup> 10 mg of methanol extract of prickle was dissolved in 10 ml of methanol to get 1 mg/ml sample solution for the test. 500  $\mu$ L of the sample was taken in a 25 ml volumetric flask. To this, 10 ml of water and 1.5 ml of Folin-Ciocalteu reagent were added. The above mixture was kept for 5 min. and then 4ml of 20 % sodium carbonate solution was added and the volume was made up to 25 ml with distilled water. The mixture was kept for 30 min. And the absorbance of the blue color developed was recorded at 765 nm in UV- visible spectrophotometer Shimadzu, UV-1700, Japan. The total phenolic content was calculated from the calibration curve of Gallic acid plotted by using the above procedure. The total phenolic content was expressed in terms of mg GAE/g of dry extract equivalent to Gallic acid.

Statistical analysis All the experiments were carried out in triplicate, and the results were expressed as mean  $\pm$  SEM.

#### Thin layer chromatography analysis

TLC analysis was carried out according to the method described by Harborne.<sup>20</sup> Methanol and petroleum ether extract of prickle of *Bombax ceiba* were selected for the



development of the mobile phase for thin-layer chromatography analysis. Glass plates were coated with silica gel G and allowed to dry followed by activation of plates in hot air oven at 110 °C for 10min. Pilot TLC was developed for methanol extract and petroleum ether extract by preparing various mobile phases using various solvents like toluene, chloroform, n-butanol, ethyl acetate, methanol and distilled water in different proportion. 1mg/ml of extracts were prepared and spotted onto the TLC plates. After the development of TLC with the mobile phase, plates were air-dried. Detection of  $R_f$  values was done in UV light 366 nm, and after spraying with anisaldehyde sulphuric acid followed by heating at 110 °C for 10 min. The movement of the active compound was expressed by its retention factor ( $R_f$ ) values, calculated as:

$$R_f = \frac{D_{\text{solute}}}{D_{\text{solvent}}} \quad (2)$$

where

$D_{\text{solute}}$  = distance traveled by solute

$D_{\text{solvent}}$  = distance traveled by solvent front

### HPTLC Fingerprinting profile

HPTLC fingerprint profile was developed for methanol and petroleum ether extract of prickles of *Bombax ceiba*. Samples were prepared by dissolving dried methanol and petroleum ether extract of prickles in methanol and petroleum ether to obtain a concentration of 5 µg/ml. 10 µl of sample solution was applied on 10 X 10 cm HPTLC aluminum plate precoated with silica gel 60 F<sub>254</sub> (0.2 mm thickness) of Merck Pvt. Ltd. (India). The most recent automatic device, 'CAMAG LINOMAT-5' was used for the present analysis. The plates were developed with mobile phase Toluene: Ethyl acetate (9:1) and Toluene: Ethyl acetate (9.5:0.5) for Methanolic extract and Petroleum ether extract of prickles, respectively. The plate was scanned at UV 366 nm (CAMAG TLC SCANNER 3).  $R_f$  values of each compound that were separated on the plate were recorded.<sup>21</sup>

## RESULTS AND DISCUSSION

### Macroscopy and microscopy

Prickles were present surrounding the stem and stem branches. Prickles were a conical shape, sharp and hard. Prickle color was reddish-brown to grey. The size of the prickle was found 0.5 cm to 2 cm bottom diameter and 1 cm to 1.5 cm in height. (Figure 1) It does not have any characteristic odor.

Microscopy study of prickle showed the presence of stone cells, numerous clusters of prism shape calcium oxalate crystals, epidermal cells and no. of brown-colored, double-walled, polygonal cork cells with the size of  $30 \pm 1.5$  µm and cells with orange content. (Figure 2)

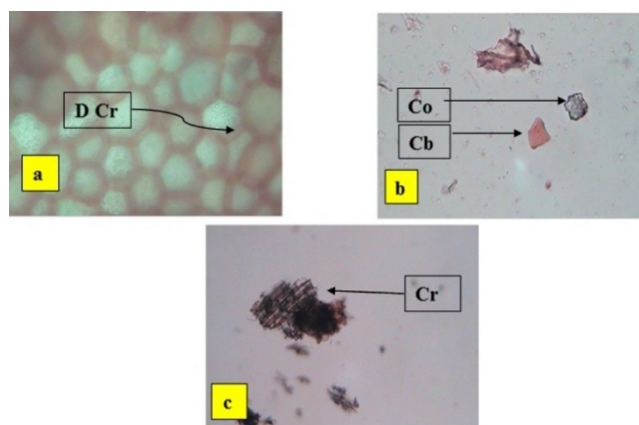


**Figure 2.** Microscopy of prickle of *Bombax ceiba*. a) Transverse section of prickle, b) & c) Powder microscopy, where D Cr- Double-wall polygonal cork cell, Co- Cluster of prism shape calcium oxalate crystal, Cb - Cells with orange content, Cr- Cork cell in powder study.

### Physico-chemical investigation

Physio-chemical investigation of *Bombax ceiba* prickle powder was carried out according to WHO guidelines<sup>13</sup>. Results of parameters such as loss on drying, ash values, extractive values, foaming index and swelling index are as depicted in Table 1.

**Table 1.** Physico-chemical investigation of prickles of *Bombax ceiba*.

No.	Parameters	Average values *
		Prickle
1	Loss on drying	4.60±0.23 %w/w
2	Total ash	3.50±0.11 %w/w
3	Acid insoluble ash	0.35±0.05 %w/w
4	Water-soluble ash	1.60±0.10 %w/w
5	Alcohol extractive value	19.20±0.22 %w/w
6	Hot water extractability	16.50±0.16 %w/w
7	Coldwater extractability	11.40±0.19 %w/w
8	Foaming index	111
9	Swelling index	4.64±0.14 mL

Results are presented in Mean±SEM (n=3). Values given here are expressed as % w/w of air-dried material.

### Fluorescence analysis

A powdered prickle of *Bombax ceiba* was subjected to successive solvent extraction and the consistency, percentage yield, fluorescence examination of all successive extracts by color in daylight and ultraviolet light at 366 nm were recorded. The results of fluorescence analysis are presented in Table 2. Methanol successive solvent extract of prickle revealed the highest extractive value of 12.16 %w/w followed by acetone and petroleum ether extract, whereas water, chloroform and benzene extracts were of low % yield value. Characteristic colors and fluorescent properties recorded can be used for identification and authentication of different extracts prepared from prickle of *Bombax ceiba*.

**Table 2.** Fluorescence analysis for prickles of *Bombax ceiba*.

No.	Extract	Colour		Consistency	Yield, %w/w
		Under daylight	Under UV light (366 nm)		
1	PEP	Light yellow	Yellowish green	Dry non-sticky	6.30
2	BEP	Yellow	Yellow	Dry non-sticky	2.48
3	CEP	Dark yellow	Dark yellow	Sticky	1.00
4	AEP	Brown	Light brown	Sticky	12.00
5	MEP	Dark brown	Magenta	Sticky	12.16
6	WEP	Orange-brown	Dark brown	Dry non-sticky	2.82

PEP- Petroleum ether (60-80°C) extract of *Bombax ceiba* prickles, BEP-Benzene extract of *Bombax ceiba* prickles, CEP- Chloroform extract of *Bombax ceiba* prickles, AEP-Acetone extract of *Bombax ceiba* prickles, MEP- Methanol extract of *Bombax ceiba* prickles, WEP-Water extract of *Bombax ceiba* prickles

**Table 3.** Preliminary phytochemical analysis of prickles of *Bombax ceiba*.

No.	Class of compound	PEP	BEP	CEP	AEP	MEP	WEP	MPBC
1	Alkaloids	-	-	-	-	-	-	-
2	Cardiac Glycoside	-	-	-	-	-	-	-
3	Phenolics/Tannins	-	-	-	+	+	+	+
4	Flavonoids	-	-	-	+	+	+	+
5	Saponins	-	-	-	-	+	+	+
6	Fixed oils & Fats	-	-	-	-	-	-	-
7	Proteins & Amino acids	-	-	-	-	-	-	-
8	Gums/mucilage	-	-	-	-	-	-	-
9	Volatile oil	-	-	-	-	-	-	-
10	Carbohydrates	-	-	-	-	+	+	+
11	Phytosterols/ Triterpenoids	+	+	+	-	-	-	+

- Negative, + - Positive, PEP- Petroleum ether (60-80°C) extract of *Bombax ceiba* prickles, BEP-Benzene extract of *Bombax ceiba* prickles, CEP- Chloroform extract of *Bombax ceiba* prickles, AEP-Acetone extract of *Bombax ceiba* prickles, MEP- Methanol extract of *Bombax ceiba* prickles, WEP-Water extract of *Bombax ceiba* prickles, MPBC- Crude methanol extract of *Bombax ceiba* prickles

### Preliminary phytochemical investigation

Successive extracts of prickles of *Bombax ceiba* were then subjected to phytochemical screening by various qualitative chemical tests. Results of phytochemical screening of successive extracts of prickles powder were depicted in Table 3.

Preliminary qualitative chemical tests of prickles have shown the presence of phenolics, tannins, flavonoids, saponins, carbohydrates and phytosterols/ triterpenoids. The methanol extract of prickles of *Bombax ceiba* revealed the presence of the highest number of phytoconstituents e.g., phenolics, tannins, flavonoids, saponins, carbohydrates and phytosterols/ triterpenoids.

### Total tannin content

The total tannin content of *Bombax ceiba* methanol extract of prickles was determined by the Lowenthal Permanganate titration method<sup>17,18</sup>. The method relies on the oxidation of phenolics by potassium permanganate solution in the presence of indigo carmine as a 'redox indicator' to show the endpoint. The total tannin content of prickles was found 4.98±0.22 %w/w, as shown in Table 4.

**Table 4.** The total tannin content of the prickles of *Bombax ceiba*.

No.	Sample	Mean±SEM % w/w
1	MPBC	4.98±0.22

The values given here are expressed as % w/w of dry weight. MPBC – methanol extract of prickles of *Bombax ceiba*, values are expressed as Mean±SEM, where, n=3

**Table 5.** Estimation of total phenolic content for methanol extract of prickles of *Bombax ceiba* in µg mg<sup>-1</sup> gallic acid equivalent

Sample	Total phenolics )			Mean ± SEM
	I	II	III	
MPBC	325.60	328.87	328.87	327.78±1.09

MPBC–Methanol extract of prickles of *Bombax ceiba*, values are expressed as Mean (µg mg<sup>-1</sup> gallic acid equivalent)±SEM, where n=3

### Determination of total phenolic content

The total phenolic content of the methanol extract of prickles was determined by Folin-Ciocalteu method<sup>19</sup>. Table 5 showed the total amount of phenolic content present in the methanol extract of *Bombax ceiba* prickles. 1mg of methanol extract of prickles of *Bombax ceiba* contains 327.78±1.09 µg gallic acid equivalent of phenols.

**Table 6.** Thin-layer chromatography of petroleum ether and methanol extract of *Bombax ceiba*.

Extract and solvent system	Detection under UV 366 nm light			Detection after spraying of anisaldehyde/sulphuric acid reagent		
	Spot no.	Color	R <sub>f</sub>	Spot no.	Color	R <sub>f</sub>
Petroleum ether extract of prickles, toluene:ethyl acetate (9.5: 0.5)	1	Pink	0.33	1	Violet	0.20
	2	Fluorescent yellow	0.43	2	Violet	0.36
	3	Pink	0.48	3	Dark Violet	0.60
Methanol extract of prickles, toluene:ethyl acetate (9: 1)	1	Fluorescent Green	0.05	1	Navy blue	0.13
	2	Blue	0.2	2	Grey	0.16
	3	Fluorescent Green	0.55	3	Violet	0.41
	-	-	-	4	Violet	0.56
	-	-	-	5	Violet	0.66
	-	-	-	5	Green	0.71
	-	-	-	6	Greenish blue	0.82
	-	-	-	7	Blue	0.99

### Thin layer chromatography analysis

The methanol and petroleum ether extracts were obtained by Soxhlet solvent extraction process. Extracts were subjected to thin-layer chromatography (TLC) to optimize the mobile phase for further HPTLC fingerprinting. Different composition of the different mobile phases was tested in order to obtain high resolution and reproducible spots. The mobile phases developed for petroleum ether and methanol extract were toluene: ethyl acetate (9.5:0.5) and toluene: ethyl acetate (9:1), respectively. The number of spots found, their color in UV 366 nm and in daylight after spraying and related R<sub>f</sub> values obtained from the TLC study as shown in Table 6 and Figure 3.

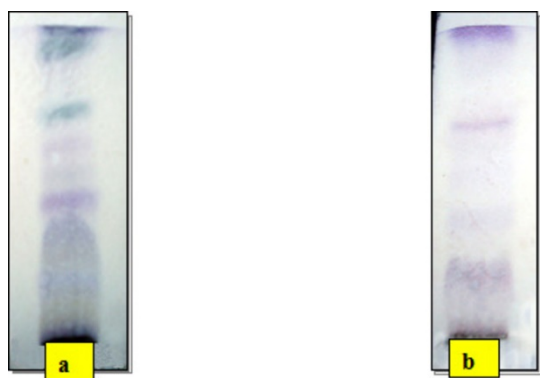


**Figure 3.** Thin-layer chromatography of *Bombax ceiba* prickles after spraying in visible light a) - methanol extract with toluene: ethyl acetate (9:1) and b)- petroleum ether extract with toluene: ethyl acetate (9.5:0.5).

### HPTLC Fingerprinting profile

HPTLC fingerprinting was performed for both methanol and petroleum ether extracts of prickles of *Bombax ceiba* using mobile phase toluene: ethyl acetate (9:1) and toluene: ethyl acetate (9.5:0.5), respectively. Eight peaks were detected

upon HPTLC of petroleum ether extract of *Bombax ceiba* prickles at 366nm using mobile phase toluene: ethyl acetate (9.5:0.5), while three peaks were detected upon HPTLC of methanol extract of *Bombax ceiba* prickles at 366 nm using mobile phase toluene: ethyl acetate (9:1). R<sub>f</sub> values for ethyl acetate extract for peak 1 to 8 were found 0.07, 0.14, 0.25, 0.31, 0.36, 0.43, 0.5 and 0.75 respectively. R<sub>f</sub> values for methanol extract for peaks 1 to 3 were found 0.07, 0.16 and 0.53, respectively. Peaks, their R<sub>f</sub> values, area under curve and area % for petroleum ether and methanol extract of prickles of *Bombax ceiba* are depicted in Table 7 and Table 8. 2D chromatogram, 3D chromatogram and HPTLC fingerprint profile of petroleum ether extract of *Bombax ceiba* prickles are shown in Figure 4, 5 and 6 respectively. 2D chromatogram, 3D Chromatogram and HPTLC fingerprint profile of methanol extract of *Bombax ceiba* prickles are shown in Figures 7, 8 and 9.

**Table 7.** HPTLC fingerprinting of petroleum ether extract of *Bombax ceiba* prickles.

Peak	R <sub>f</sub>	Area under curve	Area %
1	0.07	7884	13.77
2	0.14	4656	8.13
3	0.25	986.5	1.72
4	0.31	1858	3.24
5	0.36	3155	5.51
6	0.43	8001	13.97
7	0.5	1842	3.22
8	0.75	28892	50.44

**Table 8.** HPTLC fingerprinting of methanol extract of *Bombax ceiba* prickles.

Peak	R <sub>f</sub>	Area under curve	Area %
1	0.07	13671	84.57
2	0.16	919.8	5.69
3	0.53	1575	9.74

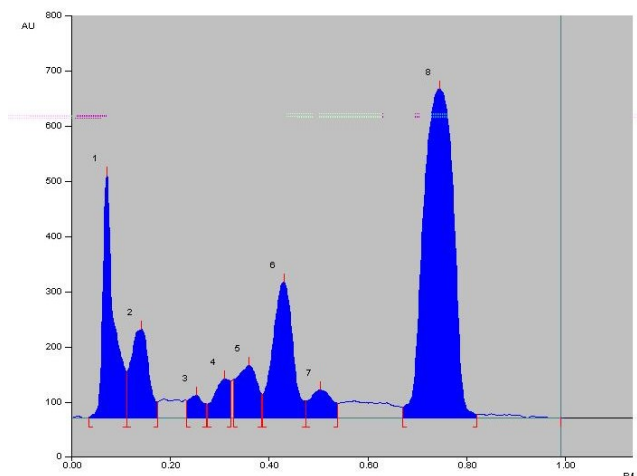


**Figure 4.** HPTLC 2D chromatogram of petroleum ether extract of *Bombax ceiba* prickles at 366nm (toluene:ethyl acetate 9.5:0.5).

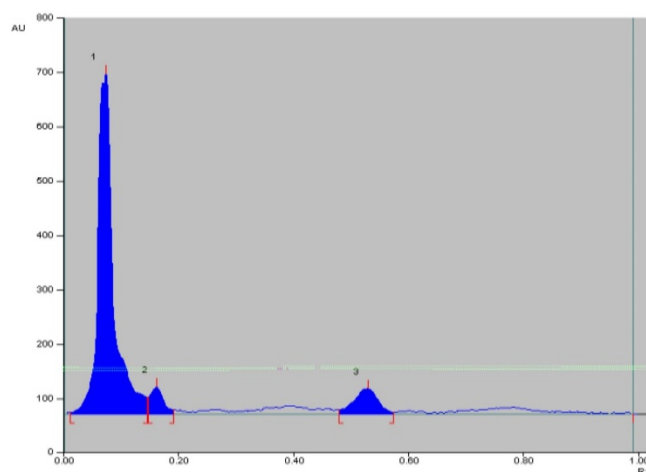


**Figure 7.** HPTLC 2D chromatogram of methanol extract of *Bombax ceiba* prickles at 366nm (toluene:ethyl acetate 9:1).

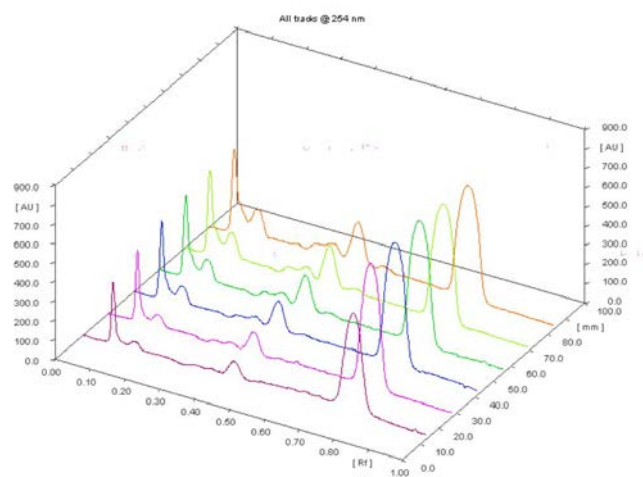


**Figure 5.** HPTLC 3D chromatogram of petroleum ether extract of *Bombax ceiba* prickles at 366nm (toluene:ethyl acetate 9.5:0.5).

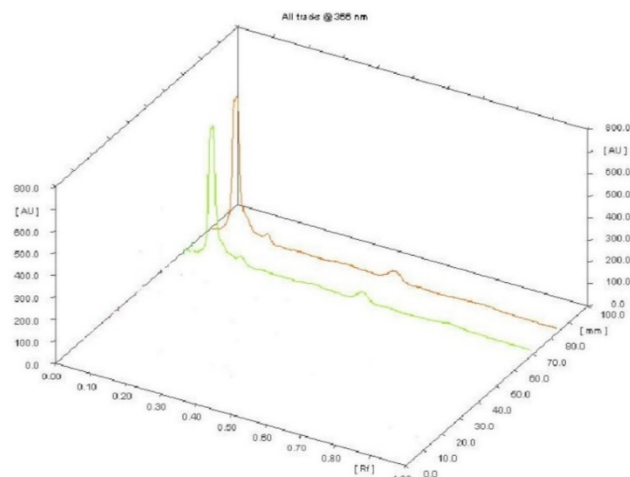


**Figure 8.** HPTLC 3D chromatogram of methanol extract of *Bombax ceiba* prickles at 366nm (toluene:ethyl acetate 9:1).

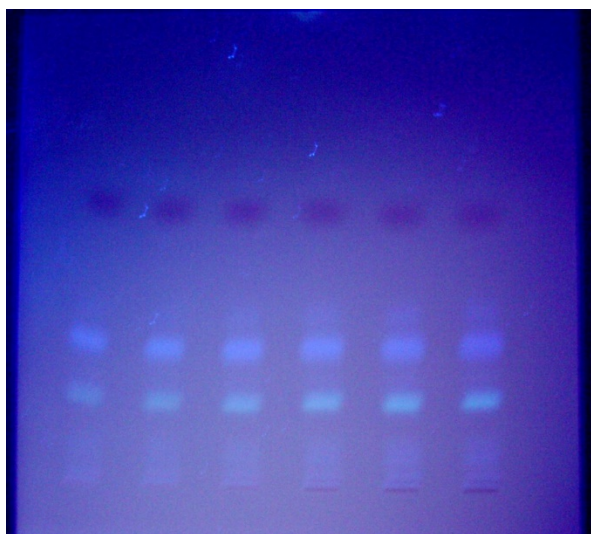


**Figure 6.** HPTLC profile of petroleum ether extract of *Bombax ceiba* prickles at 366nm (toluene:ethyl acetate 9.5:0.5).

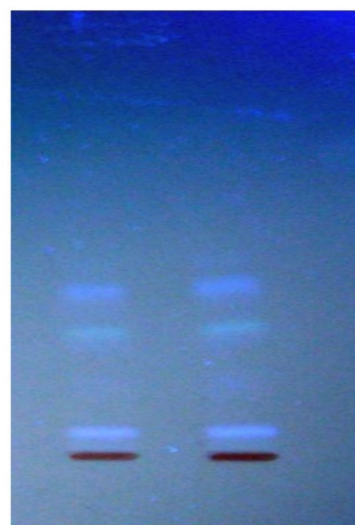


**Figure 9.** HPTLC profile of methanol extract of *Bombax ceiba* prickles at 366nm (toluene:ethyl acetate 9:1).



## CONCLUSION

Standardization of herbal drugs can be used as an important scientific tool to ensure the quality of the crude drug, extracts and formulation prepared from crude drugs. The present study was planned to establish pharmacognostic standards for prickle of *Bombax ceiba* so as to have a reliable scientific parameter to authenticate the prickles, prickle powder, and extracts. The macroscopical and microscopical study provided important data to identify crude as well as a powder form of prickle of *Bombax ceiba*. Preliminary phytochemical screening revealed the presence of phenolics, tannins, flavonoids, saponins, carbohydrates and phytosterols/triterpenoids in the extracts of prickle of *Bombax ceiba*. Further total phenol and total tannin content of methanol extract can be used as an important standardization parameter for the alcoholic formulation of prickle of *Bombax ceiba*. The physico-chemical analysis provided important data on loss on drying, ash values, extractive values, foaming index and swelling index of prickle of *Bombax ceiba* that can be used to authenticate it in raw as well as powder form. TLC and HPTLC fingerprinting have provided important data for both polar and non-polar extracts, which can be further useful for standardization of both types of extracts used to prepare formulation.

The present study can be specifically useful for authentication of the raw material of the prickles, identification in powder and raw form and in the detection of adulteration, which will ultimately benefit the people who use *Bombax ceiba* prickle formulations.

## REFERENCES

- <sup>1</sup>Kirtikar, K. R., and Basu, B. D., *Indian medicinal plants*, International Book Distributor, Dehradun, India, **2005**, 1, 354-357.
- <sup>2</sup>Vartika, J., Verma S. K. and Katewa, S. S., Myths, traditions and fate of multipurpose *Bombax ceiba* L. - An appraisal, *Indian J. Tradit. Knowl.*, **2009**, 8(4), 638-644. <http://nopr.niscair.res.in/handle/123456789/6288>
- <sup>3</sup>*The Ayurvedic Pharmacopoeia of India*, Government of India, Ministry of Health & Family Welfare, 1st ed., **2001**, 3(1), 183.
- <sup>4</sup>Agnivesha, Charak & Dridhabala, *Charak Samhita Sidhithana*, Verse-35, 10<sup>th</sup> Chapter, Chaukhamba Sanskrit Pratishthan, New Delhi, **2002**, 967.
- <sup>5</sup>Sushruta, *Sushruta Samhita Sutrasthana*, Verse-45-46, 12th ed., 38<sup>th</sup> Chapter, Chaukhamba Sanskrit Sansthan, Varanasi, **2001**, 144-5.
- <sup>6</sup>Patanakar, S. P., *Phytochemical Investigation and Pharmacological Evaluation of Aerial Parts of Salmalia malabarica. Schott and Endl. For Antiacne Activity*, M. Pharma Dissertation. Rajiv Gandhi University of Health Sciences, Bangalore, **2005**.
- <sup>7</sup>Shantha, T. R., Venkateshwarlu G, Ammal MJI, Gopa kumar K & Sridhar BN, Pharmacognostical and preliminary phytochemical studies on the thorns of *Bombax ceiba* L., *Aryavaidyan.*, **2009**, 22(2), 74-81.
- <sup>8</sup>Wallis, T. E., *Textbook of Pharmacognosy*, 5<sup>th</sup> Edition, CBS Publisher and Distributor, New Delhi, India, **2005**, 571.
- <sup>9</sup>Betty, P. J., and Derek, W. S., *Atlas of Microscopy of Medicinal Plants Culinary Herbs and Spices*, 1st Edition, CBS Publishers and Distributors, New Delhi, India, **2000**, 9-11.
- <sup>10</sup>Khandelwal, K. R., *Preliminary phytochemical screening*, In: *Practical Pharmacognosy*, 19th Edition, Nirali Prakashan, Pune, India, **2008**, 162-166.
- <sup>11</sup>Ravichandran, G., Bharadwaj, V. S., and Kolhapure, S. A., Evaluation of efficacy and safety of acne-N-pimple cream in acne vulgaris, *Antiseptic.*, **2004**, 101, 249-54.
- <sup>12</sup>Dangi, A., Mewada, A., Lodhi, Y. and Patel, M., Pharmacognostical and phytochemical studies of *Bombax ceiba* thorns, *Panacea J. Pharm. Pharm. Sci.*, **2014**, 3(4), 53-56.
- <sup>13</sup>*Quality Control Methods for Medicinal Plant Materials*, WHO, Geneva, **2002**.
- <sup>14</sup>Selvam, A. B. D., Bandyopadhyay, S., Fluorescence analysis on the roots of *Rauwolfia serpentina* (L.) Benth. ex Kurz under UV radiation, *Anc. Sci. Life*, **2005**, 24(4), 1-4.
- <sup>15</sup>Harborne, J. B., *Phytochemical methods*, Chapman and Hall: London, UK, **1973**, 49-188.
- <sup>16</sup>Kokate, C. K., Purohit, A. P., & Gokhale, S. B., *Pharmacognosy*, 7th edition, Nirali Prakashan, Pune, India, **1997**, 108-109.
- <sup>17</sup>*Indian Pharmacopoeia*, Government of India, Ministry of Health & Family, controller of publication, Delhi, India, Vol-2, App. 13.2, **1996**, A-171.
- <sup>18</sup>Lowenthal, J., About determination of tannin, *Z. Anal. Chem.*, **1877**, 16, 33-48. <https://doi.org/10.1007/BF01355993>
- <sup>19</sup>Singleton, V. L., Rossi, J. A., Colorimetry of total phenolics with phosphomolybdic-phosphotungstic acid reagents, *Am. J. Enol. Viticult.*, **1965**, 16(3), 144-158. <http://www.ajevonline.org/content/16/3/144.full.pdf+html>
- <sup>20</sup>Harborne, J. B., *Phytochemical methods*, 3<sup>rd</sup> Edition, Chapman and Hall, London, UK, **1998**, 34-37.
- <sup>21</sup>Anonymous, *Protocol for testing of Ayurvedic, Siddha & Unani Medicines*, Pharmacopoeial Laboratory for Indian Medicines, Ghaziabad, India, **2007**, 54-56.

Received: 04.12.2020.

Accepted: 21.12.2020.



# CALCULATION OF ABRAHAM MODEL L-DESCRIPTOR AND STANDARD MOLAR ENTHALPIES OF VAPORIZATION FOR LINEAR C<sub>7</sub>-C<sub>14</sub> ALKYNES FROM GAS CHROMATOGRAPHIC RETENTION INDEX DATA

Neel Shanmugam<sup>[a]</sup>, Shrika Eddula<sup>[a]</sup>, William E. Acree, Jr<sup>[a]\*</sup> and Michael H. Abraham<sup>[b]</sup>

**Keywords:** Linear alkynes, Abraham model, solute descriptors, enthalpy of vaporization, Kovats retention indices.

Abraham model **L** solute descriptors have been determined for an additional 33 linear C<sub>7</sub>-C<sub>14</sub> alkynes based on published gas chromatographic retention indices for solutes eluted from capillary columns coated with squalane and apiezon L stationary phases. Standard molar enthalpies of vaporization and sublimation at 298 K are calculated for the 33 linear alkynes using the reported solute descriptors and our recently published Abraham model correlations. Calculated vaporization enthalpies derived from the Abraham model compare very favourably with values based on a popular atom-group additivity model.

\* Corresponding Authors

Fax: (940) 565-3543

E-Mail: acree@unt.edu

[a] Department of Chemistry, University of North Texas, Denton, Texas 76203, USA

[b] Department of Chemistry, University College of London, 20 Gordon Street, London WC1H 0AJ, UK

## INTRODUCTION

Thousands of new organic and organometallic compounds are either discovered or synthesized each year by the scientific community and chemical manufacturing sector. New chemicals (such as medical drugs, pesticides, herbicides) are synthesized to address specific needs or are discovered during the characterization of chemical constituents of natural products. Practical utilization of newly discovered and newly synthesized compounds requires knowledge of their physical, toxicological and thermodynamic properties. Experimental measurements of properties are often expensive and time-consuming. It is not feasible for experimental measurements to be performed on every newly discovered and newly synthesized organic and organometallic compound. Predictive methods are often used to estimate physical and thermodynamic properties in the absence of measured experimental quantities.

The Abraham solvation parameter model is among the better of the predictive linear free energy relationships developed during the past 30 years. The model has been shown to provide reasonably accurate predictions for a wide range of solute transfer processes. Specific solute properties, *SP*, for which predictive expressions have been reported include: the logarithms of the water-to-organic solvent and gas-to-organic solvent partition coefficients,  $\log P$  and  $\log K$ ,<sup>1-7</sup> logarithms of blood-to-body tissue/fluid partition coefficients,  $\log P_{\text{blood/tissue}}$ ,<sup>8-12</sup> logarithms of the median lethal concentration of various organic compounds to aquatic organisms,  $\log LC_{50}$ ,<sup>13-16</sup> enthalpies of solvation of organic vapors and inorganic gases in organic solvents,

$\Delta H_{\text{solv}}$ ,<sup>17-27</sup> logarithms of molar solubility ratios,<sup>28-31</sup> isothermal gas chromatographic retention factors and retention indices, *RI*, Draize eye scores and eye irritation thresholds,<sup>32-34</sup> nasal pungency,<sup>32,35-37</sup> skin permeabilities,<sup>38,39</sup> and several other biological response solute properties.<sup>40,41</sup> More recently, the model was successfully extended to the prediction of enthalpies of vaporization<sup>42</sup> and sublimation,<sup>43</sup> vapor pressures of liquid and crystalline organic and organometallic compounds,<sup>44</sup> and isobaric heat capacities.<sup>45</sup>

The popularity of the Abraham model results from the model's simplistic mathematical forms (eqns.1 and 2), coupled with the fact that a single set of solute descriptors (**E**, **S**, **A**, **B**, **V** and **L**) is used in every predictive application. One does not have to compute a different set of solute descriptors for each individual property that one wishes to predict. The common mathematical form that results from having one set of descriptor values facilitates comparisons between the different solute transfer processes using either the Euclidean distance formula or Principal Component Analysis. Such comparisons have been presented in several earlier publications.

$$SP = c_p + e_p \cdot \mathbf{E} + s_p \cdot \mathbf{S} + a_p \cdot \mathbf{A} + b_p \cdot \mathbf{B} + v_p \cdot \mathbf{V} \quad (1)$$

$$SP = c_k + e_k \cdot \mathbf{E} + s_k \cdot \mathbf{S} + a_k \cdot \mathbf{A} + b_k \cdot \mathbf{B} + l_k \cdot \mathbf{L} \quad (2)$$

Unlike strictly empirical predictive methods the Abraham model is grounded on a firm understanding of molecular interactions. Each term on the right-hand side of eqns. 1 and 2 represents a different type of solute-solvent interaction that governs solute transfer between two condensed phases, eqn. (1), or solute transfer from the gas phase to a condensed phase, eqn. (2). Molecular interactions are quantified in the Abraham model as the product of a solute descriptor times the complementary condensed phase/solvent property ( $c_p$ ,  $e_p$ ,  $s_p$ ,  $a_p$ ,  $b_p$ ,  $v_p$ ,  $c_k$ ,  $e_k$ ,  $s_k$ ,  $a_k$ ,  $b_k$ , and  $l_k$ ). Solute descriptors are identified by the uppercase alphabetic characters in eqns. (1) and (2), and are defined as follows: **E** corresponds to the

molar refraction of the given solute in excess of that of a linear alkane having a comparable molecular size, **S** is a combination of the electrostatic polarity and polarizability of the dissolved solute, **A** and **B** quantify the respective hydrogen-bond donating and hydrogen-bond accepting abilities of the solute, **V** refers to the solute's McGowan molecular volume and **L** denotes the logarithm of the solute's measured gas-to-hexadecane partition coefficient at 298.15 K. The lowercase alphabetic characters on the right-hand side of eqns. (1) and (2) denote the complementary properties of the solute transfer process, and their numerical values are determined through regression analysis of experimental partition coefficient data, molar solubility ratios, gas chromatographic retention factors and retention indices, and other measured solute properties as illustrated in earlier publications.<sup>28-31,46-48</sup> Readers are referred to several review articles<sup>49-52</sup> for a more detailed discussion of the Abraham model and its predictive applications.

Continued development of the Abraham model requires determining solute descriptor values for more chemical compounds and developing correlation expressions for additional transfer processes/properties of chemical and biological significance. Our recent efforts in this area have been to publish predictive Abraham model correlations for vapor pressures, enthalpies of vaporization and sublimation and heat capacities of organic and organometallic compounds. Concurrent with developing the fore-mentioned predictive expressions we have calculated solute descriptors for several high-energy nitrogen compounds,<sup>53</sup> several adamantane derivatives<sup>54</sup> and approximately 300 different monoalkylated and polymethylated linear alkanes.<sup>55,56</sup>

The current communication is devoted to obtaining a complete set of solute descriptor values for linear C<sub>7</sub>-C<sub>14</sub> alkynes so that we can predict both their physical and thermodynamic properties. Our private database of solute descriptors has numerical values of **E**, **S**, **A**, **B** and **V** for the complete set of linear C<sub>7</sub> – C<sub>14</sub> alkynes. **L**-descriptor values, however, are available for only a small fraction of the C<sub>7</sub>-C<sub>14</sub> alkynes. Numerical values of the **E** and **V** solute descriptors, listed in Table 1 were calculated based on the alkynes refractive index and molecular structure (atomic sizes and number of chemical bonds) as described elsewhere<sup>50-52</sup>. The **S**, **A** and **B** descriptors were estimated from known experimental-based values for non-1-yne, dec-1-yne, dodec-1-yne, and the smaller C<sub>4</sub>-C<sub>8</sub> alkynes for which a **L**-descriptor value is given. The tabulated values of the **L**-solute descriptors were computed from experimental partition coefficient data. We note that the **S**, **A** and **B** solute descriptors of alkynes are numerically very small, and their contribution to the solute transfer processes defined by eqns. (1) and (2) are also small. The **L** solute descriptor, on the other hand, is much larger and its numerical value cannot be reasonably estimated by comparisons with other linear alkyne molecules. We note that an earlier version of our private solute descriptor database is available on the public UFZ-LSER website<sup>57</sup> (referenced as Abraham Absolv), and that the website will have numerical **L** solute descriptors values for several of the linear alkyne molecules whose solute descriptor values are not given in Table 1. The reference given for the **L**-descriptor in the website is LSER Dataset 2017 for CompTox users. Numerical values for the **L** solute descriptors referenced as LSER Dataset 2017 might be estimated values based on a derived mathematical

correlation between other Abraham model solute descriptors or other estimation scheme. The website for UFZ-LSER Database does have provisions for estimating solute descriptors from a molecule's canonical Smiles code. Our past experience has been that solute descriptors obtained from actual experimental data provide superior predicted values than solute descriptors calculated entirely by estimation methods.

In this study we calculate the **L** solute descriptors of the larger alkyne molecules from the published isothermal gas chromatographic retention index data of Rang and co-workers.<sup>58</sup> The authors measured the retention indices of linear C<sub>6</sub>-C<sub>14</sub> alkynes on capillary columns coated with squalane, apiezon L, polyphenyl ether and polyethylene glycol 4000 stationary phases. The computational methodology will be the same as that used in our two recent papers published in this journal,<sup>55,56</sup> which reported the numerical values of the **L** solute descriptors for approximately 300 large monoalkylated and polymethylated linear alkanes.

## CALCULATION OF ABRAHAM MODEL SOLUTE DESCRIPTORS

The computational methodology that we will use to calculate the **L** solute descriptor involves establishing an Abraham model relationship (eqn.3):

$$RI = c_{ri} + e_{ri} \cdot \mathbf{E} + s_{ri} \cdot \mathbf{S} + a_{ri} \cdot \mathbf{A} + b_{ri} \cdot \mathbf{B} + l_{ri} \cdot \mathbf{L} \quad (3)$$

using the measured Kovats retention indices, *RI*, for those alkane, alkene, and alkynes solutes for which we already have a complete set of solute descriptors. In order to have a sufficient number of experimental data points to establish meaningful Abraham model correlations we augmented the retention index datasets for the squalane and apiezon L stationary phases with experimental values determined by Sojak et al.<sup>59</sup> for linear C<sub>6</sub>-C<sub>14</sub> alkenes on a squalane stationary phase, and with experimental values determined by Vigdergauz et al.<sup>60</sup> and Sojak et al.<sup>61</sup> for several miscellaneous organic compounds on an apiezon L stationary phase. In total we had 100 and 44 experimental data points to use in the regression analyses for constructing the Abraham model correlations for the squalane and apiezon L stationary phases, respectively. The numerical values of the solute descriptors for the alkanes, alkenes and miscellaneous organic compounds used in constructing the Abraham model correlations are tabulated in Table 2. Numerical values of the solute descriptors for the smaller alkyne solutes are listed in Table 1.

We first establish an Abraham model correlation for describing the retention indices of alkane, alkene and alkyne solutes dissolved in the squalane stationary at 110 °C using the experimental *RI* values given in Table 3. Retention indices of linear alkanes are defined to be 100 times the number of carbon atoms. Squalane (more formally named 2,6,10,15,19,24-hexamethyltetracosane) is a saturated hydrocarbon, and would not be capable of hydrogen-bond formation ( $a_k = 0$  and  $b_k = 0$ ) and dipole-dipole interactions ( $s_k = 0$ ). Our published correlation<sup>1</sup> for describing gas-to-liquid partition coefficients into squalane at 298.15 K shows

**Table 1.** Abraham model solute descriptors of alkynes taken from our private solute descriptor database.

Compound	E	S	A	B	Bo	V	L
But-1-yne	0.178	0.250	0.120	0.100	0.100	0.5862	1.520
But-2-yne	0.261	0.230	0.000	0.210	0.210	0.5862	1.856
Pent-1-yne	0.172	0.230	0.120	0.120	0.120	0.7271	2.010
Pent-2-yne	0.241	0.290	0.000	0.200	0.200	0.7271	2.236
Hex-1-yne	0.166	0.220	0.100	0.120	0.120	0.8680	2.510
Hex-2-yne	0.236	0.300	0.000	0.150	0.150	0.8680	2.765
Hex-3-yne	0.224	0.300	0.000	0.150	0.150	0.8680	2.659
Hept-1-yne	0.160	0.230	0.090	0.100	0.100	1.0089	3.000
Hept-2-yne	0.237	0.300	0.000	0.150	0.150	1.0089	
Hept-3-yne	0.232	0.300	0.000	0.150	0.150	1.0089	
Oct-1-yne	0.155	0.220	0.090	0.100	0.100	1.1498	3.521
Oct-2-yne	0.225	0.300	0.000	0.150	0.150	1.1498	3.850
Oct-3-yne	0.210	0.300	0.000	0.150	0.150	1.1498	
Oct-4-yne	0.208	0.300	0.000	0.150	0.150	1.1498	3.609
Non-1-yne	0.150	0.220	0.090	0.100	0.100	1.2907	4.019
Non-2-yne	0.225	0.300	0.000	0.150	0.150	1.2907	
Non-3-yne	0.204	0.300	0.000	0.150	0.150	1.2907	
Non-4-yne	0.207	0.300	0.000	0.150	0.150	1.2907	
Dec-1-yne	0.143	0.220	0.090	0.100	0.100	1.4316	4.537
Dec-2-yne	0.217	0.300	0.000	0.150	0.150	1.4316	
Dec-3-yne	0.195	0.300	0.000	0.150	0.150	1.4316	
Dec-4-yne	0.205	0.300	0.000	0.150	0.150	1.4316	
Dec-5-yne	0.193	0.300	0.000	0.150	0.150	1.4316	
Undec-1-yne	0.139	0.220	0.090	0.100	0.100	1.5725	
Undec-2-yne	0.213	0.300	0.000	0.150	0.150	1.5725	
Undec-3-yne	0.196	0.300	0.000	0.150	0.150	1.5725	
Undec-4-yne	0.196	0.300	0.000	0.150	0.150	1.5725	
Undec-5-yne	0.191	0.300	0.000	0.150	0.150	1.5725	
Dodec-1-yne	0.133	0.220	0.090	0.100	0.100	1.7134	5.657
Dodec-2-yne	0.207	0.300	0.000	0.150	0.150	1.7134	
Dodec-3-yne	0.190	0.300	0.000	0.150	0.150	1.7134	
Dodec-4-yne	0.190	0.300	0.000	0.150	0.150	1.7134	
Dodec-5-yne	0.190	0.300	0.000	0.150	0.150	1.7134	
Dodec-6-yne	0.190	0.300	0.000	0.150	0.150	1.7134	
Tridec-1-yne	0.136	0.220	0.090	0.100	0.100	1.8543	
Tridec-2-yne	0.209	0.300	0.000	0.150	0.150	1.8543	
Tridec-3-yne	0.209	0.300	0.000	0.150	0.150	1.8543	
Tridec-4-yne	0.209	0.300	0.000	0.150	0.150	1.8543	
Tridec-5-yne	0.209	0.300	0.000	0.150	0.150	1.8543	
Tridec-6-yne	0.209	0.300	0.000	0.150	0.150	1.8543	
Tetradec-1-yne	0.144	0.220	0.090	0.100	0.100	1.9952	
Tetradec-2-yne	0.206	0.300	0.000	0.150	0.150	1.9952	
Tetradec-3-yne	0.206	0.300	0.00	0.15	0.150	1.9952	
Tetradec-4-yne	0.206	0.300	0.000	0.150	0.150	1.9952	
Tetradec-5-yne	0.206	0.300	0.000	0.150	0.150	1.9952	
Tetradec-6-yne	0.206	0.300	0.000	0.150	0.150	1.9952	
Tetradec-7-yne	0.206	0.300	0.000	0.150	0.150	1.9952	



**Table 2.** Abraham model solute descriptors for alkanes, alkenes and miscellaneous organic compounds.

Compound	E	S	A	B	L	V
Hexane	0.000	0.000	0.000	0.000	2.668	0.9540
Heptane	0.000	0.000	0.000	0.000	3.173	1.0949
Octane	0.000	0.000	0.000	0.000	3.677	1.2358
Nonane	0.000	0.000	0.000	0.000	4.182	1.3767
Decane	0.000	0.000	0.000	0.000	4.686	1.5176
Undecane	0.000	0.000	0.000	0.000	5.191	1.6585
Dodecane	0.000	0.000	0.000	0.000	5.696	1.7994
Tridecane	0.000	0.000	0.000	0.000	6.200	1.9403
Tetradecane	0.000	0.000	0.000	0.000	6.705	2.0812
Pentadecane	0.000	0.000	0.000	0.000	7.209	2.2221
Hexadecane	0.000	0.000	0.000	0.000	7.714	2.3630
Heptadecane	0.000	0.000	0.000	0.000	8.218	2.5039
Octadecane	0.000	0.000	0.000	0.000	8.722	2.6448
Hex-1-ene	0.078	0.080	0.000	0.070	2.572	0.9110
<i>cis</i> -Hex-2-ene	0.143	0.080	0.000	0.070	2.684	0.9110
<i>trans</i> -Hex-2-ene	0.122	0.080	0.000	0.060	2.655	0.9110
<i>cis</i> -Hex-3-ene	0.128	0.080	0.000	0.070	2.664	0.9110
<i>trans</i> -Hex-3-ene	0.126	0.080	0.000	0.060	2.659	0.9110
Hept-1-ene	0.092	0.080	0.000	0.070	3.063	1.0519
<i>cis</i> -Hept-2-ene	0.136	0.080	0.000	0.070	3.210	1.0519
<i>trans</i> -Hept-2-ene	0.119	0.080	0.000	0.070	3.180	1.0519
<i>cis</i> -Hept-3-ene	0.130	0.080	0.000	0.070	3.143	1.0519
<i>trans</i> -Hept-3-ene	0.121	0.080	0.000	0.070	3.125	1.0519
Oct-1-ene	0.094	0.080	0.000	0.070	3.568	1.1928
<i>cis</i> -Oct-2-ene	0.135	0.080	0.000	0.070	3.683	1.1928
<i>trans</i> -Oct-2-ene	0.123	0.070	0.000	0.070	3.668	1.1928
<i>cis</i> -Oct-3-ene	0.125	0.060	0.000	0.070	3.663	1.1928
<i>trans</i> -Oct-3-ene	0.119	0.060	0.000	0.060	3.647	1.1928
<i>cis</i> -Oct-4-ene	0.133	0.080	0.000	0.070	3.607	1.1928
<i>trans</i> -Oct-4-ene	0.114	0.080	0.000	0.070	3.593	1.1928
Non-1-ene	0.090	0.080	0.000	0.070	4.073	1.3337
<i>cis</i> -Non-2-ene	0.136	0.060	0.000	0.060	4.245	1.3337
<i>trans</i> -Non-2-ene	0.119	0.060	0.000	0.060	4.188	1.3337
<i>cis</i> -Non-3-ene	0.127	0.060	0.000	0.060	4.151	1.3337
<i>trans</i> -Non-3-ene	0.119	0.060	0.000	0.060	4.148	1.3337
<i>cis</i> -Non-4-ene	0.132	0.060	0.000	0.060	4.173	1.3337
<i>trans</i> -Non-4-ene	0.116	0.060	0.000	0.060	4.141	1.3337
Dec-1-ene	0.093	0.080	0.000	0.070	4.533	1.4746
<i>cis</i> -Dec-2-ene	0.131	0.060	0.000	0.060	4.745	1.4746
<i>trans</i> -Dec-2-ene	0.118	0.060	0.000	0.060	4.670	1.4746
<i>cis</i> -Dec-3-ene	0.131	0.060	0.000	0.060	4.680	1.4746
<i>trans</i> -Dec-3-ene	0.118	0.060	0.000	0.060	4.671	1.4746
<i>cis</i> -Dec-4-ene	0.131	0.060	0.000	0.060	4.669	1.4746
<i>trans</i> -Dec-4-ene	0.115	0.060	0.000	0.060	4.638	1.4746
<i>cis</i> -Dec-5-ene	0.123	0.060	0.000	0.060	4.665	1.4746
<i>trans</i> -Dec-5-ene	0.112	0.060	0.000	0.060	4.637	1.4746
Undec-1-ene	0.091	0.080	0.000	0.070	5.023	1.6155
<i>cis</i> -Undec-2-ene	0.134	0.060	0.000	0.060	5.258	1.6155
<i>trans</i> -Undec-2-ene	0.117	0.060	0.000	0.060	5.192	1.6155
<i>cis</i> -Undec-3-ene	0.125	0.060	0.000	0.060	5.178	1.6155
<i>trans</i> -Undec-3-ene	0.115	0.060	0.000	0.060	5.150	1.6155
<i>cis</i> -Undec-4-ene	0.129	0.060	0.000	0.060	5.168	1.6155

<i>trans</i> -Undec-4-ene	0.111	0.060	0.000	0.060	5.138	1.6155
<i>cis</i> -Undec-5-ene	0.122	0.060	0.000	0.060	5.153	1.6155
<i>trans</i> -Undec-5-ene	0.095	0.060	0.000	0.060	5.126	1.6155
Dodec-1-ene	0.089	0.080	0.000	0.070	5.515	1.7564
<i>cis</i> -Dodec-2-ene	0.132	0.060	0.000	0.060	5.766	1.7564
<i>trans</i> -Dodec-2-ene	0.116	0.060	0.000	0.060	5.699	1.7564
<i>cis</i> -Dodec-3-ene	0.132	0.060	0.000	0.060	5.692	1.7564
<i>trans</i> -Dodec-3-ene	0.115	0.060	0.000	0.060	5.656	1.7564
<i>cis</i> -Dodec-4-ene	0.123	0.060	0.000	0.060	5.667	1.7564
<i>trans</i> -Dodec-4-ene	0.112	0.060	0.000	0.060	5.641	1.7564
<i>cis</i> -Dodec-5-ene	0.116	0.060	0.000	0.060	5.653	1.7564
<i>trans</i> -Dodec-5-ene	0.092	0.060	0.000	0.060	5.636	1.7564
<i>cis</i> -Dodec-6-ene	0.120	0.060	0.000	0.060	5.655	1.7564
<i>trans</i> -Dodec-6-ene	0.119	0.060	0.000	0.060	5.647	1.7564
Tridec-1-ene	0.093	0.060	0.000	0.070	6.046	1.8973
<i>cis</i> -Tridec-2-ene	0.131	0.060	0.000	0.070	6.261	1.8973
<i>trans</i> -Tridec-2-ene	0.115	0.060	0.000	0.070	6.249	1.8973
<i>cis</i> -Tridec-3-ene	0.122	0.060	0.000	0.070	6.255	1.8973
<i>trans</i> -Tridec-3-ene	0.114	0.060	0.000	0.070	6.249	1.8973
<i>cis</i> -Tridec-4-ene	0.127	0.060	0.000	0.070	6.172	1.8973
<i>trans</i> -Tridec-4-ene	0.111	0.060	0.000	0.070	6.142	1.8973
<i>cis</i> -Tridec-5-ene	0.110	0.060	0.000	0.070	6.146	1.8973
<i>trans</i> -Tridec-5-ene	0.089	0.060	0.000	0.070	6.125	1.8973
<i>cis</i> -Tridec-6-ene	0.119	0.060	0.000	0.070	6.144	1.8973
<i>trans</i> -Tridec-6-ene	0.117	0.060	0.000	0.070	6.144	1.8973
Tetradec-1-ene	0.090	0.060	0.000	0.070	6.536	2.0382
<i>cis</i> -Tetradec-2-ene	0.130	0.060	0.000	0.070	6.840	2.0382
<i>trans</i> -Tetradec-2-ene	0.114	0.060	0.000	0.070	6.743	2.0382
<i>cis</i> -Tetradec-3-ene	0.121	0.060	0.000	0.070	6.755	2.0382
<i>trans</i> -Tetradec-3-ene	0.113	0.060	0.000	0.070	6.719	2.0382
<i>cis</i> -Tetradec-4-ene	0.126	0.060	0.000	0.070	6.776	2.0382
<i>trans</i> -Tetradec-4-ene	0.110	0.060	0.000	0.070	6.731	2.0382
<i>cis</i> -Tetradec-5-ene	0.114	0.060	0.000	0.070	6.753	2.0382
<i>trans</i> -Tetradec-5-ene	0.086	0.060	0.000	0.070	6.696	2.0382
<i>cis</i> -Tetradec-6-ene	0.118	0.060	0.000	0.070	6.762	2.0382
<i>trans</i> -Tetradec-6-ene	0.116	0.060	0.000	0.070	6.726	2.0382
<i>cis</i> -Tetradec-7-ene	0.109	0.060	0.000	0.070	6.734	2.0382
<i>trans</i> -Tetradec-7-ene	0.091	0.060	0.000	0.070	6.713	2.0382
Isopropylbenzene	0.602	0.490	0.000	0.160	4.084	1.1391
Propylbenzene	0.604	0.500	0.000	0.150	4.230	1.1391
1,3,5-Trimethylbenzene	0.649	0.520	0.000	0.190	4.344	1.1391
1,2,4-Trimethylbenzene	0.677	0.560	0.000	0.190	4.441	1.1391
1-Methyl-4-isopropylbenzene	0.607	0.490	0.000	0.190	4.590	1.2800
1,2,3-Trimethylbenzene	0.728	0.610	0.000	0.190	4.565	1.1391
1,2-Diethylbenzene	0.688	0.500	0.000	0.180	4.732	1.2800
1,3-Diisopropylbenzene	0.605	0.460	0.000	0.200	5.170	1.5618
1,2,3,5-Tetramethylbenzene	0.748	0.610	0.000	0.190	5.052	1.2800
1,4-Diisopropylbenzene	0.616	0.470	0.000	0.200	5.315	1.5618
1-Hexanol	0.210	0.420	0.370	0.480	3.610	1.0127
1-Nonanol	0.193	0.420	0.370	0.480	5.120	1.4354
Pentadec-1-ene	0.083	0.060	0.000	0.070	7.008	2.1791
Hexadec-1-ene	0.081	0.080	0.000	0.070	7.586	2.3200

that the squalane solvent does have a non-zero  $e_k$  coefficient. Analysis of the  $RI$  values in Table 3 in accordance with eqn. (3) yielded the following Abraham model expression.

**Table 3.** Retention indices,  $r_i$  (at 383 K) on a squalane stationary phase column, and Abraham model **L** solute descriptors for linear alkanes, alkenes and alkynes.

Compound	$RI/100$	L Value database	L Value Eqn. (5)
Hex-1-yne	5.839	2.510	2.565
Hex-2-yne	6.384	2.765	2.864
Hex-3-yne	6.199	2.659	2.765
Hept-1-yne	6.842	3.000	3.084
Hept-2-yne	7.420		3.402
Hept-3-yne	7.158		3.265
Oct-1-yne	7.837	3.521	3.598
Oct-2-yne	8.418	3.850	3.916
Oct-3-yne	8.163		3.780
Oct-4-yne	8.103	3.609	3.749
Non-1-yne	8.841	4.019	4.118
Non-2-yne	9.406		4.428
Non-3-yne	9.147		4.289
Non-4-yne	9.097		4.264
Dec-1-yne	9.842	4.537	4.635
Dec-2-yne	10.408		4.946
Dec-3-yne	10.131		4.797
Dec-4-yne	10.068		4.767
Dec-5-yne	10.080		4.770
Undec-1-yne	10.842		5.152
Undec-2-yne	11.401		5.460
Undec-3-yne	11.124		5.312
Undec-4-yne	11.048		5.273
Undec-5-yne	11.043		5.269
Dodec-1-yne	11.844	5.657	5.670
Dodec-2-yne	12.398		5.975
Dodec-3-yne	12.114		5.824
Dodec-4-yne	12.033		5.782
Dodec-5-yne	12.017		5.773
Dodec-6-yne	12.003		5.766
Hexane	6.000	2.668	2.609
Heptane	7.000	3.173	3.128
Octane	8.000	3.677	3.646
Nonane	9.000	4.182	4.164
Decane	10.000	4.686	4.683
Undecane	11.000	5.191	5.201
Dodecane	12.000	5.696	5.720
Tridecane	13.000	6.200	6.238
Tetradecane	14.000	6.705	6.756
Pentadecane	15.000	7.209	7.275

Hexadecane	16.000	7.714	7.793
Heptadecane	17.000	8.218	8.312
Octadecane	18.000	8.722	8.830
Hex-1-ene	5.840	2.572	2.545
cis-Hex-2-ene	6.054	2.684	2.671
trans-Hex-2-ene	5.964	2.655	2.619
cis-Hex-3-ene	5.937	2.664	2.607
trans-Hex-3-ene	5.906	2.659	2.590
Hept-1-ene	6.835	3.063	3.064
cis-Hept-2-ene	7.051	3.210	3.186
trans-Hept-2-ene	6.987	3.180	3.149
cis-Hept-3-ene	6.923	3.143	3.118
trans-Hept-3-ene	6.874	3.125	3.091
Oct-1-ene	7.829	3.568	3.579
cis-Oct-2-ene	8.036	3.683	3.696
trans-Oct-2-ene	7.973	3.668	3.661
cis-Oct-3-ene	7.902	3.663	3.625
trans-Oct-3-ene	7.880	3.647	3.612
cis-Oct-4-ene	7.886	3.607	3.618
trans-Oct-4-ene	7.841	3.593	3.590
Non-1-ene	8.828	4.073	4.096
cis-Non-2-ene	9.026	4.245	4.210
trans-Non-2-ene	8.966	4.188	4.175
cis-Non-3-ene	8.881	4.151	4.133
trans-Non-3-ene	8.865	4.148	4.122
cis-Non-4-ene	8.860	4.173	4.123
trans-Non-4-ene	8.844	4.141	4.111
Dec-1-ene	9.827	4.533	4.615
cis-Dec-2-ene	10.022	4.745	4.725
trans-Dec-2-ene	9.966	4.670	4.693
cis-Dec-3-ene	9.864	4.680	4.643
trans-Dec-3-ene	9.855	4.671	4.635
cis-Dec-4-ene	9.834	4.669	4.627
trans-Dec-4-ene	9.827	4.638	4.620
cis-Dec-5-ene	9.821	4.665	4.619
trans-Dec-5-ene	9.847	4.637	4.630
Undec-1-ene	10.826	5.023	5.132
cis-Undec-2-ene	11.019	5.258	5.242
trans-Undec-2-ene	10.965	5.192	5.210
cis-Undec-3-ene	10.858	5.178	5.157
trans-Undec-3-ene	10.853	5.150	5.152
cis-Undec-4-ene	10.811	5.168	5.133
trans-Undec-4-ene	10.812	5.138	5.130
cis-Undec-5-ene	10.789	5.153	5.120
trans-Undec-5-ene	10.820	5.126	5.130
Dodec-1-ene	11.834	5.515	5.654
cis-Dodec-2-ene	12.023	5.766	5.762

<i>trans</i> -Dodec-2-ene	11.969	5.699	5.731
<i>cis</i> -Dodec-3-ene	11.857	5.692	5.676
<i>trans</i> -Dodec-3-ene	11.852	5.656	5.670
<i>cis</i> -Dodec-4-ene	11.806	5.667	5.648
<i>trans</i> -Dodec-4-ene	11.811	5.641	5.648
<i>cis</i> -Dodec-5-ene	11.766	5.653	5.625
<i>trans</i> -Dodec-5-ene	11.811	5.636	5.643
<i>cis</i> -Dodec-6-ene	11.760	5.655	5.623
<i>trans</i> -Dodec-6-ene	11.801	5.647	5.644
Tridec-1-ene	12.835	6.046	6.174
<i>cis</i> -Tridec-2-ene	13.022	6.261	6.280
<i>trans</i> -Tridec-2-ene	12.970	6.249	6.249
<i>cis</i> -Tridec-3-ene	12.851	6.255	6.189
<i>trans</i> -Tridec-3-ene	12.851	6.249	6.187
<i>cis</i> -Tridec-4-ene	12.798	6.172	6.163
<i>trans</i> -Tridec-4-ene	12.803	6.142	6.162
<i>cis</i> -Tridec-5-ene	12.750	6.146	6.134
<i>trans</i> -Tridec-5-ene	12.803	6.125	6.157
<i>cis</i> -Tridec-6-ene	12.725	6.144	6.123
<i>trans</i> -Tridec-6-ene	12.781	6.144	6.152
Tetradec-1-ene	13.832	6.536	6.690
<i>cis</i> -Tetradec-2-ene	14.015	6.840	6.794
<i>trans</i> -Tetradec-2-ene	13.969	6.743	6.767
<i>cis</i> -Tetradec-3-ene	13.841	6.755	6.702
<i>trans</i> -Tetradec-3-ene	13.846	6.719	6.703
<i>cis</i> -Tetradec-4-ene	13.777	6.776	6.670
<i>trans</i> -Tetradec-4-ene	13.793	6.731	6.675
<i>cis</i> -Tetradec-5-ene	13.720	6.753	6.638
<i>trans</i> -Tetradec-5-ene	13.784	6.696	6.664
<i>cis</i> -Tetradec-6-ene	13.686	6.762	6.621
<i>trans</i> -Tetradec-6-ene	13.757	6.726	6.657
<i>cis</i> -Tetradec-7-ene	13.667	6.734	6.609
<i>trans</i> -Tetradec-7-ene	13.745	6.713	6.645

$$RI/100 = 0.967(0.058) - 0.458(0.245) \mathbf{E} + 1.929(0.008) \mathbf{L} \quad (4)$$

$$(N = 100, SD = 0.111, R^2 = 0.998, F = 30284)$$

where  $N$  is the number of experimental data points,  $SD$  is the standard deviation,  $R^2$  is the squared correlation coefficient, and  $F$  is the Fisher F-statistic. Standard errors in the equation coefficients are given in parentheses immediately following the respective coefficient.

We first establish Equation (4) provides a reasonably accurate mathematical description of the gas chromatographic elution behaviour of the 100 alkane, alkene and alkyne solutes on the squalane stationary phase. Through suitable mathematical rearrangement of eqn. (4)

$$\mathbf{L} = [(RI/100) - 0.967 + 0.458 \mathbf{E}]/1.929 \quad (5)$$

one can calculate the  $\mathbf{L}$  solute descriptors of the remaining 20  $C_7$ - $C_{12}$  alkynes for which  $RI$  values are available on a squalane stationary phase. The numerical values of our calculated  $\mathbf{L}$  solute descriptors are given in the last column of Table 3. The average error and average absolute error between the  $\mathbf{L}$  values in our database and those calculated based on eqn. (5) are  $AE = -0.001$  and  $AAE = 0.043$ , respectively. We do note that the tabulated numerical values of the  $\mathbf{L}$  solute descriptor based on eqn. (5) differ somewhat from the numerical values given UFZ-LSER Database<sup>57</sup> that are referenced to LSER Dataset 2017.

Rang and coworkers<sup>58</sup> also determined the isothermal Kovats retention indices of linear  $C_7$ - $C_{14}$  alkynes on capillary columns coated with apiezon L, polyphenyl ether and polyethylene glycol 4000 stationary phases at elevated temperatures. Of particular interest are the chromatographic measurements for the linear tridecynes and tetradecynes for which we do not have numerical values of the  $\mathbf{L}$  solute descriptors. A search of the published chemical and engineering literature found Kovats retention indices<sup>60,61</sup> for isopropylbenzene, propylbenzene, 1,3,5-trimethylbenzene, 1,2,4-trimethylbenzene, 1-methyl-4-isopropylbenzene, 1,2,3-trimethylbenzene, 1-hexanol, 1,2-diethylbenzene, 1,3-diisopropylbenzene, 1,2,3,5-tetramethylbenzene, 1,4-diisopropylbenzene, 1-pentadecene, 1-hexadecene, 1-heptadecene, and 1-nonanol on an apiezon L stationary phase column at 423 K. Including the retention index data of Rang et al.<sup>58</sup> for the linear decynes, undecynes and dodecynes for which we just computed  $\mathbf{L}$  solute descriptors (see Table 3), there are 44 experimental data points to use in constructing an Abraham model correlation. This should be sufficient to develop a meaningful Abraham model correlation for describing the retention behaviour of organic compounds on an apiezon L stationary phase. It takes between 30 to 40 experimental values to develop an Abraham model correlation.

Analysis of the experimental data in the second column of Table 4 yielded the following Abraham model expression:

$$RI/100 = 0.686(0.066) + 2.788(0.161) \mathbf{E} - 2.011(0.199) \mathbf{S} + 2.115(0.197) \mathbf{A} + 1.988(0.011) \mathbf{L} \quad (6)$$

$$(N = 44, SD = 0.088, R^2 = 0.999, F = 9996)$$

Preliminary analysis showed that the  $b_k \cdot \mathbf{B}$  term made a negligible contribution to the  $RI/100$  calculation (with  $s_k$  being  $-0.029$ ) and this term was removed from the final regression. Eqn. (6) provides a reasonably accurate mathematical description of the observed gas chromatographic elution behavior of the 44 organic solutes on the apiezon stationary phase.

$$\mathbf{L} = [(RI/100) - 0.686 - 2.788 \mathbf{E} + 2.011 \mathbf{S} - 2.115 \mathbf{A}]/1.988 \quad (7)$$

Through suitable mathematical rearrangement of eqn. (6), one can calculate the  $\mathbf{L}$  solute descriptors of the linear tridecynes and tetradecynes for which  $RI$  values are available on an apiezon stationary phase. The numerical values of our calculated  $\mathbf{L}$  solute descriptors are given in the last column of Table 4. The average error and average absolute error between the  $\mathbf{L}$  values in our database and those calculated based on eqn. (5) are  $AE = 0.001$  and  $AAE$



= 0.026, respectively. Solute descriptors for the linear tridecynes and tetradecynes are contained in the UFZ-LSER Database, however, numerical values can be estimated based on the molecule's canonical Smiles code. We were not able to find sufficient *RI* data for solutes eluted from polyphenyl ether and polyethylene glycol 4000 stationary phases to develop Abraham model correlations.

**Table 4.** Retention indices, *RI* (at 423 K) on an Apiezon L phase column, and Abraham model **L** solute descriptors for linear alkanes, linear alkynes and miscellaneous organic compounds used in the construction of eqn. (7).

Compound	<i>RI</i> /100	L Value Database	L Value Eqn. (7)
Dec-1-yne	9.972	4.537	4.597
Dec-2-yne	10.506	4.946	4.939
Dec-3-yne	10.174	4.797	4.803
Dec-4-yne	10.108	4.767	4.755
Dec-5-yne	10.129	4.770	4.783
Undec-1-yne	10.952	5.152	5.096
Undec-2-yne	11.508	5.460	5.448
Undec-3-yne	11.169	5.312	5.302
Undec-4-yne	11.099	5.273	5.267
Undec-5-yne	11.092	5.269	5.270
Dodec-1-yne	11.952	5.657	5.607
Dodec-2-yne	12.505	5.975	5.958
Dodec-3-yne	12.164	5.824	5.811
Dodec-4-yne	12.086	5.782	5.771
Dodec-5-yne	12.074	5.773	5.765
Dodec-6-yne	12.060	5.766	5.758
Tridec-1-yne	12.955		6.108
Tridec-2-yne	13.506		6.459
Tridec-3-yne	13.158		6.284
Tridec-4-yne	13.071		6.240
Tridec-5-yne	13.055		6.232
Tridec-6-yne	13.026		6.218
Tetradec-1-yne	13.957		6.600
Tetradec-2-yne	14.507		6.967
Tetradec-3-yne	14.149		6.787
Tetradec-4-yne	14.069		6.746
Tetradec-5-yne	14.039		6.731
Tetradec-6-yne	14.011		6.717
Tetradec-7-yne	14.002		6.713
Hexane	6.000	2.668	2.673
Heptane	7.000	3.173	3.176
Octane	8.000	3.677	3.679
Nonane	9.000	4.182	4.182
Decane	10.000	4.686	4.685
Undecane	11.000	5.191	5.188
Dodecane	12.000	5.696	5.691
Tridecane	13.000	6.200	6.194
Tetradecane	14.000	6.705	6.697
Pentadecane	15.000	7.209	7.200
Hexadecane	16.000	7.714	7.703
Heptadecane	17.000	8.218	8.206
Octadecane	18.000	8.722	8.709
Isopropylbenzene	9.550	4.084	4.110

Propylbenzene	9.860	4.230	4.273
1,3,5-Trimethylbenzene	10.127	4.344	4.365
1,2,4-Trimethylbenzene	10.370	4.441	4.488
1-Methyl-4-isopropylbenzene	10.540	4.590	4.601
1,2,3-Trimethylbenzene	10.701	4.565	4.634
1,2-Diethylbenzene	10.870	4.732	4.664
1,3-Diisopropylbenzene	11.440	5.170	5.026
1,2,3,5-Tetramethylbenzene	11.690	5.052	5.103
1,4-Diisopropylbenzene	11.880	5.315	5.242
Hexan-1-ol	8.420	3.610	3.627
Nonan-1-ol	11.360	5.120	5.130
Pentadec-1-ene	14.888	7.008	7.088
Hexadec-1-ene	15.881	7.586	7.611
Heptadec-1-ene	16.876	8.031	8.113

<sup>a</sup>Solute descriptors for heptadec-1-ene are: **E** = 0.080; **S** = 0.080; **A** = 0.000; **B** = 0.080; **V** = 2.4609; and **L** = 8.031

## PREDICTION OF MOLAR ENTHALPIES OF VAPORIZATION OF LINEAR ALKYNES

Now that we have calculated the **L** solute descriptors of  $C_7$ - $C_{14}$  linear alkynes we wish to illustrate how the numerical values can be used by the scientific community and manufacturing sector to predict unmeasured physical and chemical properties. Of the properties for which we have reported Abraham model correlations enthalpies of vaporization seem the most logical choice for the linear alkynes. Large alkynes have very limited solubility in water. The likelihood that the scientific community will want to predict the compounds' water-to-organic solvents and lethal molar concentrations towards aquatic organisms is small. Even if large alkynes were to be accidentally released in the environment their aqueous molar concentration would be too small to do significant harm to fish and other aquatic organisms. Large alkynes are not medicinal compounds and there is little demand in the pharmaceutical community to estimate their distribution in the body.

Knowledge of gas chromatographic Kovats retention indices of linear alkynes would aid practical analytical chemists in selecting an appropriate stationary phase to separate alkynes from other hydrocarbons that might be present in petroleum-based samples. These calculations are essentially the reverse of the calculations that we just employed in calculating the **L**-solute descriptors. There would not be much in the way of new information by performing more repetitive-like calculations. After considerable thought we decided to illustrate the practical applications by predicting enthalpies of vaporization as these quantities might be needed in the design of high temperature industrial processes. Enthalpies of vaporization describe how the vapor pressure of a compound varies with temperature.

Our published Abraham model correlation<sup>42</sup> (eqn. 8)

$$\Delta H_{\text{vap},298\text{K}} (\text{kJ mol}^{-1}) = 6.100 - 7.363 \mathbf{E} + 9.733 \mathbf{S} + 4.025 \mathbf{A} + 2.123 \mathbf{B} + 9.537 \mathbf{L} - 1.180 \mathbf{S} \cdot \mathbf{S} + 77.871 \mathbf{A} \cdot \mathbf{B} - 5.781 \mathbf{I}_{\text{amine}} - 14.783 \mathbf{I}_{\text{non-}\alpha,\omega\text{-diol}} - 17.873 \mathbf{I}_{\alpha,\omega\text{-diol}} \quad (8)$$

(with  $N = 703$ ,  $SD = 2.09$ ,  $R^2 = 0.986$ ,  $F = 4925.6$ )

provides reasonably accurate predictions of the standard molar enthalpies of vaporization,  $\Delta H_{\text{vap},298\text{K}}$ , as evidence by the correlation's standard deviations of  $SD = 2.09 \text{ kJ mol}^{-1}$ , which is slightly larger than the experimental uncertainty associated with the measured  $\Delta H_{\text{vap},298\text{K}}$  values. For the linear C<sub>7</sub>-C<sub>14</sub> alkynes considered in the current study only the first eight terms on the right-hand side of eqn. (8) contribute to the calculations. The last three terms in eqn. (8) pertain to organic compounds having amino- and hydroxyl-functional groups. Results of our  $\Delta H_{\text{vap},298\text{K}}$  predictions are reported in the second column of Table 5.

**Table 5.** Comparison of the Enthalpies of Vaporization,  $\Delta H_{\text{vap},298\text{K}}$  ( $\text{kJ mol}^{-1}$ ), Predicted by the Abraham Model, eqn. (8), and the Group-Additivity Method of Naef and Acree, eqn. (10).

Compound	$\Delta H_{\text{vap},298\text{K}}$ Eqn. (8)	$\Delta H_{\text{vap},298\text{K}}$ Eqn. (10)
Hept-2-yne	39.93	40.23
Hept-3-yne	38.66	40.23
Oct-3-yne	43.74	44.81
Non-2-yne	49.81	49.39
Non-3-yne	48.63	49.39
Non-4-yne	48.37	49.39
Dec-2-yne	54.80	53.97
Dec-3-yne	53.54	53.97
Dec-4-yne	53.18	53.97
Dec-5-yne	53.30	53.97
Undec-1-yne	57.57	56.52
Undec-2-yne	59.73	58.55
Undec-3-yne	58.45	58.55
Undec-4-yne	58.07	58.55
Undec-5-yne	58.07	58.55
Dodec-2-yne	64.69	63.12
Dodec-3-yne	63.37	63.12
Dodec-4-yne	62.97	63.12
Dodec-5-yne	62.89	63.12
Dodec-6-yne	62.83	63.12
Tridec-1-yne	66.71	65.68
Tridec-2-yne	69.29	67.71
Tridec-3-yne	67.62	67.71
Tridec-4-yne	67.20	67.71
Tridec-5-yne	57.13	67.71
Tridec-6-yne	66.99	67.71
Tetradec-1-yne	71.34	70.26
Tetradec-2-yne	74.16	72.29
Tetradec-3-yne	72.44	72.29
Tetradec-4-yne	72.05	72.29
Tetradec-5-yne	71.91	72.29
Tetradec-6-yne	71.78	72.29
Tetradec-7-yne	71.74	72.29

We were unable to find experimental  $\Delta H_{\text{vap},298\text{K}}$  data in the published chemical literature to compare our calculated values against. What we offer in the way of a comparison is to compare our calculated values against the calculated values of a popular group-additivity method proposed by Naef and Acree<sup>62</sup> that has been shown to predict  $\Delta H_{\text{vap},298\text{K}}$  values for a wide range of organic and organometallic compounds to within a standard deviation of  $SD = 4.30 \text{ kJ mol}^{-1}$  for 3,460 compounds. The basic method sums the contributions that each atomic group makes to the given thermodynamic or physical property:

$$\text{Property} = \sum_i A_i a_i + \sum_j B_j b_j + \text{constant} \quad (9)$$

where  $A_i$  is the number of occurrences of the  $i$ th atom group,  $B_j$  is the number of times each special group occurs,  $a_i$  and  $b_j$  are the numerical values of each atom group and special group, and  $C$  is a constant.

The atom group-additivity method, proposed by Naef and Acree,<sup>62</sup> fragments linear alkyne molecules into two types of sp hybridized carbon atoms and two types of sp<sup>3</sup> hybridized carbon atoms. Each carbon atom type is based on the number of each type of atoms bonded to the carbon atom. One of the sp carbon atom-groups will be bonded to one hydrogen atom (HC#) and the second carbon atom type will be bonded to zero hydrogen atoms (CC#). The symbol “#” was used by Naef and Acree to denote a carbon-carbon atom triple bond. In the case of the sp<sup>3</sup> hybridized carbon atoms one carbon atom is bonded to three hydrogen atoms and one carbon atom (CH<sub>3</sub> group), and the second carbon atom type is bonded to two hydrogen atoms and two carbon atoms (CH<sub>2</sub> group). There is also one special group that is defined as the number of carbon atoms in the unsaturated hydrocarbon molecule.

In eqn. (10) below we have filled in the numerical group values and constants for predicting  $\Delta H_{\text{vap},298\text{K}}$  of linear alkynes:

$$\Delta H_{\text{vap},298\text{K}} (\text{kJ mol}^{-1}) = 3.07 n_{\text{CH}_3} + 4.67 n_{\text{CH}_2} + 2.42 n_{\text{HC\#}} + 6.05 n_{\text{CC\#}} - 0.09 n_{\text{carbon unsat}} + 8.61 \quad (10)$$

Examination of the numerical entries in the last two columns of Table 5 reveals that the predictions based on the Abraham model are similar to predictions based on the group-additivity model of Naef and Acree.<sup>61</sup> Except for the 1-alkynes the group-additivity method though is not able to distinguish between the placement of the triple bond in the molecule, and gives the same predicted values for a given molecular formula. In other words, the predicted values of all 2-tetradecyne through 7-tetradecyne molecules are the same. The group additivity model also does not distinguish between “cis” and “trans” isomers. This limitation is a common feature of most group-additivity and group contribution methods. The Abraham model, on the other hand, would provide different predicted values for the different alkyne isomers, and does not require fragmentation of the molecule into atom groups or functional groups. Fragmentation of molecules into functional groups can be difficult at times, particularly in the case of more complex molecules having many different functional groups.

## CONCLUSION

Numerical values of the Abraham model **L** solute descriptor have been reported for the first time for 33 linear C<sub>7</sub>-C<sub>14</sub> alkynes. The numerical values were determined by regression analysis of published isothermal gas chromatographic retention indices on squalane and apiezon L stationary phases. Calculated **L** solute descriptors completed our set of solute descriptors for linear C<sub>7</sub>-C<sub>14</sub> alkynes. Prior to this study our private database of descriptor values contained only the **E**, **S**, **A**, **B** and **V** solute descriptors for these 33 alkyne molecules. Solute descriptors were used to predict the standard molar enthalpies of vaporization based on a previously published Abraham model correlation.<sup>42</sup> The predicted values compare very favourably with calculated values based on an atom-group additivity model.<sup>62</sup> Unlike the additivity model the Abraham model provides different predicted values of  $\Delta H_{\text{vap},298\text{K}}$  for each linear alkyne isomer that structurally differ from each other by the placement of the triple bond in the molecule.

## REFERENCES

- Abraham, M. H., Acree, W. E. Jr., Gas-solvent and water-solvent partition of trans-stilbene at 298 K, *J. Mol. Liq.*, **2017**, 238, 58-61. <https://doi.org/10.1016/j.molliq.2017.04.119>
- Abraham, M. H. Acree, W. E. Jr., Descriptors for the prediction of partition coefficients of 8-hydroxyquinoline and its derivatives, *Sep. Sci. Technol.*, **2014**, 49, 2135-2141. <https://doi.org/10.1080/01496395.2014.928768>
- Hart, E., Klein, A., Barrera, M., Jodray, M., Rodriguez, K., Acree, W. E. Jr., Abraham, M. H., Development of Abraham model correlations for describing the transfer of molecular solutes into propanenitrile and butanenitrile from water and from the gas phase, *Phys. Chem. Liq.*, **2018**, 56, 821-833. <https://doi.org/10.1080/00319104.2017.1399268>
- Fischer R., Jodray, M., Qian, E., Wang, L., Lee, G., Yue, D., Che, M., Liu, Y., Acree, W. E. Jr., Abraham, M. H., Abraham model correlations for solute transfer into benzyl alcohol from both water and the gas phase, *Phys. Chem. Liq.*, **2020**, 58, 116-126. <https://doi.org/10.1080/00319104.2018.1550778>
- Rabhi, F., Mutelet, F., Sifaoui, H., Wagle, D. V., Baker, G. A., Churchill, B., Acree, W. E. Jr., Characterization of the solubilizing ability of tetraalkylammonium ionic liquids containing a pendant alkyl chain bearing a basic N,N-dimethylamino or N,N-dimethylaminoethoxy functionality, *J. Mol. Liq.*, **2019**, 283, 380-390. <https://doi.org/10.1016/j.molliq.2019.03.066>
- Mutelet, F., Baker, G. A., Ravula, S., Qian, E., Wang, L., Acree, W. E. Jr., Infinite dilution activity coefficients and gas-to-liquid partition coefficients of organic solutes dissolved in 1-sec-butyl-3-methylimidazolium bis(trifluoromethylsulfonyl)imide and in 1-tert-butyl-3-methylimidazolium bis(trifluoromethylsulfonyl)imide, *Phys. Chem. Liq.*, **2019**, 57, 453-472. <https://doi.org/10.1080/00319104.2018.1491045>
- Mutelet, F., Ravula, S., Baker, G. A., Woods, D., Tong, X., Acree, W. E. Jr., Infinite dilution activity coefficients and gas-to-liquid partition coefficients of organic solutes dissolved in 1-benzylpyridinium bis(trifluoromethylsulfonyl)imide and 1-cyclohexylmethyl-1-methylpyrrolidinium bis(trifluoromethylsulfonyl)imide, *J. Solut. Chem.*, **2018**, 47, 308-335. <https://doi.org/10.1007/s10953-018-0720-5>
- Abraham, M. H., Ibrahim, A., Acree, W. E. Jr., Air to brain, blood to brain and plasma to brain distribution of volatile organic compounds: linear free energy analyses, *Eur. J. Med. Chem.*, **2006**, 41, 494-502. <https://doi.org/10.1016/j.ejmech.2006.01.004>
- Abraham, M. H., Ibrahim, A., Acree, W. E. Jr., Air to muscle and blood/plasma to muscle distribution of volatile organic compounds and drugs: linear free energy analyses. *Chem. Res. Toxicol.*, **2006**, 19, 801-808. <https://doi.org/10.1021/tx050337k>
- Abraham, M. H., Ibrahim, A., Acree, W. E., Air to liver partition coefficients for volatile organic compounds and blood to liver partition coefficients for volatile organic compounds and drugs, *Eur. J. Med. Chem.*, **2007**, 42, 743751. <https://doi.org/10.1016/j.ejmech.2006.12.011>
- Abraham, M. H., Ibrahim, A., Acree, W. E., Air to lung partition coefficients for volatile organic compounds and blood to lung partition coefficients for volatile organic compounds and drugs, *Eur. J. Med. Chem.*, **2008**, 43, 478485. <https://doi.org/10.1016/j.ejmech.2007.04.002>
- Abraham, M. H., Ibrahim, A., Air to fat and blood to fat distribution of volatile organic compounds and drugs: Linear free energy analyses. *Eur. J. Med. Chem.*, **2006**, 41: 14301438. <https://doi.org/10.1016/j.ejmech.2006.07.012>
- Hoover, K. R., Acree, W. E. Jr., Abraham, M. H., Chemical toxicity correlations for several fish species based on the Abraham solvation parameter model, *Chem. Res. Toxicol.*, **2005**, 18, 1497-505. <https://doi.org/10.1021/tx050164z>
- Hoover, K. R., Flanagan, K. B., Acree, W. E. Jr., Abraham, M. H. Chemical toxicity correlations for several protozoas, bacteria, and water fleas based on the Abraham solvation parameter model, *J. Environ. Eng. Sci.*, **2007**, 6, 165-174. <https://doi.org/10.1139/s06-041>
- Bowen, K. R., Flanagan, K. B., Acree, W. E., Abraham, M. H., Rafols, C., Correlation of the toxicity of organic compounds to tadpoles using the Abraham model, *Sci. Total Environ.*, **2006**, 371, 99-109. <https://doi.org/10.1016/j.scitotenv.2006.08.030>
- Bowen, K. R., Flanagan, K. B., Acree, W. E., Abraham, M. H., Correlating toxicities of organic compounds to select protozoa using the Abraham model, *Sci. Total Environ.*, **2006**, 369, 109-118. <https://doi.org/10.1016/j.scitotenv.2006.05.008>
- Lu, J. Z., Acree, W. E. Jr., Abraham, M. H., Abraham model correlations for enthalpies of solvation of organic solutes dissolved in N,N-dimethylacetamide, 2-butanone and tetrahydrofuran (UPATED) at 298.15 K, *Phys. Chem. Liq.*, **2020**, 58, 675-692. <https://doi.org/10.1080/00319104.2019.1633528>
- Lu, J. Z., Acree, W. E. Jr., Abraham, M. H., Abraham model correlations for enthalpies of solvation of organic solutes dissolved in methyl acetate and octane, *Phys. Chem. Liq.*, **2020**, 58, 18-30. <https://doi.org/10.1080/00319104.2018.1534234>
- Lu, J. Z., Acree, W. E. Jr., Abraham, M. H., Updated Abraham model correlations for enthalpies of solvation of organic solutes dissolved in benzene and acetonitrile, *Phys. Chem. Liq.*, **2019**, 57, 84-99. <https://doi.org/10.1080/00319104.2018.1423565>
- Higgins, E., Acree, W. E. Jr., Abraham, M. H., Development of Abraham model correlations for enthalpies of solvation of organic solutes dissolved in 1,3-dioxolane, *Phys. Chem. Liq.*, **2016**, 54, 786-796. <https://doi.org/10.1080/00319104.2016.1161043>
- Schmidt, A., Zad, M., Acree, W. E. Jr., Abraham M. H., Development of Abraham model correlations for predicting enthalpies of solvation of nonionic solutes dissolved in formamide, *Phys. Chem. Liq.*, **2016**, 54: 313-324. <https://doi.org/10.1080/00319104.2015.1084882>
- Hart, E., Grover, D., Zettl, H., Koshevarova, V., Acree, W. E. Jr., Abraham M. H., Development of Abraham model expressions for predicting the enthalpies of solvation of solutes dissolved in acetic acid, *Phys. Chem. Liq.*, **2016**, 54, 141-154. <https://doi.org/10.1080/00319104.2015.1079194>
- Hart, E., Grover, D., Zettl, H., Acree, W. E. Jr., Abraham, M. H., Abraham model enthalpy of solvation correlations for solutes



- dissolved in dimethyl carbonate and diethyl carbonate, *Phys. Chem. Liq.*, **2015**, *53*, 732-747. <https://doi.org/10.1080/00319104.2015.1042478>
- <sup>24</sup>Hart, E., Zettl, H., Grover, D., Acree, W. E. Jr., Abraham, M. H., Abraham model enthalpy of solvation correlations for solutes dissolved in 1-alkanol solvents (C4-C6), *Phys. Chem. Liq.*, **2015**, *53*, 638-659. <https://doi.org/10.1080/00319104.2015.1018259>
- <sup>25</sup>Mintz, C., Clark, M., Burton, K., Acree, W. E. Jr., Abraham, M. H., Enthalpy of solvation correlations for gaseous solutes dissolved in benzene and in alkane solvents based on the Abraham model, *QSAR Comb. Sci.*, **2007**, *26*, 881-888. <https://doi.org/10.1002/qsar.200630152>
- <sup>26</sup>Mintz, C., Burton, K., Acree, W. E. Jr., Abraham, M. H., Enthalpy of solvation correlations for gaseous solutes dissolved in linear alkanes (C<sub>5</sub>-C<sub>16</sub>) based on the Abraham model, *QSAR Comb. Sci.*, **2008**, *27*, 179-186. <https://doi.org/10.1002/qsar.200730040>
- <sup>27</sup>Mintz, C., Burton, K., Ladlie, T., Clark, M., Acree, W. E. Jr., Abraham, M. H., Enthalpy of solvation correlations for organic solutes and gases dissolved in N,N-dimethylformamide and tert-butanol, *J. Mol. Liq.*, **2009**, *144*, 23-31. <https://doi.org/10.1016/j.molliq.2008.09.002>
- <sup>28</sup>Abraham, M. H. Acree, W. E. Jr., Descriptors for the  $\alpha,\omega$ -dicarboxylic acids from oxalic acid to sebacic acid, *Fluid Phase Equilib.*, **2018**, *467*, 17-24. <https://doi.org/10.1016/j.fluid.2018.03.017.0378-3812>
- <sup>29</sup>Acree, W. E. Jr., Jodray, M., Abraham, M. H., Illustration of the calculation of solute descriptors for maltol from published solubility data, *Phys. Chem. Liq.*, **2018**, *56*, 403-409. <https://doi.org/10.1080/00319104.2017.1376061>
- <sup>30</sup>Acree W. E. Jr., Bowen, K. R., Horton, M. Y., Abraham, M. H., Computation of Abraham model solute descriptors for 3-methyl-4-nitrobenzoic acid from measured solubility data, *Phys. Chem. Liq.*, **2017**, *55*, 482-491. <https://doi.org/10.1080/00319104.2016.1227813>
- <sup>31</sup>Abraham, M. H., Acree, W. E. Jr., Brumfield, M., Hart, E., Pipersburgh, L., Mateja, K., Dai, C., Grover, D., Zhang, S., Deduction of physicochemical properties from solubilities: 2,4-dihydroxy-benzophenone, biotin, and caprolactam as examples, *J. Chem. Eng. Data*, **2015**, *60*, 1440-1446. <https://doi.org/10.1021/je501140p>
- <sup>32</sup>Abraham, M. H., Gola, J. M. R., Cometto-Muniz, J. E., Cain, W. S., The correlation and prediction of VOC thresholds for nasal pungency, eye irritation and odour in humans, *Indoor+Built Environ.*, **2001**, *10*, 252-257. <https://doi.org/10.1177/1420326X0101000320>
- <sup>33</sup>Abraham, M. H., Hassanisadi, M., Jalali-Heravi, M., Ghafourian, T., Cain, W. S., Cometto-Muniz, J. E., Draize rabbit eye test compatibility with eye irritation thresholds in humans: A quantitative structure-activity relationship analysis, *Toxicol. Sci.*, **2003**, *76*, 384-391. <https://doi.org/10.1093/toxsci/kfg242>
- <sup>34</sup>Abraham, M. H., Kumarsingh, R., Cometto-Muniz, J. E., Cain, W. S., Draize eye scores and eye irritation thresholds in man can be combined into one QSAR, *Ann. New York Acad. Sci.*, **1998**, *855*, 652-656. <https://doi.org/10.1111/j.17496632.1998.tb10641.x>
- <sup>35</sup>Cometto-Muniz, J. E., Cain, W. S., Abraham, M. H., Determinants for nasal trigeminal detection of volatile organic compounds, *Chem. Senses*, **2005**, *30*, 627-642. <https://doi.org/10.1093/chemse/bji056>
- <sup>36</sup>Abraham, M. H., Kumarsingh, R., Cometto-Muniz, J. E., Cain, W. S., An algorithm for nasal pungency thresholds in man, *Arch. Toxicol.*, **1998**, *72*, 227-232. <https://doi.org/10.1007/s002040050493>
- <sup>37</sup>Abraham, M. H., Andonian-Haftvan, J., Cometto-Muniz, J. E., Cain, W. S., An analysis of nasal irritation thresholds using a new solvation equation, *Fund. Appl. Toxicol.*, **1996**, *31*, 71-76. <https://doi.org/10.1006/faat.1996.0077>
- <sup>38</sup>Abraham, M. H., Martins, F., Human skin permeation and partition: general linear free-energy relationship analyses, *J. Pharm. Sci.*, **2004**, *93*, 1508-1523. <https://doi.org/10.1002/jps.20070>
- <sup>39</sup>Zhang, K., Abraham, M. H., Liu, X., An equation for the prediction of human skin permeability of neutral molecules, ions and ionic species, *Int. J. Pharm.*, **2017**, *521*, 259-266. <https://doi.org/10.1016/j.ijpharm.2017.02.059>
- <sup>40</sup>Abraham, M. H., Acree, W. E. Jr., Mintz, C., Payne, S., Effect of anesthetic structure on inhalation anesthesia: implications for the mechanism, *J. Pharm. Sci.*, **2008**, *97*, 2373-2384. <https://doi.org/10.1002/jps.21150>
- <sup>41</sup>Abraham, M. H., Acree, W. E. Jr., Prediction of convulsant activity of gases and vapors, *Eur. J. Med. Chem.*, **2009**, *44*, 885-890. <https://doi.org/10.1016/j.ejmech.2008.05.027>
- <sup>42</sup>Churchill, B., Acree, W. E. Jr., Abraham, M. H., Development of Abraham model expressions for predicting the standard molar enthalpies of vaporization of organic compounds at 298.15 K, *Thermochim. Acta*, **2019**, *681*, 178372/1-178372/6. <https://doi.org/10.1016/j.tca.2019.178372>
- <sup>43</sup>Abraham, M. H., Acree, W. E. Jr., Estimation of enthalpies of sublimation of organic, organometallic and inorganic compounds, *Fluid Phase Equilib.*, **2020**, *515*, 112575/1-112475/5. <https://doi.org/10.1016/j.fluid.2020.112575>
- <sup>44</sup>Abraham, M. H., Acree, W. E. Jr., Estimation of vapor pressures of liquid and solid organic and organometallic compounds at 298.15 K, *Fluid Phase Equilib.*, **2020**, *519*, 112595/1-112595/5. <https://doi.org/10.1016/j.fluid.2020.112595>
- <sup>45</sup>Abraham, M. H., Acree, W. E., Estimation of heat capacities of gases, liquids and solids, and heat capacities of vaporization and of sublimation of organic chemicals at 298.15 K, *J. Mol. Liq.*, **2020**, *317*, 113969/1-113969/4. <https://doi.org/10.1016/j.molliq.2020.113969>
- <sup>46</sup>Abraham, M. H., Acree, W. E. Jr., Descriptors for artemisinin and its derivatives; estimation of physicochemical and biochemical data, *Eur. Chem. Bull.*, **2013**, *2*, 1027-1037. <http://dx.doi.org/10.17628/ecb.2013.2.1027-10>
- <sup>47</sup>Bowen, K. R., Stephens, T. W., Lu, H., Satish, K., Shan, D., Acree, W. E. Jr., Abraham, M. H., Experimental and predicted solubilities of 3,4-dimethoxybenzoic acid in select organic solvents of varying polarity and hydrogen-bonding character, *Eur. Chem. Bull.*, **2013**, *2*, 577-583. <http://dx.doi.org/10.17628/ecb.2013.2.577-58>
- <sup>48</sup>Wilson, A., Tian, A., Chou, V., Quay, A. N., Acree, W. E. Jr., Abraham, M. H., Experimental and predicted solubilities of 3,4-dichlorobenzoic acid in select organic solvents and in binary aqueous-ethanol mixtures, *Phys. Chem. Liq.*, **2012**, *50*, 324-335. <https://doi.org/10.1080/00319104.2012.673166>
- <sup>49</sup>Poole, C. F., Ariyasena, T. C., Lenca, N., Estimation of the environmental properties of compounds from chromatographic properties and the solvation parameter method. *J. Chromatogr. A.*, **2013**, *1317*, 85-104. <https://doi.org/10.1016/j.chroma.2013.05.045>
- <sup>50</sup>Clarke, E. D., Mallon, L., The Determination of Abraham descriptors and their Application to Crop Protection Research, in *Modern Methods in Crop Protection Research*, ed. Jeschke, P., Krämer, W., Schirmer, E., Witschel, M., Wiley-VCH Verlag GmbH & Co., **2012**.
- <sup>51</sup>Endo, S., Goss, K.-U., Applications of polyparameter linear free energy relationships in environmental chemistry, *Environ. Sci. Technol.*, **2014**, *48*, 12477-12491. <https://doi.org/10.1021/es503369t>
- <sup>52</sup>Jalan, A., Ashcraft, R. W., West, R. H., Green, W. H., Predicting solvation energies for kinetic modeling, *Ann. Rep. Prog. Chem. Sect. C: Phys. Chem.*, **2010**, *106*, 211-258. <https://doi.org/10.1039/B811056P>
- <sup>53</sup>Abraham, M. H., Acree, W. E. Jr., Liu, X., Descriptors for high-energy nitro compounds; Estimation of thermodynamic, physicochemical and environmental properties, *Prop. Explos. Pyrotech.*, in press. <https://doi.org/10.1002/prep.202000117>



- <sup>54</sup>Abraham, M. H., Acree, W. E. Jr., Liu, X., Descriptors for adamantane and some of its derivatives, *J. Mol. Liq.*, submitted for publication.
- <sup>55</sup>Liu, G., Eddula, S., Jiang, C., Huang, J., Tirumala, P., Xu, A., Acree, W. E. Jr., Abraham, M. H., Abraham solvation parameter model: prediction of enthalpies of vaporization and sublimation of mono-methyl branched alkanes using measured gas chromatographic data, *Eur. Chem. Bull.*, **2020**, 9, 273-284. <http://dx.doi.org/10.17628/ecb.2020.9.273-284>
- <sup>56</sup>Tirumala, P., Huang, J., Eddula, S., Hiang, C., Xu, A., Liu, G., Acree, W. E. Jr., Abraham, M. H., Calculation of Abraham model L-descriptor and standard molar enthalpies of vaporization and sublimation for C9 - C26 mono-alkyl and polymethyl alkanes, *Eur. Chem. Bull.*, **2020**, 9, 317-328. <http://dx.doi.org/10.17628/ecb.2020.9.317-328>
- <sup>57</sup>Ulrich N., Endo S., Brown T. N., Watanabe N., Bronner G., Abraham M. H., Goss K-U., UFZ-LSER database v 3.2.1 [Internet], Leipzig, Germany, Helmholtz Centre for Environmental Research-UFZ. 2017 [accessed on 27.10.2020]. Available from <http://www.ufz.de/lserd>.
- <sup>58</sup>Rang, S., Kuningas, K., Orav, A., Eisen, O., Capillary gas chromatography of n-alkynes. I. Retention indices, *J. Chromatog.*, **1976**, 119, 451-460. [https://doi.org/10.1016/S0021-9673\(00\)86807-7](https://doi.org/10.1016/S0021-9673(00)86807-7)
- <sup>59</sup>Sojak, L., Hrivnak, J., Majer, P., Capillary gas chromatography of linear alkenes on squalane, *Anal. Chem.*, **1973**, 45, 293-302. <https://doi.org/10.1021/ac60324a039>
- <sup>60</sup>Vigdergauz, M. S., Nasybullina, R. K., Polyakova, L. A., Byl'ev, V. A., Methods of assessing fuel and oil quality: The use of apiezons as stationary phases in gas chromatography, *Khim. Tekhnol. Topliv Masel*, **1968**, 11, 57-61.
- <sup>61</sup>Sojak, L., Krupcik, J., Janak, J., Gas chromatography of all C15-C18 linear alkenes on capillary columns with very high resolution power, *J. Chromatog.*, **1980**, 195, 43-64. [https://doi.org/10.1016/S0021-9673\(00\)81542-3](https://doi.org/10.1016/S0021-9673(00)81542-3)
- <sup>62</sup>Naef, R., Acree, W. E. Jr., Calculation of five thermodynamic molecular descriptors by means of a general computer algorithm based on the group-additivity method: standard enthalpies of vaporization, sublimation and solvation, and entropy of fusion of ordinary organic molecules and total phase-change entropy of liquid crystals, *Molecules*, **2017**, 22, 1059/1-1059/41. <https://doi.org/10.3390/molecules22071059>

Received: 04.12.2020.  
Accepted: 25.12.2020.



# ELEMENTS, ALKALOIDS AND ANTIOXIDANT VALUE OF *CHELIDONIUM MAJUS* L. AND THE EXTRACTS OBTAINED BY DIFFERENT EXTRACTION METHODS

Klára Szentmihályi,<sup>[a]\*</sup> Ilona Szöllösi-Varga<sup>[b]</sup> and Mária Then<sup>[c]</sup>

**Keywords:** *Chelidonium majus* L., alkaloids, flavonoids, metal ions, antioxidant value, supercritical fluid extraction.

The active components of *Chelidonium majus* (greater celandine) is based on its sensitive and effective biologically active agents. The active components of greater celandine extracts and, therefore, their usability depends on the extraction methods. This project was to evaluate and compare the components in the extracts obtained by different new and traditional extraction methods. The extracts were obtained by aqueous and alcoholic extraction, supercritical fluid extraction, pressing-centrifugation method, microwave extraction and were examined for alkaloids, elements, and antioxidant activity. The rhizome has the highest tannin, polyphenol, and alkaloid content, while aerial parts of the plant show the highest flavonoid contents and antioxidant activities. The extracts also contain metal ions contributing to the favourable therapeutic effects that can be mainly Cu, Fe, Mn, Cr, and Zn. The traditional pressed extracts rich in alkaloids confirm their usage for the treatment of warts and these extracts also contain Cu and Fe in concentrations that are effective against viruses.

\* Corresponding Authors

Phone: +36 1 382 6506

E-Mail: szentmihalyi.klara@ttk.hu

- [a] Institute of Materials and Environmental Chemistry,  
Research Centre for Natural Sciences, 1117 Budapest,  
Magyar tudósok körútja 2, Hungary
- [b] Department of Biochemistry and Molecular Biology, Szeged  
University, Szeged, Hungary
- [c] Institute of Pharmacognosy, Semmelweis University,  
Budapest, Hungary

America as well. Besides effective bioactive alkaloid components (coptisine, chelidonine, chelerythrine, sanguinarine, berberine, protopine, etc.), greater celandine contains flavonoids, chelidonine acid, resin, fruit acids (malic acid, citric acid, tartaric acid), vitamin C, volatile oil and metals as well.<sup>2,3</sup> The main use of greater celandine is externally against warts and corns, internally for healing liver and gallbladder diseases.<sup>4</sup> Bioactive components of the plant extracts have wide range effects as they have antioxidant, spasmolytic, anti-inflammatory, antimicrobial, antiviral, antifungal, antitumor activity and cytotoxic properties.<sup>5-9</sup>

## INTRODUCTION

Greater celandine (*Chelidonium majus* L., Figure 1) is a member of the Papaveraceae family. Alkaloid rich orange-colored latex flows out from broken stems and roots. The dried latex is available in the herb-trade or its products in pharmacies for internal and external use and in cosmetic shops for external use.<sup>1</sup> This proves the increasing use of the natural materials in therapy.



**Figure 1.** Rhizome and flowering plant of *Chelidonium majus* L.

Greater celandine is found in the vicinity of human habitations as a weed. It grows wild in the whole of Europe and almost everywhere in Asia and today, even in North

Folk medicine indicates the antiviral activity of fresh plants and mainly to its alkaloids in freshly flowing out latex, which is used externally.<sup>10,11</sup> But after drying it, the latex loses its effective compound, which is responsible for the killing of warts. Other microbiological effects of the latex still remain that is why it becomes an important effective substance of the tooth-paste and the mouth-wash as well.<sup>12,13</sup>

For internal use of the medicinal drugs, the most often applied method is the tea making against gall bladder and liver problems. Nevertheless, other extraction methods are also applied, e.g., tincture. In the case of greater celandine pressing method for obtaining fresh latex with sensitive quaternary nitrogen agent content is the traditional extraction. Since the main bioactive components of greater celandine can change and their concentrations decrease with time, we examined different technological methods to study and get extracts of same or similar bioactive agent content as present in fresh plant or pressed latex. The metal elements are also found in the plant and extracts. These elements supposed to contribute to the favorable therapeutic effect. Therefore, the metal ion concentration in the drug and some extracts were measured as well to detect the soluble element. Antioxidant activity is connected to the polyphenolic compounds such as flavonoids.<sup>14</sup> Although there is no positive correlation between them in all cases, the higher antioxidant activity always implies a higher content of antioxidant type compound.

The primary objective was to study the *C. majus* L latex and different extracts for organic and inorganic agents as well as for antioxidant activity. A further objective was to compare and evaluate the measured parameters in different parts of the plant and extracts critically in the view of the main indication field.

## MATERIALS AND METHODS

The samples studied were greater celandine plants freshly collected from the Botanical Garden of Budapest in the flowering state in May. After identification of the plant, a sample was placed in the plant warehouse of the Institute of Pharmacognosy (213/07). All kinds of measurement and extract were made from the fresh plant right away after collection except the element content determination for which the samples were dried (Sample numbers: 778-780).

For the supercritical fluid extraction (SFE), the solvent was technical grade carbon dioxide obtained from Répcelak Gas Trade (Hungary). Alcohol (96 %), propylene glycol solvents, nitric acid (37 %), hydrogen peroxide (30 %) were high purity grade and were purchased from Reanal Ltd (Budapest, Hungary). Chelidonine was purchased from Merck Ltd (Germany) while berberine obtained from Sigma-Aldrich (Hungary). High purity water (18.3 M $\Omega$ .cm) was made by Millipore equipment (Merck Ltd).

ICP multi-element standards (CPAchem Ltd; Stara Zagora, Bulgaria) were used as standard solutions.

### Preparation of extracts

The aqueous extract was made from 6 g plant sample with 100 mL of deionized boiling water. After standing 24 h, it was filtered.

For the pressed method, a fresh plant (100 g) was pressed with a pressing machine obtaining 17.6 g latex (Sample number: SB.CH-12/5).

For the pressed with water method, fresh plant (53.28 g) was pressed with seizing fluid of water and centrifuged, obtaining 37.52 g filtrate (Sample number: SB.H-12/6).

Alcoholic extract was made from 5 g sample with 100 mL of alcohol (96 %). The suspension was kept for 3 days. Then it was filtered (Sample number: TM.CH-A/96).

SFE with water, propylene glycol and alcohol was made in a high-pressure flow-up stream extraction system (University of Veszprém) similarly, as was published earlier. Nevertheless, some parameters (e.g., temperature) and plant to solvent ratio are different.<sup>15,16</sup> SFE with water was made from 62.5 g fresh wet plant with 237 g of carbon dioxide at 35 °C and 250 bar. The extract (6.5882 g, 10.54 %) was received in 100 mL of water (Sample number: IV-62). SFE with propylene glycol was prepared from 97.65 g plant with 198 g carbon dioxide in the first step obtaining 6.55 g extract (6.71 %). At the second step, the plant residue was extracted once more with 280 g carbon dioxide and 51.50 g propylene glycol. The cumulated extract was 25.99 g solution (Sample number: IV-63). SFE with alcohol (96 %)

was prepared from 31.48 g plant with 290 g of carbon dioxide in the first step. The extract yield was 1.8478 g (5.87 %). After this, the residue was extracted again with 96 g carbon dioxide and 10.90 g alcohol. The cumulated extract was 8.59 g solution (Sample number: IV-61).

Microwave extraction was carried out in a MarsX apparatus. The fresh plant (1 g) was extracted in 10 mL of deionized water at 100 °C for 3x3 min. with 500 W (Sample number: MW.CH-32).

The amount of fresh plant used for different extraction methods, and the gained extracts are summarized in Table 1. The extracts are stable for a long time in the refrigerator.

**Table 1.** Amount of initial greater celandine and the gained extracts.

Type of extraction	Amount of initial material (g)	Gained extract
Tea	6	100 mL
Pressed latex	100	17.6 g
Pressed latex with water	53.28	37.52 g
Alcoholic (96 %)	5	100 mL
SFE with water	62.5	100 mL
SFE with propylene glycol	97.65	25.99 g
SFE with alcohol	31.48	1.85 g
Microwave with water	1	10 mL

### Measurements of organic compounds

Total flavonoid content was measured by spectrophotometry at 420 nm according to the German Pharmacopoeia (DAB10), after formation aluminum complex.<sup>17,18</sup>

The polyphenol content was measured by spectrophotometry according to the Singleton and Rossi method.<sup>19</sup> The absorbance of the samples was read at 760 nm with a Hitachi U-2000 spectrophotometer. Three parallel measurements of each sample were made against a blank that was prepared under the same conditions as the samples. Gallic acid was used as a reference solution, and the results were expressed in gallic acid equivalent. Tannic acid content was determined according to the description of Hungarian Pharmacopoeia (Ph.Hg.VIII).<sup>20</sup>

Total alkaloid content was determined by spectrometry at 570 nm after complex formation with chromotropic acid according to the guideline of the German Pharmacopoeia (DAB10), and it was expressed in chelidonine content.<sup>18</sup> This method is official in the Hungarian Pharmacopoeia and the European Pharmacopoeia (Ph. Eur. 5) as well.<sup>20,21</sup>

Alkaloid components from the samples were determined by thin-layer chromatographic techniques with densitometry after extraction with methanol since this is an appropriate method for celandrine alkaloids nowadays as well.<sup>22</sup> Separation of coptisine and berberine from the other alkaloids, then the measurement of the samples was performed on precoated silicagel (Kieselgel60 F254).

**Table 2.** Bioactive agent content and  $\pm$  standard deviation (% , g 100 g<sup>-1</sup>, n=3) in the plant parts of fresh greater celandine.

Part	Flavonoid	Tannin	Polyphenol	Alkaloid
Rhizome	0.120 $\pm$ 0.008	9.21 $\pm$ 0.12	15.90 $\pm$ 0.96	1.98 $\pm$ 0.020
Stem	0.278 $\pm$ 0.005	6.25 $\pm$ 0.21	11.99 $\pm$ 0.58	0.582 $\pm$ 0.110
Leaf	0.404 $\pm$ 0.008	6.54 $\pm$ 0.16	13.38 $\pm$ 0.45	0.691 $\pm$ 0.025
Herb	0.392 $\pm$ 0.004	6.26 $\pm$ 0.27	11.71 $\pm$ 0.39	1.85 $\pm$ 0.02

**Table 3.** Amount of alkaloid components with  $\pm$  standard deviation (% , g 100 g<sup>-1</sup>, n=3) in the plant parts of fresh greater celandine.

Part	Berberine, %	Coptisine, %	Chelidonine, %
Rhizome	0.024 $\pm$ 0.004	0.072 $\pm$ 0.004	1.28 $\pm$ 0.02
Stem	0.012 $\pm$ 0.002	0.063 $\pm$ 0.003	0.45 $\pm$ 0.03
Leaf	0.065 $\pm$ 0.004	0.021 $\pm$ 0.001	0.52 $\pm$ 0.03
Herb	0.0024 $\pm$ 0.0003	0.023 $\pm$ 0.010	0.44 $\pm$ 0.02

Eluent was 1-propanol, formic acid and water (90:1:9) recommended by Wagner and Blatt.<sup>23</sup> The standard was 1 % solution of chelidonine and berberine. For the quantitative examination, the extent of the spot was measured by the densitometer (Shimadzu 169). Other alkaloid content (coptisine) was expressed in chelidonine content.

#### Measurements of inorganic elements

The concentration of elements in samples was determined by inductively coupled plasma optical emission spectrometry (ICP-OES). The instrument was Spectro Genesis ICP-OES (Kleve, Germany). The plant samples were digested in an open digestion system with a mixture of HNO<sub>3</sub> (5 mL) and H<sub>2</sub>O<sub>2</sub> (2 mL) then made up to 25 mL with deionized water.<sup>24</sup> In the case of extracts, the solvents were evaporated first, then it was digested as the plant samples. Three parallel solutions were made from each sample and the measurements for the micro- and macroelement (Al, B, Ba, Ca, Cd, Cr, Co, Cu, Fe, Hg, K, Li, Mg, Mn, Mo, Na, Ni, P, Pb, S, Ti, V, Zn) were performed three times. The elements whose concentrations were below the detection limit in all samples were omitted from the tables.

#### Antioxidant value by FRAP method

The FRAP (the ferric reducing ability of plants) measurement was carried out by the following modified Benzie and Strain method.<sup>25</sup> Blank is FRAP reagent, the sample is 1.5 mL FRAP reagent and 50  $\mu$ L sample solution then monitoring at 593 nm up to 5 min in 1 cm light path at 37 °C. An aqueous solution of known FeSO<sub>4</sub>.7H<sub>2</sub>O was used for calibration, and the result was calculated according to the calibration curve.<sup>26</sup> For measuring of the samples, extractions were made from 1.5 g powdered dry latex with 200 mL of water. After standing at room temperature for 30 min, it was filtered than measured with FRAP reagent.<sup>27,28</sup> The extracts were measured with FRAP reagent. The antioxidant values of samples expressed in  $\mu$ mol L<sup>-1</sup>, since they refer to the solutions made.

FRAP reagent: The reagent solution contains 25 mL acetate buffer (300 mmol L<sup>-1</sup>, pH 3.6; 3.1 g sodium acetate trihydrate and 16 mL acetic acid in 1000 mL distilled water), 2.5 mL TPTZ solution (10 mmol/l 2,4,6-tripyridyl-S-triazine in 40 mmol L<sup>-1</sup> HCl ) and 2.5 mL FeCl<sub>3</sub>.6H<sub>2</sub>O solution (20 mmol L<sup>-1</sup> FeCl<sub>3</sub>.6H<sub>2</sub>O in distilled water).

#### Statistical analyses

The calculations of means and standard deviation as well as the statistical analysis were performed using Microsoft Office Excel 2016 and Statistica 7 (StatSoft Inc., Tulsa, USA) software. A significant difference was set at  $P < 0.05$ .

## RESULTS AND DISCUSSION

#### Organic agents of greater celandine drug

According to the officially accepted spectroscopic determination of the total active substance content, greater celandine has significant active substance content (Table 2). Greater celandine is a plant with valuable active ingredients, flavonoids, alkaloids, polyphenols, and tannins. The tannin, polyphenol, and alkaloid content of the rhizome is particularly outstanding, which is significantly ( $P < 0.05$ ) higher than that of the other parts of the plant. Flavonoids, on the other hand, were found to be significantly higher ( $P < 0.05$ ) amounts in the leaf and herb, although they were not in extremely high concentrations (Table 2). The highest alkaloid content is accumulated in the rhizome, but it is also significant in the other parts of the plant. Although the plant is of alkaloid content mainly, the tannin and polyphenol contents in all parts are outstanding also and according to the correlation calculation, the tannin content (Table 2) is a significant positive correlation with the polyphenol content ( $R = 0.955$ ,  $P < 0.05$ ). The active agents in the plant and plant parts of greater celandine are in good accordance with the data in the literature,<sup>29,30</sup> and the highest alkaloid content was measured in the rhizome that is not surprising.



The amount of alkaloid components was determined by HPLC and densitometry. The results showed that chelidonine is the major alkaloid component, whereas coptisine is present in smaller amounts (Table 3). The alkaloid composition also varies according to the plant parts, but the main alkaloid chelidonine is present in all parts of the plant. The amount of alkaloid components was correlated well with the results obtained by HPLC<sup>31</sup> and is in good agreement with earlier data in the literature.<sup>32</sup>

#### Elements in greater celandine drug

The element content in the parts of greater celandine is represented in Table 4. The concentration of most elements is in the order of average plant concentration. An exception to this is that the concentration of Al, Cr, Fe, and Ti in rhizome is high.

There are significant differences ( $P < 0.05$ ) between most of the element content (Al, B, Ba, Ca, Cu, Fe, Mg, Mn, Ti, and Zn) in the plant parts of greater celandine. The highest Al, Fe, and Ti concentration is found in the rhizome. The stem accumulates B, K, and P to the greatest extent. The leaf contains the highest amount of Ba, Ca, Cr, Cu, Mg, Na, S, and Zn, while the herb is rich in Mn. The stem contains most elements (Ba, Ca, Cr, Cu, Fe, Mg, Mn, Na, S, Ti, Zn) in the lowest concentration compared to the other parts of the plant (Table 4). The results for rhizome and herb are similar to those that we get in an earlier experiment for plants obtained from different places and years.<sup>3</sup>

**Table 4.** Element content  $\pm$  standard deviation ( $\mu\text{g g}^{-1}$  of dry weight,  $n=3$ ) in the dried plant parts of greater celandine.

Element	Rhizome	Stem	Leaf	Herb
Al	1054 $\pm$ 13	260.7 $\pm$ 5.0	195.8 $\pm$ 5.6	184.1 $\pm$ 2.7
B	22.69 $\pm$ 0.32	71.81 $\pm$ 0.66	29.10 $\pm$ 4.41	19.92 $\pm$ 0.52
Ba	21.82 $\pm$ 0.47	8.32 $\pm$ 0.06	22.02 $\pm$ 0.16	16.61 $\pm$ 0.16
Ca	15540 $\pm$ 39	4785 $\pm$ 12	22690 $\pm$ 96	11723 $\pm$ 72
Cr	2.04 $\pm$ 0.48	0.593 $\pm$ 0.428	2.22 $\pm$ 0.19	2.01 $\pm$ 0.18
Cu	17.56 $\pm$ 0.21	12.12 $\pm$ 0.15	19.83 $\pm$ 0.42	13.34 $\pm$ 0.21
Fe	814.7 $\pm$ 14.8	77.55 $\pm$ 1.92	234.0 $\pm$ 2.2	216.2 $\pm$ 1.7
K	36828 $\pm$ 610	52346 $\pm$ 1136	38369 $\pm$ 504	32285 $\pm$ 161
Li	0.864 $\pm$ 0.360	< dl	< dl	< dl
Mg	1821 $\pm$ 56	836.3 $\pm$ 10.2	2132 $\pm$ 57	1729 $\pm$ 29
Mn	27.57 $\pm$ 0.47	9.64 $\pm$ 0.10	16.86 $\pm$ 0.26	42.60 $\pm$ 5.01
Na	297.9 $\pm$ 4.6	218.1 $\pm$ 4.5	522.1 $\pm$ 10.7	298.8 $\pm$ 2.0
P	3514 $\pm$ 31	4911 $\pm$ 60	3557 $\pm$ 44	3887 $\pm$ 515
Pb	1.86 $\pm$ 0.43	< dl	1.56 $\pm$ 0.79	< dl
S	1405 $\pm$ 32	893.4 $\pm$ 10.3	2006 $\pm$ 7	1478 $\pm$ 10
Ti	18.23 $\pm$ 1.98	2.99 $\pm$ 0.06	5.69 $\pm$ 0.29	4.99 $\pm$ 0.62
Zn	31.04 $\pm$ 0.22	27.85 $\pm$ 0.46	52.64 $\pm$ 0.78	45.53 $\pm$ 0.14

<dl under detection limit

The element content in the parts of greater celandine is similar to the average plant concentration except in the case of Al, Cr, Fe and Ti where the concentration of rhizome is high compared to the average plant concentration ( $< 200 \mu\text{g g}^{-1}$ ,  $< 1 \mu\text{g g}^{-1}$ ,  $< 30 \mu\text{g g}^{-1}$ ,  $< 10 \mu\text{g g}^{-1}$ , respectively). The Cr and Fe concentrations of leaf and herb are also high, and the concentration of Ca and S in the stem is less than the average plant concentration ( $10\text{-}30000 \mu\text{g g}^{-1}$  and  $1000\text{-}5000 \mu\text{g g}^{-1}$ , respectively).<sup>33</sup> The combined high concentrations of

Al, Cr, Fe, and Ti in the rhizome indicate soil contamination, suggesting that the soil was not properly washed out of the sample.<sup>34</sup> The partly parallel change of these elements is signed by the positive correlation of Al-Fe, Al-Ti, and Fe-Ti ( $R=0.957, 0.971$  and  $0.998, P < 0.05$ ).

The coptisine content showed a tight correlation with the Cr, Cu, and Mg content in the drug ( $-0.989; 0.976$  and  $-0.972; P < 0.05$ ). This is confirmed by other analytical measurements and mathematical calculations<sup>35</sup> that the alkaloid metabolism is regulated by some elements, for example, Mg, Cr and Zn.

#### Antioxidant activity of greater celandine drug

The antioxidant activity of the plant parts is shown in Table 5. The highest antioxidant value is connected to the leaf, and the lower ones are to the rhizome. There are a lot of compounds with antioxidant properties in the plant, such as vitamin C, vitamin E, flavonoids, carotenoids, polyphenols.<sup>36</sup> Better antioxidant value can be connected, for example, to the extracts or antioxidants with higher flavonoid (e.g., quercetin or rutin) and polyphenol content.<sup>14</sup> Leaves with the highest flavonoid content (Table 2) showed the highest antioxidant value, while the rhizome the least. Nevertheless, according to the correlation calculation, the antioxidant value is not correlated with the flavonoid or polyphenol content, rather a positive correlation was found with Zn content ( $R=0.979$ ) at  $P < 0.05$ . Zn is also of antioxidant property,<sup>37</sup> but the clear connection of the antioxidant value of greater celandine with its Zn content needs more data and further examinations.

**Table 5.** Antioxidant activity of the plant parts of dried greater celandine measured by FRAP method.

Part	FRAP value, $\mu\text{mol L}^{-1}$
Rhizome	82.6 $\pm$ 0.9
Stem	119.5 $\pm$ 1.8
Leaf	426.6 $\pm$ 2.6
Herb	325.1 $\pm$ 2.5
Quercetin	3798 $\pm$ 3
Rutin	5219 $\pm$ 4

#### Organic agents in the greater celandine extracts

Although the rhizome contains the highest amount of alkaloids, the aerial part of the plant also has a significant amount of it, and the herb is more easily collected and does not contain higher concentrations of unwanted elements from soil. Therefore the herb of the plant was used for extraction.

The dry material and total alkaloid content of the extracts are presented in Table 6. Here it can be seen the differences that give more information for extraction as a method. The highest dry material and alkaloid content can be connected to the pressed latex, while the other extracts have similar but lower dry material content. Since the dry material content greatly depends on the amount of solvent as well, the yield of dry material may show more relevant information about the organic components of the extracts. According to this, the tea and alcoholic extract contain the highest amount of organic agents (20.18 and 20.24 %, respectively) followed by microwave extraction with water (9.88 %).

**Table 6.** Dry material content (% w V<sup>-1</sup>, n=3) in the greater celandine extracts, as well as the yields of dry material and alkaloids (wt. %, g 100 g<sup>-1</sup>).

Method	Dry material content, g in 100 mL	The yield of dry material, wt. %	Total alkaloid content, %, g chelidonine 100 mL <sup>-1</sup> extract	Yield of alkaloid, wt. %
Tea	1.211±0.025	20.18	0.060±0.015	54.4
Pressed latex	2.915±0.012	0.513	1.98±0.06	18.8
Pressed latex withwater	1.293±0.036	0.258	1.09±0.05	41.5
Alcoholic extract (96 %)	1.012±0.011	20.24	0.0164±0.02	17.7
SFE with water	1.087±0.026	1.74	0.266±0.004	23.0
SFE with propylene glycol	1.270±0.029	0.338	0.072±0.002	1.03
SFE with alcohol	1.112±0.031	0.494	0.211±0.003	3.11
Microwave extraction with water	0.988±0.013	9.88	0.049±0.001	26.5

First of all, we were interested in the total amount of effective substances in the extracts of fresh plants. The total alkaloid contents expressed in chelidonine of the different solutions are very different because of the different method applied, and the dissolution of bioactive compounds change with the seizing fluid and solvent, so it was observed the difference e.g., between the alkaloid content of aqueous and alcoholic extracts (Table 6). The tea, the alcoholic extract and the microwave extract contain the less amounts of total alkaloids. This means that the alkaloid dissolution at different rates depends on other parameters as well. If an alkaloid yield is calculated from the initial alkaloid content of fresh herb, we can see that more than half (54.4 %) of the alkaloid content of the plant is gained by tea making, 41.5 % is gained by pressed latex with water. By the use of water at pressed latex, we got a diluted extract for alkaloid, but the alkaloid yield increased from 18.8 % to 41.5 %. These results show that the pressed latex and the pressed latex with water gave extract rich in alkaloids, while the tea and the pressed latex with water gained the highest amount of total alkaloid from the plant. The SFE almost independently from the servant solvent seems not to be a good method for obtaining alkaloid rich extracts and alkaloid gaining.

The results obtained for the extraction strengthen our earlier examination on this topic that the extracts (latex, tea, microwave, SFEs) have significant effective compounds and elements, although the different parameters applied in the extractions did not give an outstanding difference in the results.<sup>15,38</sup> According to the correlation calculations, the dry material content has a high positive correlation with the total alkaloid content ( $R=0.907$ ,  $P<0.05$ ).

However, the amounts of individual components was also important for us. That's why the alkaloid combinations of extracts were observed by thin-layer chromatography and densitometry. The separation of the components was achieved by Wagner's recommended eluents.<sup>23</sup> The main alkaloid component contents in the extracts are summarized in Table 7. It can be seen that the main alkaloids are coptisine and chelidonine. The loss of alkaloids is high in the case of pressed latex since only trace amounts of alkaloids present in the latex (0.05-5.2 %). Nevertheless, this extract contains alkaloids in high concentrations. By supercritical fluid extraction (SFE), we didn't get homogeneous solutions, and the SFE extracts show rare alkaloid composition. They contain only a small amount of berberine, coptisine, and chelidonine (Table 7).

**Table 7.** Main alkaloid content (wt. %) in the extracts measured by TLC and densitometry, and the dissolution rate of alkaloid components (%) in parenthesis.

Method	Berberine	Coptisine	Chelidonine
Tea	0.01 (69)	0.11 (80)	0.059 (2.2)
Pressed latex	0.15 (5.2)	0.45 (1.0)	0.42 (0.05)
Pressed latex (H <sub>2</sub> O)	0.13 (38)	0.352 (11)	0.350 (0.6)
Alcoholic extract (96 %)	0.01 (83)	0.04 (35)	0.94 (43)
SFE (water)	0.071 (4.7)	0.136 (9.5)	0.12 (0.44)
SFE (propylene glycol)	0.009 (1.0)	0.063 (0.73)	0.24 (0.15)
SFE (alcohol)	0.028 (0.32)	0.555 (6.6)	0.72 (0.45)
Microwave extraction (water)	0.01 (42)	0.112 (49)	0.034 (0.77)

Alkaloid combinations of extracts represent a rare alkaloid dispersion mainly with coptisine and chelidonine, although the high berberine content of fresh latex seems to be the reason for its anti-inflammatory and antiviral activity.<sup>39</sup> The dissolution of alkaloid components from the drug into the extracts varies to a large extent by extracts.

In some cases, a high amount of loss was observed mainly in pressed latex and SFEs, while the tea making and extraction with alcohol seem to be a good method for gaining berberine and coptisine (Table 7). The total alkaloid content in the extracts is in correlation only with their berberine content ( $R=0.937$ ,  $P<0.05$ ).

#### Inorganic elements in the greater celandine extracts

The element concentrations of the examined extracts are in Table 8. In the drug, we found a significant amount of Cr and Mn compared to the average concentration of plants. The element concentrations in the extracts are not big in view of their absolute values except for K and Ca. But anyway, it is important to know that elements are also present in the aqueous, alcoholic extracts and the pressed latexes, and these elements may contribute to the therapeutic effect of extracts.

**Table 8.** Element content in the greater celandine extracts  $\pm$  standard deviations ( $\mu\text{g mL}^{-1}$ , n=3) and dissolution rate in parenthesis (%).

Element	Tea	Pressed latex	Pressed latex with water	Alcoholic extract	Microwave extract with water
Al	4.26 $\pm$ 0.60 (39)	4.47 $\pm$ 0.19 (0.4)	2.83 $\pm$ 0.08 (1.1)	0.84 $\pm$ 0.06 (9.1)	1.43 $\pm$ 0.07 (7.7)
B	0.39 $\pm$ 0.02 (33)	2.38 $\pm$ 0.03 (2.1)	3.09 $\pm$ 0.08 (10)	0.29 $\pm$ 0.01 (29)	0.94 $\pm$ 0.22 (47)
Ba	0.21 $\pm$ 0.01 (21)	0.31 $\pm$ 0.01 (0.3)	0.28 $\pm$ 0.01 (1.2)	0.06 $\pm$ 0.01 (7.5)	0.08 $\pm$ 0.01 (4.7)
Ca	224 $\pm$ 14 (32)	2028 $\pm$ 10 (3.0)	589 $\pm$ 15 (3.5)	139 $\pm$ 3 (24)	488 $\pm$ 23 (41)
Cr	0.012 $\pm$ 0.001(9.6)	0.04 $\pm$ 0.01 (0.4)	0.04 $\pm$ 0.01 (1.4)	<dl	<dl
Cu	0.08 $\pm$ 0.01 (9.8)	0.26 $\pm$ 0.01 (0.4)	0.29 $\pm$ 0.01 (1.5)	0.006 $\pm$ 0.001 (0.9)	0.11 $\pm$ 0.01 (8.1)
Fe	0.73 $\pm$ 0.04 (5.6)	2.97 $\pm$ 0.07 (0.2)	5.11 $\pm$ 0.06 (1.7)	0.22 $\pm$ 0.01 (2.0)	1.69 $\pm$ 0.14 (7.8)
K	1518 $\pm$ 18 (78)	7042 $\pm$ 63 (3.8)	1928 $\pm$ 42 (4.2)	261 $\pm$ 4 (16)	1538 $\pm$ 36 (47)
Mg	42.3 $\pm$ 2.6 (41)	420 $\pm$ 9 (4.3)	134 $\pm$ 1 (5.4)	33.5 $\pm$ 0.7 (39)	54 $\pm$ 5 (31)
Mn	0.92 $\pm$ 0.01 (36)	2.49 $\pm$ 0.03 (1.0)	1.37 $\pm$ 0.01 (2.3)	0.40 $\pm$ 0.01 (19)	0.85 $\pm$ 0.15 (20)
Na	15.6 $\pm$ 0.4 (87)	26.3 $\pm$ 0.4 (1.5)	8.62 $\pm$ 0.19 (2.0)	6.2 $\pm$ 0.4 (41)	25.8 $\pm$ 0.6 (86)
P	179 $\pm$ 9 (77)	612 $\pm$ 2 (2.8)	64.3 $\pm$ 0.9 (1.2)	40.0 $\pm$ 0.5 (21)	38.1 $\pm$ 1 (9.7)
S	37.8 $\pm$ 1.2 (43)	155 $\pm$ 1 (1.8)	57.1 $\pm$ 0.8 (2.7)	29.6 $\pm$ 0.6 (40)	10.3 $\pm$ 1 (6.9)
Zn	0.10 $\pm$ 0.01 (3.8)	2.97 $\pm$ 0.03 (1.1)	0.94 $\pm$ 0.01 (1.5)	0.04 $\pm$ 0.01 (1.7)	0.08 $\pm$ 0.01 (1.9)

<dl below detection limit

More than 70 % of the Na, K, and P content, about 40 % of the Al, Mg, and S content, more than 30 % of the B, Ba, Mn, Ca content are dissolved into the tea from the drug with the organic compounds. On an average, hardly 2-4 percent of the elements get to the pressed latex (e.g., 4.3 % Mg, 3.8 % K, 3.0 % Ca, 2.8 % P, 1.8 % S and 1.5 % Na), and it can be seen a little bit higher dissolution in the case of pressed latex with water. The dissolution rate of elements was significant in the alcoholic and microwave extracts, but their concentrations do not reach the values of tea in most cases (Table 8). Altogether the highest element dissolution was observed into the tea while the micro amounts of microelements were present (e.g., 0.04  $\mu\text{g g}^{-1}$  Cr) in the locally applied pressed latex but anyhow our organism needs micro amount from some elements<sup>40</sup> and these small amounts depending on many factors and the circumstances can be transferred in high rate via the skin.<sup>41</sup>

The element content of SFEs was not analyzed because of the limited amounts of extracts, which was used for the determination of main active agents. Therefore, the element content of the residue of SFEs was determined (Table 9). Some accumulation of Al, Cu, and Na can be seen in the residues of the SFEs, which means that only a little amount of element gets into the extracts from these elements. The Ba, Ca, Cr, K, Mg, K, P, S, and Zn contents of SFE residues are lower than that of the plant, which means that the extracts contain these elements in a relatively higher amount. In our earlier examination in another kind of SFE, we obtained similar results.<sup>15</sup>

Some metals such as gold, copper, zinc, arsenic, silver, have antiviral activities and they effects are proved against several types of viruses, such as human immunodeficiency virus (HIV), herpes simplex virus (HSV), hepatitis A, B, C, influenza.<sup>42-44</sup> In general the reduced transition metals (e.g. Fe, Cu, Cr, Mn) have antiviral activity and cause oxidative stress via Fenton and Fenton-like reaction.<sup>24,45-47</sup> It is also known for a long time that certain metals can act synergetic with other agents, bioactive molecules. Copper and gold kill microorganisms in the water in the presence of chloride.<sup>48</sup> The copper concentrations of the pressed extracts are of a similar order of magnitude, while the iron concentration is

higher than that found to be effective (10 mM metal alone or in combination) against *Streptococcus mutans*.<sup>45</sup>

**Table 9.** Element content of the residue of SFEs made from greater celandine  $\pm$  standard deviations ( $\mu\text{g g}^{-1}$ , n=3).

Element	SFE		
	water	propylene glycol	alcohol
Al	202.8 $\pm$ 8.9	214.7 $\pm$ 2.1	46.08 $\pm$ 0.63
B	14.31 $\pm$ 0.53	13.5 $\pm$ 3.2	10.11 $\pm$ 0.22
Ba	16.4 $\pm$ 0.41	5.65 $\pm$ 0.11	6.22 $\pm$ 0.26
Ca	9906 $\pm$ 152	5625 $\pm$ 48	3456 $\pm$ 35
Cr	1.97 $\pm$ 0.61	0.618 $\pm$ 0.109	2.11 $\pm$ 0.29
Cu	14.1 $\pm$ 1.8	17.72 $\pm$ 0.45	17.4 $\pm$ 5.1
Fe	218.3 $\pm$ 9.2	115.7 $\pm$ 0.6	77.95 $\pm$ 2.50
K	8361 $\pm$ 181	14883 $\pm$ 178	12708 $\pm$ 272
Mg	955.6 $\pm$ 20.6	862.3 $\pm$ 10.8	373.1 $\pm$ 6.7
Mn	20.01 $\pm$ 0.36	11.22 $\pm$ 0.05	5.82 $\pm$ 0.12
Mo	0.537 $\pm$ 0.408	0.836 $\pm$ 0.286	0.695 $\pm$ 0.576
Na	266.7 $\pm$ 11.7	344.0 $\pm$ 19.0	282.5 $\pm$ 5.7
P	996.0 $\pm$ 11.7	1949 $\pm$ 50	1093 $\pm$ 32
S	911.3 $\pm$ 38.6	1822 $\pm$ 42	484.4 $\pm$ 8.6
Ti	14.46 $\pm$ 1.82	2.30 $\pm$ 0.05	2.74 $\pm$ 1.11
Zn	37.11 $\pm$ 0.66	39.00 $\pm$ 0.98	58.80 $\pm$ 1.06

The copper concentration found to be effective against the HSV is 100  $\text{mg L}^{-1}$ ,<sup>46</sup> and this copper concentration exists in the microwave extract and a little bit higher concentration in the pressed latex extracts (Table 8). There is no information yet on the effectiveness of metals against human papilloma viruses (HPV) that cause warts although the antiviral activity seems to occur by similar mechanism in all type of viruses.<sup>42</sup> According to these the copper and iron concentration of pressed latex and pressed latex with water, beside their high alkaloid content, contribute certainly to their antiviral effect against warts and antibacterial activity.

#### Antioxidant activity of greater celandine extracts

The antioxidant activity of extracts shows that the highest values belong to the SFE prepared with alcohol (presumably due to its polyphenol content) and SFE with propylene

glycol while the pressed latex, pressed latex with water and microwave extraction with water show relatively low activity (Table 10). The antioxidant activity of extracts represents higher values mainly for SFEs compared to our earlier examinations for alcoholic extracts, where we found 90.6 and 91.4  $\mu\text{mol L}^{-1}$  antioxidant activity for 20 and 40 % alcoholic extracts of greater celandine and Nadova and co-authors also published potential antioxidant activity.<sup>27,49</sup> So these extracts, mainly the SFEs have prominently high FRAP values.

There is no correlation of FRAP values with any other parameters. This calculation is confirmed by Khodabande and coauthors, who examined the antioxidant activity of greater celandine by the FRAP method also, and they did not find any relationship with any parameters measured.<sup>50</sup> This means that in the extract there are many compounds, from which one part represents antioxidant activity, while the other has prooxidant property.

According to these results it can be summarised that extracts with higher FRAP values presumable have higher content of antioxidant agents.

**Table 10.** Antioxidant activity of the greater celandine extracts measured by FRAP method.

Test material	FRAP value, $\mu\text{mol L}^{-1}$
Tea	299.5 $\pm$ 2.8
Pressed latex	132.8 $\pm$ 5.6
Pressed latex with water	112.5 $\pm$ 2.6
Alcoholic extract (96 %)	289.5 $\pm$ 2.8
SFE with water	672.8 $\pm$ 3.8
SFE with propylene glycol	2895 $\pm$ 3.1
SFE with alcohol	3795 $\pm$ 10
Microwave extraction with water	92.9 $\pm$ 3.3

## CONCLUSION

The supercritical fluid extraction seems to result a biomass that can be modified according to the use or stored for further processing with water, alcohol, or propylene glycol. Although there is no data for element content of SFEs, the outstanding FRAP values of aqueous and alcoholic SFEs suggest that the active ingredients, such as flavonoids with their anti-inflammatory activities and berberine or Mg, Cr, and Zn, can do much in the treatment of acne-prone skin, microtrum skin surface.

Since the greater celandine is a plant containing sensitive active ingredients, the pressed latex extracts are still the most suitable ones for gaining alkaloid rich preparations against warts. In addition to the high alkaloid content, these extracts also contain transition metals (e.g., Cu, Fe) in concentrations that are effective against viruses. In summarising the metal element content of the pressed extracts presumably contributes to the beneficial antiviral effect of greater celandine. The other methods made with water (tea, microwave extract) also give the extracts with relative high alkaloid and transition metal content.

## ACKNOWLEDGMENT

The authors would like to express their grateful thanks to Dr. Vendel Illés for the careful making of supercritical fluid extractions and Dr. Béla Simándi for making the pressed latex with water. To our great regret, they are no longer among us and not listed among the authors.

## REFERENCES

- Zdarilova, A., Malikova, J., Dvorak, Z., Ulrichová J., Šimánek, V., Quaternary isoquinoline alkaloids sanguinarine and chelerythrine. In vitro and in vivo effects. *Chem. Listy*, **2006**, *100*, 30-41. <http://www.chemicke-listy.cz/ojs3/index.php/chemicke-listy/article/view/1961/1961>
- Colombo, M. L., Bosisio, E., Pharmacological activities of *Chelidonium majus* L. *Pharm. Res.*, **1996**, *33*, 127-134. <https://doi.org/10.1006/phrs.1996.0019>
- Sárközi, Á., Then, M., Szentmihályi, K., Mineral element content of greater celandine (*Chelidonium majus* L.) *Acta Aliment.*, **2005**, *34*, 113-120. <https://doi.org/10.1556/AAlim.34.2005.2.3>
- Gerenčér, M., Turecek, P. L., Kistner, O., Mitterer, A., Savidis-Dacho, H., Barrett, N. P., In vitro and in vivo antiretroviral activity of the substance purified from the aqueous extract of *Chelidonium majus* L. *Antiviral Res.*, **2006**, *72*, 153-156. <https://doi.org/10.1016/j.antiviral.2006.03.008>
- Capistrano, I. R., Wouters, A., Lardon F., Gravekamp, C., Apers, S., Pieters, L., In vitro and in vivo investigation on the antitumor activity of *Chelidonium majus*. *Phytomed.*, **2015**, *22*, 1279-1287. <https://doi.org/10.1016/j.phymed.2015.10.013>
- Hejtmanekova, N., Walterova, D., Preiningeret, D., Simanek V., Antifungal activity of quaternary benzo(c)phenanthridine alkaloids from *Chelidonium majus*. *Fitoterapia*, **1984**, *5*, 291-294.
- Kim, H. K., Farnsworth, N. R., Blomster, R. N., Fong, H. H. S., Biological and phytochemical evaluation of plants V: Isolation of two cytotoxic alkaloids from *Chelidonium majus*. *J. Pharm. Sci.*, **1969**, *58*, 372-374. <https://doi.org/10.1002/jps.2600580323>
- Lenfeld, J., Kroutil, M., Marsalek, E., Slavik, V., Antiinflammatory activity of quaternary benzophenanthridine alkaloids from *Chelidonium majus*. *J. Med. Plant Res.*, **1981**, *43*, 191-165. <https://doi.org/10.1055/s-2007-971493>
- Maji, A. K., Banerji P., *Chelidonium majus* L. (Greater celandine) – A review on its phytochemical and therapeutic perspectives. *Int. J. Herbal Med.*, **2015**, *3*, 10-27. <https://doi.org/10.22271/flora.2015.v3.i1.03>
- Kéry, Á., Horváth, I. Nász, I., Verzar-Petri, G., Kulcsár, G., Antiviral alkaloid in *Chelidonium majus* L. *Acta Pharm. Hung.*, **1987**, *57*, 19-25.
- Monavari, S. H. R., Shahrabadi, M. S., Keyvani, H., Salim, F. B., Evaluation of in vitro antiviral activity of *Chelidonium majus* L. against herpes simplex virus type-1. *African J. Microbiol. Res.*, **2012**, *6*, 4360-4364. DOI: 10.5897/AJMR11.1350
- Mozsgai, K., Huth, J., Kéry, Á., Vidéki, M., Budavári, O., Váradi, J., Banoczy, J., Nyarasi, I., Rigó, O., Ember, G., Characteristics and clinical study of *Chelidonium* medical toothpaste and mouthwash. *Mediflora*, **1988**, *1*, 21-23.
- Parson, L. G., Thomas, L. G., Southard, G. L., Woodall, I. R., Jones, B. J. B., Effect of sanguinaria extract on established plaque and gingivitis when supragingival delivered as a manual rinse or under pressure in oral irrigation. *J. Clin. Periodontol.*, **1987**, *14*, 381-385. <https://doi.org/10.1111/j.1600-051X.1987.tb01540.x>



- <sup>14</sup>Burda, S., Oleszek, W., Antioxidant and antiradical activities of flavonoids. *J. Agric. Food Chem.*, **2001**, *49*, 2774-2779. <https://doi.org/10.1021/jf001413m>
- <sup>15</sup>Then, M., Szentmihályi, K., Sárközi, Á., Illés, V., Forgács, E., Effect of sample handling on alkaloid and element content in aqueous extract of *Chelidonium majus* L. *J. Chromatogr. A*, **2000**, *889*, 69-74. [https://doi.org/10.1016/S0021-9673\(00\)00236-3](https://doi.org/10.1016/S0021-9673(00)00236-3)
- <sup>16</sup>Then, M., Sárközi, Á., Illés, V., Szöllösi-Varga, I., Szentmihályi, K., Critical evaluation of the use of co-solvents in the case of supercritical extraction (*Chelidonium majus* L.). *Olaj Szappan Kozmetika*, **2002**, *51*(suppl.), 55-60.
- <sup>17</sup>Glasl, H., Photometrische normierung von Flavonoid-O und C-Glycosiden *Fresenius Z. Anal. Chem.* **1985**, *321*, 325-330. <https://doi.org/10.1007/BF00469376>
- <sup>18</sup>German Pharmacopoeia-Deutsches Arzneibuch 10, Deutscher Apotheker Verlag, Stuttgart, **1991**.
- <sup>19</sup>Singleton, V. L., Rossi, J. A., Colorimetry of total phenolics with phosphomolybdic-phosphotungstic acid reagents. *Am. J. Enol. Viticult.*, **1965**, *16*, 144-158.
- <sup>20</sup>Hungarian Pharmacopoeia, VIII Edition (Ph. Hg. VIII), Medicina Könyvkiadó, **2004**.
- <sup>21</sup>European Pharmacopoeia, 5<sup>th</sup> Edition (Ph. Eur. 5.), Council of Europe, **2004**.
- <sup>22</sup>Bogucka-Kocka, A., Zalewski D., Main alkaloids of *Chelidonium majus* L. using thin layer chromatographic-densitometric method. *Acta Chromatogr.*, **2017**, *29*, 385-397. <https://doi.org/10.1556/1326.2017.29.3.09>
- <sup>23</sup>Wagner, H., Bladt, S., *Plant Drug Analysis: A Thin Layer Chromatography Atlas*, Springer Science & Business Media, **1996**. <https://doi.org/10.1007/978-3-642-00574-9>
- <sup>24</sup>Szentmihályi, K., Significance of the examination of the metal element content of herbal extracts in adjuvant therapy. *Orv. Hetil.*, **2018**, *159*, 713-719. <https://doi.org/10.1556/650.2018.30955>
- <sup>25</sup>Benzie, I. E. F., Strain, J. J., Ferric reducing/antioxidant power assay: Direct measure of the total antioxidant activity of biological fluids and modified version for simultaneous measurement of total antioxidant power and ascorbic acid concentration. *Method Enzymol.*, **1999**, *299*, 15-27. <https://doi.org/10.1111/j.2050-411X.1999.tb00232.x>
- <sup>26</sup>Lado, C., Then, M., Varga, I., Szöke, É., Szentmihályi, K., The antioxidant property of volatile oils determined by the ferric reducing ability. *Z. Naturforsch.*, **2004**, *59c*, 354-358. <https://doi.org/10.1515/znc-2004-5-611>
- <sup>27</sup>Then, M., Szentmihályi, K., Sárközi, Á., Szöllösi Varga, I., Examination on antioxidant activity in the greater celandine (*Chelidonium majus* L.) extracts by FRAP method. *Acta Biol. Szeged.*, **2003**, *47*, 115-117. <http://abs.bibl.u-szeged.hu/index.php/abs/article/view/2357/2349>
- <sup>28</sup>Džambić, A., Muratović, S., Veljović, E., Softić, A., Dautović, E., Šljivić Husejnović, M., Horozić, E., Smajlović, A., Evaluation of antioxidative, antimicrobial and cytotoxic activity of the synthesized arylmethylenbis(3-hydroxy-5,5-dimethyl-2-cyclohexen-1-one) derivatives. *Eur. Chem. Bull.*, **2020**, *9*(9), 285-290. <https://doi.org/10.17628/ecb.2020.9.285-290>
- <sup>29</sup>Rojsanga, P., Gritsanapan, W., Suntornsuk, L., Determination of berberine content in the stem extracts of *Coscinium fenestratum* by TLC densitometry. *Med. Princ. Pract.*, **2006**, *15*, 373-378. <https://doi.org/10.1159/000094272>
- <sup>30</sup>Zielińska, S., Jezierska-Domaradzka, A., Wójciak-Kosior, M., Sowa, I., Junka, A., Matkow, A. M., Greater celandine's ups and downs – 21. Centuries of medicinal uses of *Chelidonium majus* from the viewpoint of today's pharmacology. *Pharmacol.*, **2018**, *9*, Article 299. <https://doi.org/10.3389/fphar.2018.00299>
- <sup>31</sup>Sárközi, Á., Janicsák, G., Kursinszki, L., Kéry, Á., Alkaloid composition of *Chelidonium majus* L. studied by different chromatographic techniques. *Chromatogr.* **2006**, *63*, S81-S86. <https://doi.org/10.1365/s10337-006-0728-7>
- <sup>32</sup>Seidler-Lozykowska, K., Kedzia, B., Bocianowski, J., Gryszczynska, A., Lowicki, Z., Opala, B., Pietrowiak, A., Content of alkaloids and flavonoids in celandine (*Chelidonium majus* L.) herb at the selected developmental phases. *Acta Sci. Pol. HortorumCultus*, **2016**, *15*(4), 161-172. [https://www.researchgate.net/profile/Agnieszka\\_Gryszczynska2/publication/307607560\\_CONTENT\\_OF\\_ALKALOIDS\\_AND\\_FLAVONOIDS\\_IN\\_CELANDINE\\_Chelidonium\\_majus\\_L\\_HERB\\_AT\\_THE\\_SELECTED\\_DEVELOPMENTAL\\_PHASES/links/57cd569a08ae89cd1e897cc9/CONTENT-OF-ALKALOIDS-AND-FLAVONOIDS-IN-CELANDINE-Chelidonium-majus-L-HERB-AT-THE-SELECTED-DEVELOPMENTAL-PHASES.pdf](https://www.researchgate.net/profile/Agnieszka_Gryszczynska2/publication/307607560_CONTENT_OF_ALKALOIDS_AND_FLAVONOIDS_IN_CELANDINE_Chelidonium_majus_L_HERB_AT_THE_SELECTED_DEVELOPMENTAL_PHASES/links/57cd569a08ae89cd1e897cc9/CONTENT-OF-ALKALOIDS-AND-FLAVONOIDS-IN-CELANDINE-Chelidonium-majus-L-HERB-AT-THE-SELECTED-DEVELOPMENTAL-PHASES.pdf)
- <sup>33</sup>Kabata-Pendias, A., Pendias, H., *Trace Elements in Soil and Plants*, 3<sup>rd</sup> edition, CRC Press, Boca Raton, London, **2001**. <https://doi.org/10.1201/9781420039900>
- <sup>34</sup>Szentmihályi, K., May, Z., Then, M., Hajdú, M., Böszörményi, A., Fodor, J., Balázs, A., Lemberkovics, E., Marczal, G., Szöke, É., Metal elements, organic agents in herbal remedy, *Species thymi composite*, and its drug-constituents. *Eur. Chem Bull.*, **2012**, *1*, 14-21. DOI: 10.17628/ecb.2012.1.14-21
- <sup>35</sup>Buzuk, N. G., Lovkova, M. I., Sokolova, S. M., Tiutekin, I. V., Relationship between celandine isoquinoline alkaloids with macro- and microelements. *Prikl. Biokhim. Mikrobiol.*, **2011**, *37*, 586-92.
- <sup>36</sup>Xu, D. P., Li, Y., Meng, X., Zhou, T., Zhou, Y., Zheng, J., Zhang, J. J., Li, H. B., Natural antioxidants in foods and medicinal plants: Extraction, assessment, and resources. *Int. J. Mol. Sci.*, **2017**, *5*, 18. <https://doi.org/10.3390/ijms18010096>
- <sup>37</sup>Marreiro, D. D., Cruz, K. J., Morais, J. B., Beserra, J. B., Severo, J. S., de Oliveira, A. R., Zinc and oxidative stress: Current mechanisms. *Antioxidants (Basel, Switzerland)*, **2017**, *6*, 24. <https://doi.org/10.3390/antiox6020024>
- <sup>38</sup>Ganan, N. A., Dias, M. A., Bombaldi, F., Zigadio, J. A., Brignole, E. A., DeSouza, H. C., Braga, M. E. M., Alkaloids from *Chelidonium majus* L.: Fractionated supercritical CO<sub>2</sub> extraction with co-solvents. *Separ. Purific. Techn.*, **2016**, *165*, 199-207. <https://doi.org/10.1016/j.seppur.2016.04.006>
- <sup>39</sup>Pencikova, K., Kollar, P., Zavalova, V., Müller, Z. V., Táborská, E., Urbanová, J., Hošek, J., Investigation of sanguinarine and chelerythrine effects on LPS-induced inflammatory gene expression in the THP-1 cell line. *Phytomed.*, **2012**, *19*, 890-895. <https://doi.org/10.1016/j.phymed.2012.04.001>
- <sup>40</sup>Dietary Reference Intakes for vitamin A, vitamin K, arsenic, boron, chromium, copper, iodine, iron, manganese, molybdenum, nickel, silicon, vanadium, and zinc. Institute of Medicine, Food and Nutrition Board, National Academy Press, Washington, DC, **2001**. <https://www.google.hu/search?client=opera&q=gmail&sourceid=opera&ie=UTF-8&oe=UTF-8>
- <sup>41</sup>Radloff, C., Vaia, R. A., Brunton, J., Bouwer, G. T., Ward, V. K., Metal nanoshell assembly on a virus bioscaffold. *Nano Lett.*, **2005**, *5*, 1187-1191. <https://doi.org/10.1021/nl050658g>
- <sup>42</sup>Yadavalli, T., Shukla, D., Role of metal and metal oxide nanoparticles as diagnostic and therapeutic tools for highly prevalent viral infections. *Nanomedicine*, **2017**, *13*, 219-230. <https://doi.org/10.1016/j.nano.2016.08.016>
- <sup>43</sup>Akhtar, A., Wang, S. X., Ghali, L., Bell, C., Wen, X., Effective delivery of arsenic trioxide to HPV-positive cervical cancer cells using optimised liposomes: A size and charge study. *Int. J. Mol. Sci.*, **2018**, *19*, 1081. <https://doi.org/10.3390/ijms19041081>
- <sup>44</sup>Kass, L., Rosanoff, A., Tanner, A., Sullivan, K., McAuley, W., Plessat, M., Effect of transdermal magnesium cream on serum and urinary magnesium levels in humans: A pilot study. *PLoS One*, **2017**, *12*, e0174817. <https://doi.org/10.1371/journal.pone.0174817>
- <sup>45</sup>Dunning, J. C., Ma, Y., Marquis, R.E., Anaerobic killing of oral streptococci by reduced, transition metal cations. *Appl.*

- Environm. Microbiol.*, **1998**, *64*, 27–33. <https://doi.org/10.1128/AEM.64.1.27-33.1998>
- <sup>46</sup>Sagripanti, J. L., Routson, L. B., Bonifacin, A. C., Lytle, C. L., Mechanism of copper-mediated inactivation of herpes simplex virus. *Antimicrob. Agents Chemother.*, **1997**, *41*, 812–817. <https://doi.org/10.1128/AAC.41.4.812>
- <sup>47</sup>Szentmihályi K., Metal element homeostasis and oxidative stress in pathological processes. *Orv. Hetil.*, **2019**, *160*, 1407–1416. <https://doi.org/10.1556/650.2019.31499>
- <sup>48</sup>Zheng, Y., Lin, Q., Xie, L., Observation on synergetic efficacy of chlorine and metal ion killing microorganisms in water. *Chin. J. Disinfect.*, **2004**, 2004-03.
- <sup>49</sup>Nadova, S., Miadokova, E., Alfoldiova, L., Kopaskova, M., Hasplova, K., Hudcova, A., Vaculcikova, D., Gregan, F., Cipak, L., . Potential antioxidant activity, cytotoxic and apoptosis-inducing effects of *Chelidonium majus* L. extract on leukemia cells. *Neuro. Endocrinol. Lett.*, **2008**, *29*(5), 649–652. [https://www.researchgate.net/profile/Eva-Miadokova/publication/23454806\\_Potential\\_antioxidant\\_activity\\_cytotoxic\\_and\\_apoptosis-inducing\\_effects\\_of\\_Chelidonium\\_majus\\_L\\_extract\\_on\\_leukemia\\_cells/links/0a85e537359baa4ce7000000.pdf](https://www.researchgate.net/profile/Eva-Miadokova/publication/23454806_Potential_antioxidant_activity_cytotoxic_and_apoptosis-inducing_effects_of_Chelidonium_majus_L_extract_on_leukemia_cells/links/0a85e537359baa4ce7000000.pdf)
- <sup>50</sup>Khodabande, Z., Jafarian, V., Sariri, R., Antioxidant activity of *Chelidonium majus* extract at phenological stages. *Appl. Biol. Chem.*, **2017**, *60*, 497-503. <https://doi.org/10.1007/s13765-017-0304-x>

Received: 07.12.2020.

Accepted: 28.12.2020.



# SYNTHESIS OF NOVEL ANTI-INFLAMMATORY USNIC ACID-BASED IMIDAZOLIUM SALTS

Tiruveedhula Somasekhar,<sup>[a,c]</sup> Monisha Javadi,<sup>[b]</sup> Ramakrishna Sistla<sup>[b,c]</sup> and  
Uppuluri Venkata Mallavadhani<sup>[a,c\*]</sup>

**Keywords:** Usnic acid; imidazolium salts; anti-inflammatory activity; cytokine proteins; U937 cells.

Ten novel usnic acid based imidazolium salts were synthesized by employing a two-step protocol. The anti-inflammatory potential of the newly synthesised compounds was evaluated *in vitro* against cytokine proteins TNF- $\alpha$  and IL-1 $\beta$  secreted from U937 cells. Some of the imidazolium salts exhibited promising anti-inflammatory activity against the TNF- $\alpha$  and IL-1 $\beta$  with IC<sub>50</sub> values ranging between 5.3  $\mu$ M - 7.5  $\mu$ M, which are many folds lower than that of the parent compound (>100  $\mu$ M). Most significantly, substitution with electronegative groups in imidazolium salts of usnic acid found to be more potent and exhibiting enhanced anti-inflammatory activity.

\*Corresponding Author

E-Mail: uvmavadani@yahoo.com (U.V. Mallavadhani)

- [a] Centre for Natural Products & Traditional Knowledge, CSIR-Indian Institute of Chemical Technology, Hyderabad 500007, India.
- [b] Applied Biology Department & Toxicology, CSIR-Indian Institute of Chemical Technology, Hyderabad 500007, India.
- [c] Academy of Scientific and Innovative Research (AcSIR), CSIR-Indian Institute of Chemical Technology, Hyderabad 500007, India.

## INTRODUCTION

Usnic acid, a natural dibenzofuran lichen metabolite, has attracted the attention as 'Hot Natural Scaffold' in view of its structural diversity and therapeutic potential. Usnic acid is reported to exhibit a wide range of biological activities such as anti-inflammatory, antioxidant as well as pro-oxidant, antimicrobial, antiviral, antibiotic, and antitumor activities etc.<sup>1</sup> It was isolated from different genera of lichens such as *Usnea* (Usneaceae), *Lecanora* (Lecanoraceae) and *Cladonia* (Cladoniaceae) in large quantity (up to 26%).<sup>2</sup> It plays a crucial role in restricting prostaglandin and it acts like an anti-inflammatory drug.<sup>3</sup> The anti-inflammatory property of usnic acid<sup>4</sup> has been shown by down-regulating the expression of TNF- $\alpha$ , MIP-2, IL-8, IL-6. Huang et al. have explored the mechanism of usnic acid against inflammation by encouraging the lipopolysaccharide from the RAW264.7 cell line. It acts in a dose dependent manner towards pro-inflammatory mediators and cytokines that leads to attenuate the IL-6, IL-1 $\beta$ , iNOS, to COX-2 through dwindling the NF $\kappa$ B factor.<sup>5</sup> Usnic acid possesses a wide range of functional groups and associated with intramolecular hydrogen bonding between the functional groups. D. N. Sokolov et al. have analysed some usnic acid-amine hybrids of both enantiomers, against influenza virus A (H1N1)pdm09. Interestingly, (+)-usnic acid enamine derivatives explored with good antiviral activity than (-)-usnic acid-amine hybrids.<sup>6</sup> Usnic acid consists of three rings such as A, B & C rings. Out of these, A and C rings are amenable for a wide range of chemical transformations by introducing pharmacophore moieties such as chalcones, thiazoles, aurones, enamines, coumarins,

and flavones. Among these analogues, enamines have shown the best biological profiles.<sup>7</sup> Enamines such as usenamines were identified as chemically and biologically diversified structures in lichens and exhibited a broad spectrum of biological activities.<sup>2</sup> Bruno et al. explored the wound repairing mechanism of usnic acid enamine hybrids by employing *in vitro* and *in vivo* assays.<sup>8</sup> Imidazole is a five-membered N-heterocyclic ring contains two nitrogen atoms and is an important pharmacophore in medicinal chemistry.<sup>9</sup> Imidazolium salts are obtained by the alkylation of Imidazole nitrogen atoms.<sup>10</sup> Zheng et.al reported two naturally occurring imidazolium salts such as lepidiline A & lepidiline B from *Lepidium meyenii*.<sup>11</sup> These imidazolium salts and their hybrids possess multiple biological activities such as antimicrobial<sup>12</sup>, antitumor<sup>13</sup>, antioxidants, anti-fibrotic, HIV-integrase inhibition etc.,<sup>14</sup> Yang et.al has reported the synthesis of a series of imidazolium salts bearing different functional groups by refluxing alkyl halides and imidazole in toluene. The resultant salts were tested against various cancer cell lines.<sup>15</sup> With this background in view, the chemical transformation of usnic acid has now been done by incorporating pharmacophore moiety of imidazolium salts through the key bioactive enamine linkage to afford the desired usnic acid-based imidazolium salts and evaluation of the resultant products for their anti-inflammatory potential.

## EXPERIMENTAL

### Isolation of (+)- usnic acid (1)

(+)-Usnic acid was isolated from the lichen *Usnea longissima* and *Usnea orientalis* as per our reported procedure.<sup>2</sup> The lichen material was collected from NBRI, Lucknow, India. The lichen material (250+200 g) was air-dried, powdered and extracted with n-hexane (3 L) using a Soxhlet extractor for 12 h. Concentration of the n-hexane extract under vacuum gave the residue (8.8 g), which was chromatographed over silica gel column to afford (+)-usnic acid (1) as pale yellow shining crystals, (8.6 g, mp: 204 °C, [ $\alpha$ ]<sub>D</sub> = +490° (CHCl<sub>3</sub>) in 1.91 % yield. IR (KBr)  $\nu_{max}$ : 2650-

3254, 1692, 1632, 1541, 1454, 1374, 1357, 1288, 1190  $\text{cm}^{-1}$ ;  $^1\text{H}$  NMR (500 MHz,  $\text{CDCl}_3$ ):  $\delta$  1.76 (3H, s, H-10), 2.11 (3H, s, H-15), 2.66 (3H, s, H-12), 2.68 (3H, s, H-14), 5.98 (1H, s, H-4), 11.03 (1H, s, 9-OH), 13.34 (1H, s, 7-OH);  $^{13}\text{C}$  NMR (75 MHz,  $\text{CDCl}_3$ ):  $\delta$  7.47, 27.80, 31.19, 32.07, 59.01, 98.25, 101.45, 103.89, 105.17, 109.22, 155.13, 157.42, 163.80, 179.27, 191.63, 197.98, 200.23, 201.68; ESI-HRMS (m/z)  $[\text{M}+\text{H}]^+$  calcd for  $\text{C}_{18}\text{H}_{17}\text{O}_7$  345.0968, found 345.0970.

### Isolation of methyl barbatate (2)

The molecule **2** has been achieved with successive treatment of *Usnea longissima* and *Usnea orientalis* with ethyl acetate solvent. Concentration of the ethyl acetate extract under vacuum gave the residue (1.3 g, 0.28 %), which was chromatographed over silica gel column to afford methyl barbatate (2) as colourless crystals, (1.3 g, mp: 187-192  $^\circ\text{C}$  in 0.28 % yield. IR (KBr)  $\nu_{\text{max}}$ : 2551-3452, 1738, 1637, 1572, 1493, 1462, 1398, 1314, 1259, and 1228;  $^1\text{H}$  NMR (400 MHz,  $\text{CDCl}_3$ ): 2.16 (3H,S), 2.18 (3H,S), 2.47 (3H,S), 2.61 (3H,S), 3.85 (3H,S), 3.86(3H,S), 6.54 (1H,S), 6.62 (1H,S), 11.75 (1H,S);  $^{13}\text{C}$  NMR (75 MHz,  $\text{CDCl}_3$ ): 8.86, 9.09, 20.18, 24.10, 55.69, 62.08, 108.11, 116.66, 117.38, 117.75, 119.55, 135.45, 140.85, 154.10, 157.21, 160.05, 163.81, 166.19, 174.85. ESI-HRMS (m/z)  $[\text{M}+\text{H}]^+$  calcd. for  $\text{C}_{20}\text{H}_{23}\text{O}_7$  375.1444, found 375.1444.

### Synthesis of compound 3

A solution of compound **1** (1.5 g, 4.360 mmol) and 3-(1H-imidazol-1-yl)propan-1-amine (4.360 mmol) in methanol (12 mL) was stood at 60  $^\circ\text{C}$  and refluxed for four hours under stirring conditions. The reaction mixture was then concentrated under reduced pressure and the resulting residue was chromatographed over silica gel column using n-hexane: ethyl acetate mixture as eluent to afford pure compound **3**.

### (R,E)-6-Acetyl-2-[1-(3-(1H-imidazol-1-yl)propylamino)ethylidene]-7,9-dihydroxy-8,9b-dimethyl dibenzofuran-1,3(2H,9bH)-dione (3).

Pale yellow solid (0.157 g, 48%); mp: 80-82  $^\circ\text{C}$ ; IR (KBr)  $\nu_{\text{max}}$ : 2650-3444, 1701, 1626, 1555, 1467, 1368, 1283, 1186  $\text{cm}^{-1}$ ;  $^1\text{H}$  NMR (300 MHz,  $\text{CDCl}_3+\text{DMSO}-d_6$ ):  $\delta$  1.71 (3H, s, H-10), 2.06 (3H, s, H-15), 2.24 (2H, m, H-17), 2.59 (3H, s, H-12), 2.68 (3H, s, H-14), 3.46 (2H, m, H-16), 4.17 (2H, t, J = 6.6 Hz, H-18), 5.79 (1H, s, H-4), 7.01 (1H, S, H-4'), 7.07 (1H, S, H-5'), 7.55 (1H, S, H-2'), 11.90 (1H, s, 9-OH), 13.36 (1H, s, 7-OH), 13.51 (1H, brs, NH);  $^{13}\text{C}$  NMR (75 MHz,  $\text{CDCl}_3+\text{DMSO}-d_6$ ):  $\delta$  6.9 (C-15), 17.6 (C-12), 29.6 (C-17), 30.6 (C-14), 31.4 (C-10), 39.9 (C-16), 43.2 (C-18), 56.5 (C-9b), 100.6 (C-6), 101.7 (C-4), 101.8 (C-2), 104.4 (C-9a), 107.1 (C-8), 118.1 (C-5'), 129.3 (C-4'), 136.5 (C-2'), 155.2 (C-5a), 157.6 (C-9), 162.7 (C-7), 173.4 (C-11), 174.7 (C-4a), 189.5 (C-3), 197.6 (C-1), 200.1 (C-13); ESI-HRMS (m/z)  $[\text{M}+\text{H}]^+$  calcd. for  $\text{C}_{24}\text{H}_{26}\text{N}_3\text{O}_6$  452.1816, found 452.1798.

### General procedure for the synthesis of salts

To a solution of compound **3** (0.1 g, 0.221 mmol) in dry toluene (5 mL) was added appropriate phenacyl bromide (0.221 mmol) and the resulting mixture were refluxed at 80  $^\circ\text{C}$  for 4-12 hours under stirring. Colourless precipitate

was formed in the round-bottom flask after reaction was completed. This precipitate was filtered and washed with toluene (3 $\times$ 10 mL), to achieve the imidazolium salts (**4-13**) in 72-93% yield.

### (E)-1-(3-((1-(6-Acetyl-7,9-dihydroxy-8-methyl-1,3-dioxo-1,9b-dihydrodibenzo[b,d]furan-2(3H)-ylidene)ethyl)amino)propyl)-3-(2-oxo-2-phenylethyl)-1H-imidazol-3-ium (4).

Colourless solid (0.122 g, 85%); mp: 148-150  $^\circ\text{C}$ ; IR (KBr)  $\nu_{\text{max}}$ : 2926-3411, 1700, 1623, 1555, 1460, 1366, 1281, 1231, 1181  $\text{cm}^{-1}$ ;  $^1\text{H}$  NMR (300 MHz,  $\text{CDCl}_3+\text{DMSO}-d_6$ ): 1.68 (3H, S), 2.03 (3H, s), 2.34 (3H, s), 2.42 (2H, t, J= 6.877), 2.65 (3H, s), 2.67 (3H, s), 3.74 (2H, broad peak), 4.62 (2H, t, J= 6.877), 5.74 (1H, s), 6.18 (2H, s), 7.55 (2H, t, J=6.602), 7.68 (1H, t, J= 6.877), 7.74 (1H, s), 7.90 (1H, s), 8.04 (2H, d, J= 6.602), 9.72 (1H, s), 11.96 (1H, s), 13.34 (2H, broad peak).  $^{13}\text{C}$  NMR (75 MHz,  $\text{CDCl}_3+\text{DMSO}-d_6$ ): 6.72, 17.80, 28.92, 30.41, 31.14, 46.52, 54.96, 56.18, 100.41, 101.59, 104.30, 106.74, 121.22, 123.78, 124.46, 127.59, 128.31, 131.82, 132.79, 133.86, 137.13, 155.05, 157.37, 162.47, 173.00, 174.82, 189.09, 189.80, 197.32, 199.84. ESI-HRMS (m/z)  $[\text{M}+\text{H}]^+$  calcd. for  $\text{C}_{32}\text{H}_{32}\text{N}_3\text{O}_7$  570.2240, found 570.2241.

### (E)-1-(3-((1-(6-Acetyl-7,9-dihydroxy-8-methyl-1,3-dioxo-1,9b-dihydrodibenzo[b,d]furan-2(3H)-ylidene)ethyl)amino)propyl)-3-(2-(4-chlorophenyl)-2-oxo ethyl)-1H-imidazol-3-ium (5).

Pale yellow solid (0.115 g, 76%); mp: 137-139  $^\circ\text{C}$ ; IR (KBr)  $\nu_{\text{max}}$ : 2925-3414, 1700, 1625, 1554, 1465, 1372, 1283, 1232, 1187  $\text{cm}^{-1}$ .  $^1\text{H}$  NMR (300 MHz,  $\text{CDCl}_3+\text{DMSO}-d_6$ ): 1.67 (3H, s), 2.02 (3H, s), 2.33 (3H, s), 2.41 (2H, t, J= 6.877), 2.64 (3H, s), 2.66 (3H, s), 3.25 (2H, broad peak), 3.69-3.78 (2H, m), 4.61 (2H, t, J=6.602), 5.74 (1H, s), 6.21(2H, s), 7.52 (2H, d, J=8.253), 7.78 (1H, S), 7.93 (1H, s), 8.03 (2H, d, J= 8.52), 9.69 (1H, s), 11.97 (1H, S), 13.34 (2H, broad peak).  $^{13}\text{C}$  NMR (75 MHz,  $\text{CDCl}_3+\text{DMSO}-d_6$ ): 6.49, 17.49, 20.35, 28.65, 30.16, 30.87, 46.19, 54.61, 55.86, 100.12, 101.25, 101.35, 104.02, 106.35, 120.98, 123.49, 124.22, 127.12, 127.90, 128.28, 128.90, 131.05, 136.83, 139.68, 154.78, 157.08, 162.17, 172.63, 174.48, 188.69, 196.99, 199.54. ESI-HRMS (m/z)  $[\text{M}+\text{H}]^+$  calcd for  $\text{C}_{32}\text{H}_{31}\text{N}_3\text{O}_7\text{Cl}$  570.2240, found 570.2241.

### (E)-1-(3-((1-(6-Acetyl-7,9-dihydroxy-8-methyl-1,3-dioxo-1,9b-dihydrodibenzo[b,d]furan-2(3H)-ylidene)ethyl)amino)propyl)-3-(2-(4-nitrophenyl)-2-oxoethyl)-1H-imidazol-3-ium (6).

Pale yellow solid (0.134 g, 87%); mp: 136-138  $^\circ\text{C}$ ; IR (KBr)  $\nu_{\text{max}}$ : 2927-3410, 1705, 1623, 1556, 1465, 1351, 1282, 1184  $\text{cm}^{-1}$ ;  $^1\text{H}$  NMR (300 MHz,  $\text{CDCl}_3+\text{DMSO}-d_6$ ):  $\delta$  1.68 (3H, s), 2.00 (3H, S), 2.36-2.45 (2H, m), 2.59 (2H, broad peak), 2.65 (3H, s), 2.67(3H, s), 3.70-3.79 (2H, m), 4.58 (2H, broad peak), 5.76 (1H, s), 6.27 (2H,S), 7.79 (1H, s), 7.94 (1H, s), 8.27-8.42 (4H, m), 9.51 (1H, s), 12.02 (3H, s), 13.27 (3H, s), 13.33 (3H, S).  $^{13}\text{C}$  NMR (75 MHz,  $\text{CDCl}_3+\text{DMSO}-d_6$ ):  $\delta$  6.29, 17.24, 29.93, 30.65, 45.99, 54.85, 55.60, 100.01, 101.14, 103.83, 106.03, 120.91, 123.29, 128.58, 136.53, 137.10, 149.49, 154.58, 156.85, 161.89, 172.37, 174.27, 188.41, 188.95, 196.71, 199.35. ESI-HRMS (m/z)  $[\text{M}+\text{H}]^+$  calcd. for  $\text{C}_{32}\text{H}_{31}\text{N}_4\text{O}_9$  615.2091, found 615.2090.



**(E)-1-(3-((1-(6-Acetyl-7,9-dihydroxy-8-methyl-1,3-dioxo-1,9b-dihydrodibenzo[*b,d*]furan-2(3H)-ylidene)ethyl)amino)propyl)-3-(2-(3-methoxyphenyl)-2-oxoethyl)-1H-imidazol-3-ium (7)**

Pale yellow solid (0.108 g, 72%); mp: 219-221 °C; IR (KBr)  $\nu_{\text{max}}$ : 2927-3420, 1698, 1627, 1551, 1467, 1367, 1286, 1190  $\text{cm}^{-1}$ ;  $^1\text{H}$  NMR (300 MHz,  $\text{CDCl}_3+\text{DMSO}-d_6$ ):  $\delta$  1.69 (3H, s), 2.03 (3H, s), 2.38-2.45 (2H, m), 2.66 (3H, s), 2.67 (3H, s), 3.71-3.78 (2H, m), 3.88 (3H, S), 4.60 (2H, t,  $J=6.602$ ), 7.47 (1H, t,  $J=7.825$ ), 7.53 (1H, bp), 7.62-.65 (2H, m), 7.71 (1H, s), 7.86 (1H, S), 9.65 (1H, s), 11.96 (1H, s), 13.32 (1H, s), 13.34 (1H, s).  $^{13}\text{C}$  NMR (75 MHz,  $\text{CDCl}_3+\text{DMSO}-d_6$ ):  $\delta$  6.74, 17.79, 28.91, 30.43, 31.14, 46.52, 54.89, 54.89, 56.20, 100.44, 101.62, 104.31, 106.78, 112.2, 120.02, 121.17, 123.76, 129.43, 134.07, 137.18, 155.07, 157.37, 159.20, 162.50, 173.06, 174.84, 189.12, 189.64, 193.36, 199.86. ESI-HRMS (m/z)  $[\text{M}+\text{H}]^+$  calcd. for  $\text{C}_{33}\text{H}_{34}\text{N}_3\text{O}_8$  600.2346, found 600.2346.

**(E)-1-(3-((1-(6-Acetyl-7,9-dihydroxy-8-methyl-1,3-dioxo-1,9b-dihydrodibenzo[*b,d*]furan-2(3H)-ylidene)ethyl)amino)propyl)-3-(2-(3-carbamoyl-4-hydroxyphenyl)-2-oxo-ethyl)-1H-imidazol-3-ium (8)**

Colourless solid (0.132 g, 84%); mp: 196-198 °C; IR (KBr)  $\nu_{\text{max}}$ : 2925-3416, 1663, 1625, 1554, 1465, 1368, 1315, 1283, 1242, 1189  $\text{cm}^{-1}$ ;  $^1\text{H}$  NMR (400 MHz,  $\text{CDCl}_3+\text{DMSO}-d_6$ ):  $\delta$  1.69 (3H, s), 2.03 (3H, s), 2.34 (2H, s), 2.37-2.47 (2H, m), 2.66 (3H, s), 2.67 (3H, s), 3.68-3.76 (2H, m), 4.56 (2H, t,  $J=6.602$ ), 5.77 (1H, s), 6.13 (2H, s), 7.00 (1H, d,  $J=8.803$ ), 7.61 (1H, s), 7.73 (2H, S), 7.84 (1H, s), 8.01 (1H, d,  $J=8.803$ ), 8.61(1H, s), 9.53 (1H, S), 11.97 (1H, s), 13.35 (2H, m).  $^{13}\text{C}$  NMR (75 MHz,  $\text{CDCl}_3+\text{DMSO}-d_6$ ):  $\delta$  6.58, 17.55, 3.26, 46.28, 54.56, 55.99, 64.37, 100.26, 101.46, 104.12, 106.51, 113.08, 117.94, 120.96, 123.51, 127.23, 129.60, 132.79, 136.86, 154.89, 157.18, 162.29, 166.22, 170.92, 172.85, 174.63, 187.81, 188.88, 197.12, 199.68. ESI-HRMS (m/z)  $[\text{M}+\text{H}]^+$  calcd. for  $\text{C}_{33}\text{H}_{33}\text{N}_4\text{O}_9$  629.2248, found 629.2240.

**(E)-1-(3-((1-(6-Acetyl-7,9-dihydroxy-8-methyl-1,3-dioxo-1,9b-dihydrodibenzo[*b,d*]furan-2(3H)-ylidene)ethyl)amino)propyl)-3-(2-(3,4-dihydro-2H-benzo[*b*][1,4]dioxepin-7-yl)-2-oxoethyl)-1H-imidazol-3-ium (9)**

Colourless solid (0.145 g, 91%); mp: 204-206 °C; IR (KBr)  $\nu_{\text{max}}$ : 2927-3423, 1694, 1625, 1556, 1465, 1366, 1271, 1191  $\text{cm}^{-1}$ ;  $^1\text{H}$  NMR (400 MHz,  $\text{CDCl}_3+\text{DMSO}-d_6$ ):  $\delta$  1.69 (3H, s), 2.04 (3H, s), 2.22-2.30 (2H, m), 2.38-2.47 (2H, m), 2.66 (3H, s), 2.67 (3H, s), 3.71-3.78 (2H, m), 4.28-4.37 (4H, m), 4.62 (2H, t,  $J=5.77$ ), 5.75 (1H, s), 6.05 (2H, s), 7.03 (1H, d,  $J=7.978$ ), 7.61 (1H, s), 7.65 (2H, s), 7.83 (1H, S), 9.79 (1H, s), 11.94 (1H, S), 13.35 (2H, bp).  $^{13}\text{C}$  NMR (75 MHz,  $\text{CDCl}_3+\text{DMSO}-d_6$ ):  $\delta$  5.95, 16.77, 27.83, 29.06, 29.54, 30.24, 45.49, 53.59, 55.10, 68.76, 68.89, 99.45, 100.79, 103.43, 105.44, 120.30, 122.34, 122.87, 127.10, 136.23, 149.06, 154.19, 154.79, 156.42, 161.46, 171.84, 173.76, 187.38, 187.77, 196.16, 198.87. ESI-HRMS (m/z)  $[\text{M}+\text{H}]^+$  calcd. for  $\text{C}_{35}\text{H}_{36}\text{N}_3\text{O}_9$  642.2452, found 642.2458

**(E)-1-(3-((1-(6-Acetyl-7,9-dihydroxy-8-methyl-1,3-dioxo-1,9b-dihydrodibenzo[*b,d*]furan-2(3H)-ylidene)ethyl) amino)propyl)-3-(2-(4-fluorophenyl)-2-oxoethyl)-1H-imidazol-3-ium (10)**

Colourless solid (0.115 g, 78%); mp: 118-120 °C; IR (KBr)  $\nu_{\text{max}}$ : 2927-3415, 1699, 1623, 1555, 1465, 1368, 1282, 1231, 1188  $\text{cm}^{-1}$ ;  $^1\text{H}$  NMR (300 MHz,  $\text{CDCl}_3+\text{DMSO}-d_6$ ):  $\delta$  1.67 (3H, s), 2.04 (3H, s), 2.39-2.48 (2H, bp), 2.65 (6H, s), 3.74 (2H, bp), 4.62 (2H, bp), 5.73 (1H, s), 6.21 (2H, s), 7.18 (2H, bp), 7.68 (1H, s), 7.79 (1H, s), 8.11 (2H, bp), 9.83 (1H, s), 11.90 (1H, s), 13.34 (2H, s).  $^{13}\text{C}$  NMR (100 MHz,  $\text{CDCl}_3+\text{DMSO}-d_6$ ):  $\delta$  7.38, 18.11, 28.82, 30.91, 31.55, 46.67, 55.17, 56.22, 100.75, 101.70, 102.22, 104.96, 106.25, 116.00, 116.22, 121.97, 124.12, 130.33, 131.12, 131.22, 137.42, 155.60, 157.52, 162.42, 172.92, 175.14, 188.77, 189.77, 197.17, 200.71. ESI-HRMS (m/z)  $[\text{M}+\text{H}]^+$  calcd for  $\text{C}_{32}\text{H}_{31}\text{N}_3\text{O}_7\text{F}$  588.2146, found 588.2153.

**(E)-1-(3-((1-(6-Acetyl-7,9-dihydroxy-8-methyl-1,3-dioxo-1,9b-dihydrodibenzo[*b,d*]furan-2(3H)-ylidene)ethyl)amino)propyl)-3-(2-oxo-2-(*p*-tolyl)ethyl)-1H-imidazol-3-ium (11)**

Colourless solid (0.120 g, 82%); mp: 98-100 °C; IR (KBr)  $\nu_{\text{max}}$ : 2924-3414, 1697, 1623, 1555, 1464, 1368, 1282, 1236, 1183  $\text{cm}^{-1}$ ;  $^1\text{H}$  NMR (300 MHz,  $\text{CDCl}_3+\text{DMSO}-d_6$ ):  $\delta$  1.69 (3H, s), 2.03 (3H, s), 2.34 (2H, s), 2.42 (6H, s), 3.75 (2H, bp), 4.63 (2H, t,  $J=6.327$ ), 5.73 (1H, s), 6.12 (2H, s), 7.31 (2H, d,  $J=7.427$ ), 7.67 (1H, s), 7.85 (1H, s), 7.91 (2H, d,  $J=7.427$ ), 9.72 (1H, s), 11.94 (1H, s), 13.30 (1H, bp), 13.34 (1H, s).  $^{13}\text{C}$  NMR (75 MHz,  $\text{CDCl}_3+\text{DMSO}-d_6$ ):  $\delta$  6.88, 17.98, 21.18, 29.11, 30.57, 31.30, 46.68, 54.97, 56.37, 100.59, 101.73, 104.45, 106.96, 121.36, 123.87, 127.85, 129.13, 130.38, 137.28, 145.23, 155.20, 157.52, 162.52, 162.66, 173.20, 175.00, 189.31, 189.40, 197.51, 200.02. ESI-HRMS (m/z)  $[\text{M}+\text{H}]^+$  calcd. for  $\text{C}_{32}\text{H}_{34}\text{N}_3\text{O}_7$  584.2397, found 584.2399.

**(E)-1-(3-((1-(6-Acetyl-7,9-dihydroxy-8-methyl-1,3-di-oxo-1,9b-dihydrodibenzo[*b,d*]furan-2(3H)-ylidene)eth-yl)amino)propyl)-3-(2-(naphthalen-2-yl)-2-oxoethyl)-1H-imidazol-3-ium bromide (12)**

Colourless solid (0.144 g, 93%); mp: 224-226 °C; IR (KBr)  $\nu_{\text{max}}$ : 2927-3414, 1693, 1625, 1554, 1467, 1365, 1282, 1180  $\text{cm}^{-1}$ ;  $^1\text{H}$  NMR (300 MHz,  $\text{CDCl}_3+\text{DMSO}-d_6$ ):  $\delta$  1.65 (3H, s), 2.03 (3H, s), 2.34 (2H, s), 2.38-2.46 (2H, m), 2.62 (3H, s), 2.66 (3H, s), 3.70-3.79 (2H, m), 4.62 (2H, t,  $J=5.777$ ), 5.72 (1H, s), 6.30 (2H, s), 7.57-7.66 (3H, m), 7.75 (1H, s), 7.88 (1H, s), 7.91-8.06 (4H, m), 8.70 (1H, S), 9.76 (1H, s), 11.94 (1H, s), 13.30 (1H, s), 13.33 (1H, S).  $^{13}\text{C}$  NMR (75 MHz,  $\text{CDCl}_3+\text{DMSO}-d_6$ ):  $\delta$  6.88, 17.96, 29.05, 30.55, 31.28, 46.70, 55.13, 56.13, 100.57, 101.71, 104.43, 106.94, 121.35, 122.54, 123.92, 126.63, 127.14, 128.27, 128.76, 129.25, 130.12, 130.33, 131.64, 135.36, 137.34, 155.16, 157.49, 162.63, 173.20, 174.99, 189.30, 189.90, 197.49, 199.99. ESI-HRMS (m/z)  $[\text{M}+\text{H}]^+$  calcd. for  $\text{C}_{36}\text{H}_{34}\text{N}_3\text{O}_7$  620.2397, found 620.2396.

**(E)-1-(3-((1-(6-Acetyl-7,9-dihydroxy-8-methyl-1,3-dioxo-1,9b-dihydrodibenzo[*b,d*]furan-2(3H)-ylidene)ethyl)amino)propyl)-3-(2-(4-bromophenyl)-2-oxoethyl)-1H-imidazol-3-ium bromide (13)**

Colourless solid (0.127g, 79%); mp: 97-99 °C; IR (KBr)  $\nu_{\max}$ : 2926-3417, 1698, 1622, 1556, 1462, 1369, 1281, 1231, 1179  $\text{cm}^{-1}$ ;  $^1\text{H}$  NMR (300 MHz,  $\text{CDCl}_3 + \text{DMSO}-d_6$ ):  $\delta$  1.68 (3H, s), 2.04 (3H, s), 2.39-2.49 (2H, m), 2.59 (2H, s), 2.660 (3H, s), 2.668 (3H, s), 4.15-4.22 (2H, m), 4.61 (2H, t,  $J=6.327$ ), 5.75 (1H, s), 6.20 (2H, s), 7.68 (2H, d,  $J=7.978$ ), 7.73 (1H, s), 7.86 (1H, s), 7.94 (2H, d,  $J=7.703$ ), 9.71 (1H, s), 11.45 (1H, s), 11.95 (1H, s), 13.35 (2H, bp).  $^{13}\text{C}$  NMR (75 MHz,  $\text{CDCl}_3 + \text{DMSO}-d_6$ ):  $\delta$  6.37, 17.31, 17.33, 20.21, 28.42, 29.00, 30.02, 30.73, 46.05, 54.42, 55.70, 99.99, 101.24, 103.93, 106.17, 120.89, 123.38, 124.09, 127.00, 127.77, 128.86, 131.12, 136.63, 154.68, 156.96, 162.01, 172.51, 174.11, 174.37, 188.90, 188.54, 196.82, 199.42. ESI-HRMS ( $m/z$ )  $[\text{M}+\text{H}]^+$  calcd. for  $\text{C}_{32}\text{H}_{31}\text{N}_3\text{O}_7$  648.1345, found 648.1354.

## RESULTS AND DISCUSSION

### Isolation of (+) - usnic acid and methyl barbatate from the fruticose lichen species *Usnea longissima* and *Usnea orientalis*.

Usnic acid was isolated as the major metabolite from two fruticose *Usnea* lichen species viz. *Usnea longissima* (250 g) and *Usnea orientalis* (200 g) by soxhlet extraction using *n*-hexane as solvent at 60 °C for 12 hours. Usnic acid was separated during soxhlet extraction as an insoluble substance. The insoluble substance was purified by column chromatography followed by recrystallisation from chloroform - hexane solvent mixture to afford (+)-usnic acid (**1**) in 2.0 and 1.8 % yields respectively (Chart 1) mp: 204 °C.

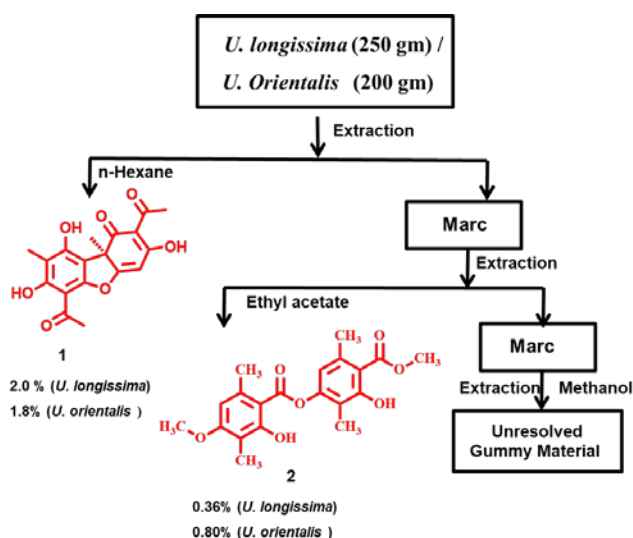


**Chart 1.** Extraction of Usnic acid from *U. longissima* and *U. orientalis*

The IR spectrum, of usnic acid showed three peaks at 1692, 1632 and 1630  $\text{cm}^{-1}$  corresponding to C1, C6 and C2 groups respectively. In its  $^1\text{H}$  NMR spectrum, five singlet's appeared at  $\delta$  1.76, 2.11, 2.66, 2.68 and 5.98 confirms 9b-

$\text{CH}_3$ , 8- $\text{CH}_3$ , 2-CO $\text{CH}_3$ , 6-CO $\text{CH}_3$  and 4-CH protons respectively. In its  $^{13}\text{C}$  NMR spectrum, three signals appeared at  $\delta$  201.68, 200.23 and 197.98 ppm corresponding to C2-carbonyl, C6-carbonyl and C1-carbonyl groups respectively. Further, its structure was confirmed by its HRMS spectrum, which showed the protonated molecular ion  $[\text{M}+\text{H}]^+$  at 345.0970 corresponding to the molecular formula  $\text{C}_{18}\text{H}_{17}\text{O}_7$ . In addition to usnic acid, methyl barbatate (**2**) was also isolated from the fruticose lichens of *usnea longissima* (0.36%) and *usnea orientalis* (0.8%) from the ethyl acetate extract (Figure 1).

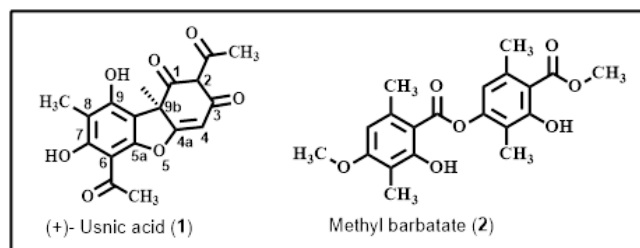
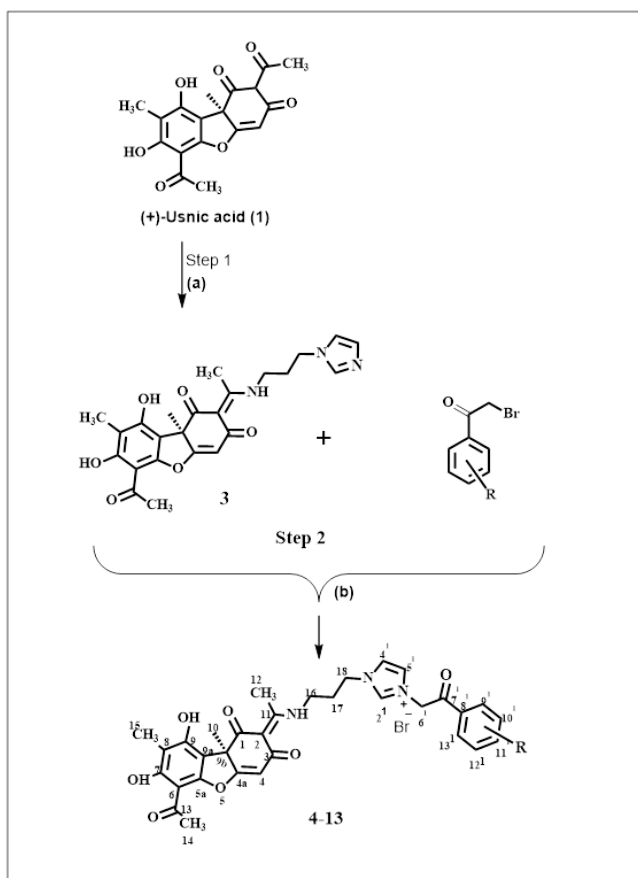


**Figure 1.** Natural products isolated from *Usnea longissima* and *Usnea orientalis*.

The IR spectrum of methyl barbatate showed peaks at 3452, 1738 and 1637  $\text{cm}^{-1}$  corresponding to hydroxyl and carbonyl functionalities. The  $^1\text{H}$  NMR spectrum of the compound showed six singlets at  $\delta$  2.16, 2.18, 2.47, 2.61, 3.85, and 3.86. The first four values representing aromatic methyl groups and the preceding values corresponding to two methoxy groups. It also showed the signals corresponding to two aromatic protons at  $\delta$  6.54, and 6.62 ppm. The  $^{13}\text{C}$  NMR spectrum of the compound showed peak  $\delta$  174.85 ppm corresponding to the ester carbonyl carbon and the peaks appeared between  $\delta$  8.86-62.08 ppm corresponding to aromatic methyl and methoxy carbons. Further, the structure was confirmed as methyl barbatate by its HRMS spectrum, which showed the protonated molecular ion  $[\text{M}+\text{H}]^+$  at 375.1444 corresponding to the molecular formula  $\text{C}_{20}\text{H}_{23}\text{O}_7$ .

### Synthesis of novel (+)-usnic acid based imidazolium salts

The protocols adopted for the synthesis of novel (+)-usnic acid based imidazolium salt hybrids are presented in Scheme 1. In the first step (+)- usnic acid (**1**) was treated with 3-(1H-imidazol-1-yl)propan-1-amine in methanol at 60 °C to synthesise the corresponding enamine (**3**) in 48% yield as per our earlier reported procedure.<sup>16</sup> Compound **3** was thoroughly characterised by its spectroscopic data. In the  $^1\text{H}$  NMR spectrum of compound **3**, three peaks appeared at  $\delta$  7.01,  $\delta$  7.07 and  $\delta$  7.55 corresponding to imidazole moiety. The  $^{13}\text{C}$  NMR spectrum while confirming these observations exhibited the characteristic carbon signals of imidazole moiety at  $\delta$  118.1,  $\delta$  129.3 and  $\delta$  136.5 ppm. In the second step, compound **3** was refluxed with various phenacyl bromides in toluene at 90 °C (Table 1) to afford the corresponding imidazolium salt derivatives (**4-13**) in very good to excellent (72-93%) yields (Scheme 1). Compounds **4-13** were thoroughly characterised by their spectral data ( $^1\text{H}$  and  $^{13}\text{C}$  NMR, IR and HRMS). The IR spectra of compounds **4-13** showed the characteristic ester functionality between 1663-1705  $\text{cm}^{-1}$ .



(a) 3-(1H-imidazol-1-yl)propan-1-amine, methanol, reflux at 60 °C, 48 %; (b) phenacyl bromide, toluene, heat at 90 °C, 72-93%

### Scheme 1. Synthesis of imidazolium salts from usnic acid (1)

The  $^1\text{H}$  NMR spectra of the compounds showed the characteristic phenacyl methylene protons between  $\delta$  6.05-6.30. The  $^{13}\text{C}$  NMR spectra of the compounds while confirming their structures exhibited the characteristic phenacyl methylene and carbonyl carbons between  $\delta$  55.10-56.37 and  $\delta$  187.77-189.90 respectively.

Table 1. Synthesis of compounds from 4 to 13.

Compounds	R	Yield, %
4	$\text{C}_6\text{H}_5\text{COCH}_2-$	85
5	$4-\text{ClC}_6\text{H}_4\text{COCH}_2-$	76
6	$4-\text{O}_2\text{NC}_6\text{H}_4\text{COCH}_2-$	87
7	$3-\text{MeOC}_6\text{H}_4\text{COCH}_2-$	72
8	$3-(\text{H}_2\text{NCO})-4-\text{HOC}_6\text{H}_3\text{COCH}_2-$	84
9	$3,4-[\text{CH}_2(\text{CH}_2\text{O})_2]\text{C}_6\text{H}_3\text{COCH}_2-$	91
10	$4-\text{FC}_6\text{H}_4\text{COCH}_2-$	78
11	$4-\text{CH}_3\text{C}_6\text{H}_4\text{COCH}_2-$	82
12	$\beta\text{-C}_{10}\text{H}_7\text{COCH}_2-$	93
13	$4\text{-BrC}_6\text{H}_4\text{COCH}_2-$	79

The anti-inflammatory activity of the synthesized compounds 4-13 was tested *in vitro* by estimating the amount of cytokines, TNF- $\alpha$  and IL-1 $\beta$ , secreted in the LPS challenged U937 cell lines on treatment with the test compounds. Though the parent compound 1 displayed weak anti-inflammatory activity, the majority of the synthesized hybrids showed promising anti-inflammatory activity against TNF- $\alpha$  at a concentration of 10  $\mu\text{M}$ . As shown in Table 2, compound 5 (80.10%), exhibited good inhibitory

potential against TNF- $\alpha$  and the compounds 6 (90.4%) and 13 (85.5%) exhibited potential inhibitory activities against IL-1 $\beta$ . However, it is seen from the study that most of the compounds failed to show inhibition activity against IL-1 $\beta$ .

Table 2. Anti-inflammatory activity of synthesised compounds in percentage of inhibition.

Compound	Inhibition, %	
	TNF- $\alpha$	IL-1 $\beta$
1	4.84	-1.24
3	-8.1	25.5
4	50.9	16.7
5	80.1	25.4
6	17.3	90.4
7	-3.6	44.0
8	24.5	-24.6
9	7.0	21.8
10	-24.5	-3.5
11	21.4	2.5
12	31.9	24.9
13	4.7	85.5
Dexamethasone	81.4	80.5

Table 3. IC<sub>50</sub> values of synthesized compounds.

Compound	IC <sub>50</sub> , $\mu\text{M}$	
	TNF- $\alpha$	IL-1 $\beta$
1	>100	>100
5	$5.3 \pm 0.005$	>100
6	>100	$7.5 \pm 0.1$
13	>100	$6.8 \pm 0.5$
Dexamethasone	$1.5 \pm 0.04$	$2.9 \pm 0.05$

Compounds with good TNF- $\alpha$  inhibitory activity were further screened to identify their IC<sub>50</sub> values. As shown in Table 3, the above compounds proved to possess good anti-inflammatory activity with IC<sub>50</sub> values  $5.3 \pm 0.005$   $\mu\text{M}$  (5),  $7.5 \pm 0.1$   $\mu\text{M}$  (6), and  $6.8 \pm 0.5$   $\mu\text{M}$  (13), when compared to the parent compound 1 (>100  $\mu\text{M}$ ).

The anti-inflammatory activities of the synthetic analogues were also found to be comparable with that of the standard dexamethasone [IC<sub>50</sub>:  $4.18 \pm 0.1$  (TNF- $\alpha$ );  $2.9 \pm 0.05$  (IL-1 $\beta$ )]. From the close analysis of the results (Table 2 and 3), it is evident that the introduction of enamine functionality at the C-2 position of (+)- usnic acid (5, 6 and 13) increases the TNF- $\alpha$  & IL-1 $\beta$  inhibitory activity many folds (IC<sub>50</sub>: 5.3  $\mu\text{M}$  - 7.5  $\mu\text{M}$ ). Interestingly, the synthesized imidazolium salts with electron-withdrawing groups on phenacyl moiety such as chloro, nitro and bromo groups (5, 6 and 13) showed potent activity (IC<sub>50</sub>: 5.3  $\mu\text{M}$  - 7.5  $\mu\text{M}$ ) against TNF- $\alpha$  and IL-1 $\beta$ , whereas imidazolium salts with an aromatic or heteroaromatic substituent's (4 and 8-12) showed weak activity. Most significantly, imidazoles 5 (IC<sub>50</sub>:  $5.3 \pm 0.005$   $\mu\text{M}$ ), 6 (IC<sub>50</sub>:  $7.5 \pm 0.1$   $\mu\text{M}$ ) and 13 (IC<sub>50</sub>:  $6.8 \pm 0.5$   $\mu\text{M}$ ) found to be many folds more active than the parent compound (1). Because of significant activities exhibited by compounds 5, 6 and 13, they can be considered as lead compounds for further development to synthesise highly potent anti-inflammatory agent.

## CONCLUSION

In total, ten novel hybrids of (+)-usnic acid based imidazolium salts were synthesized and evaluated for their anti-inflammatory potential against the cytokine proteins TNF- $\alpha$  and IL-1 $\beta$  secreted from U937 cells. The imidazolium salts (**5**, **6**, and **13**) exhibited promising anti-inflammatory activity against the TNF- $\alpha$  and IL-1 $\beta$  with IC<sub>50</sub> values ranging between 5.3  $\mu$ M - 7.5  $\mu$ M, which are many folds lower than that of the parent compound (>100  $\mu$ M). Most significantly, imidazolium salts with electronegative groups (**5**, **6** and **13**) found to be more potent and exhibiting enhanced anti-inflammatory activity. Hence, these compounds can be considered as lead molecules for further fine tuning to make highly potent anti-inflammatory therapeutic agents.

## ACKNOWLEDGEMENTS

This work was supported by CSIR, Government of India in the form of Research fellowship to TS. We thank Director CSIR-IICT for the support (IICT/Pubs./2019/390).

## REFERENCES

- <sup>1</sup>Araujo, A. A. S., De Melo, M. G. D., Rabelo, T. K., Nunes, P. S., Santos, S. L., Serafini, M. R., Santos, M. R. V., Quintans-Junior, L. J., Gelain, D. P., Review of the biological properties and toxicity of usnic acid, *Nat. Prod. Res.*, **2015**, 29(23), 2167-2180. DOI:10.1080/14786419.2015.1007455.
- <sup>2</sup>Xuelong, Y., Guo, Q., Guozhu, S. U., Yang, A., Zhongdong, H.U., Changhai, Q. U., ZheWan., Ruoyu, L. I., Pengfei ,T.U., Xingyun, C., Usnic Acid Derivatives with Cytotoxic and Antifungal Activities From the Lichen Usnea longissima, *J. Nat. Prod.*, **2016**, 79, 1373. DOI:10.1021/acs.jnatprod.6b00109.
- <sup>3</sup>Vijayakumar, C. S., Viswanathan, S., Reddy, M. K., Parvathavarthini, S., Kundu, A. B., Sukumar, E., Anti-inflammatory activity of (+)- usnic acid, *Fitoterapia*, **2000**, 71(5), 564-566. DOI: 10.1016/s0367- 326x(00)00209-4.
- <sup>4</sup>Zu-Qing, S., Zhi-Zhun, M., Jin-Bin, L., Xue-Xuan, F., Yong-Zhuo, L., Xie Zhang., Yu-Hong, L., Xiao-Ying, Chen., Zhi-Wei, C., Zi-Ren, S., Xiao-Ping, L., Usnic acid protects LPS-induced acute lung injury in mice through attenuating inflammatory responses and oxidative stress, *Int. Immunopharmacol.*, **2014**, 22, 371-378. DOI:10.1016/j.intimp.2014.06.043.
- <sup>5</sup>Huang, Z., Zheng, G., Tao, J., Ruan, J., Anti-inflammatory Effects and Mechanisms of Usnic Acid, *J. Wuhan Univ. Technol. Mater.*, **2011**, 26, 955. DOI: 10.1007/s11595-011-0344-8.
- <sup>6</sup>Sokolov, D.N., Zarubaev, V. V., Shtro, A. A., Polovinka, M. P., Luzina, O.A., Komarova, N. I., Salakhutdinov, N. F., Kiselev, O. I., Anti-viral activity of (-) and (+)-usnic acids and their derivatives against influenza virus A(H1N1)2009, *Bioorg. Med. Chem. Lett.*, **2012**, 22, 7060-7064. DOI:10.1016/j.bmcl.2012.09.084.
- <sup>7</sup>Luzina, O. A., Salakhutdinov, N. F., Biological Activity of Usnic Acid and Its Derivatives: Part 1. Activity against Unicellular Organisms, *Russ. J. Bioorg. Chem.*, **2016**, 42(2), 129-149. DOI:10.1134/S1068162016020084.
- <sup>8</sup>Bruno, M., Trucchi, B., Burlando, B., Ranzato, E., Martinotti, S., Akkol, E. K., Suntar, I., Keles, H., Verotta, L., (+)-Usnic acid enamines with remarkable cicatrizing properties, *Bioorg. Med. Chem.*, **2013**, 21, 1834. DOI:10.1016/j.bmc.2013.01.045.
- <sup>9</sup>Siti, N. R., Yugen, Z., Imidazolium salts and their polymeric materials for biological applications, *Chem. Soc. Rev.*, **2013**, 42(23), 9055-9070. DOI: 10.1039/c3cs60169b.
- <sup>10</sup>Xiao-Liang, X ., Chun-Lei, Y., Wen Chen, Ying-Chao, L., Li-Juan, Y., Yan, L., Hong-Bin, Z., Xiao- Dong, Y., Synthesis and antitumor activity of novel 2-substituted indoline imidazolium salt derivatives, *Org. Biomol. Chem.*, **2015**, 13, 1550. DOI: 10.1039/C4OB02385D.
- <sup>11</sup>Baoliang, C., Bo Lin, Z., Kan He., Qun, Y. Z., Imidazole Alkaloids from *Lepidium meyenii*, *J. Nat. Prod.* **2003**, 66(8), 1101. DOI: 10.1021/np030031i.
- <sup>12</sup>Ewa, L. B., Dorota, G., Imidazolium salts and their polymeric materials for biological applications, *J. Biosci. Bioeng.*, **2013**, 115, 71. DOI: 10.1039/C3CS60169B.
- <sup>13</sup>Hindi, K. M., Panzner, M. J., Cannon, C. L., Youngs, W. J., The Medicinal Applications of Imidazolium Carbene-Metal Complexes, *Chem. Rev.*, **2009**, 109, 3859. DOI: 10.1021/cr800500u.
- <sup>14</sup>Del Bufalo, A., Bernad, J., Dardenne, C., Verda, D., Meunier, J. R., Rousset, F., Martinozzi-Teissier, S., Pipy, B., Contact sensitizers modulate the arachidonic acid metabolism of PMA-differentiated U-937 monocytic cells activated by LPS, *Toxicol. Appl. Pharmacol.*, **2011**, 256(1), 35-43. DOI:10.1016/j.taap.2011.06.025.
- <sup>15</sup>Yang, X. D., Zeng, X. H., Zhang, Y. L., Qing, C., Song, W. J., Li, L., Zhang, H. B., Synthesis and cytotoxic activities of novel phenacylimidazolium bromides, *Bioorg. Med. Chem. Lett.*, **2009**, 19, 1892. DOI: 10.1016/j.bmcl.2009.02.065.
- <sup>16</sup>Mallavadhani, U. V., Nagi Reddy, V., Balabhaskara Rao, K., Nishanth, J., Synthesis and antiproliferative activity of novel (+)- usnic acid analogues, *J. Asian Nat. Prod. Res.*, **2019**, 22(6), 562-577. DOI:10.1080/10286020.2019.1603220.

Received: 22.11.2020.

Accepted: 25.12.2020.